UC DAVIS CHEM 205: SYMMETRY, SPECTROSCOPY, & STRUCTURE

Delmar Larsen
LibreTexts

UC Davis Chem 205: Symmetry, Spectroscopy, & Structure

LibreTexts

The LibreTexts libraries are Powered by NICE CXOne and are supported by the Department of Education Open Textbook Pilot Project, the UC Davis Office of the Provost, the UC Davis Library, the California State University Affordable Learning Solutions Program, and Merlot. This material is based upon work supported by the National Science Foundation under Grant No. 1246120, 1525057, and 1413739.

Any opinions, findings, and conclusions or recommendations expressed in this material are those of the author(s) and do not necessarily reflect the views of the National Science Foundation nor the US Department of Education.

TABLE OF CONTENTS

Licensing

0: Agenda

1: Basics of Spectroscopy

- 1.1: Electromagnetic Radiation (Component 1)
- 1.2: Matter (Component 2)
- 1.3: Experimental Details of Absorption spectroscopy

2: Electronic Spectroscopy

- 2.1: Transition Integrals
- 2.2: Vibronic Transitions
- 2.3: Broadening Mechanisms
- 2.4: The Fate of Electronic Transitions
- 2.5: Electronic State and Transitions
- 2.6: Introduction to Symmetry
- 2.7: The Carbonyl Group
- 2.8: Symmetry and Formaldehyde
- 2.9: Configuration Interaction
- 2.10: Measures of Transition Amplitudes
- 2.11: Term Symbols
- 2.12: Absorption Spectrum of Formaldehyde
- 2.13: Assignment of Bands Based on Solvent Effects
- 2.14: Solvent Effect of Fluorescence
- 2.15: Breaking Symmetries
- 2.16: Charge Transfer Bands
- 2.17: Conjugation Length

3: Vibrational Spectroscopy

- 3.1: Introduction to Vibrations
- 3.2: Polyatomic Molecules
- 3.3: Raman vs. IR Spectroscopies
- 3.4: Resonant Raman Spectroscopy
- 3.5: Classification of Normal Modes
- 3.6: IR and Raman Activity
- 3.7: Non-Fundamental Transations - Hot Bands, Combination Bands, and Fermi Resonances
- 3.8: Fourier Transform IR Spectroscopy
- 3.9: Spectra of Gases - Rovibronic Transitions

4: X-ray Spectroscopy

- 4.1: Physical Principles
- 4.2: Photoelectron Spectroscopy - Valence Ionization
- 4.3: Back to Basics
- 4.4: Experimental Details
- 4.5: X-ray Photoelectron (XPS) Spectroscopy
- 4.6: X-ray Absorption Spectroscopies

- 4.7: Experimental modes and Data Analysis
- 4.8: Introduction to X-ray Absorption Spectroscopy (XAS)
- 4.9: X-Ray Absorption Near Edge Structure (XANES)
- 4.10: X-ray absorption fine structure (XAFS)

5: Magnetic Resonance Spectroscopies

- 5.1: Nuclear Magnetic Resonance (NMR) - Intrinsic Spins
- 5.2: Nuclear Magnetic Resonance (NMR) - Turning on the Field
- 5.3: Spin 1/2 Spectra
- 5.4: Chemical Shifts
- 5.5: Boltzmann Statistics
- 5.6: Larmour Frequency
- 5.7: Ensemble Effects
- 5.8: Precession and Relaxation
- 5.9: Chemical Shifts
- 5.10: Fourier Transform (pulsed) NMR - The way things are really done these days
- 5.11: Spin-Spin, J-Coupling or indirect dipole-dipole coupling (all the same phenomenon)
- 5.12: 13-C NMR Spectroscopy
- 5.13: Nuclear Overhauser Effect (NOE) and 2-D NMR
- 5.14: Electron Paramagnetic Resonance
- 5.15: EPR Instrumentation
- 5.16: EPR Signals
- 5.17: EPR - Hyperfine Structure

6: Miscellaneous Topics

7: Writing Topics

- 7.1: Polarization Sensitive Electronic Spectra (Anisotropy)
- 7.2: Circular Dichroism (Electronic)
- 7.3: Influence of Absorption Spectra based on Molecular Structure
- 7.4: Two-Photon Absorption
- 7.5: Electronic Absorption Selection Rules
- 7.6: Resonant Raman Scattering
- 7.7: Circular Dichroism (Vibrational)
- 7.8: FTIR Operation
- 7.9: Fourier Transform Algorithms in FTIR
- 7.10: Rotational Raman Spectroscopy -Li Wang
- 7.11: Vibrational Absorption Selection Rules
- 7.12: Microwave Rotational Spectroscopy
- 7.13: Two-photon Fluorescence -Rachel Siegel
- 7.14: 2D NMR (General Properties)
- 7.15: Spin Echos
- 7.16: X-ray Photoelectron Spectroscopy (XPS) - Nick Mrachek
- 7.17: Sensitivity of XANES on Oxidation State of Elements - Ivan Opara
- 7.18: Sensitivity of XANES on Chemical Environment (e.g., bonding)
- 7.19: X-Ray Generation and Detection Sources
- 7.20: Analysis of XAFS Spectra -Kingston Robinson
- 7.21: X-Ray Photoelectron Spectroscopy
- 7.22: Magic Angle Spinning Solid-State NMR -Kayla Osumi
- 7.23: Electron-Nuclear Double Resonance (ENDOR) -Liam Twomey
- 7.24: Double Electron-Electron Resonance (DEER)

- 7.25: Nuclear Resonance Vibrational Spectroscopy (NRVS)
- 7.26: Nuclear Overhauser Effect
- 7.27: Total Correlation Spectroscopy (TOCSY)
- 7.28: Nuclear Overhauser Effect Spectroscopy (NOESY) - Joel Shirey
- 7.29: ^{1}H-^{1}H COSY (COrrelated SpectroscopY) - Chris Suarez
- 7.30: Heteronculear Single Quantum Coherence (HSQC) NMR
- 7.31: Rotating frame Overhauser Effect SpectroscopY (^{1}H-^{1i}H ROESY)
- 7.32: scanning near-field optical microscopy (SNOM) - Xavier Holmes
- 7.33: Surface-enhanced Raman spectroscopy - Chris Suarez

Index

Glossary

Detailed Licensing

Licensing

*A detailed breakdown of this resource's licensing can be found in **Back Matter/Detailed Licensing**.*

CHAPTER OVERVIEW

1: Basics of Spectroscopy

Spectroscopy is the study of the absorption and emission of electromagnetic radiation by matter. Spectroscopy is an important tool that can be used to find the molecular structures, composition, and vibration frequencies of a substance. It can also be used to find the concentrations of reactants as functions of time to find the reaction intermediates. The defining characteristic of spectroscopy is interaction of light (electromagnetic spectrum) and matter. Knowledge of both is required to fully interpret the measured data.

- To the **Physical Chemist**, spectroscopy is the natural consequence of the application of the time-dependent Schrödinger equation to a well defined quantum mechanical system, which by definition has well defined quantized energy levels. Detailed knowledge of the underlying quantum mechanical description of the interaction of applied radiation and a desired sample is the primary goal of this class (*Theory*).
- To the **Analytical Chemist**, spectroscopy is a technique (or series of techniques) capable of providing either quantitative or qualitative analysis of unknown samples with the aid of instruments either complex or simple. Detailed knowledge of the operation and application of spectroscopic instruments is the primary goal of this class (*Application*).
- To the **Inorganic Chemist**, spectroscopy is a technique (or series of techniques) that provides useful and constructive interpretation of, often newly synthesized, compounds generated in the laboratory. Detailed knowledge of interpreting spectroscopic signals is the primary goal of this class (*Interpretation*).

Spectroscopy is the study of the interaction of radiation (Component 1) with matter (Component 2).

1.1: Electromagnetic Radiation (Component 1)
1.2: Matter (Component 2)
1.3: Different types of Spectroscopy
1.4: Absorbance and Concentration
1.5: Multicomponent Samples

1.1: Electromagnetic Radiation (Component 1)

Spectroscopy is the study of the interaction of **radiation** with **matter**. Electromagnetic radiation is a form of energy that is produce by oscillating electric and magnetic disturbance. It travels at the speed of light as a quantized harmonic wave. The electric and magnetic waves travel perpendicular to each other. Characteristics of waves include amplitude, wavelength, and frequency.

The electromagnetic spectrum consists of Radio/TV, Microwaves, Infrared, Visible, Ultraviolet, X-rays, and Gamma-rays (Figure 1.1.1). The longest waves, radio waves, are approximately 10^3 m in wavelength. As the name implies, radio waves are transmitted by radio broadcasts, TV broadcasts, and even cell phones. The shortest waves, Gamma rays, are approximately 10^{-12} m in wavelength. Out this huge spectrum, the human eyes can only detect waves from 390 nm to 780 nm.

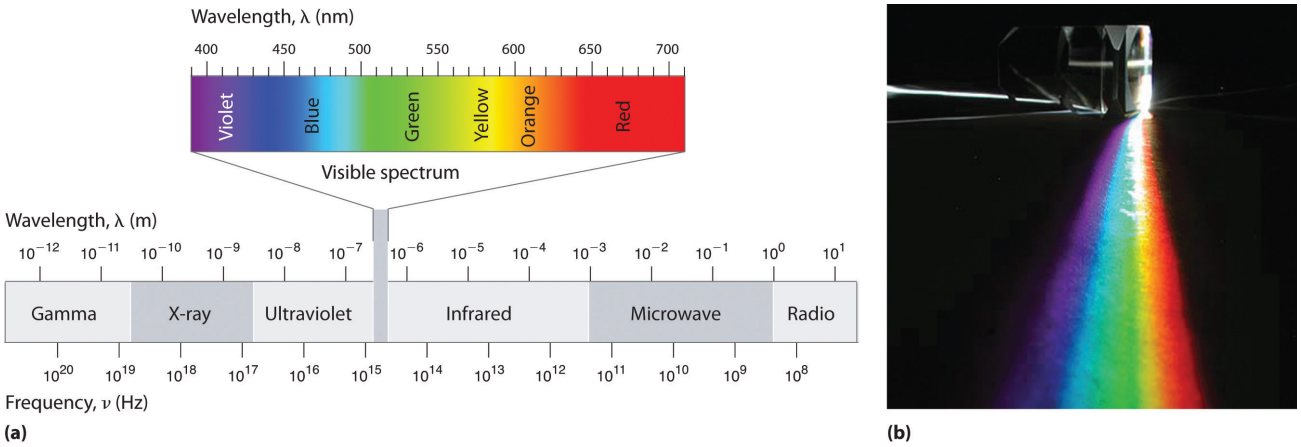

Figure 1.1.1: The Electromagnetic Spectrum. (a) This diagram shows the wavelength and frequency ranges of electromagnetic radiation. The visible portion of the electromagnetic spectrum is the narrow region with wavelengths between about 400 and 700 nm. (b) When white light is passed through a prism, it is split into light of different wavelengths, whose colors correspond to the visible spectrum. (CC BY-NC-SA; anonymous)

Within this visible range our eyes perceive radiation of different wavelengths (or frequencies) as light of different colors, ranging from red to violet in order of decreasing wavelength. The components of white light—a mixture of all the frequencies of visible light—can be separated by a prism (Figure 1.1.1*b*). A similar phenomenon creates a rainbow, where water droplets suspended in the air act as tiny prisms.

Table 1.1.1: Common Wavelength Units for Electromagnetic Radiation

Unit	Symbol	Wavelength (m)	Type of Radiation
picometer	pm	10^{-12}	gamma ray
angstrom	Å	10^{-10}	x-ray
nanometer	nm	10^{-9}	x-ray
micrometer	μm	10^{-6}	infrared
millimeter	mm	10^{-3}	infrared
centimeter	cm	10^{-2}	microwave
meter	m	10^{0}	radio

We know that EM radiation of photons whose energy each with energies given by **Planck's law**:

$$E = h\nu \tag{1.1.1}$$

where h is Planck's constant = $6.626068 \times 10^{-34}\ m^2 kg/s$ and ν is the frequency ($1/s$ or Hz).

The speed of the electromagnetic radiation in vacuum is c, which is equal to 299,792,458 m/s. Since

$$c = \lambda\nu$$

EEquation 1.1.1 can be written in the following two alternate forms:

$$E = \frac{hc}{\lambda} = hc\tilde{\nu}$$

or

$$\tilde{\nu} = \frac{1}{\lambda}.$$

where $1/\lambda$ is the inverse wavelength or wavenumber (cm^{-1}).

The effect that a photon will have on matter or molecule will depend on E, and thus on v.

- For $\tilde{\nu} < 10^{-2}$ cm^{-1} ($\lambda \sim 1$ m), we have **radio frequencies**. These are too low an energy photons for anything except to affect the magnetic energy of a nucleus in an external magnetic field (NMR Spectroscopy)
- For 10^{-2} $cm^{-1} < \tilde{\nu} < 10$ cm^{-1} ($\lambda \sim 1$ cm), we have **microwave frequencies**. Photons have enough energy to be absorbed by unpaired electrons spins in an externally magnetic field (ESR) or to change the rotational energy of a molecule (microwave rotational spectroscopy)
- For 10 $cm^{-1} < \tilde{\nu} < 10^{4}$ cm^{-1} ($\lambda \sim 5$ μm), we have **infrared frequencies**. Photons have sufficient energy to be absorbed in the rotational motion of the molecules. This is called vibrational spectroscopy.
- For 10^{-2} $cm^{-1} < \tilde{\nu} < 10^{5}$ cm^{-1} ($\lambda < 1$ μm), we have **visible and UV spectroscopy** which involves excitations of electrons (valence) from stable orbits to higher energy orbits in the molecule. Electronic spectroscopy (UV-VIS)
- For 10^{5} $cm^{-1} < \tilde{\nu} < 10^{6}$ cm^{-1}, we have **vacuum UV**, where the photons have enough energy that if absorbed by a valence electron, the electron can be “knocked” out of the molecule. This is called photoelectron spectroscopy
- For 10^{6} $cm^{-1} < \tilde{\nu} < 10^{8}$ cm^{-1}, these are **X-rays** and have enough energy to ionize not only valence electrons, but also core electrons. This spectroscopy is call X-ray Photo-electron spectroscopy (XPS) and also Extended X-ray absorption fine structure (EXAFS) and X-ray Absorption Near Edge Structure (XANES).
- For $\tilde{\nu} < 10^{8}$ cm^{-1}. These are very energetic **gamma rays** and are not used extensively for spectroscopy with chemists. One key exception is Mössbauer spectroscopy which is enough energy to promote changes in the nuclei of the atoms.

That is a quick run-down of the spectroscopies we will be address in this course. We will not be discussing mass spectroscopy or diffraction techniques although used quite constructively for many scientific endeavors.

1.2: Matter (Component 2)

A typical molecule will have thousands of possible energy levels involving rotational, vibrational and electronic excitations and combinations thereof. However, relatively few transitions between these states will be allowed. Rules restricting transitions between states are call **Selection Rules**. They all have a basis in symmetry of the molecules. Thus, Group theory is a powerful tool to develop selection rules, and thus, to interpret the observed spectra.

From undergraduate quantum mechanics, you are familiar with the solutions to the time-*independent* Schrödinger Equation

$$H^{(0)}\psi_n(\vec{r}) = E_n\psi_n(\vec{r})$$

or in bra/ket notation

$$\hat{H}^{(0)}|n\rangle = E_n|n\rangle$$

which can be solved exactly for many systems, such as the harmonic oscillator, the rotating diatomic (rigid) molecule, and the H-atom and numerically for the rest. The wavefunctions, $\{|n\rangle\}$, are called **stationary** states with energies $\{E_n\}$. These are solutions to the time-independent Schrödinger equation.

If $\hat{H}$ is absolutely independent of time, then a molecule described by a particular ψ_n will stay in that state forever. There will no possibility for transitions between different ψ_n, which is the essence of spectroscopy. Transitions between stationary states can only happen in the presence of a time-dependent Hamiltonian. This is provided by the oscillating electric and magnetic fields of the radiation. So the total Hamiltonian is now

$$H_{tot} = H^{(0)} + H^{(1)}(t)$$

where $H^{(1)}(t)$ us the time-dependent Hamiltonian that describes the interaction with the electromagnetic radiation.

Electric Dipole Coupling

Ultraviolet and visible radiation interacts with matter which causes electronic transitions (promotion of electrons from the ground state to a high energy state). The ultraviolet region falls in the range between 190-380 nm, the visible region falls between 380-750 nm. For the interaction of the oscillating electric field, $\vec{E}(t)$ of monochromatic radiation of frequency, ν, with the electrons of the molecules,

$$H^{(1)}(t) = \vec{E}\cdot\vec{\mu}\cos(\pi\nu t) \tag{1.2.1}$$

where $\vec{E}$ is the amplitude of the oscillating **electric field vector** and $\vec{\mu}$ is the **electric dipole moment** of the molecule and ν is the frequency of the radiation. The electric dipole moment is a summation of all charges in the species.

$$\vec{\mu} = -e\sum_i \vec{R}_i$$

$\vec{E}$ is polarized in a plane to the direction of propagation. Generally, light is depolarized meaning that polarization is uniformly distributed in the XY place for Z direction. Laser radiation, in contrast, is often plane polarized, with a simple polarization in the XY plane or at some angle.

For Reference

The energy of 285 nm photons is $6.97\times10^{-19}J$ and for one mole of photon $419.7\,kJ/mol$

The mean wavelength in visible is 565 nm. The energy of 565 nm photons is $3.52\times10^{-19}J$ and for one mole of photon $211.7\,kJ/mol$

If the radiation is not strong, then $H^{(1)}(t) \ll H^{(0)}$ and the change introduced by $H^{(1)}(t)$ can be treated as a perturbation, e.g., 1st order transition theory. We will not go through the steps here, which are covered in many standard textbooks in Quantum Mechanics.

From such approaches, we get an expression for the transition probability is often called "**Fermi's Golden Rule**"

$$W_{i\to f} = \left(\frac{4\pi}{h}\right)\left|H_{fi}^{(1)}\right|^2 \rho(\Delta E)$$

where

- i and f label the initial and final states in the transition
- $W_{i\to f}$ is the probability per unit time that a transition occurs.
- $\rho_N(\Delta E)$ is the density of final states and
- $\Delta E = abs(E_f - E_i)$ in dimensions of energy^{-1}. This important part of is $W_{i\to f}$ is $H_{fi}^{(1)}$

$$H_{fi}^{(1)} = \langle f|H^{(1)}|i\rangle \tag{1.2.2}$$

For example, for the **electric dipole-induced transition** (Equation 1.2.1), the coupling element is

$$H_{fi}^{(1)} = \vec{E}\cdot\langle f|\vec{\mu}|i\rangle \tag{1.2.3}$$

other transitions (e.g., electric quadrupole-induced transition, magnetic dipole-induced transitions, etc) will have different expressions.

If this matrix element of the perturbed Hamiltonian is non-zero, then transitions **CAN** be induced from $|i\rangle$ to $|f\rangle$. The importance of symmetry is that the integrals (Equation 1.2.2 or 1.2.3) can often be shown to be ZERO, using group theory arguments. **We will be getting to this later.** Transitions can be assigned because we know that some for them cannot occur or can only occur with some probability with a weak absorption from the applied radiation (within 1st order perturbation theory).

Separation of Eigenstates

Born-Oppenheimer approximation: energy separated into three types rotational levels superimposed on vibrational levels and vibrational levels superimposed on electronic levels.

$$\Delta E = \Delta_{Eelectronic} + \Delta E_{vibration} + \Delta E_{rotation}$$

And there is a strong separation of magnitude in these energies (Figure 1.2.1):

$$\Delta E_{electronic} > \Delta E_{vibration} > \Delta E_{rotation}$$

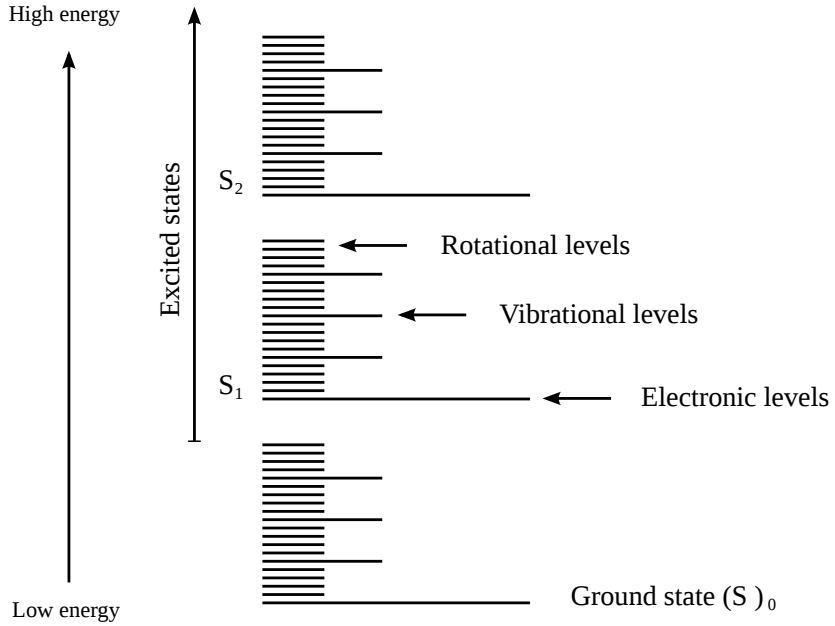

Figure 1.2.1: A diagram representing singlet energy-levels in a molecule to help explain the concept of electronic, rotational and vibrational energy-levels to my students. (CC BY-SA 3.0; Lvzon via Wikipedia)

The energy levels (eigenstates) can be rated in the following order **electronic > vibrational > rotational**. Each of these transitions differ by an order of magnitude. Rotational transitions occur at lower energies (longer wavelengths) and this energy is insufficient

and cannot cause vibrational and electronic transitions, but vibrational (near infra-red) and electronic transitions (ultraviolet region of the electromagnetic spectrum) require higher energies. The diagram below illustrates possible transitions that occur.

- transitions represents pure rotational changes (far infrared).
- transitions rotational-vibrational (rovibrational) transitions;
- transitions are rotational-vibrational-electronic transitions (visible and ultraviolet) S_o is electronic ground state and S_1 and S_2 are electronic excited states.

For a transition to be spectroscopically observed

1. There must exist a coupling mechanism (via $H^{(1)}$) between initial and final eigenstates
2. The initial eigenstate ($|i\rangle$) must be **populated** (e.g., d^0 d-d electronic transition). Since most spectroscopies involve molecules/systems that are **thermally populated**, then the Boltzmann distribution is required

$$p_i = \frac{e^{-E_{i/kT}}}{Q}$$

with

$$Q = \sum_i^{\infty} e^{-E_i/kT}$$

(assuming non-degenerate eigenstates)

3. The final eigenstate ($|f\rangle$) must be **unpopulated** (e.g., d^{10} d-d electronic transitions)

Note

At room temperature ($kT = 200\,cm^{-1}$), most electronic transitions occur from $v = 0$, but not from $J = 0$ eigenstate. So potentially multiple excitation transitions typically coexist.

1.3: Different types of Spectroscopy

There are many different types of spectroscopy, each tailored to a specific type of analysis, interaction of light with matter, and the information it provides. Here's a summary of some of the most common and widely used types of spectroscopy: Different types of spectroscopy focus on the absorption, emission, or scattering of light by molecules or atoms. Here's a summary of the three major types:

- **Absorption/Transmission Spectroscopy** measures light absorbed by the sample to identify and quantify substances.
- **Emission Spectroscopy** measures light emitted by excited atoms or molecules as they return to lower energy states.
- **Scattering Spectroscopy** measures the redirected light when it interacts with particles or molecules, providing information about molecular vibrations or particle size.

Each type of spectroscopy has its own advantages and applications, depending on the nature of the sample and the information required.

Absorption/Transmission Spectroscopies

Absorption spectroscopy involves the measurement of the amount of light absorbed by a sample as a function of its wavelength or frequency. When light passes through a substance, certain wavelengths of light are absorbed by the sample, causing transitions in the energy levels of atoms or molecules. The intensity of absorption is related to the concentration of the absorbing species in the sample.

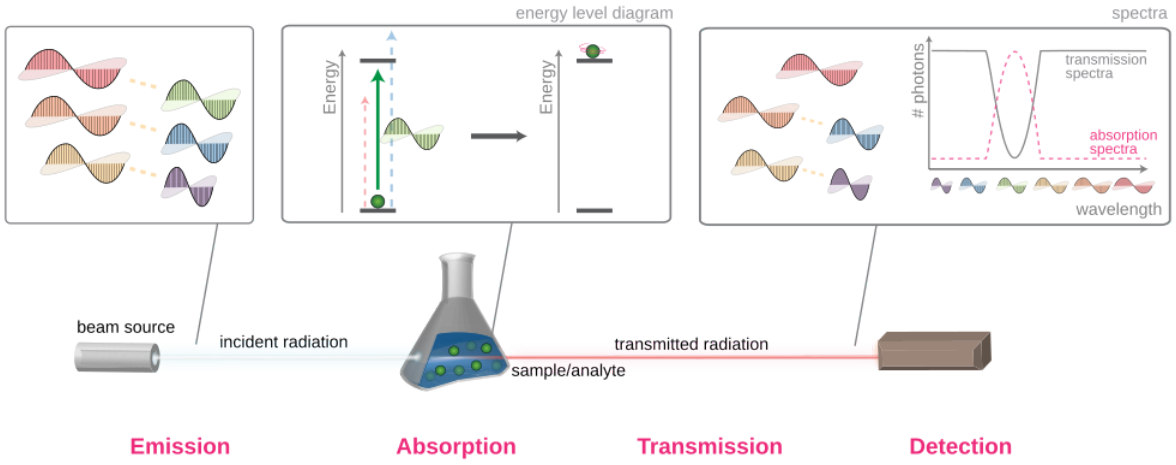

Figure 1.3.1: An overview of electromagnetic radiation absorption. This example discusses the general principle using visible light. A white beam source – emitting light of multiple wavelengths – is focused on a sample (the complementary color pairs are indicated by the yellow dotted lines). Upon striking the sample, photons that match the energy gap of the molecules present (green light in this example) are absorbed in order to excite the molecule. Other photons transmit unaffected and, if the radiation is in the visible region (400–700 nm), the sample color is the complementary color of the absorbed light. By comparing the attenuation of the transmitted light with the incident, an absorption spectrum can be obtained. (CC BY-SA 3.0; Jon Chui via Wikipedia)

The absorption of light at a given λ, can be used to measure concentration in solution. Electronic absorption spectra of solutes in liquid solution are generally broadened due to several factors including inhomogeneities in the local environment that do not average out – fluctuations that are too slow.

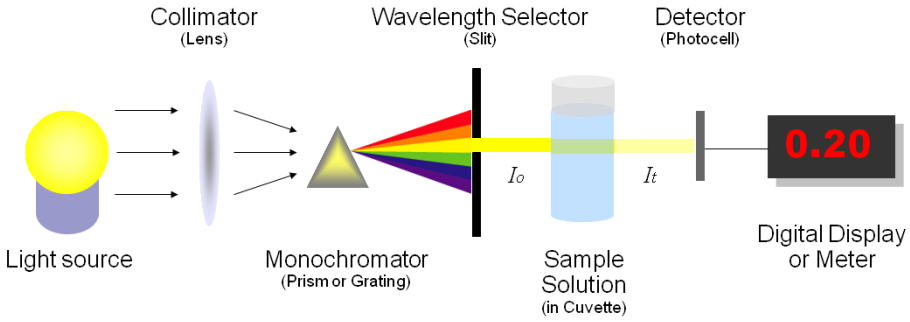

Figure 1.3.1: Basic structure of spectrophotometers (CC BY-4.0; Heesung Shim via LibreTexts)

Timescales

The characteristic timescale for the electronic transition is ~1 fs, while several fluctuations in the solvent are much slower ~ps. These local fluctuations of the solvent results in a “static inhomogeneity” of the absorption band. Thus rotational structure is not revealed and vibrational structure partially so (if at all) and are referred to as bands in the absorption.

The amount of photons that goes through the cuvette and into the detector is dependent on the length of the cuvette and the concentration of the sample. Once you know the intensity of light after it passes through the cuvette, you can relate it to **transmittance** (T) (Figure 1.3.2). Transmittance is the fraction of light that passes through the sample. This can be calculated using the equation:

$$\text{Transmittance}(T) = \frac{I_t}{I_o}$$

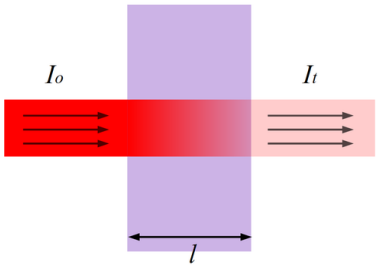

Figure 1.3.2: Transmittance (CC BY-4.0; Heesung Shim via LibreTexts)

Key Types of Absorption Spectroscopies

Ultraviolet-Visible (UV-Vis) Spectroscopy

- **Principle**: Measures the absorption of ultraviolet and visible light (200–800 nm) by a sample. Molecules absorb light at specific wavelengths corresponding to electronic transitions.
- **Applications**: Used to determine concentrations of organic compounds, metals, and transition metal complexes. It's also widely used in chemical and biochemical analysis.
- **Example**: Determining the concentration of a compound in solution by measuring the absorption of UV or visible light.

Infrared (IR) Spectroscopy

- **Principle**: Measures the absorption of infrared light (typically in the 4000–400 cm^{-1} range) by a sample, which causes molecular vibrations (stretching, bending, etc.).
- **Applications**: Identifies functional groups in organic molecules and characterizes chemical bonds. It’s commonly used in organic chemistry, environmental monitoring, and material science.
- **Example**: Identifying functional groups like -OH (hydroxyl), -NH (amine), and C=O (carbonyl) in organic compounds.

X-ray Absorption Spectroscopy (XAS)

- **Principle**: Measures the absorption of X-rays by a sample, which excites inner electrons, providing information about the local structure and electronic environment of specific elements.
- **Applications**: Used for the analysis of materials, especially in materials science, chemistry, and catalysis. It provides insights into coordination, oxidation state, and electronic structure.
- **Example**: Characterizing the local structure of metal ions in catalysts or materials.

Atomic Absorption Spectroscopy (AAS)

- **Principle**: Measures the absorption of light by free atoms in the gas phase, typically produced by a flame or graphite furnace. The absorption is characteristic of the element being analyzed.
- **Applications**: Commonly used to determine trace amounts of metals in samples, including environmental, pharmaceutical, and food analysis.
- **Example**: Measuring concentrations of metals such as lead, mercury, and calcium in water or soil samples.

Near-Infrared (NIR) Spectroscopy

- **Principle**: Measures the absorption of near-infrared light (1000–2500 nm), which interacts with overtones and combinations of molecular vibrations, especially in organic compounds.
- **Applications**: Used in agricultural, pharmaceutical, and food industries for non-destructive analysis, including moisture content, fat, and protein levels.
- **Example**: Determining moisture content in grains or pharmaceutical formulations.

Example 1.3.1: UV-Visible Spectroscopy

Many transition metal ions, such as Cu^{2+} and Co^{2+}, form colorful solutions because the metal ion absorbs visible light. The transitions that give rise to this absorption are valence electrons in the metal ion's *d*-orbitals.

Figure 1.3.1: Transition Metal Rainbow (Copyright; tgent_007 via Reddit)

For a free metal ion, the five *d*-orbitals are of equal energy. In the presence of a complexing ligand or solvent molecule, however, the *d*-orbitals split into two or more groups that differ in energy. For example, in an octahedral complex of $Cu(H_2O)_6^{2+}$ the six water molecules perturb the *d*-orbitals into the two groups shown in Figure 1.3.3 . The resulting $d \rightarrow d$ transitions for transition metal ions are relatively weak.

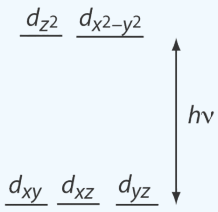

Figure 1.3.3 . Splitting of the *d*-orbitals in an octahedral field.

Emission Spectroscopies

Emission spectroscopy is based on the principle that atoms or molecules emit light (photons) when they transition from a higher energy state to a lower energy state. This emission occurs after the sample is excited by an external energy source (e.g., heat, light, or electrical energy). The emitted light is typically analyzed to determine the composition and concentration of the elements or compounds in the sample.

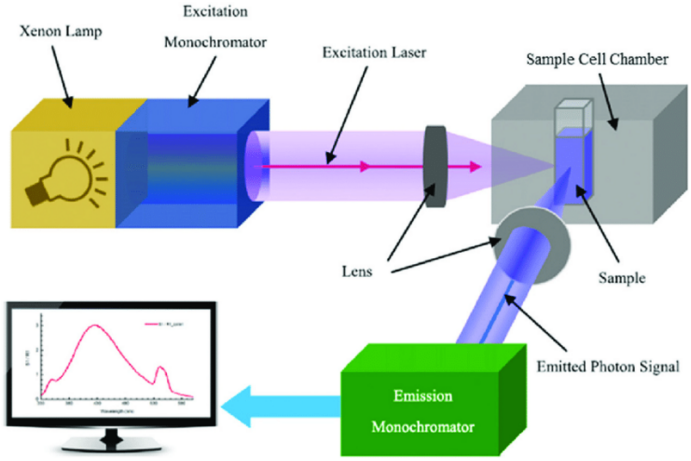

Figure 1.3.2: Schematic diagram of the arrangement of optical components in a typical fluorometer. (CC BY-SA 3.0 Unported; Changzheng Li and Yanan Yue via Wikipedia)

Key Types of Emission Spectroscopies

Fluorescence Spectroscopy

- **Principle**: Molecules absorb light (usually in the ultraviolet or visible range) and then emit light at a longer wavelength (lower energy) as they return to a lower energy state.
- **Applications**: Used for detecting and quantifying trace amounts of compounds, especially in biological, environmental, and chemical studies. It's highly sensitive and selective.
- **Example**: Detecting pollutants, biomarkers, or DNA sequences in medical diagnostics.

Atomic Emission Spectroscopy (AES)

- **Principle**: Atoms in a sample are excited (often by a flame, plasma, or electric arc) and then emit light at characteristic wavelengths as they relax to their ground state.
- **Applications**: Used to analyze the elemental composition of a sample, particularly in environmental, industrial, and pharmaceutical analysis.
- **Example**: Measuring the concentration of metals like sodium, potassium, and calcium in samples.

Inductively Coupled Plasma Optical Emission Spectroscopy (ICP-OES)

- **Principle**: A sample is introduced into a plasma (a high-temperature ionized gas), which excites the atoms. The emitted light is analyzed to determine the sample's composition.
- **Applications**: Provides sensitive and multi-element analysis, commonly used in environmental testing, food safety, and materials analysis.
- **Example**: Detecting trace elements in water, soil, and food products.

Flame Emission Spectroscopy (FES)

- **Principle**: A sample is introduced into a flame, where it is atomized and excited. The emitted light is analyzed, which is characteristic of the elements in the sample.
- **Applications**: Primarily used for the determination of metal ions in aqueous solutions.
- **Example**: Testing for sodium or potassium levels in blood or urine.

X-ray Emission Spectroscopy

- **Principle**: X-rays interact with a sample, causing inner shell electrons to be ejected. The atoms then release energy as X-ray fluorescence, which is measured.

- **Applications**: Used for elemental analysis, particularly in materials science and geology.
- **Example**: Identifying and quantifying elements in rocks, minerals, and metals.

Example 1.3.2: Flame Emission Spectroscopy (FES)

A common technique used for detecting metals in a sample by measuring the emitted light when a sample is heated in a flame. The emitted light has a characteristic wavelength corresponding to the energy difference between the excited and ground states of atoms or molecules.

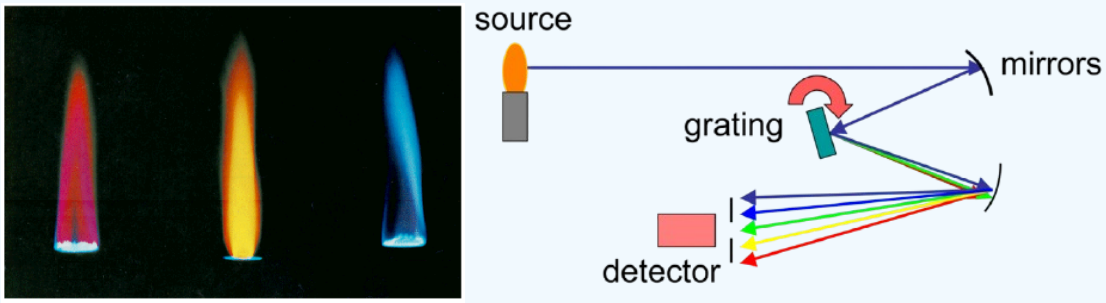

Figure 1.3.3: Many elements will still produce distinctive colors under such conditions, simple flame tests can be used to identify these elements. In fact, flame tests were used to identify elements long before the invention of modern techniques, such as emission spectroscopy. (left) flames from specific elements in a bunsen burner. (right) Schematic of a flame emission spectrometer. (CC BY-SA 3.0 Unported; Kkmurray via Wikipedia)

Scattering Spectroscopies

Scattering spectroscopy involves the scattering of light by molecules or particles in the sample. Unlike absorption, where light is absorbed by the sample, scattering occurs when light interacts with the sample and is redirected in different directions. The intensity and pattern of scattered light can provide information about the size, shape, and properties of particles, as well as the molecular structure of the sample.

Key Types of Scattering Spectroscopies

Raman Spectroscopy

- **Principle**: Measures the inelastic scattering of light (Raman scattering) when photons interact with molecular vibrations. The scattered light is shifted in frequency, providing information about molecular structure and bonding.
- **Applications**: Used to study molecular vibrations, chemical structure, and functional groups. It is widely used in material science, chemistry, and biological research.
- **Example**: Identifying chemical bonds, functional groups, and molecular structures in organic compounds.

Rayleigh Scattering

- **Principle**: Involves the elastic scattering of light by molecules or particles that are much smaller than the wavelength of the incident light. The scattered light has the same frequency as the incident light.
- **Applications**: Often used to study the size, shape, and concentration of small particles (e.g., in aerosols, colloids, and nanomaterials).
- **Example**: Determining particle size distribution in suspensions or colloidal systems.

Dynamic Light Scattering (DLS)

- **Principle**: A technique that measures fluctuations in the intensity of scattered light as particles move in a liquid. This can be used to determine the size and distribution of particles in solution.
- **Applications**: Primarily used for characterizing nanoparticles, colloids, and biomolecules in suspension.
- **Example**: Measuring the size of nanoparticles, proteins, or polymers in solution.

Neutron Scattering

- **Principle**: Uses neutrons instead of light to scatter off a sample. Neutron scattering provides information about atomic and molecular structures, especially for materials with lighter elements like hydrogen.

- **Applications**: Used in materials science, biology, and chemistry to study structures at the atomic and molecular level, including soft matter and complex materials.
- **Example**: Studying the structure of proteins, polymers, and crystalline materials.

Compton Scattering

- **Principle**: Involves the inelastic scattering of X-rays or gamma rays by electrons. The change in energy and direction of the scattered photons provides information about the electron density and the material's properties.
- **Applications**: Primarily used in physics and materials science to study the electronic structure and density of materials.
- **Example**: Investigating the electronic properties of metals and semiconductors.

Example 1.3.3: Raman Spectroscopy

In Raman scattering, most of the light is scattered at the same frequency (Rayleigh scattering), but a small portion of light is shifted to different frequencies (Stokes and Anti-Stokes scattering), providing insights into the sample's molecular vibrations. Measures the scattering of light when it interacts with vibrational modes of molecules. Raman spectroscopy provides information about molecular vibrations and can be used for structural analysis of compounds.

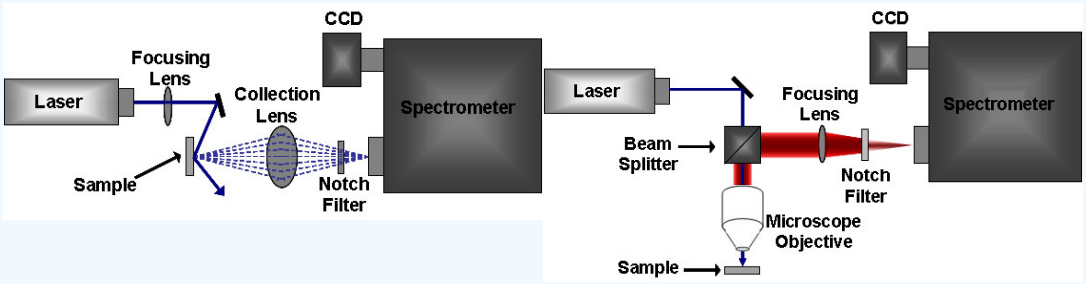

Figure 1.3.4: (left) Schematic of a macro-Raman spectrometer. (right) Schematic of a micro-Raman spectrometer where illumination and collection are performed through microscope objective. (CC BY 3.0; Pavan M. V. Raja & Andrew R. Barron via OpenStax CNX)

1.4: Absorbance and Concentration

When monochromatic electromagnetic radiation passes through an infinitesimally thin layer of sample of thickness *dx*, it experiences a decrease in its power of *dP* (Figure 1.4.1).

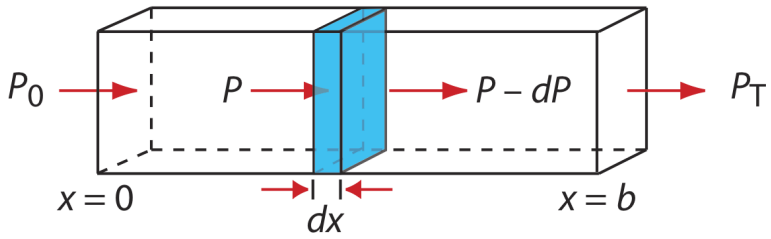

Figure 1.4.1. Factors used to derive the Beer's law.

This fractional decrease in power is proportional to the sample's thickness and to the analyte's concentration, *C*; thus

$$-\frac{dP}{P} = \alpha C dx \tag{1.4.1}$$

where *P* is the power incident on the thin layer of sample and α is a proportionality constant. Integrating the left side of Equation 1.4.1 over the sample's full thickness

$$-\int_{P=P_0}^{P=P_t} \frac{dP}{P} = \alpha C \int_{x=0}^{x=b} dx$$

$$\ln \frac{P_0}{P_T} = \alpha b C$$

converting from ln to log, and substituting into the equation relating transmittance to absorbance

$$A = -\log T = -\log \frac{P_T}{P_0}$$

gives

$$A = abC \tag{1.4.2}$$

where *a* is the analyte's absorptivity with units of cm^{-1} $conc^{-1}$. If we express the concentration using molarity, then we replace *a* with the molar absorptivity, ε, which has units of cm^{-1} M^{-1}.

$$A = \varepsilon b C \tag{1.4.3}$$

The absorptivity and the molar absorptivity are proportional to the probability that the analyte absorbs a photon of a given energy. As a result, values for both *a* and ε depend on the wavelength of the absorbed photon.

Example 1.4.1

A 5.00×10^{-4} M solution of analyte is placed in a sample cell that has a pathlength of 1.00 cm. At a wavelength of 490 nm, the solution's absorbance is 0.338. What is the analyte's molar absorptivity at this wavelength?

Solution

Solving Equation 1.4.3 for ϵ and making appropriate substitutions gives

$$\varepsilon = \frac{A}{bC} = \frac{0.338}{(1.00 \text{ cm})\left(5.00 \times 10^{-4} \text{ M}\right)} = 676 \text{ cm}^{-1} \text{ M}^{-1}$$

Exercise 1.4.1

A solution of the analyte from Example 1.4.1 has an absorbance of 0.228 in a 1.00-cm sample cell. What is the analyte's concentration?

Answer

Making appropriate substitutions into Beer's law

$$A = 0.228 = \varepsilon b C = \left(676\ \text{M}^{-1}\ \text{cm}^{-1}\right)(1\ \text{cm})C$$

and solving for *C* gives a concentration of 3.37×10^{-4} M.

Equation 1.4.2 and Equation 1.4.3, which establish the linear relationship between absorbance and concentration, are known as Beer's law. Calibration curves based on Beer's law are common in quantitative analyses.

As is often the case, the formulation of a law is more complicated than its name suggests. This is the case, for example, with Beer's law, which also is known as the Beer-Lambert law or the Beer-Lambert-Bouguer law. Pierre Bouguer, in 1729, and Johann Lambert, in 1760, noted that the transmittance of light decreases exponentially with an increase in the sample's thickness.

$$T \propto e^{-b}$$

Later, in 1852, August Beer noted that the transmittance of light decreases exponentially as the concentration of the absorbing species increases.

$$T \propto e^{-C}$$

Together, and when written in terms of absorbance instead of transmittance, these two relationships make up what we know as Beer's law.

Limitations to Beer's Law

Beer's law suggests that a plot of absorbance vs. concentration—we will call this a Beer's law plot—is a straight line with a *y*-intercept of zero and a slope of *ab* or εb. In some cases a Beer's law plot deviates from this ideal behavior (see Figure 1.4.2), and such deviations from linearity are divided into three categories: fundamental, chemical, and instrumental.

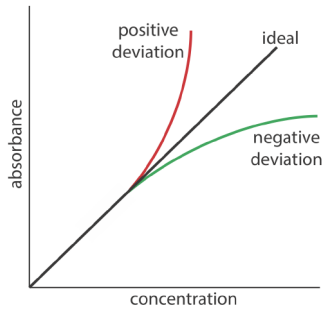

Figure 1.4.2. Plots of absorbance vs. concentration showing positive and negative deviations from the ideal Beer's law relationship, which is a straight line.

1.5: Multicomponent Samples

We can extend Beer's law to a sample that contains several absorbing components. If there are no interactions between the components, then the individual absorbances, A_i, are additive. For a two-component mixture of analyte's X and Y, the total absorbance, A_{tot}, is

$$A_{tot} = A_X + A_Y = \varepsilon_X b C_X + \varepsilon_Y b C_Y$$

Generalizing, the absorbance for a mixture of n components, A_{mix}, is

$$A_{mix} = \sum_{i=1}^{n} A_i = \sum_{i=1}^{n} \varepsilon_i b C_i \tag{1.5.1}$$

Determining Concentrations from Spectra

Simultaneous determination of concentration of two simultaneously present absorbers (B and C) is possible from measuring @ two wavelengths, λ_1 and λ_2. In a 1 cm pathlength cell,

$$A_1 = A(\lambda_1) = \varepsilon_b(\lambda_1)c_b + \varepsilon_c(\lambda_1)c_c$$

$$A_2 = A(\lambda_2) = \varepsilon_b(\lambda_2)c_b + \varepsilon_c(\lambda_2)c_c$$

Simultaneous solutions of this linear system of equations are possible provided

$$\det \begin{vmatrix} \varepsilon_B(\lambda_1) & \varepsilon_C(\lambda_1) \\ \varepsilon_B(\lambda_2) & \varepsilon_C(\lambda_2) \end{vmatrix} \neq 0$$

If this is 0 (or close to it), then the equations are **linearly dependent** and no unique solution for c_b and c_b possible. The wavelengths, λ_1 and λ_2 should be chosen to yield a large value for the determinant.

Isosbestic Points

If there are only two species present in solution that absorbs, S and ES, for instance, and they have overlapping spectra, there will be at least one wavelength, λ_o, where

$$\varepsilon_S(\lambda_o) = \varepsilon_{ES}(\lambda_o).$$

The absorbance @ λ_o will be constant irrespective of the condition of the sample (in equilibrium or out of equilibrium) assuming constant sum of populations.

$$\begin{aligned} A(\lambda)_o) &= x\varepsilon_S(\lambda_o) + y\varepsilon_S(\lambda_o) \\ &= (x+y)\varepsilon_S(\lambda_o) \end{aligned}$$

λ_o defines an **isobestic point**. If we know the spectrum of S and ES, λ_o can be determined.

Example 1.5.1: p-nitrophenol vs. p-nitrophenolate

You need a spectrometer to produce a variety of wavelengths because different compounds absorb best at different wavelengths. For example, p-nitrophenol (acid form) has the maximum absorbance at approximately 320 nm and p-nitrophenolate (basic form) absorbs best at 400 nm (Figure 1.5.3).

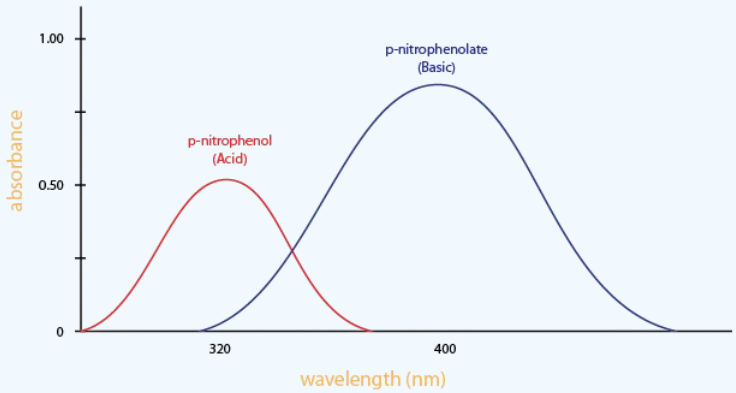

Figure 1.5.3: Absorbance of two different compounds. (CC BY 4.0; Heesung Shim via LibreTexts)

Looking at the graph that measures absorbance and wavelength, an isosbestic point can also be observed. An **isosbestic point** is the wavelength in which the absorbance of two or more species are the same. The appearance of an isosbestic point in a reaction demonstrates that an intermediate is NOT required to form a product from a reactant. Figure 1.5.4 shows an example of an isosbestic point.

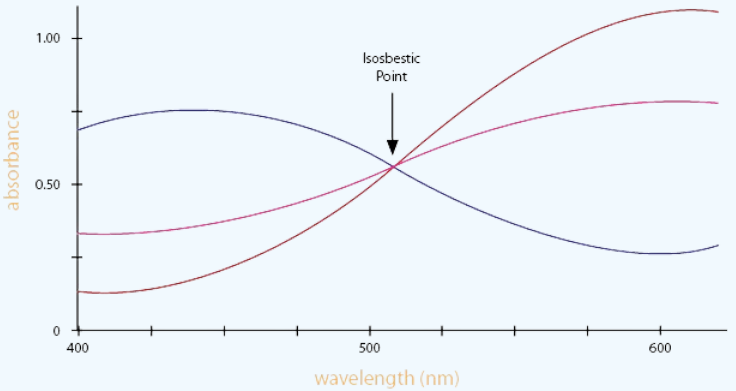

Figure 1.5.4: An example of isosbestic point. (CC BY 4.0; Heesung Shim via LibreTexts)

CHAPTER OVERVIEW

2: Electronic Spectroscopy

Electron spectroscopy is an analytical technique to study the electronic structure and its dynamics in atoms and molecules. In general an excitation source such as x-rays, electrons or synchrotron radiation will eject an electron from an inner-shell orbital of an atom.

2.1: Transition Integrals
2.2: Vibronic Transitions
2.3: Broadening Mechanisms
2.4: The Fate of Electronic Transitions
2.5: Electronic State and Transitions
2.6: Introduction to Symmetry
2.7: The Carbonyl Group
2.8: Symmetry and Formaldehyde
2.9: Configuration Interaction
2.10: Measures of Transition Amplitudes
2.11: Term Symbols
2.12: Absorption Spectrum of Formaldehyde
2.13: Assignment of Bands Based on Solvent Effects
2.14: Solvent Effect of Fluorescence
2.15: Breaking Symmetries
2.16: Charge Transfer Bands
2.17: Conjugation Length

2.1: Transition Integrals

If the electronic transition dipole moment, $\mu_{f,i}$ has a nonzero value then the particular transition can be detected by optical spectroscopy.

$$\mu_{\mathrm{f,i}} = \int \Psi_{\mathrm{final}}\, \hat{\mu} \Psi_{\mathrm{initial}}\, \mathrm{d}\tau \neq 0$$

The intensities of spectroscopic transitions are proportional to the transition integral. The μ is related to a dipole and therefore charge times distance.

$$\hat{\mu} = -e \sum_i \vec{r}_i$$

where e is the elementary charge of an electron. Now,

$$\mu_{\mathrm{fi}} = -e \int \psi_{\mathrm{final}}\, \vec{r}\, \psi_{\mathrm{initial}}\, \mathrm{d}\tau$$

The applicable wave functions of two states can be vibrational wave functions if we are talking about vibrational spectroscopy, electronic wavefunctions if we are talking about electronic spectroscopy etc.

Electronic Transitions (cause of UV-Visible absorption)

Electronic transitions in organic molecules lead to UV and visible absorption. As a rule, energetically favored electron promotion will be from the highest occupied molecular orbital (HOMO) to the lowest unoccupied molecular orbital (LUMO), and the resulting species is called an **excited state.** The molecular orbital picture for the hydrogen molecule (H_2) consists of one bonding σ MO, and a higher energy antibonding σ* MO. When the molecule is in the ground state, both electrons are paired in the lower-energy bonding orbital – this is the Highest Occupied Molecular Orbital (HOMO). The antibonding σ* orbital, in turn, is the Lowest Unoccupied Molecular Orbital (LUMO).

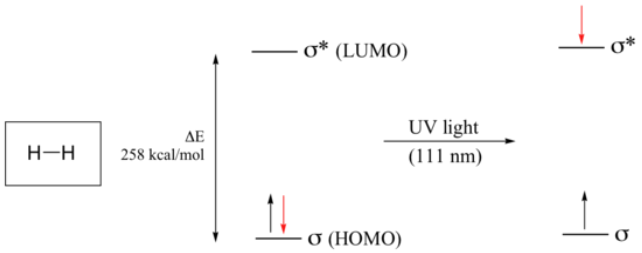

If the molecule is exposed to light of a wavelength with energy equal to ΔE, the HOMO-LUMO energy gap, this wavelength will be absorbed and the energy used to bump one of the electrons from the HOMO to the LUMO – in other words, from the σ to the σ* orbital. This is referred to as a $\sigma - \sigma^*$ transition. ΔE for this electronic transition is 258 kcal/mol, corresponding to light with a wavelength of 111 nm.

When a double-bonded molecule such as ethene (common name ethylene) absorbs light, it undergoes a $\pi - \pi^*$ transition. Because $\pi - \pi^*$ energy gaps are narrower than $\sigma - \sigma^*$ gaps, ethene absorbs light at 165 nm - a longer wavelength than molecular hydrogen.

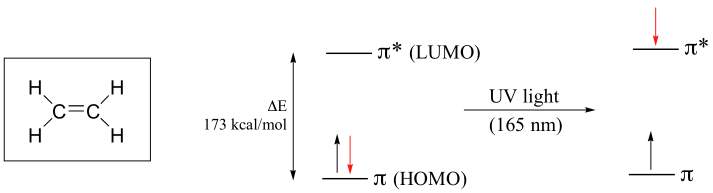

A diagram highlighting the various kinds of electronic excitation that may occur in organic molecules is shown below. Of the six transitions outlined, only the two lowest energy ones, n to π^* and π to π^* (colored blue) are achieved by the energies available in the 200 to 800 nm range of a UV/VIs spectrum. These energies are sufficient to promote or excite a molecular electron to a higher energy orbital in many conjugated compounds.

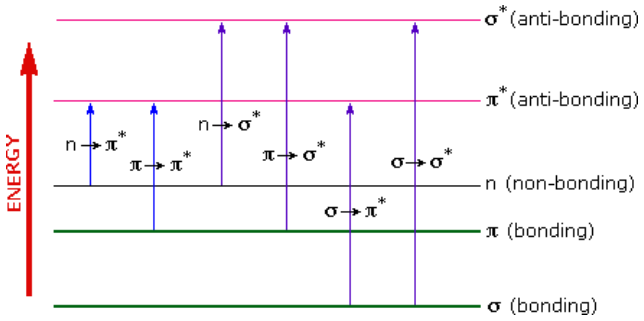

The resulting spectrum is presented as a graph of absorbance (A) versus wavelength, as in the isoprene spectrum shown below. Since isoprene is colorless, it does not absorb in the visible part of the spectrum and this region is not displayed on the graph. Notice that the convention in UV-vis spectroscopy is to show the baseline at the bottom of the graph with the peaks pointing up. Wavelength values on the x-axis are generally measured in nanometers (nm) rather than in cm^{-1} as is the convention in IR spectroscopy.

λ_{max}, which is the wavelength at maximal light absorbance. As you can see, isoprene has λ_{max}, = 222 nm. The second valuable piece of data is the absorbance at the λ_{max}. In the isoprene spectrum the absorbance at the value λ_{max} of 222 nm is about 0.8.

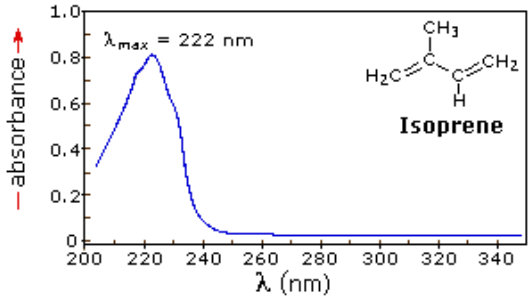

The only molecular moieties likely to absorb light in the 200 to 800 nm region are functional groups that contain pi-electrons and hetero atoms having non-bonding valence-shell electron pairs. Such light absorbing groups are referred to as **chromophores**. A list of some simple chromophores and their light absorption characteristics are provided below. The oxygen non-bonding electrons in alcohols and ethers do not give rise to absorption above 160 nm. Consequently, pure alcohol and ether solvents may be used for spectroscopic studies.

Chromophore	Example	Excitation	λmax, nm	ε @ λmax	Solvent
C=C	Ethene	$\pi \rightarrow \pi^*$	171	15,000	hexane
C≡C	1-Hexyne	$\pi \rightarrow \pi^*$	180	10,000	hexane
C=O	Ethanal	$n \rightarrow \pi^*$ $\pi \rightarrow \pi^*$	290 180	15 10,000	hexane hexane
N=O	Nitromethane	$n \rightarrow \pi^*$ $\pi \rightarrow \pi^*$	275 200	17 5,000	ethanol ethanol
C-X X=Br X=I	Methyl bromide Methyl Iodide	$n \rightarrow \sigma^*$ $n \rightarrow \sigma^*$	205 255	200 360	hexane hexane

2.2: Vibronic Transitions

As mentioned Earlier, electronic excitations occur with wavelengths in the visible and ultraviolet regions of the EM spectrum. Transitions also usually involve vibrational excitations (as previously discussed with the diatomic molecule). Plot the total energy of molecule (except for nuclear translational kinetic energy) vs. r, the intermolecular distance. This is effectively, the potential energy function, $V(r)$, for the intramolecular nuclear motion (vibration). This is due to the Born-Oppenheimer approximation. Often, we introduce vibrations as a quadratic function (Harmonic Oscillator), however, a Morse potential function gives a good fit to the true potential (within the BO approximation).

$$V(r) = D\left(1 - \mathrm{e}^{-v_o\left(2\pi^2/D\right)^{1/2}(r-r_{eq})}\right)^2$$

where D is the dissociation energy, μ is the reduced mass, r_{eq} is the equilibrium bond length and ν_o is the fundamental vibrational frequency.

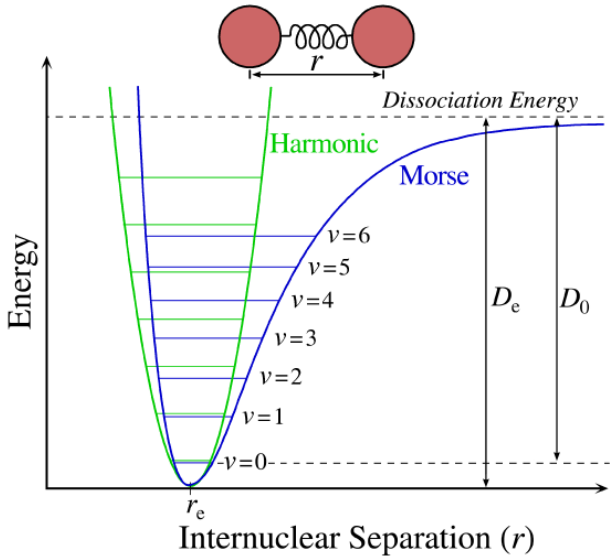

Figure 2.2.1: Copy and Paste Caption here. (CC BY-SA 4.0; Somoza via Wikipedia)

The actual energy levels for the molecule are shown by the horizontal lines. These lie above $V(r)$ and represent the contributions of nuclear kinetics energy of the total energy of the molecule. The classical turning points for a given vibrational state ($v = 3$) are shown by point A and B. At these points, classically, the nuclear kinetic energy is 0 and the vibrational energy is all potential. At $r = r_{eq}$, the kinetic Energy of the nuclear, classically, is at the maximum, which is where $V(r)$ is 0.

In quantum mechanics, it does not quite work that way. The only things we know is that $\langle V \rangle_{av} = \langle T \rangle$ on the average. Note that the spacing between the vibration energy levels decrease with increasing vibrational energy. If enough energy is absorbed, the molecule will dissociate into atoms. The vibration spacing becomes smaller since the bond is not an ideal Hook's law spring: $V(r) = 1/2k(r - r_{eq})$, and becomes weaker as it is stretched, thus $\Delta\nu$ **decreases** between adjacent energy levels.

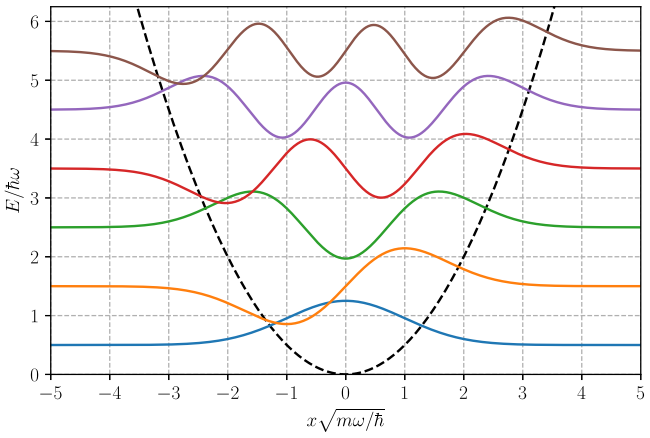

Figure 2.2.2: First six wavefunctions of the quantum harmonic oscillator. (Public Domain; AkanoToE via Wikipedia)

Each bound state also can be described by a different (in general) Morse potential curve, displaced upwards by the electronic energy different. V_o, r_{eq}, and D will differ in principle for each vibration (if more than two atoms in the molecule) in each electronic state (Figure 2.2.3).

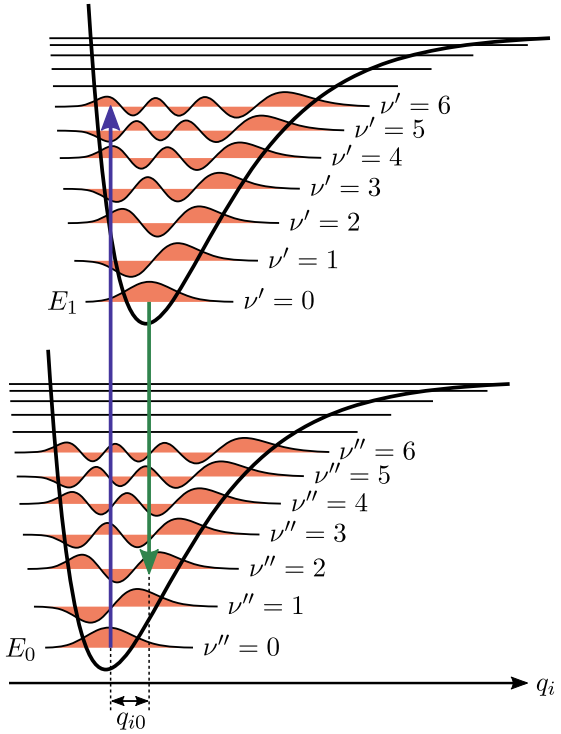

Figure 2.2.3: Franck–Condon principle energy diagram. Since electronic transitions are very fast compared with nuclear motions, the vibrational states to and from which absorption and emission occur are those that correspond to a minimal change in the nuclear coordinates. As a result, both absorption and emission produce molecules in vibrationally excited states. The potential wells are shown favoring transitions with changes in ν. (CC BY-SA 4.0; Original author was Samoza and was converted to SVG by Frenzie23 via Wikipedia)

Transitions usually originate from the v=0 (because they are not thermally occupied at kT=200 cm^{-1}), but can end up in $v' = 0$, $v' = 1$, $v'' = 2$ etc. No selection rules on this transition. Electronic transitions in molecules are governed by the Frank-Condon approximation. Since an electronic transition task place in a short time (1fs), the nuclei do not have time to move during an electronic transition **(similar separation of velocities as in the Born Oppenheimer approximation, but that did not involve spectroscopic transitions).** Thus, all transitions are vertical on a potential energy diagram (plotted energy versus nuclear position) = r is fixed in a diatomic. Note: the vibrational wavefunctions are drawn above.

The **Born-Oppenheimer** approximation allows us to write the wavefunction of a state as

$$\Psi_{\text{int}} = \Psi_{el}\Psi_{\text{nucl}}\,(Q)$$

where Q is the nuclear distances or positions. To be more exact, we should

$$\psi_{\text{int}} = \Psi_{el}(q;Q)\psi_{\text{nucl}}\,(Q)$$

with q representing the electron distances (or positions). The semi-colon represents a parametric dependence on Q.

The separation of the internal wavefunction (excluding transitional effects) into a product of two functions is the same as splitting the Hamiltonian into a sum of two components

$$H_{\text{int}} = \Psi_{el}(q;Q) + \Psi_{mcl}(q)$$

and the corresponding energies

$$E_{\text{int}} = E_{el} + E_{\text{nucl}}\,.$$

If $\mathrm{H}^{(1)}$ is the interaction of the electromagnetic radiation with the electrons, then the integral

$$\int \psi^{i}_{\text{int}}\, H^{(1)} \psi^{f}_{\text{int}}\, d\Gamma$$

can be factored and do NOT depend on vibration (just parametrically). So

$$\int \psi^{i}_{\text{int}}\, H^{(1)} \psi^{f}_{\text{int}}\, d\Gamma = \int \psi^{i}_{el} H^{(1)} \psi^{f}_{el} d\Gamma \times \int \psi^{i}_{\text{mucl}}\, \psi^{f}_{\text{mucl}}\, dQ$$

And the transition probability is

$$W_{i\to f} \propto \left| \int \psi^{i}_{el} H^{(1)} \psi^{f}_{el} d \right|^{2} \times \left| \int \psi^{i}_{\text{nucl}}\, \psi^{f}_{\text{nucl}}\, dQ \right|^{2}$$

The last term is the square of the nuclear overlap integral and is call the **Frank-Condon (FC) Factor**. This first term is an integral over the electronic wavefunction as this does not depend strongly on the nuclear coordinate (well, parametrically). So the intensity of the v=0 to v'=0, v=0 to v'=1, and v=0 to v'=2, transitions is mainly controlled by the Franck-Condon factor also referred to as S.

> **Note**
>
> To see which vibrational mode changes can accompany an electronic transition, we need to look at the Franck-Condon (FC) factors

Franck-Condon Progressions

To understand the significance of the above formula for the FC factor, let us examine a ground and excited state potential energy surface at $T = 0$ Kelvin. Shown below are two states separated by 8,000 cm^{-1} in energy. This is energy separation between the bottoms of their potential wells, but also between the respective zero-point energy levels. Let us assume that the wavenumber of the vibrational mode is 1,000 cm^{-1} and that the bond length is increased due to the fact that an electron is removed from a bonding orbital and placed in an anti-bonding orbital upon electronic excitation.

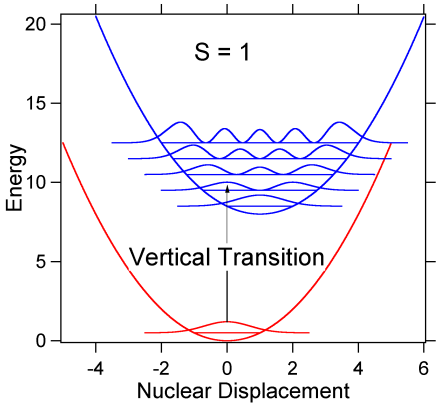

Figure 2.2.2: Wavefunctions transitions for a harmonic oscillator model system with moderate displacement (S=1). (Stefan Franzen)

According to the above model for the Franck-Condon factor we would generate a "stick" spectrum (Figure 2.2.3) where each vibrational transition is infinitely narrow and transition can only occur when $E = h\nu$ exactly. For example, the potential energy surfaces were given for $S = 1$ and the transition probability at each level is given by the sticks (black) in Figure 2.2.3.

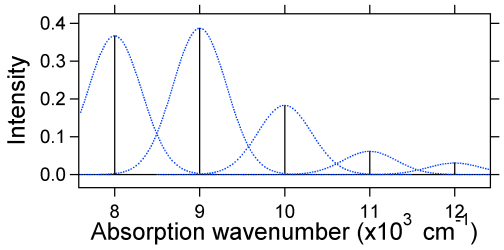

Figure 2.2.3: Stick spectrum, dressed with Gaussians, for the moderate displacement (S=1) harmonic oscillator system from Figure 2.2.2. (Stefan Franzen)

The dotted Gaussians that surround each stick give a more realistic picture of what the absorption spectrum should look like. In this first place each energy level (stick) will be given some width by the fact that the state has a finite lifetime. Such broadening is called homogeneous broadening since it affects all of the molecules in the ensemble in a similar fashion. There is also broadening due to small differences in the environment of each molecule. This type of broadening is called inhomogeneous broadening. Regardless of origin the model above was created using a Gaussian broadening

The nuclear displacement between the ground and excited state determines the shape of the absorption spectrum. Let us examine both a smaller and a large excited state displacement. If $S = ½$ and the potential energy surfaces in this case are:

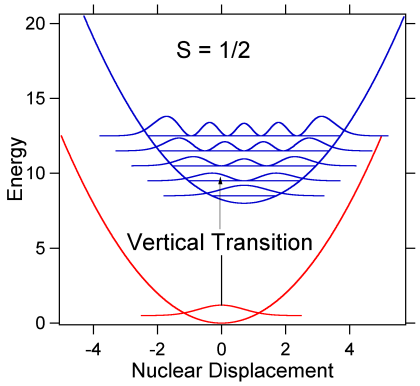

Figure 2.2.4: Wavefunctions transitions for a harmonic oscillator model system with small displacement (S=1/2). (Stefan Franzen)

For this case the "stick" spectrum has the appearance in Figure 2.2.5

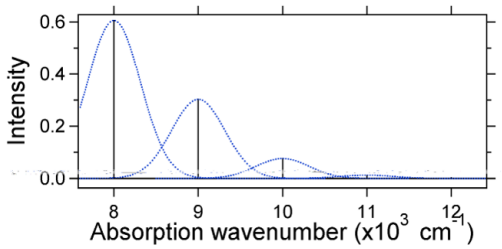

Figure 2.2.5: Stick spectrum, dressed with Gaussians, for the small displacement (S=1/2) harmonic oscillator system from Figure 2.2.4. (Stefan Franzen)

Note that the zero-zero or $S_{0,0}$ vibrational transition is much large in the case where the displacement is small.

> As a general rule of thumb the S constant gives the ratio of the intensity of the $v = 2$ transition to the $v = 1$ transition. In this case since $S = 0.5$, the $v = 2$ transition is 0.5 the intensity of $v = 1$ transition.

As an example of a larger displacement the disposition of the potential energy surfaces for S = 2 is shown below.

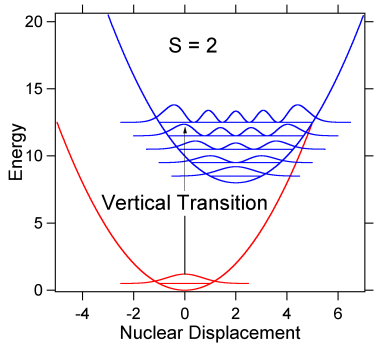

Figure 2.2.6: Wavefunctions transitions for a harmonic oscillator model system with strong displacement (S=2). (Stefan Franzen)

The larger displacement results in decreased overlap of the ground state level with the v = 0 level of the excited state. The maximum intensity will be achieved in higher vibrational levels as shown in the stick spectrum.

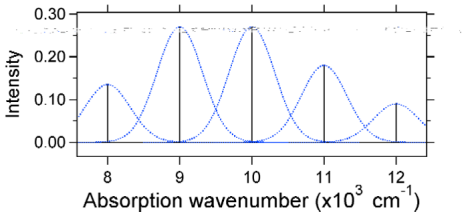

Figure 2.2.7: Stick spectrum, dressed with Gaussians, for the large displacement (S=2) harmonic oscillator system from Figure 2.2.6. (Stefan Franzen)

The absorption spectra plotted below all have the same integrated intensity, however their shapes are altered because of the differing extent of displacement of the excited state potential energy surface.

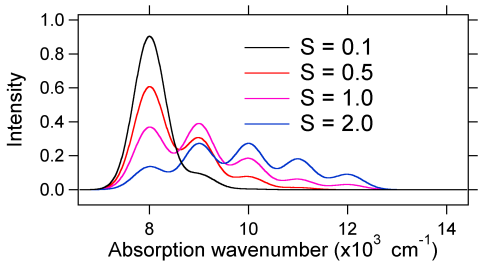

Figure 2.2.8: Stick spectra, dressed with Gaussians, for the small to large displacements in harmonic oscillator system described above. (Stefan Franzen)

So the nature of the relative vibronic band intensities can tell us whether there is a displacement of the equilibrium nuclear coordinate that accompanied a transition. When will there be an increase in bond length (i.e., $Q_e > R_e$)? This occurs when an electron is promoted from a bonding molecular orbital to a non-bonding or anti-bonding molecular orbitals (i.e., when the bond order is less in the excited state than the ground state).

- Non-bonding molecular orbital $\rightarrow$ bonding molecular orbital
- Anti-bonding molecular orbital $\rightarrow$ bonding molecular orbital
- Anti-bonding molecular orbital $\rightarrow$ non-bonding molecular orbital

In short, when the bond order is lower in the excited state than in the ground state, then $Q_e > R_e$; an increase in bond length will occur when this happens.

2.3: Broadening Mechanisms

Spectrum lines are not infinitesimally narrow; they have a finite width. A graph of radiance or intensity per unit wavelength (or frequency) versus wavelength (or frequency) is the *line profile*. There are several causes of line broadening, some internal to the atom, others external, and each produces its characteristic profile. Some types of profile, for example, have a broad core and small wings; others have a narrow core and extensive, broad wings. Analysis of the exact shape of a line profile may give us information about the physical conditions, such as temperature and pressure, in a stellar atmosphere.

An absorption lineshape can represent the dynamics of the dipole or be broadened by energy relaxation, for instance through coupling to a continuum. However, there are numerous processes that can influence the lineshape. These can be separated by dynamic processes intrinsic to the molecular system, which is termed **homogeneous broadening**, and static effects known as **inhomogeneous broadening**, which can be considered an ensemble averaging effect.

2.3.1: Homogeneous Broadening

Several dynamical mechanisms can potentially contribute to damping and line-broadening. These intrinsically molecular processes, often referred to as homogeneous broadening, are commonly assigned a time scale $T_2 = \Gamma^{-1}$.

2.3.1.1: Population Relaxation

Atoms and molecules emit (or absorb) light when their electrons jump from one energy state to another. In the case of the H-alpha line, the transition involves the n=3 and n=2 states of hydrogen.

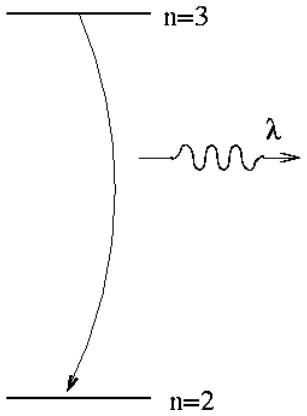

If we knew the energy difference *exactly*, then we would know the wavelength of the photon *exactly*. However, due to **Heisenberg's Uncertainty Principle,** we do NOT know the energies exactly. One way to look at is that atoms very quickly jump from an excited state to a lower state; that means that you don't have very long to measure the energy in the upper state. The limit on the time available to measure the excited state's energy places a limit on the precision of the energy measurement:

$$\Delta E \Delta t \simeq \hbar$$

The lifetime of hydrogen atoms in their excited states is very short. For example, the lifetime of hydrogen in the $n = 2$ and $n = 3$ states is about 10^{-8} seconds.

Population relaxation refers to decay in the coherence created by the light field as a result of the finite lifetime of the coupled states, and is often assigned a time scale T_1. This can have contributions from radiative decay, such as spontaneous emission, or non-radiative processes such as relaxation as a result of coupling to a continuum.

$$\frac{1}{T_1} = \frac{1}{\tau_{rad}} + \frac{1}{\tau_{NR}} \tag{2.3.1}$$

The observed population relaxation time depends on both the relaxation times of the upper and lower states (m and n) being coupled by the field:

$$1/T_1 = w_{mn} + w_{nm}.$$

When the energy splitting is high compared to k_BT, only the downward rate contributes, which is why the rate is often written $1/2T_1$.

2.3.1.2: Pure Dephasing (Collisional Broadening)

Pure dephasing is characterized by a time constant T_2^* that characterizes the randomization of phase within an ensemble as a result of molecular interactions. This is a dynamic effect in which memory of the phase of oscillation of a molecule is lost as a result of intermolecular interactions that randomize the phase. Examples include collisions in a dense gas, or fluctuations induced by a solvent. This process does not change the population of the states involved.

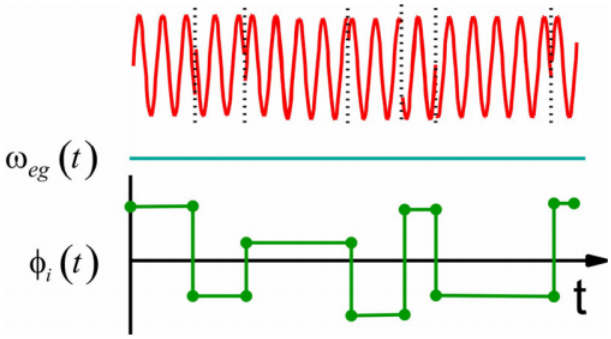

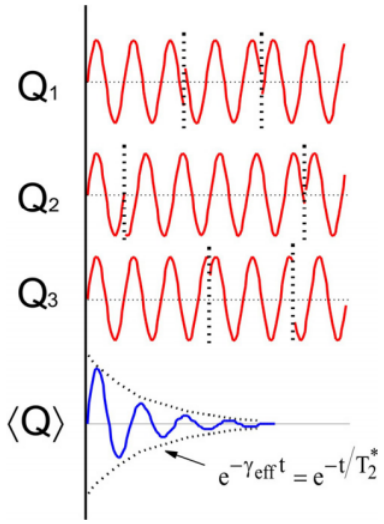

2.3.1.3: Orientational Relaxation

Orientational relaxation (τ_{or}) also leads to relaxation of the dipole correlation function and to line-broadening. Since the correlation function depends on the projection of the dipole onto a fixed axis in the laboratory frame, randomization of the initial dipole orientations is an ensemble averaged dephasing effect. In solution, this process is commonly treated as an orientational diffusion problem in which τ_{or} is proportional to the diffusion constant.

If these homogeneous processes are independent, the rates for different processes contribute additively to the damping and line width:

$$\frac{1}{T_2} = \frac{1}{T_1} + \frac{1}{T_2^*} + \frac{1}{\tau_{or}} \tag{2.3.2}$$

2.3.2: Inhomogeneous Broadening

Absorption lineshapes can also be broadened by a static distribution of frequencies.

2.3.2.1: Doppler broadening

When thermal motion causes a particle to move towards the observer, the emitted radiation will be shifted to a higher frequency. Likewise, when the emitter moves away, the frequency will be lowered. For non-relativistic thermal velocities, the Doppler shift in frequency will be:

$$\nu = \nu_0 \left(1 + \frac{v}{c}\right), \tag{2.3.3}$$

where ν is the observed frequency, ν_0 is the rest frequency, v is the velocity of the emitter towards the observer, and c is the speed of light.

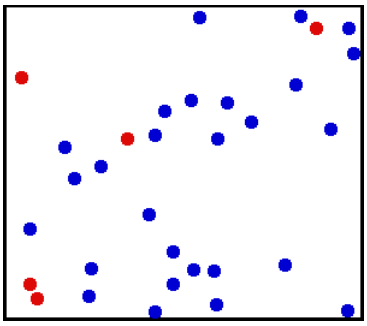

Figure 2.3.1: CMotion of gas molecules. The randomized thermal vibrations of fundamental particles such as atoms and molecules —gives a substance its “kinetic temperature.” . (Public Domain; Greg L via Wikipedia)

Since there is a distribution of speeds both toward and away from the observer in any volume element of the radiating body, the net effect will be to broaden the observed line. Propagating the Maxwell-Boltzmann Distribution law for velocities of a gas with the Doppler shifting (Equation 2.3.3) results in a line broadening (of a Gaussian distribution).

$$\Delta v_{\mathrm{FWHM}} = \sqrt{\frac{8kT\ln 2}{mc^2}}v_0$$

where FWHM is the full width at half maximum of the line.

2.3.2.2: Static Broadening

If molecules within the ensemble are influenced static environmental variations more than other processes, then the observed lineshape reports on the distribution of environments. This inhomogeneous broadening is a static ensemble averaging effect, which hides the dynamical content in the homogeneous linewidth. The origin of the inhomogeneous broadening can be molecular (for instance a distribution of defects in crystals) or macroscopic (i.e., an inhomogeneous magnetic field in NMR).

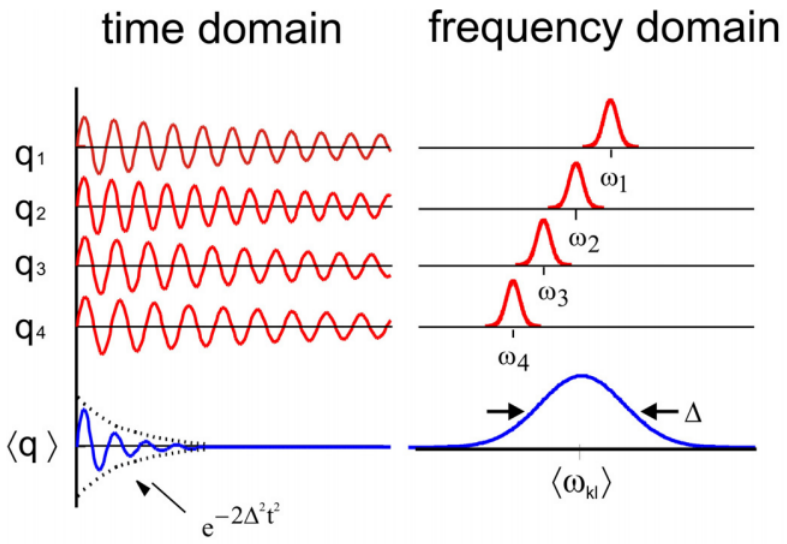

The inhomogeneous linewidth is dictated the width of the distribution Δ.

2.3.3: Total Linewidth

The total observed broadening of the absorption lineshape reflects the contribution of all of these effects. All of these effects can be present simultaneously in an absorption spectrum.

2.4: The Fate of Electronic Transitions

Aleksander Jablonski was a Polish academic who devoted his life to the study of molecular absorbance and emission of light. He developed a written representation that generally shows a portion of the possible consequences of applying photons from the visible spectrum of light to a particular molecule. These schematics are referred to as Jablonski diagrams.

A refresher on Electronic States

Excited states may be classified as **singlet** or **triplet** based upon their electron spin angular momentum. The electrons in most non-metallic organic compounds are paired (opposite spins) in bonding and non-bonding orbitals, resulting in a net zero spin diamagnetic molecule for the ground state. Such states have a single energy state in an applied magnetic field, and are called singlets. Electronic states in which two electrons with identical spin occupy different orbitals (the Pauli exclusion principle) have a net spin of 1 (2 • 1/2) and are paramagnetic. In a magnetic field such states have three energy levels (+1, 0, -1) and are called triplets. Molecular oxygen is a rare example of a triplet ground electronic state.

Introduction

A Jablonski diagram is basically an energy diagram, arranged with energy on a vertical axis. The energy levels can be quantitatively denoted, but most of these diagrams use energy levels schematically. The rest of the diagram is arranged into columns. Every column usually represents a specific spin multiplicity for a particular species. However, some diagrams divide energy levels within the same spin multiplicity into different columns. Within each column, horizontal lines represent eigenstates for that particular molecule. Bold horizontal lines are representations of the limits of electronic energy states. Within each electronic energy state are multiple vibronic energy states that may be coupled with the electronic state. Usually only a portion of these vibrational eigenstates are represented due to the massive number of possible vibrations in a molecule. Each of these vibrational energy states can be subdivided even further into rotational energy levels; however, typical Jablonski diagrams omit such intense levels of detail. As electronic energy states increase, the difference in energy becomes continually less, eventually becoming a continuum that can be approach with classical mechanics. Additionally, as the electronic energy levels get closer together, the overlap of vibronic energy levels increases.

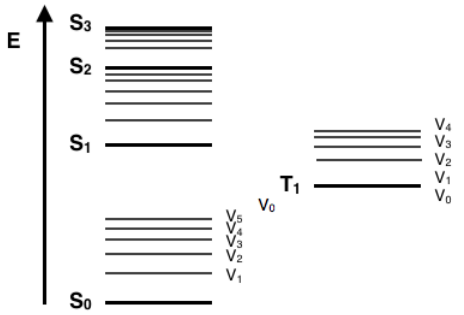

Figure 2.4.1: The Foundation of a typical Jablonski Diagram

Through the use of straight and curved lines, these figures show transitions between eigenstates that occur from the exposure of a molecule to a particular wavelength of light. Straight lines show the conversion between a photon of light and the energy of an electron. Curved lines show transitions of electrons without any interaction with light. Within a Jablonski diagram several different pathways show how an electron may accept and then dissipate the energy from a photon of a particular wavelength. Thus, most diagrams start with arrows going from the ground electronic state and finish with arrows going to the ground electronic state.

Absorbance

The first transition in most Jablonski diagrams is the absorbance of a photon of a particular energy by the molecule of interest. This is indicated by a straight arrow pointing up. Absorbance is the method by which an electron is excited from a lower energy level to a higher energy level. The energy of the photon is transferred to the particular electron. That electron then transitions to a different eigenstate corresponding to the amount of energy transferred. Only certain wavelengths of light are possible for absorbance, that is, wavelengths that have energies that correspond to the energy difference between two different eigenstates of the particular molecule. Absorbance is a very fast transition, on the order of 10^{-15} seconds. Most Jablonski diagrams, however, do not indicate a time scale for the phenomenon being indicated. This transition will usually occur from the lowest (ground) electronic state due to

the statistical mechanical issue of most electrons occupying a low lying state at reasonable temperatures. There is a Boltzmann distribution of electrons within this low lying levels, based on the the energy available to the molecules. This energy available is a function of the Boltzmann's constant and the temperature of the system. These low lying electrons will transition to an excited electronic state as well as some excited vibrational state.

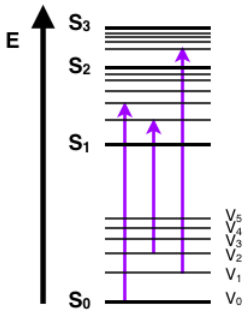

Figure 2.4.2: Three possible absorption transitions represented.

Vibrational Relaxation and Internal Conversion

Once an electron is excited, there are a multitude of ways that energy may be dissipated. The first is through vibrational relaxation, a non-radiative process. This is indicated on the Jablonski diagram as a curved arrow between vibrational levels. Vibrational relaxation is where the energy deposited by the photon into the electron is given away to other vibrational modes as kinetic energy. This kinetic energy may stay within the same molecule, or it may be transferred to other molecules around the excited molecule, largely depending on the phase of the probed sample. This process is also very fast, between 10^{-14} and 10^{-11} seconds. Since this is a very fast transition, it is extremely likely to occur immediately following absorbance. This relaxation occurs between vibrational levels, so generally electrons will not change from one electronic level to another through this method.

However, if vibrational energy levels strongly overlap electronic energy levels, a possibility exists that the excited electron can transition from a vibration level in one electronic state to another vibration level in a lower electronic state. This process is called internal conversion and mechanistically is identical to vibrational relaxation. It is also indicated as a curved line on a Jablonski diagram, between two vibrational levels in different electronic states. Internal Conversion occurs because of the overlap of vibrational and electronic energy states. As energies increase, the manifold of vibrational and electronic eigenstates becomes ever closer distributed. At energy levels greater than the first excited state, the manifold of vibrational energy levels strongly overlap with the electronic levels. This overlap gives a higher degree of probability that the electron can transition between vibrational levels that will lower the electronic state. Internal conversion occurs in the same time frame as vibrational relaxation, therefore, is a very likely way for molecules to dissipate energy from light perturbation. However, due to a lack of vibrational and electronic energy state overlap and a large energy difference between the ground state and first excited state, internal conversion is very slow for an electron to return to the ground state. This slow return to the ground state lets other transitive processes compete with internal conversion at the first electronically excited state. Both vibrational relaxation and internal conversion occur in most perturbations, yet are seldom the final transition.

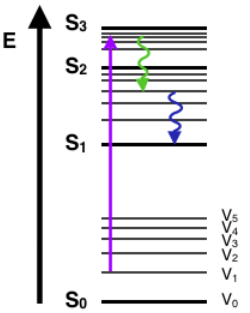

Figure 2.4.3: Possible scenario with absorption, internal conversion, and vibrational relaxation *processes shown.*

Fluorescence

Another pathway for molecules to deal with energy received from photons is to emit a photon. This is termed fluorescence. It is indicated on a Jablonski diagram as a straight line going down on the energy axis between electronic states. Fluorescence is a slow process on the order of 10^{-9} to 10^{-7} seconds; therefore, it is not a very likely path for an electron to dissipate energy especially at electronic energy states higher than the first excited state. While this transition is slow, it is an allowed transition with the electron staying in the same multiplicity manifold. Fluorescence is most often observed between the first excited electron state and the ground state for any particular molecule because at higher energies it is more likely that energy will be dissipated through internal conversion and vibrational relaxation. At the first excited state, fluorescence can compete in regard to timescales with other non-radiative processes. The energy of the photon emitted in fluorescence is the same energy as the difference between the eigenstates of the transition; however, the energy of fluorescent photons is always less than that of the exciting photons. This difference is because energy is lost in internal conversion and vibrational relaxation, where it is transferred away from the electron. Due to the large number of vibrational levels that can be coupled into the transition between electronic states, measured emission is usually distributed over a range of wavelengths.

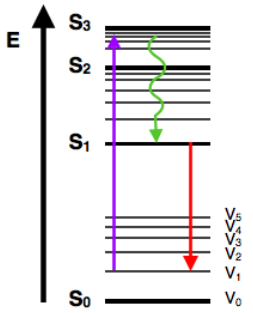

Figure 2.4.4: Possible scenario with absorption, internal conversion and vibrational relaxation, and fluorescence processes shown.

Intersystem Crossing

Yet another path a molecule may take in the dissipation of energy is called intersystem crossing. This where the electron changes spin multiplicity from an excited singlet state to an excited triplet state. It is indicated by a horizontal, curved arrow from one column to another. This is the slowest process in the Jablonski diagram, several orders of magnitude slower than fluorescence. This slow transition is a forbidden transition, that is, a transition that based strictly on electronic selection rules should not happen. However, by coupling vibrational factors into the selection rules, the transition become weakly allowed and able to compete with the time scale of fluorescence. Intersystem crossing leads to several interesting routes back to the ground electronic state. One direct transition is phosphorescence, where a radiative transition from an excited triplet state to a singlet ground state occurs.This is also a very slow, forbidden transition. Another possibility is delayed fluorescence, the transition back to the first excited singlet level, leading to the emitting transition to the ground electronic state.

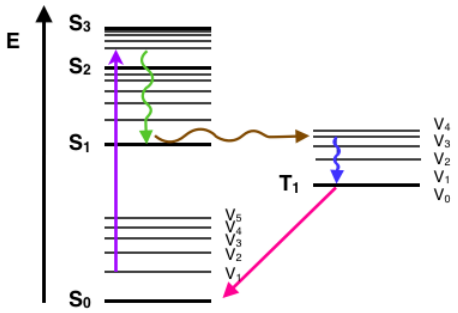

Figure 2.4.5: *Possible scenario with absorption, internal conversion, vibrational relaxation, intersystem crossing, and phosphorescence processes shown.*

Other non-emitting transitions from excited state to ground state exist and account for the majority of molecules not exhibiting fluorescence or phosphorescent behavior. One process is the energy transfer between molecules through molecular collisions (e.g., external conversion). Another path is through quenching, energy transfer between molecules through overlap in absorption and fluorescence spectra. These are non-emitting processes that will compete with fluorescence as the molecule relaxes back down to

the ground electronic state. In a Jablonski diagram, each of these processes are indicated with a curved line going down to on the energy scale.

All together

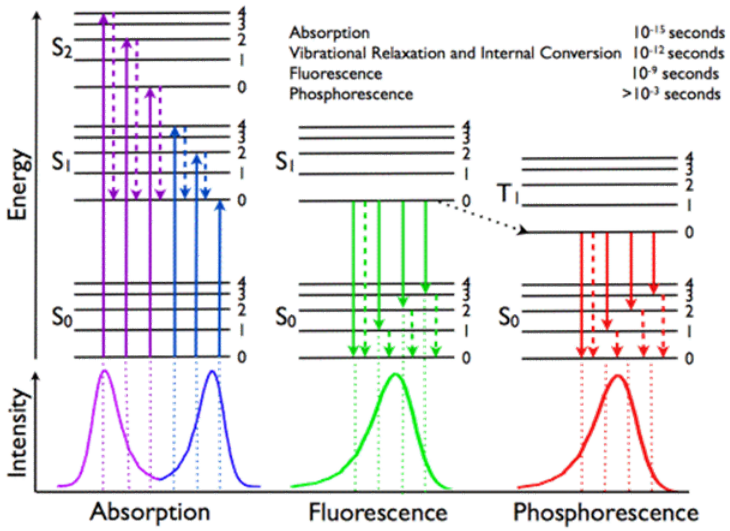

Jablonki Diagram (http://www2.chemistry.msu.edu/facult...l/photchem.htm**)**

Time Scales

It is important to note that a Jablonski diagram shows what sorts of transitions that can possibly happen in a particular molecule. Each of these possibilities is dependent on the time scales of each transition. The faster the transition, the more likely it is to happen as determined by selection rules. Therefore, understanding the time scales each process can happen is imperative to understanding if the process may happen. Below is a table of average time scales for basic radiative and non-radiative processes.

Table 1: Average timescales for radiative and non-radiative processes

Transition	Time Scale	Radiative Process?
Internal Conversion	10^{-14} - 10^{-11} s	no
Vibrational Relaxation	10^{-14} - 10^{-11} s	no
Absorption	10^{-15} s	yes
Phosphorescence	10^{-4} - 10^{-1} s	yes
Intersystem Crossing	10^{-8} - 10^{-3} s	no
Fluorescence	10^{-9} - 10^{-7} s	yes

Each process outlined above can be combined into a single Jablonski diagram for a particular molecule to give a overall picture of possible results of perturbation of a molecule by light energy. Jablonski diagrams are used to easily visualize the complex inner workings of how electrons change eigenstates in different conditions. Through this simple model, specific quantum mechanical phenomena are easily communicated.

References

1. H. H. Jaffe and Albert L. Miller "The fates of electronic excitation energy" *J. Chem. Educ.*, 1966, 43 (9), p 469 **DOI:**10.1021/ed043p469
2. E. B. Priestley and A. Haug "Phosphorescence Spectrum of Pure Crystalline Naphthalene" J. Chem. Phys. 49, 622 (1968), DOI:10.1063/1.1670118

2.5: Electronic State and Transitions

https://chem.libretexts.org/Bookshel..._Visible_Light

The symmetry requirement for observing the electronic transition is embodies in the electronic integral.

$$\int \psi_{el}^{i} H^{(1)} \psi_{el}^{f} d\Gamma$$

which **must not equal zero** to observe the transition. This can be determined by group theory by looking at the transformation properties of $H^{(1)}$ and the wavefunctions under the symmetry properties of the point group of the molecule.

This treatment is for a diatomic but can be generalized to a polyatomic that has more than 1 degree of vibrational freedom: $3N-6$ for non-linear and $3N-5$ for linear molecules where N is the number of atoms. $V(r)$ is replace by a multi-dimensional surface $V(q_1, q_2, q_3, q_4 \ldots q_{3N-6})$ where the q's are displacements from equilibrium (often expressed as normal modes) and represent the nuclear degrees of freedom for the molecule. The normal modes are coordinates that represent combinations of bonds stretches, compressions and bends; these will be discussed later in more detail.

Electronic Transition Types

The most likely electronic transition involves the absorption of a photon by a **single electron** (as taught in general chemistry classes). Thus, if we have a one-electron MO description of the molecular electronic configuration, we can describe an electronic transition by giving the MO of the original and the MO of the state that final electron winds up in after the transition.

Orbital types: (Kasha)

- n: lone pair orbitals
- σ: bonding pair orbitals of σ local symmetry
- σ*: anti-bonding σ orbitals
- π: pi bonding MO
- π*: pi anti-bonding MO

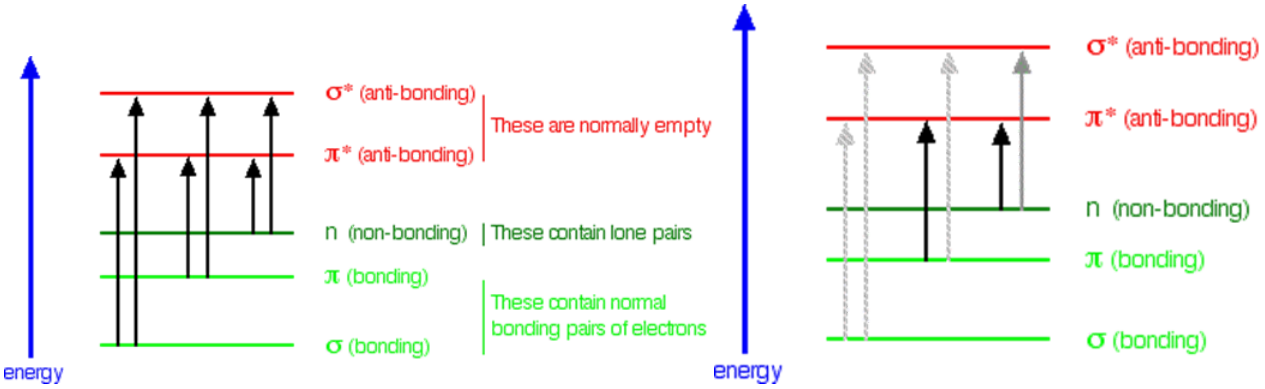

Look again at the possible jumps. This time, the important jumps are shown in black, and a less important one in grey. The grey dotted arrows show jumps which absorb light outside the region of the spectrum we are working in.

Delocalization

$CH_2=CH_2$	$CH_2=CH-CH=CH_2$	$CH_2=CH-CH=CH-CH=CH_2$
ethene	buta-1,3-diene	hexa-1,3,5-triene

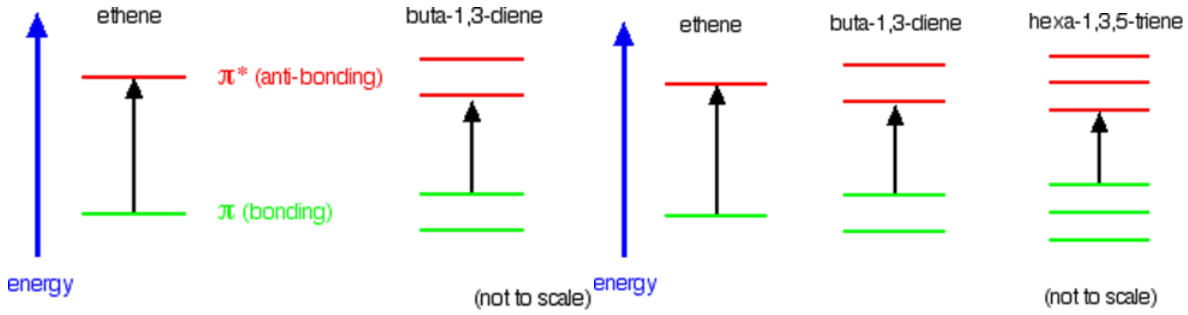

Beta-carotene has the sort of delocalization that we've just been looking at, but on a much greater scale with 11 carbon-carbon double bonds conjugated together. The diagram shows the structure of beta-carotene with the alternating double and single bonds shown in red.

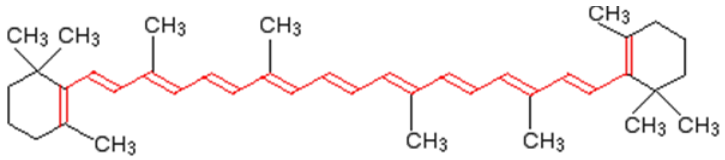

The more delocalization there is, the smaller the gap between the highest energy pi bonding orbital and the lowest energy pi anti-bonding orbital. To promote an electron therefore takes less energy in beta-carotene than in the cases we've looked at so far - because the gap between the levels is less.

2.6: Introduction to Symmetry

A *symmetry operation* is an action that leaves an object looking the same after it has been carried out. For example, if we take a molecule of water and rotate it by 180° about an axis passing through the central O atom (between the two H atoms) it will look the same as before. Each symmetry operation has a corresponding *symmetry element*, which is the axis, plane, line or point with respect to which the symmetry operation is carried out. The symmetry element consists of all the points that stay in the same place when the symmetry operation is performed. In a rotation, the line of points that stay in the same place constitute a *symmetry axis*; in a reflection the points that remain unchanged make up a *plane of symmetry*. The symmetry elements that a molecule (and any other 3-D object) may possess are discussed below.

Symmetry Operations

A symmetry operation is a permutation of atoms such that the molecule is transformed into a state **indistinguishable** from the starting state.

E: The Identity Symmetry

The identity operation consists of doing nothing, and the corresponding symmetry element is the entire molecule. Every molecule has at least this element. For example, the $CHFClBr$ molecule in Figure 2.6.1 . The identify symmetry is not indicated since all molecule exhibit this symmetry.

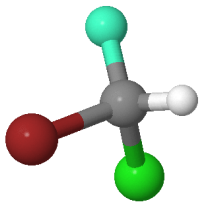

Figure 2.6.1 : Example of Identify Symmetry: The $CHFClBr$ molecule contain no other symmetry other than identity. Image created via Symmetry @ Otterbein site by Dean Johnston et al.

C_n: an n-fold Axis of Rotation

Rotation by $360^\circ/n$ leaves the molecule unchanged. The H_2O molecule has a C_2 axis (Figure 2.6.2). Some molecules have more than one C_n axis, in which case the one with the highest value of n is called the *principal axis*. Note that by convention rotations are *counterclockwise* about the axis. C_n rotations are indicated via vectors with labels as indicated below.

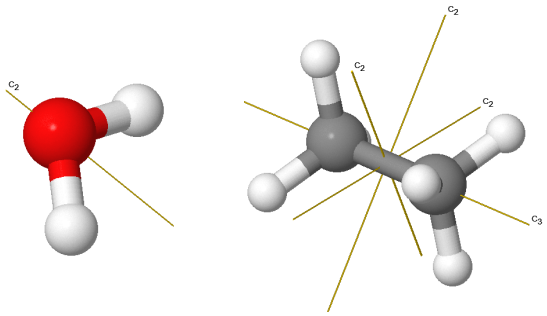

Figure 2.6.2 : Examples of n-fold Axis of Rotation: (left) The water molecule contains a C_2 axis. (right) Ethane contains both C_2 and C_3 axes. Image created via Symmetry @ Otterbein site by Dean Johnston et al.

σ: a Plane of Symmetry

Reflection in the plane leaves the molecule looking the same. In a molecule that also has an axis of symmetry, a mirror plane that includes the axis is called a vertical mirror plane and is labeled σ_v, while one perpendicular to the axis is called a horizontal mirror plane and is labeled σ_h. A vertical mirror plane that bisects the angle between two C_2 axes is called a dihedral mirror plane, σ_d. σ symmetry is indicated as a plane on molecules; since they often bisect atoms, which should be clearly indicated.

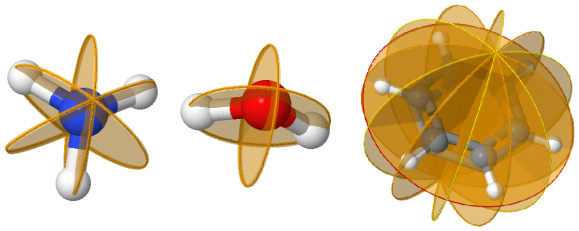

Figure 2.6.3 : Examples of reflection symmetry. (left) The ammonia molecule contains three identical reflection planes. All are designated as vertical symmetry planes (σ_v) because they contain the principle rotation axis.(middle) The water molecule contains two different reflection planes. (right) benzene contains a total of seven reflection planes, one horizontal plane (σ_h) and six vertical planes (σ_v and σ_d). Image created via Symmetry @ Otterbein site by Dean Johnston et al.

i: a Center of Inversion Symmetry

Inversion through the center of symmetry leaves the molecule unchanged. Inversion consists of passing each point through the center of inversion and out to the same distance on the other side of the molecule. Examples of molecules with centers of inversion is shown in Figure 2.6.4 . Centers of inversion are indicated via a point, which may or may not overlap with an atoms. The centers of inversion in the examples below do not overlap with atoms.

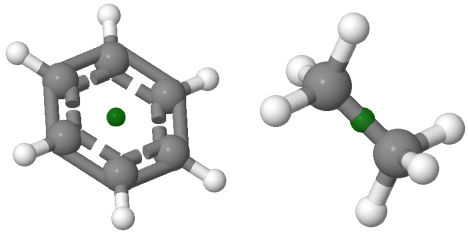

Figure 2.6.4 : Examples of Center of Inversion Symmetry. (left) Benzene and (right) staggard ethane have centers of inversion (green balls). Image created via Symmetry @ Otterbein site by Dean Johnston et al.

S_n: an n-fold axis of improper rotation Symmetry

Improper rotations are also called a rotary-reflection axis. The rotary reflection operation consists of rotating through an angle $360^\circ/n$ about the axis, followed by reflecting in a plane perpendicular to the axis. Improper rotation symmetry is indicated with both an axis and a plan as demonstrated in the examples in Figure 2.6.5 .

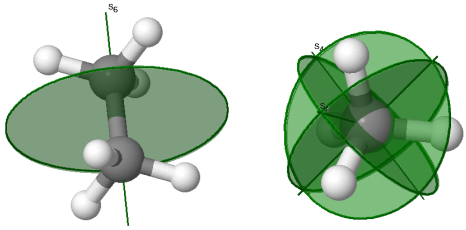

Figure 2.6.5 : Examples of Improper axis of rotation. (left) Staggered ethane contains an S_6 axis of improper rotation. (right) Methane contains three S_4 axes of improper rotation. Image created via Symmetry @ Otterbein site by Dean Johnston et al.

Note

S_1 is the same as reflection and S_2 is the same as inversion.

The identity E and rotations C_n are symmetry operations that could actually be carried out on a molecule. For this reason they are called *proper symmetry operations*. Reflections, inversions and improper rotations can only be imagined (it is not actually possible to turn a molecule into its mirror image or to invert it without some fairly drastic rearrangement of chemical bonds) and as such, are termed *improper symmetry operations*. These five symmetry elements are tabulated in Table 2.6.1 with their corresponding operators.

Table 2.6.1 : The five principal symmetry elements and their operators for 3D space

Symbol Elements	Description	Symbol Operator	Symbol
E	identity	$\hat{E}$	no change
C_n	n-fold axis of rotation	$\hat{C}_n$	Rotation by $360^\circ/n$leaves the molecule unchanged
σ	plane of symmetry	$\hat{\sigma}$	Reflection in the plane leaves the molecule unchanged
i	center of symmetry.	$\hat{i}$	Inversion through the center of symmetry leaves the molecule unchanged.
S_n	n-fold improper rotation	$\hat{S}_n$	The rotary reflection operation consists of rotating through an angle $360^\circ/n$about the axis, followed by reflecting in a plane perpendicular to the axis.

Axis Definitions

Conventionally, when imposing a set of Cartesian axes on a molecule (as we will need to do later on in the course), the z axis lies along the principal axis of the molecule, the x axis lies in the plane of the molecule (or in a plane containing the largest number of atoms if the molecule is non-planar), and the y axis makes up a right handed axis system.

Molecular Point Groups

It is only possible for certain combinations of symmetry elements to be present in a molecule (or any other object). As a result, we may group together molecules that possess the same symmetry elements and classify molecules according to their symmetry. These groups of symmetry elements are called **point groups** (due to the fact that there is at least one point in space that remains unchanged no matter which symmetry operation from the group is applied). There are two systems of notation for labeling symmetry groups, called the Schoenflies and Hermann-Mauguin (or International) systems. The symmetry of individual molecules is usually described using the **Schoenflies** notation, which is used below.

Table 2.6.2 : Common Point Groups for Molecules

Nonaxial groups	C_1	C_s	C_i	-	-	-	-	-	-
C_n groups	C_2	C_3	C_4	C_5	C_6	C_7	C_8	-	-
D_n groups	D_2	D_3	D_4	D_5	D_6	D_7	D_8	-	-
C_{nv} groups	C_{2v}	C_{3v}	C_{4v}	C_{5v}	C_{6v}	C_{7v}	C_{8v}	-	-
C_{nh} groups	C_{2h}	C_{3h}	C_{4h}	C_{5h}	C_{6h}	-	-	-	-
D_{nh} groups	D_{2h}	D_{3h}	D_{4h}	D_{5h}	D_{6h}	D_{7h}	D_{8h}	-	-
D_{nd} groups	D_{2d}	D_{3d}	D_{4d}	D_{5d}	D_{6d}	D_{7d}	D_{8d}	-	-
S_n groups	S_2	-	S_4	-	S_6		S_8	S_{10}	S_{12}
Cubic groups	T	T_h	T_d	O	O_h	I	I_h	-	-
Linear groups	$C_{\infty v}$	$D_{\infty h}$	-	-	-	-	-	-	-

Shared Names

Some of the point groups share their names with symmetry operations, so be careful you do not mix up the two. It is usually clear from the context which one is being referred to.

1. C_1 - contains only the identity (a C_1 rotation is a rotation by 360° and is the same as the identity operation) e.g. CHDFCl.

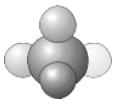

2. C_i - contains the identity E and a center of inversion i.

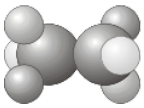

3. C_S - contains the identity E and a plane of reflection σ.

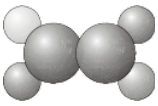

4. C_n - contains the identity and an n-fold axis of rotation.

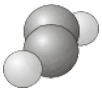

5. C_{nv} - contains the identity, an n-fold axis of rotation, and n vertical mirror planes σ_v.

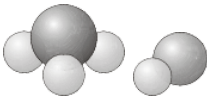

6. C_{nh} - contains the identity, an n-fold axis of rotation, and a horizontal reflection plane σ_h (note that in C_{2h} this combination of symmetry elements automatically implies a center of inversion).

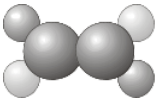

7. D_n - contains the identity, an n-fold axis of rotation, and n 2-fold rotations about axes perpendicular to the principal axis.

8. D_{nh} - contains the same symmetry elements as D_n with the addition of a horizontal mirror plane.

9. D_{nd} - contains the same symmetry elements as D_n with the addition of n dihedral mirror planes.

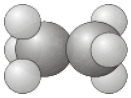

10. S_n - contains the identity and *one* S_n axis. Note that molecules only belong to S_n if they have not already been classified in terms of one of the preceding point groups (e.g. S_2 is the same as C_i, and a molecule with this symmetry would already have been classified).

The following groups are the cubic groups, which contain more than one principal axis. They separate into the tetrahedral groups (T_d, T_h and T) and the octahedral groups (O and O_h). The icosahedral group also exists, but is not included below.

11. T_d - contains all the symmetry elements of a regular tetrahedron, including the identity, 4 C_3 axes, 3 C_2 axes, 6 dihedral mirror planes, and 3 S_4 axes e.g. CH_4.

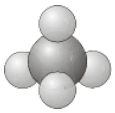

12. T - as for T_d but no planes of reflection.
13. T_h - as for T but contains a center of inversion.
14. O_h - the group of the regular octahedron e.g. SF_6.

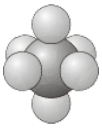

15. O - as for O_h, but with no planes of reflection.

The final group is the full rotation group R_3, which consists of an infinite number of C_n axes with all possible values of n and describes the symmetry of a sphere. Atoms (but no molecules) belong to R_3, and the group has important applications in atomic quantum mechanics. However, we won't be treating it any further here.

Once you become more familiar with the symmetry elements and point groups described above, you will find it quite straightforward to classify a molecule in terms of its point group. In the meantime, the flowchart shown below provides a step-by-step approach to the problem.

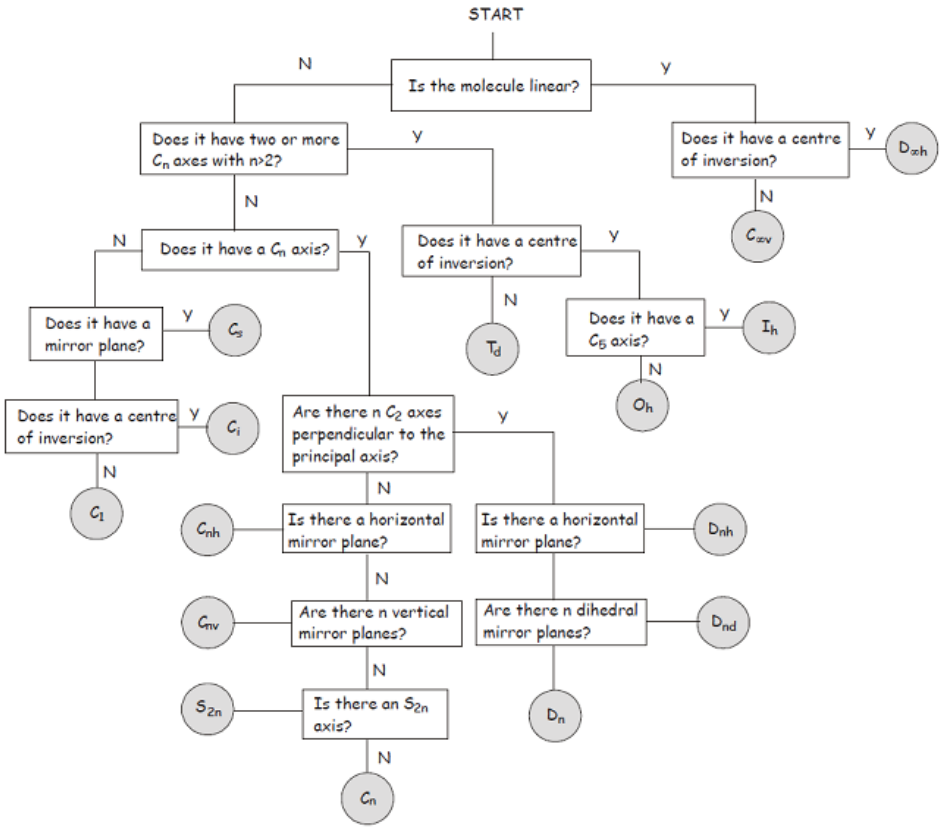

[1]Though the Hermann-Mauguin system can be used to label point groups, it is usually used in the discussion of crystal symmetry. In crystals, in addition to the symmetry elements described above, translational symmetry elements are very important. Translational symmetry operations leave no point unchanged, with the consequence that crystal symmetry is described in terms of *space groups* rather than *point groups*.

Symmetry and physical properties

Carrying out a symmetry operation on a molecule must not change any of its physical properties. It turns out that this has some interesting consequences, allowing us to predict whether or not a molecule may be chiral or polar on the basis of its point group.

For a molecule to have a permanent dipole moment, it must have an asymmetric charge distribution. The point group of the molecule not only determines whether the molecule may have a dipole moment, but also in which direction(s) it may point. If a molecule has a C_n axis with $n > 1$, it **cannot** have a dipole moment perpendicular to the axis of rotation (for example, a C_2 rotation would interchange the ends of such a dipole moment and reverse the polarity, which is not allowed – rotations with higher values of n would also change the direction in which the dipole points). Any dipole must lie parallel to a C_n axis.

Also, if the point group of the molecule contains any symmetry operation that would interchange the two ends of the molecule, such as a σ_h mirror plane or a C_2 rotation perpendicular to the principal axis, then there cannot be a dipole moment along the axis. The only groups compatible with a dipole moment are C_n, C_{nv} and C_s. In molecules belonging to C_n or C_{nv} the dipole must lie along the axis of rotation.

One example of symmetry in chemistry that you will already have come across is found in the isomeric pairs of molecules called enantiomers. Enantiomers are non-superimposable mirror images of each other, and one consequence of this symmetrical relationship is that they rotate the plane of polarized light passing through them in opposite directions. Such molecules are said to be chiral,[2] meaning that they cannot be superimposed on their mirror image. Formally, the symmetry element that precludes a molecule from being chiral is a rotation-reflection axis S_n. Such an axis is often implied by other symmetry elements present in a group.

For example, a point group that has C_n and σ_h as elements will also have S_n. Similarly, a center of inversion is equivalent to S_2. As a rule of thumb, a molecule definitely cannot have be chiral if it has a center of inversion or a mirror plane of any type (σ_h, σ_v or σ_d), but if these symmetry elements are absent the molecule should be checked carefully for an S_n axis before it is assumed to be chiral.

Chirality

The word chiral has its origins in the Greek word for hand ($\chi\epsilon\rho\iota$, pronounced ‘cheri’ with a soft ch as in ‘loch’). A pair of hands is also a pair of non-superimposable mirror images, and you will often hear chirality referred to as ‘handedness’ for this reason.

Summary

All molecules can be described in terms of their symmetry or lack thereof, which may contain symmetry elements (point, line, plane). Reflection, rotation, and inversion are symmetry operations (movement of the molecules such that after the movement, all the atoms of the molecules is coincidental with equivalent atom of the molecule in original).

Contributors and Attributions

- Claire Vallance (University of Oxford)

2.7: The Carbonyl Group

http://mutuslab.cs.uwindsor.ca/Wang/...1/341_l09c.pdf

Let's look at the electron transitions of H_2CO, formaldyhyde, for a typical description of the MO of an organic molecule.

Pretty valence-bond theory

(first year description of formaldehyde): https://www.chemtube3d.com/orbitalsformaldehyde

View 1: Before (but after hybridization)

Carbon and the oxygen are both sp^2 hybridized.

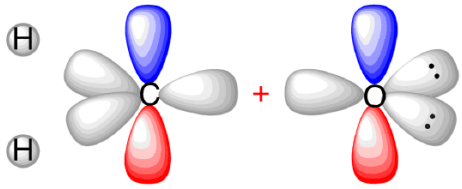

(CC BY-SA-NC; Nick Graves via ChemTube3D)

View 2: Moved together to demonstrate overlap

When moved together, there is overlap of the π and sp^2 orbitals.

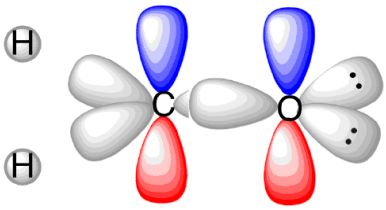

(CC BY-SA-NC; Nick Graves via ChemTube3D)

View 3: Generation of new bonds to make the carbonyl bond)

Formation of bonding interactions to form the sigma bond (from the sp^2 orbitals on C and O AND an π bond from the two non-hybridized p orbitals on C and O.

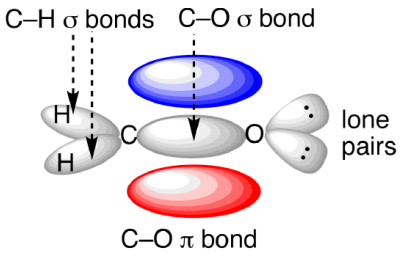

(CC BY-SA-NC; Nick Graves via ChemTube3D)

H^2CO is a planar molecule with C_{2v} symmetry. We ignore the n(1s) core electrons on C and O as well as the σ electrons in the C-H bonds. Very low energy excitations will not be involved in the UV-VIS region. The ground state valence electronic configuration of

interest is:

$$n_a^2\sigma^2\pi^2n_b^2(\pi^*)^0(\sigma^*)^0$$

This is the lowest energy MO's that originate from the **valence atomic orbitals** of the C and O.

What do they look like? http://pubs.acs.org/doi/pdf/10.1021/ed050p400

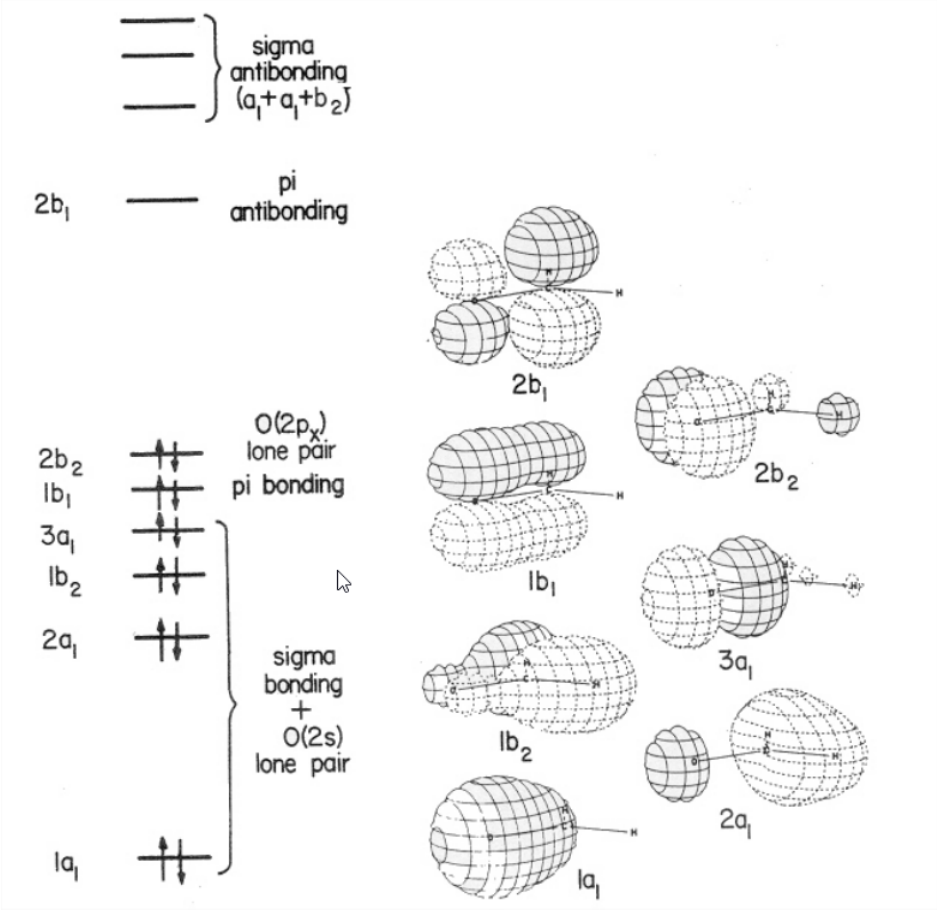

Figure XX: http://pubs.acs.org/doi/pdf/10.1021/ed050p400. All Rights Reserved ACS

The MO energies are

$$n_a < \sigma < \pi < n_b < \pi^* < \sigma^*$$

from a simple MO calculation. $n < \sigma$ because $2s \ll 2p$. Let's ignore the lowest non-bodning state and focus on the "frontier orbitals" - the higher lying MOs.

Possible Electronic Transitions

There are six outer valence e- are involved in major electronic transitions. The lowest energy transition is a $n \rightarrow \pi^*$ transition, while $\pi \rightarrow \pi^*$ and $n_a \rightarrow \sigma^*$ occur at higher ΔE and shorter λ.

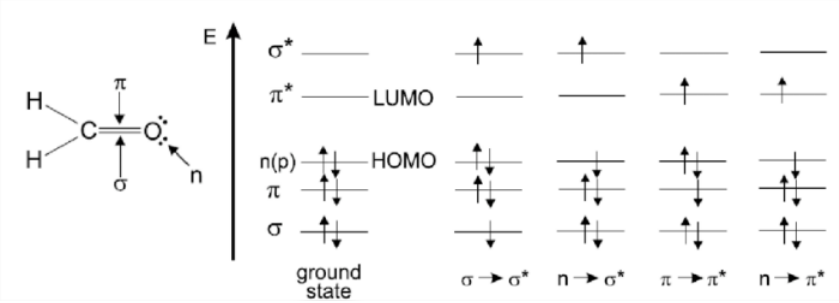

Energy levels of molecular orbitals in formaldehyde.

Molecular orbitals of formaldehyde emphasizing the transitions (after Guillet [19]).

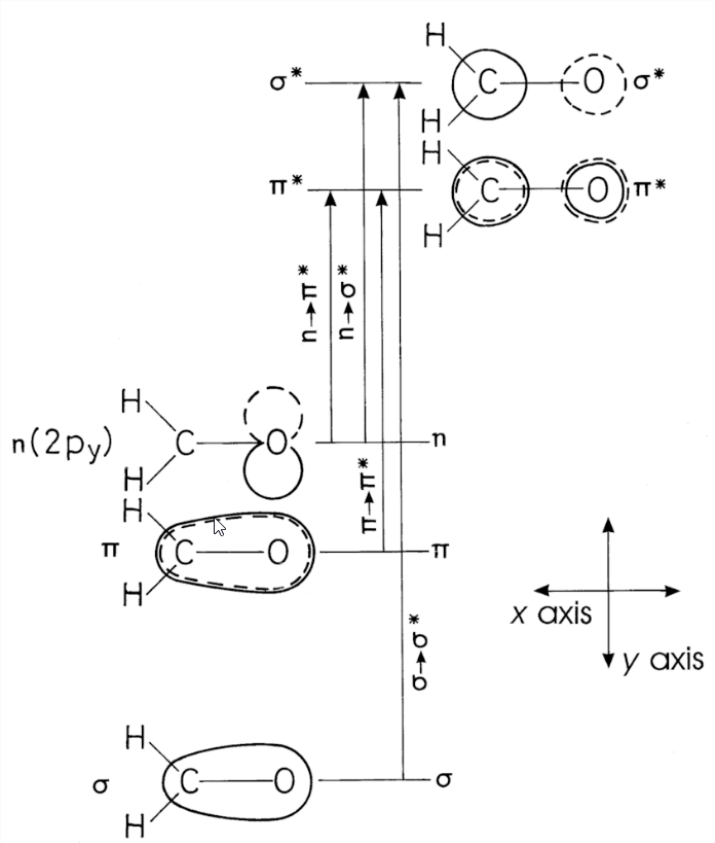

Triplet States

In addition to change in the orbital type, the excited electron may keep the same m_s, spin quantum number producing a singlet excited state. If m_s changes during the transition, the excited state had two ↑↑ electrons and is a **triplet state**. For instance, the $n \rightarrow \pi^*$ transition can lead to a $^1(n_1\pi^*)$ if the m_s does **not change**, but to $^3(n_1\pi^*)$ if it **does change (flip)**. Both the singlet and triplet states have the same configuration, but lies lower in energy because ↑↑ electrons are on average further apart than ↓↑ electrons (reducing e-e correlation).

This MO description is oversimplified. e-e interactions are different in an excited state than in the ground state. So A single configuration description is not very good; however this descriptions can be improved by allowing configurations to exit together to minimize the energy of the excited state (e.g. CI-doubles, CI-triples). We will discuss this later.

2.8: Symmetry and Formaldehyde

These five symmetry elements are tabulated in Table 2.8.1 with their corresponding operators.

Table 2.8.1 : The five principal symmetry elements and their operators for 3D space

Symbol Elements	Description	Symbol Operator	Symbol
E	identity	$\hat{E}$	no change
C_n	n-fold axis of rotation	$\hat{C}_n$	Rotation by $360^\circ/n$leaves the molecule unchanged
σ	plane of symmetry	$\hat{\sigma}$	Reflection in the plane leaves the molecule unchanged
i	center of symmetry.	$\hat{i}$	Inversion through the center of symmetry leaves the molecule unchanged.
S_n	n-fold improper rotation	$\hat{S}_n$	The rotary reflection operation consists of rotating through an angle $360^\circ/n$about the axis, followed by reflecting in a plane perpendicular to the axis.

Every molecule has a point group associated with it, which are assigned by a set for rules (explained by Group theory). The character tables takes the point group and represents all of the symmetry that the molecule has.

Symmetry Operations

A symmetry operation is a permutation of atoms such that the molecule is transformed into a state **indistinguishable** from the starting state.

Character Tables

A character table is a two dimensional chart associated with a point group that contains the irreducible representations of each point group along with their corresponding matrix characters. It also contains the Mulliken symbols used to describe the dimensions of the irreducible representations, and the functions for symmetry symbols for the Cartesian coordinates as well as rotations about the Cartesian coordinates.

A character table can be separated into 6 different parts, namely:

1. The Point Group
2. The Symmetry Operation
3. The Mulliken Symbols
4. The Characters for the Irreducible Representations
5. The Functions for Symmetry Symbols for Cartesian Coordinates and Rotations
6. The Function for Symmetry Symbols for Square and Binary Products

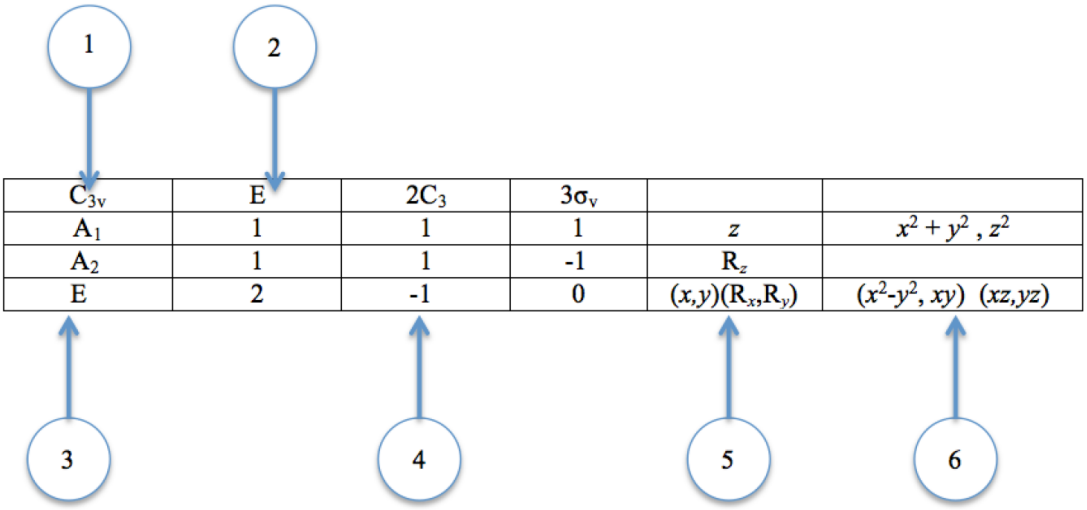

Figure 2.8.1: An example of a character table with different parts labelled

In many applications of group theory, we only need to know the characters of the representative matrices. Luckily, when each basis function transforms as a 1D **irreducible representation** (which is true in many cases of interest) there is a simple shortcut to determining the characters. All we have to do is to look at the way the individual basis functions transform under each symmetry operation.

Characters

For a given operation, step through the basis functions as follows:

i. Add 1 to the character if the basis function is unchanged by the symmetry operation (i.e. the basis function is mapped onto itself);
ii. Add -1 to the character if the basis function changes sign under the symmetry operation (i.e the basis function is mapped onto minus itself);
iii. Add 0 to the character if the basis function moves when the symmetry operation is applied (i.e the basis function is mapped onto something different from itself).

Formaldehyde

The MO's form a basis for irreducible representation of the C_{2v} **point-group** of H_2CO. Conventionally, the z-axis is along the C=O bond and the x-axis is ⊥ to place of the molecule. The symmetry operations for C_{2v} are E, C_2, $\sigma_v(xy)$ and $\sigma_{v'}(yx)$. For :

π and π^*

$$\hat{E}\pi = (+1)\pi$$

$$\hat{C}_2\pi = (-1)\pi$$

$$\hat{\sigma}_v\pi = (+1)\pi$$

$$\hat{\sigma}_{v'}\pi = (-1)\pi$$

So π and π^* transform as the B_1 irreducible representation

σ and σ^*

$$\hat{E}\sigma = (+1)\sigma$$

$$\hat{C}_2\sigma = (+1)\sigma$$

$$\hat{\sigma}_v\sigma = (+1)\sigma$$

$$\hat{\sigma}_{v'}\sigma = (+1)\sigma$$

So σ and σ^* transform as the A_1 irreducible representation

n_a

n_a also transform as B_1 it is a core electron in this orbital

n_b

$$\hat{E}n_b = (+1)n_b$$

$$\hat{C}_2 n_b = (-1)n_b$$

$$\hat{\sigma}_v n_b = (-1)n_b$$

$$\hat{\sigma}_{v'} n_b = (+1)n_b$$

So n_b transforms as the B_2 irreducible representation

Having ascertained the symmetry species of the MO's: $A_1(\sigma, \sigma^*, n_a)$; $B_1(\pi, \pi^*)$; $B_2(n)b)$, we can ask about the symmetry of the state produced by a configuration.

Direct Products of Representations

Here are listed some helpful general rules for the product of two irreducible representations. For specific combinations not listed here, one can work out the product by multiplying the characters of each irreducible representation and solving the linear combination of the irreducible representations from the point group that generates that product. Often this process is simple, especially when one or both of the irreducible representations are non-degenerate (in most cases *A* or *B*).

2. For C_2, C_3, C_6, D_3, D_6,C_{2v},C_{3v}, C_{6v},C_{2h}, C_{3h}, C_{6h}, D_{3h}, D_{6h}, D_{3d}, S_6

	A_1	A_2	B_1	B_2	E_1	E_2
A_1	A_1	A_2	B_1	B_2	E_1	E_2
A_2		A_1	B_2	B_1	E_1	E_2
B_1			A_1	A_2	E_2	E_1
B_2				A_1	E_2	E_1
E_1					$A_1 + [A_2] + E_2$	$B_1 + B_2 + E_1$
E_2						$A_1 + [A_2] + E_2$

Representation of an Electronic State

The representation of a specific quantum electronic state can be evaluated by the **direct product** of the representations of the molecular orbitals of the occupied electrons. Direct products can be extracted from the tables above. For example, the non-degenerate representations below

$$A \times A = A$$

$$B \times B = A$$

$$A \times B = B$$

Remember that the ground state valence electronic configuration of formaldehyde is:

$$n_a^2 \sigma^2 \pi^2 n_b^2 (\pi^*)^0 (\sigma^*)^0$$

so the representation of the ground-state is

$$\Gamma = (B_1 \times B_1)(A_1 \times A_1)(B_1 \times B_1)(B_2 \times B_2) \tag{2.8.1}$$

This can be simplified using the direct product tables

$$\Gamma = (A_1)(A_1)(A_1)(A_1)$$

so the ground state has a representation of A_1. We can make a general "rule" from this. This is a **“closed shell”** configuration and corresponds to a state with all molecular orbitals *doubly* occupied or *empty* and must be a singlet state! Since there are no odd electrons in the orbitals in the ground state, the configuration has a ${}^1A_1$ symmetry (totally symmetry).

Rule: Simpler Calculation

The symmetry representation of an electronic state is the direct product of the symmetry representations of each of the odd electrons orbitals. Since doubly filled orbitals do not contribute since their products are always totally symmetry:

$$B_1 \times B_1 = A_1$$

$$A_2 \times A_2 = A_1$$

etc.

There are no odd electrons in the orbitals in the ground state. Possible excited state symmetry includes:

$$n_b \rightarrow \pi^* \text{ or } {}^1\left(n_b, \pi^*\right)$$

and pay attention to only the unpair electrons give the following representation

Notation

- We use lower case representations for designating 1e- orbitals.
- We use capital case representation for designated are electronic states

$$\Gamma = b_2 \times b_1 = A_2$$

The electronic state symmetry is thus ${}^1A_2$. Conventionally, the $n_b \rightarrow \pi^*$ transition, in terms of states, is described as

$${}^1A_2 \leftarrow {}^1A_1$$

or

$${}^1A_2\left(n, \pi^*\right) \leftarrow {}^1A_1$$

Higher energy state is conventionally places on the left hand side and the arrow points in the direction of the transition.

Example 2.8.1

The ${}^1\left(\pi, \pi^*\right)$ state has the symmetry of

$$\mathrm{b_1} \times \mathrm{b_1} = \mathrm{a_1}$$

thus this transition is designated

$${}^1A_1\left(\pi, \pi^*\right) \leftarrow {}^1A_1$$

and this transition moves electron density from the O to the C, this is because

$$\pi = a\left(2p_x^C\right) + b\left(2p_x^o\right)$$

$b > a$ since O is more electronegative

$$\pi^* = b'\left(2p_x^C\right) + a'\left(p_x^O\right)$$

$b' > a'$ since for orthogonality with π.

Now, the ${}^1A_2 \leftarrow {}^1A_1$ transition also moves electron density from the O to the C. (For a similar argument).

References

- https://chem.libretexts.org/Bookshel...aracter_Tables
- http://www1.udel.edu/pchem/C444/Lect.../Lecture31.pdf

2.9: Configuration Interaction

The best energies obtained at the Hartree-Fock level are still not accurate, because they use an average potential for the electron-electron interactions. **Configuration interaction** (CI) methods help to overcome this limitation. Because electrons interact and repel each other, their motion in atoms is correlated. When one electron is close to the nucleus, the other tends to be far away. When one is on one side, the other tends to be on the other side. This motion is related to that of two people playing tag around a house. The exact wavefunction must depend upon the coordinates of both electrons simultaneously. We have shown that it is a reasonable approximation in calculating energies to neglect this correlation and use wavefunctions that only depend upon the coordinates of one electron, which assumes the electrons move independently.

This "orbital approximation" is similar to playing tag without keeping track of the other person. This independent-electron approximation gives reasonable, even good values, for the energy, and correlation can be taken into account to improve this description even more. In describing electrons in atoms, it is not necessary to be restricted to only a **single orbital configuration** given by a a single electron configuration (represented as a detrimental wavefunction e.g., a Slater determinant).

For example, for the two-electron Slater determinant wavefunction of helium, we could write

$$\psi_{CI}(r_1, r_2) = \underbrace{c_1 Det|\varphi_{1s}(r_1)\varphi_{1s}(r_2)|}_{\text{ground state: } 1s^2} + \underbrace{c_2 Det|\varphi_{1s}(r_1)\varphi_{2s}(r_2)|}_{\text{excited state: } 1s^1 2s^1} \tag{2.9.1}$$

where c_1 and c_2 are coefficients (that can be varied in variational method). This CI wavefunction adds the excited (higher energy) configuration $1s^12s^1$ to the ground (lowest energy) configuration $1s^2$. The lowest energy configuration corresponds to both electrons being in the same region of space at the same time; the higher energy configuration represents one electron being close to the nucleus and the other electron being further away. This makes sense because the electrons repel each other. When one electron is in one region of space, the other electron will be in another region. Configuration interaction is a way to account for this correlation.

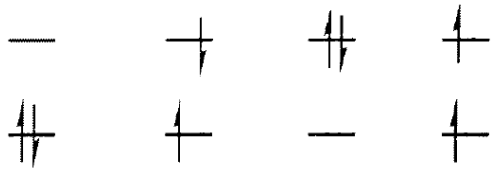

Figure 2.9.1: Within the CI approach the wavefunction for helium is a combination of all possible configurations (themselves described by Slater determinants. The wavefunction in Equation 2.9.1 would be the two left configurations

A single configuration description of an excited state is not very good because it does not take into consideration changes in the electron-electron repulsion. This is compensated for by allowing configuration of **the same symmetry** to mix CI. For instance, ${}^1(\sigma, \sigma^*)$ also has a ${}^1A_1$ symmetry, but is at a higher energy than for ${}^1(\pi, \pi^*)$. Let's define

$$\begin{aligned} {}^1A_1(\pi, \pi^*) &\equiv {}^1A_{1a} \\ {}^1A_1(\sigma, \sigma^*) &\equiv {}^1A_{1b} \end{aligned}$$

with CI, $b << a$ and we get improved energies and wavefunctions.

The new energies, E_a and E_b come from the solution of a 2x2 secular determinant, in this case:

$$0 = \begin{vmatrix} E_a - E & H_{12} \\ H_{12} & E_a - E \end{vmatrix}$$

where $H_{12} = \left\langle {}^1A'_{1a} \left| H' \right| {}^1A'_{1b} \right\rangle$ and H' is the electron-electron repulsion term in the Hamiltonian.

- If include all possible terms in sum (this is **Full CI and is** rarely done).
- Common to use all possible single and double excitations –CISD
- Choose a limited selection of configurations, optimize both configuration weights and MO's –**Multi-configurational self-consistent field (MCSCF)**
- Use perturbation theory formulism rather than variational–Perturbation is the difference between exact electron repulsion and HF representations (Møller-Plesset Perturbation Theory) MP2, MP3, MP4, etc.

Summary

A CI wavefunction is simply describes the linear combination of Slater determinants used for the wavefunction. In terms of a specification of orbital occupation (for instance, (1s)2(2s)2(2p)1...), interaction means the mixing (interaction) of different electronic configurations (states). Due to the long CPU time and immense hardware required for CI calculations, the method is limited to relatively small systems.

2.10: Measures of Transition Amplitudes

Now that we have looked at some of the possible electronic transitions from a theoretical point of view, we have some ammunition to assign spectra. Before we do this, we have to look at the expected intensities (strengths) of various possible absorption bands.

A convenient measure of intensity is the **oscillator strength**, f, that is related to the integrated intensity of an absorption band.

$$f = 4.314 \times 10^{-9} \int_{\text{whole band}} \varepsilon(\tilde{v}) d\tilde{v}$$

where $\tilde{v}$ is in units of cm^{-1}.

For allowed electronic transitions ($f > 0.1$) and for a symmetric band shape, an approximation relation can be made that is

$$f \propto 4.6 \times 10^{-9} \varepsilon_{\max} \Delta\tilde{v}_{1/2}$$

where $\Delta\tilde{v}_{1/2}$ is the bandwidth at half maximum absorbance (FWHM). Typically, $\Delta\tilde{v}_{1/2} = 10^3 \underline{\underline{\text{cm}^{-1}}}$, so for $f = 0.1$, we have

$$0.1 \propto 4.6 \times 10^{-9} \varepsilon_{\max} 10^3$$

or

$$\varepsilon_{\max} = \frac{1}{4.6 \times 10^{-5}} = 2 \times 10^4$$

So typically allowed electronic transitions in the UV or Vis will have $\varepsilon_{\max} \geq 20,000$.

Transition Moment Integrals

f is related to the **dipole strength**, D, which is the absolute squared of the transition moment integral.

$$f \propto D \equiv \left| \int_{-\infty}^{\infty} \psi_{el} \hat{M} \psi_{el}^{ex} \, d\Gamma \right|^2 = |\langle i | \hat{M} | f \rangle|^2$$

The $\hat{M}$ operator is the important part of the $H^{(1)}$ that appears in the **Fermi golden rule**. Thus, we see that f is also a measure of $W_{i->f}$.

Above,

- ψ_{el}^{ex} or $|f\rangle$ is the electronic wavefunction of the excited state (final),
- ψ_{el} or $\langle i|$ is the initial electronic state.
- $\hat{M}$ is the **electric dipole moment operator** and as a vectorial properties it has the components, $\hat{M}_x$, $\hat{M}_y$, and $\hat{M}_z$. $\hat{M}$ is a function of the electronic coordinates and is given by

$$\hat{M} = e \sum_i \vec{r}_i$$

and thus each component can be calculated independently:

$$\hat{M}_x = e \sum_i x_i$$

$$\hat{M}_y = e \sum_i y_i$$

and

$$\hat{M}_z = e \sum_i z_i$$

So the components of transform like translations along the Cartesian axis: x, y, z. In order for a transition to be allowed by electric dipole selection rules, at least one of the following integrals must be non-zero!

$$\left\langle i \left| \hat{M}_x \right| f \right\rangle \tag{2.10.1}$$

$$\left\langle i \left| \hat{M}_y \right| f \right\rangle \tag{2.10.2}$$

or

$$\left\langle i \left| \hat{M}_z \right| f \right\rangle \tag{2.10.3}$$

The particular transition moment integral that is not zero is an electronic transition defines the polarization of the transition. An oscillating electric field at this transition frequency aligned along the polarization axis **only** will induce transitions.

$$|i\rangle \rightarrow |f\rangle$$

Sometimes transitions are forbidden by symmetry since each of the three electronic transition moment integrals is zero. Sometimes transitions will weakly occur (low f) because of small interactions such as **vibronic coupling** and **spin-orbit coupling**.

Vibronic Coupling: In this case, distortions of the molecules induce by unsymmetrical vibrations can chance the symmetry of the molecule, making an otherwise forbidden transition (for symmetry reasons) slightly allowed.

Selection rule

The integrand of the transition moment integral **must have** a component that belongs to the totally symmetric (A_1 for non-centro.sym. or A_{1g} for centrosymmetric molecules) representation of the point group of the molecule. If not, the transition is symmetry **forbidden**.

Example 2.10.1: LaPort's rule for Centrosymmetric Molecules

For centrosymmetric molecules, all bands then have either a g (gerade=EVEN) or u (gerade =ODD) designation based on the character under i.

For instance, s and d orbitals are g since they do not change sign under i. But, p and f orbitals are u since they change sign under i.

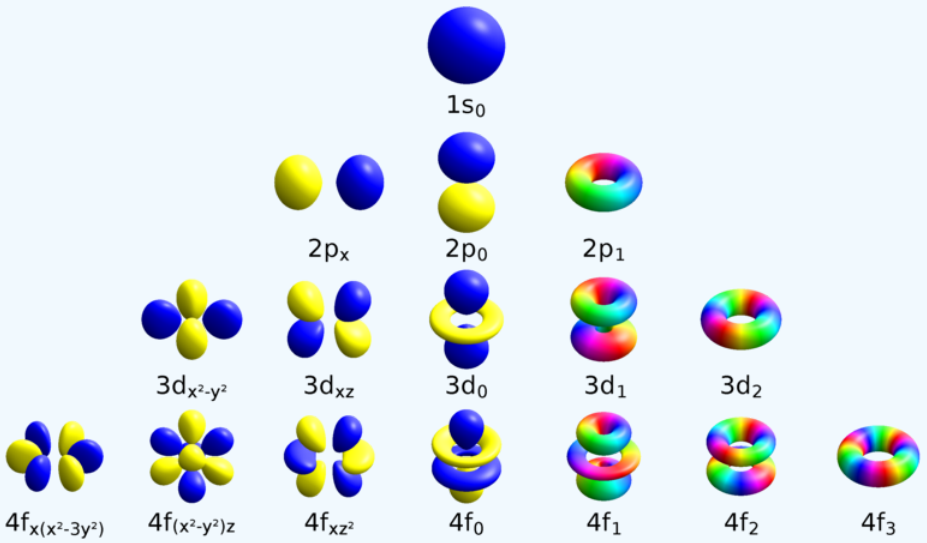

Figure: Atomic orbitals showing only the m-eigenstates. (Cc BY -SA 4.0;Geek3 via Wikipedia)

Now, $\hat{M}_x$, $\hat{M}_y$, and $\hat{M}_z$ are each u, so the integrands must contain A_{1g} to be allowed.

This means and thus must at least be g. Now,

$$u \times u = g \times g = g$$

and

$$u \times g = g \times u = u.$$

Since the $\hat{M}$ components are u, then $|i\rangle$ and $|f\rangle$ must be u and g or g and u in order that the integrand is g. Thus we get the simple LaPort rule (For centrosymmetric molecules):

$$u \longleftrightarrow u \qquad \text{Transitions are forbidden}$$

$$g \longleftrightarrow g \qquad \text{Transitions are forbidden}$$

$$g \longleftrightarrow u \qquad \text{Transitions are allowed}$$

$$u \longleftrightarrow g \qquad \text{Transitions are allowed}$$

However, the integrands must still contain the totally symeetric component (A_{1g} in this case) for it to be observed!

So for inorganic chemists in the audience, $d \longleftrightarrow d$ electronic transitions are forbidden if the group contains i as are $p \longleftrightarrow p$ and $s \longleftrightarrow s$ electronic transitions etc. [Thus, for the transitions in $\mathrm{Ni(H_2O)_6^{2+}}$ complex ion with octahedral symmetry, the ε is about 20, which is not a very intense absorption. Group has \(O_h\) symmetry and thus contains i.] LaPort's rule does say that $p \longleftrightarrow d$ and $s \longleftrightarrow p$ or transitions are allowed!

Example 2.10.2: Spin Flips

Transitions between states of differing spin multiplicities are forbidden. This is because the integral is evaluated over not only spatial coordinates, but also over "spin space." does NOT contains spins variables, thus the spin integral can be separated.

So the ground-state electronic wavefunction can be written as

$$\psi_{el}(r,s) = \psi_{el}(r)\psi_{el}(s) \text{ or } |r,s\rangle_{el} = |r\rangle_{el}|s\rangle_{el}$$

or

and the excited state wavefunction can be similarly written as

$$\psi_{el}^{ex}(r,s) = \psi_{el}^{ex}(r)\psi_{el}^{ex}(s) \text{ or } |r,s\rangle_{el}^{ex} = |r\rangle_{el}^{ex}|s\rangle_{el}^{ex}$$

or

Thus the integral

$$\int_{-\infty}^{\infty} \psi_{el}^{*}\hat{M}\psi_{el}^{ex}\,dr ds = \left\langle r|_{el} \left\langle s|_{el}\hat{M} \mid r \right\rangle_{el}^{ex} \mid s \right\rangle_{el}^{ex} = \left\langle r|_{el}\hat{M} \mid r \right\rangle_{el}^{ex} \langle s|_{el} \mid s\rangle_{el}^{ex}$$

where **r** represents spatial and **s** represents spin coordinates. If, for example, $|r,s\rangle_{el}$ is a singlet state and $|r,s\rangle_{el}^{ex}$ is a triplet state, the spin integral is

$$\langle s \text{ (singlet) } |_{el}| \, s(\text{ triplet }) \rangle_{el}^{ex} = 0$$

Since $|r,s\rangle_{el}$ as a single is orthogonal to $|r,s\rangle_{el}^{ex}$ as a triplet. However, spin-orbit coupling can mix singlet and triplet spin function together, so a weak singlet <-> triplet transition is sometimes observed. This is represented as an addition to the total Hamiltonian, H_{so}, that mixes triplet wavefunctions into singlet states and vice version.

2.11: Term Symbols

Term symbols are a shorthand method used to describe the energy, angular momentum, and spin multiplicity of an atom in any particular state. From a spectroscopic perspective, we need to know the values for the various types of angular momenta. Term symbols provide three pieces of information

- Total orbital angular momentum, L
- Multiplicity of the term, $2S+1$
- Total angular momentum, J

$$^{2S+1}L_J$$

Total Angular Momentum

$$L = l_1 + l_2 + l_3 + \ldots$$

- Maximum L is $l_1 + l_2$
- Minimum L is $|l_1 - l_2|$

$$\begin{array}{lccccc} \text{L:} & 0 & 1 & 2 & 3 & 4 \\ & \text{S} & \text{P} & \text{S} & \text{F} & \text{G} \end{array} \tag{2.11.1}$$

Spin Multiplicity

We can also determine the multiplicity options using a Clebsch-Gordan series

$$S = ½ + ½, ½ - ½$$

For two electron system S=0 and the spin multiplicity given by

$$2S+1$$

- For $S = 1$ (two unpaired electrons): $2S+1 = 3$ This is called a **triplet** state
- For $S = 0$ (no unpaired electrons): $2S+1 = 1$ This is called a **singlet** state

Total Angular Momentum

Permitted values of J again, given by a Clebsch-Gordon series

$$J = L+S, L+S-1, L+S-2 \ldots . |L-S|$$

Example 2.11.1

- *H($1s^1$) : ground state term symbol is $^2S_{1/2}$. Hence only one possible state for this "configuration"*
- *He($1s^2$) : Ground state term symbol is $^1S_0$. Hence only one state possible for this "configuration"*
- *Now, what about the excited hydrogen atom*. For case with L =1, S = ½ J = 1 + ½ or 1 - ½ the term symbols are $^2P_{3/2}$ and $^2P_{1/2}$

A portion of the hydrogen atom transition level diagram for optical spectra then, will look like

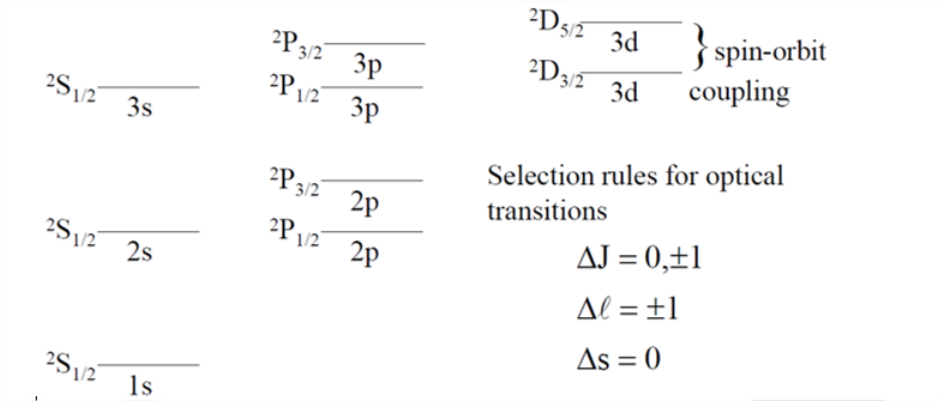

And with allowed transitions:

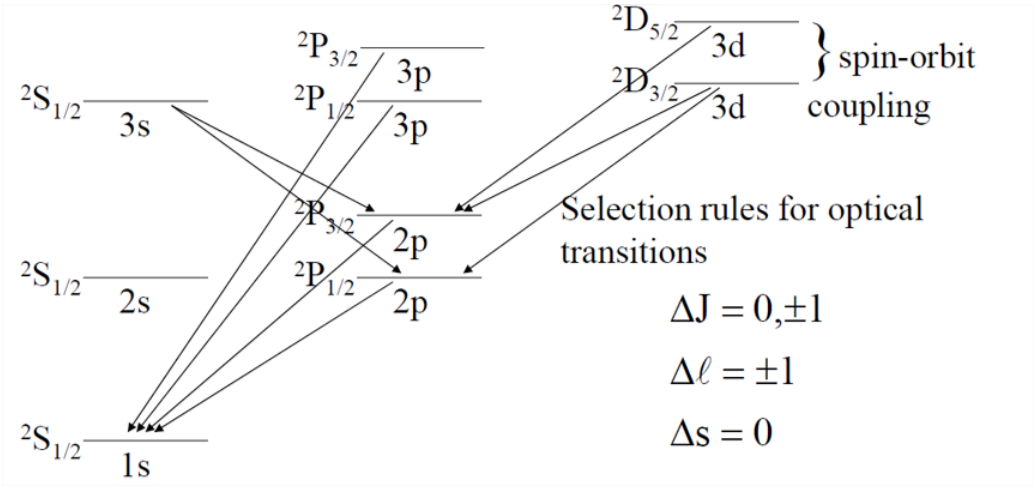

What about Ne? For $2p^6$ configuration, only one set of possible values.

$$M_L = m_1 + m_2 + m - 3 + m - 4 + m_5 + m_6 = 1 + 1 + 0 + 0 + (-1) + (-1) = 0$$

And in this case we also have

$S = |M_s| = m_{s1} + m_{s2} + m_{s3} + m_{s4} + m_{s5} + m_{s6}$

$= ½-½ + ½-½ + ½-½ = 0$

Thus, term is ^1S_o. **We will find this to be true for ANY filled subshell**. More complicated terms occur with unfilled shells (e.g., excited states). How to dictate energy levels of these states? Use Hund's rules:

1. State with the **largest** value of S is most stable and stability decreases with decreasing S.

2. For states with same values of S, the state with the **largest** value of L is the most stable.

3. If states have same values of L and S then, for a subshell that is less than half filled, state with **smallest** J is most stable; for subshells that are more than half filled, state with **largest** value of J is most stable.

Example 2.11.1

Example: Consider the terms ^3D, ^3P, ^3S, ^1D, ^1P, ^1S to describe the same electron distribution in an atom. In terms of stability we can rank these terms as:

$^1S > {}^1P > {}^1D > {}^3S > {}^3P > {}^3D$ Most stable

Given that the ^3D states are most stable, which of these terms correspond to the most stable state? Since the two p subshells are less than half filled, we would predict that the 3D1term corresponds to the most stable state! Simple approach for finding the ground state term symbol for any atom:

- Find maximum value of S consistent with the Pauli Exclusion Principle: S = S_{max}.
- For S = S_{max}, find the maximum value of L consistent with the Pauli Exclusion Principle: L = L_{max}.
- Apply Hund's Rules to find J for most stable state.

Example 2.11.2

He($1s^1 2s^1$): An Excited State Configuration
Terms: $^1S_0$, $^3S_1$
{ There is no $^3S_0$ nor $^3S_{-1}$ Term }

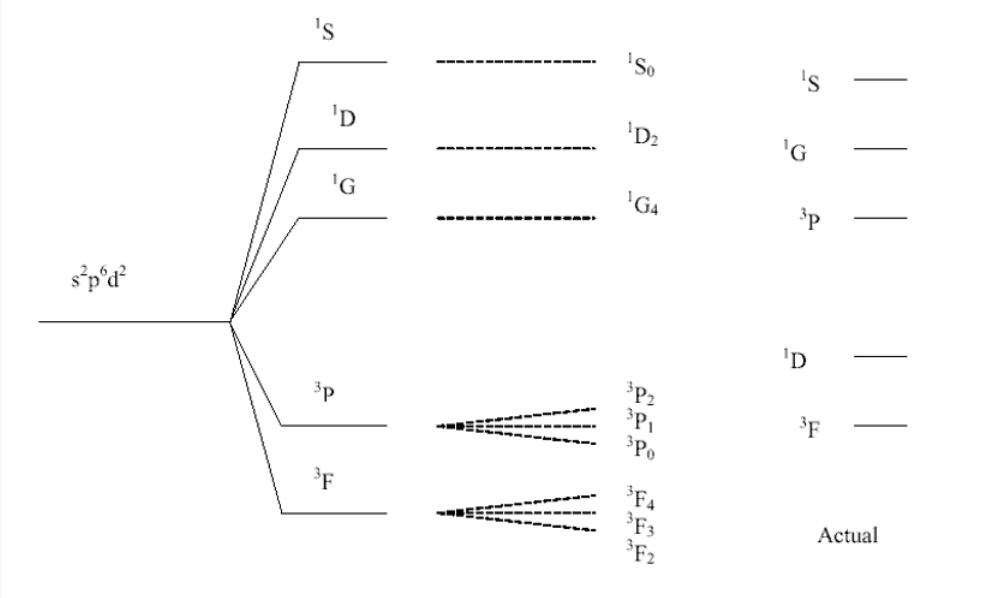

Configuration	Terms
p^1, p^5	^2P
p^2, p^4	^3P, ^1D, ^1S
p^3	^4S, ^2P, ^2D
d^1, d^9	^2D
d^2, d^8	^3P, ^3F, ^1S, ^1D, ^1G
d^3, d^7	^2P, ^2D, ^2D, ^2F, ^2G, ^2H, ^4P, ^4F
d^4, d^6	^1S, ^1S, ^1D, ^1D, ^1F, ^1G, ^1G, ^1I, ^3P, ^3P, ^3D, ^3F, ^3F, ^3G, ^3H, ^5D
d^5	^2S, ^2P, ^2D, ^2D, ^2D, ^2F, ^2F, ^2G, ^2G, ^2H, ^2I, ^4P, ^4D, ^4F, ^4G, ^6S

2.12: Absorption Spectrum of Formaldehyde

We can how turn to H_2CO again and look at the measured spectrum in the laboratory.

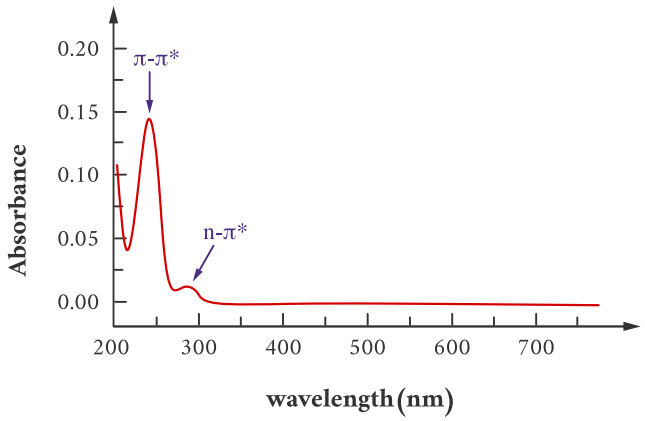

Figure 2.12.1: Electronic absorption spectrum of Formaldehyde in water. (CC BY-NC 4.0; Ümit Kaya via LibreTexts)

Two UV absorption bands are observed experimentally (Figure 2.12.1):

- 270 nm with $\varepsilon = 100$ and
- 185 nm with $\varepsilon > 10,000$

As discussed earlier, the lowest energy transitions are $n_b \rightarrow \pi^*$ and $\pi \rightarrow \pi^*$. As far as the states are concerned, the transitions are

$$^1A_2\left(n, \pi^*\right) \leftarrow {}^1A_1$$

and

$$^1A_1\left(\pi, \pi^*\right) \leftarrow {}^1A_1$$

respectively.

The Cartesian translational coordinates, x, y, z form a bases for the B_1, B_2 and A_1 representations in C_{2v}. Or course, x, y, z have the same transformation properties as $\hat{M}_x$, $\hat{M}_y$ and $\hat{M}_z$, respectively. Hence we can represent as

$$\hat{M} = \begin{pmatrix} \hat{M}_x \\ \hat{M}_y \\ \hat{M}_z \end{pmatrix}$$

or in the C_{2v} point group as

$$\begin{pmatrix} M_x \\ M_y \\ M_z \end{pmatrix} = \begin{pmatrix} B_1 \\ B_2 \\ A_1 \end{pmatrix}.$$

Class, please confirm this with the character table!

Example 2.12.1: Forbidden Transition

Let's look at $^1A_2\left(n, \pi^*\right) \leftarrow {}^1A_1$

Evaluate this integrand for all components of $\hat{M}$:

$$A_2 \otimes \begin{pmatrix} B_1 \\ B_2 \\ A_1 \end{pmatrix} \otimes A_1 = \begin{pmatrix} B_2 \\ B_1 \\ A_2 \end{pmatrix}$$

And looking at each component:

- For $\hat{M}_x$:

$$A_2 \otimes B_1 \otimes A_1 = B_2$$

- For $\hat{M}_y$:

$$A_2 \otimes B_2 \otimes A_1 = B_1$$

- For $\hat{M}_z$:

$$A_2 \otimes A_1 \otimes A_1 = A_2$$

Therefore the ${}^1A_2 \leftarrow {}^1A_1$ transition is **forbidden** by electronic symmetry since there the symmetry is ODD for all the three $\hat{M}$ components. That is, integration over all space with an integrand of non-A_1 symmetry will always results in zero!

However, in reality, other coupling elements like vibronic coupling and spin-orbit coupling will make this a weakly allow transition (Figure $2.12.1$) instead of explicitly forbidden.

Example 2.12.2: Allowed Transition

Let's look at ${}^1A_1\ (\pi, \pi^*) \leftarrow {}^1A_1$

Evaluate this integrand for all components of $\hat{M}$:

$$A_1 \otimes \begin{pmatrix} B_1 \\ B_2 \\ A_1 \end{pmatrix} \otimes A_1 = \begin{pmatrix} B_1 \\ B_2 \\ A_1 \end{pmatrix}$$

Therefore ${}^1A_1 \leftarrow {}^1A_1$ is **allowed** by since

- For $\hat{M}_x$:

$$A_1 \otimes B_1 \otimes A_1 = B_1$$

- For $\hat{M}_y$:

$$A_1 \otimes B_2 \otimes A_1 = B_2$$

- For $\hat{M}_z$:

$$A_1 \otimes A_1 \otimes A_1 = A_1$$

when $\hat{M}_z$ the dipole moment operation (A_1) is used we get an integrand that has A_1 symmetry. This electronic transition is thus polarized (preferential absorption of one polarization vs. another) and is only allowed when the oscillating electric field vector, is aligned along the molecular z-axis (along the C=O bond direction).

Example 2.12.3: Higher Lying Transitions

Let's consider higher energy transitions can occur such as

$${}^1B_1\ (\pi, \sigma^*) \leftarrow {}^1A_1$$

$$B_1 \otimes \begin{pmatrix} B_1 \\ B_2 \\ A_1 \end{pmatrix} \otimes A_1 = \begin{pmatrix} A_1 \\ A_2 \\ B_1 \end{pmatrix}$$

So this transition is $\hat{M}_x$ polarization **allowed** and is expected to lie further in the vacuum ultraviolet.

References

- https://www.chem.ucla.edu/~bacher/UV...lone.html.html
- http://web.gps.caltech.edu/~gab/ch21...ure16_2018.pdf

2.13: Assignment of Bands Based on Solvent Effects

Spectra of organic molecules containing n and π electrons can frequently be assigned based on their solvent effects.

Solvation

Solvents that do not itself absorb in the region under investigation are the most suitable for UV-visible spectroscopy. Most commonly used solvents are 95% EtOH, H_2O and hexane. Often, both the intensity (ε) and λ_{max} shift with the change of the polarity of the solvent. While all solutes species interact with the surrounding solvent molecules to affect the electronic energies of the electronic state, charged and dipolar molecules interact especially strongly often resulting in pronounced spectral shifts.

Definition: Spectropscopic Changes

- **Bathochromic shift:** shift to longer λ, also called **red shift.**
- **Hypsochromic shift:** shift to shorter λ, also called **blue shift**.
- **Hyperchromism**: increase in ε of a band.
- **Hypochromism**: decrease in ε of a band.

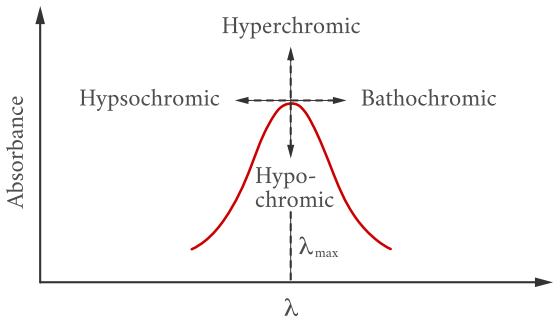

Figure 2.13.1: Terminology of Shifts in an absorption Band. (CC BY-NC 4.0; Ümit Kaya via LibreTexts)

The strength and nature of these interactions influence many properties of the solute including reaction rates. **Solvation** is the process of reorganizing solvent and solute molecules into solvation complexes and involves bond formation, hydrogen bonding, and van der Waals forces.

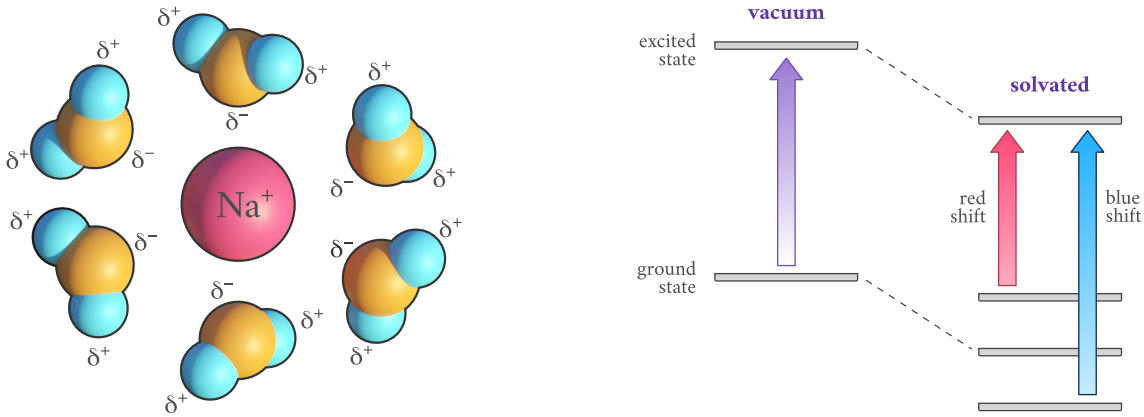

Figure 2.13.1: A sodium ion solvated by water molecules. (CC BY-NC 4.0; Ümit Kaya via LibreTexts) (left) Schematic illustration of energy level diagrams of the solute for understanding how its electronic states are changed due to the solvent effect. The vertical excitation energies required for transitions from ground to excited states are indicated with arrows. The dashed lines indicate the situation in which the excited state has the same electron distribution as the ground state. (CC BY-NC 4.0; Ümit Kaya via LibreTexts)

For compounds having n, π, and π^* orbitals (e.g. formaldyde), we can observe $n \rightarrow \pi^*$ and $\pi \rightarrow \pi^*$ transitions. The absorption wavelength $n \rightarrow \pi^*$ of is typically longer than that of $\pi \rightarrow \pi^*$ since the energy gap of $n \rightarrow \pi^*$ is smaller than $\pi \rightarrow \pi^*$. Different types of transition are affected differently with changes in polarity.

$\sigma \rightarrow \sigma^*$ Transitions (Neglible Shifts)

Molecules showing this type of transition are non-polar since σ MOs are non-polar in nature. Therefore, changing the polarity of solvents has neglibable effect on this transition. By increasing polarity of the solvent, compounds like hydrocarbons does not experience any appreciable shift. Thus, value of absorption maximum for non-polar compound is same in ethanol (polar) and hexane (non-polar).

$\pi \rightarrow \pi^*$ Transitions (Bathochromic Shifts)

In case of $\pi \rightarrow \pi^*$ transitions, the excited states are more polar than the ground state and the dipole-dipole interactions with solvent molecules lower the energy of the excited state more than that of the ground state. Therefore a polar solvent decreases the energy of $\pi \rightarrow \pi^*$ transition and absorption maximum appears ~10-20 nm red shifted in going from hexane to ethanol solvent.

For this type of transition, λ_{max} value shifts to **longer wavelength** with increasing polarity solvents. If the excited state is polar, but the ground state is neutral, polar solvent will primarily interact with the excited state to stabilizes it (decrease it absolute energy). Hence, absorption shifts to **longer wavelength**.

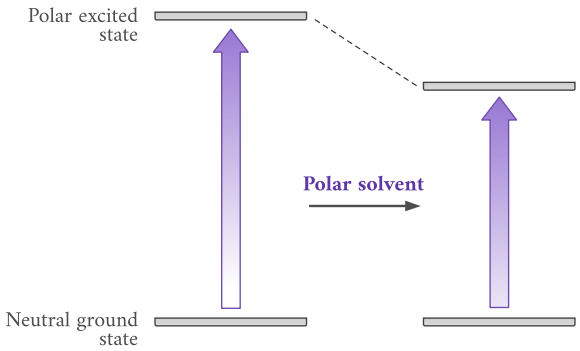

(CC BY-NC 4.0; Ümit Kaya via LibreTexts)

$n \rightarrow \sigma^*$ Transitions (Hypsochromic Shifts)

If excited state is neutral and ground states are polar. Polar solvents will preferentially solvate the ground state to lower its energy. Hence, absorption shifts to **shorter wavelength** with increasing polarity of the solvent.

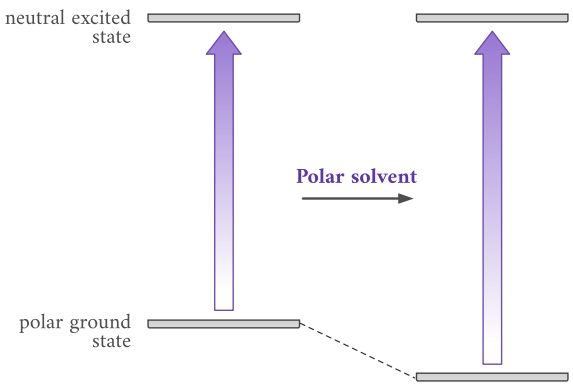

(CC BY-NC 4.0; Ümit Kaya via LibreTexts)

$n \rightarrow \pi^*$ Transitions (Hypsochromic Shifts)

Similar to $n \rightarrow \sigma^*$ transitions, the value of λ_{max} shifts to **shorter wavelength** for this transition.

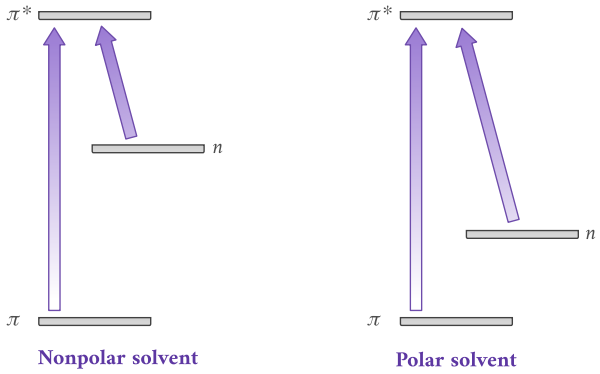

(CC BY-NC 4.0; Ümit Kaya via LibreTexts)

Example 2.13.1

Influence of solvent on the UV bands (λ_{max}) of the $n \rightarrow \pi^*$ and $\pi \rightarrow \pi^*$ transitions of 4-methylpent-3-en-2-one is tabulate below.

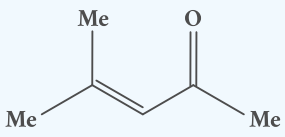

Solvent	$\pi \rightarrow \pi^*$ (nm)	$n \rightarrow \pi^*$ (nm)
n-hexane	230	327

Solvent	$\pi \rightarrow \pi^*$ (nm)	$n \rightarrow \pi^*$ (nm)
ether	230	326
ethanol	237	315
water	245	305

Note that the $\pi \rightarrow \pi^*$ increases wavelength (decreased excitation energy) and the $n \rightarrow \pi^*$ decreases wavelength (increases excitation energy).

Summary

In a polar solvent, the absorption of $n \rightarrow \pi^*$ will shift to shorter wavelengths, while the $\pi \rightarrow \pi^*$ will weakly (or not at all) shift to longer wavelengths because the polar solvent stabilizes these three orbitals in different extent, $n > \pi^* > \pi$, since π^* orbitals are more polar than π orbital as polar solvent stabilizes polar substances more (see J. Chem. Phys. **121**, 8435 (2004); doi:10.1063/1.1804957). Thus, as solvent polarity increases:

- $\pi \rightarrow \pi^*$ band shifts to longer λ_{max}
- $n \rightarrow \sigma^*$ band shifts to shorter λ_{max}
- $n \rightarrow \pi^*$ band shifts to shorter λ_{max}

2.14: Solvent Effect of Fluorescence

The concept of solvation can be understood from interactions between a fluorophore (the solute), and the surrounding solvent molecules. The dominating solute-solvent interactions arise from electrostatic dipole-dipole interactions, which lead to lowering the potential energies of all energy levels involved in absorption and fluorescence processes.

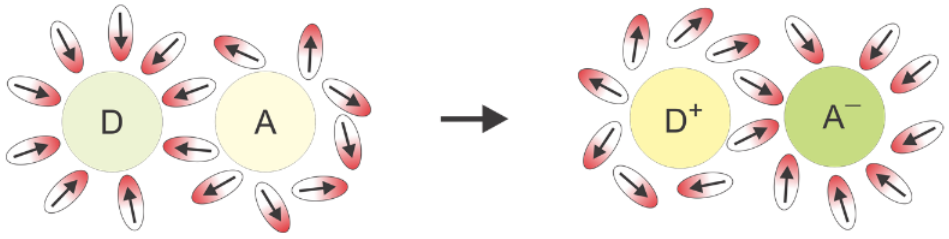

Figure 1: Changes in solute-solvent interactions lead to solvatochromic shifts in absorption and fluorescence spectra of the same fluorophore. (CC BY-SA-NC; Andrei Tokmakoff)

This effect can be explained by **Onsager's model of solvation**. According to this model, the dipole moment of the fluorophore in the ground state, μ_g, interacts with the dipole moments of the surrounding solvent molecules, rearranging them in a way that minimizes the potential energy of the whole system. If we would "freeze" the molecules for a while and remove the fluorophore, the special arrangement of the solvent dipole moments would result in a non-balanced electric field R_g, called the "reaction field" or "vacuum field"

Solvation Energies

In Onsager's model, the solute-solvent interaction is identified as an interaction of the fluorophore dipole moment, μ_g, with the reaction field R_g, namely:

$$U_g^{\text{rel}} = -\vec{\mu}_g \cdot \vec{R}_g$$

The energy level of the ground state is therefore lowered by this value. The symbol 'rel' indicates that the solvent is in a state of thermodynamic equilibrium (relaxed).

Electronic excitation of the fluorophore causes a rapid (~10^{-15} s) change of its dipole moment to μ_e. This time is much too short for the solvent molecules to rearrange their orientations. Thus, immediately after excitation the interaction energy will be:

$$U_e^{FC} = -\vec{\mu}_e \cdot \vec{R}_g$$

indicating that the reaction field will be still the same as it was before excitation. The symbol 'FC' indicates a non-equilibrated, Franck-Condon state. The solvent molecules need usually picoseconds (10^{-12}-10^{-10} s) to perform solvent relaxation achieving finally the solute-solvent interaction energy (Figure 2):

$$U_e^{\text{rel}} = -\vec{\mu}_e \cdot \vec{R}_e$$

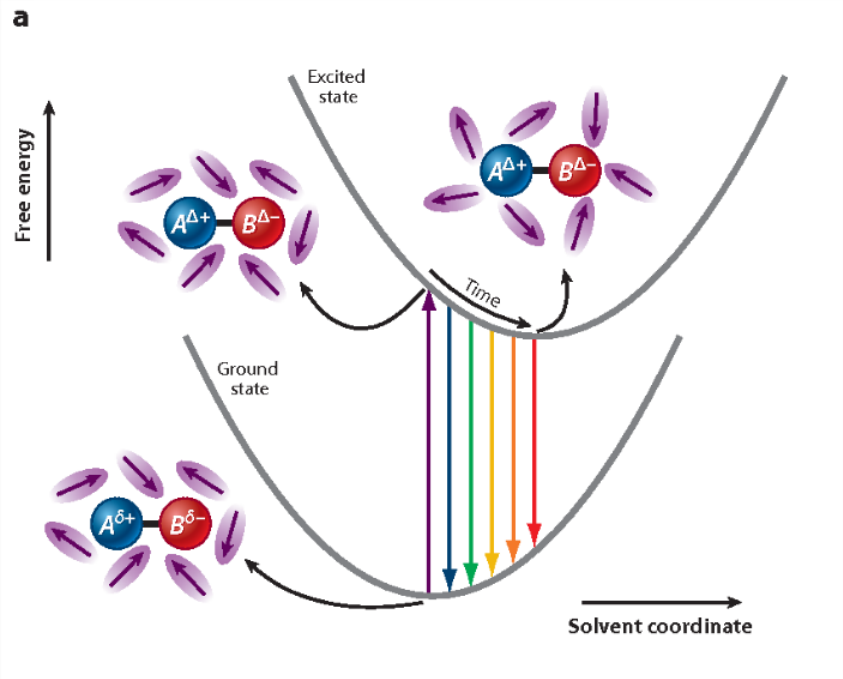

Figure 2: Schematic description of the time-dependent fluorescence (TDF) process. (a) The absorption and TDF are depicted for a dye molecule, represented as A-B with a charge-transfer transition (> δ). The purple arrows indicate solvent molecule permanent dipole moments that reorganize after excitation as measured by a collective solvent coordinate. https://www.semanticscholar.org/pape...c0d32/figure/0

The process of fluorescence brings the fluorophore dipole moment back to its ground-state value μ_g, so just after fluorescence:

$$U_e^{FC} = -\vec{\mu}_e \cdot \vec{R}_e$$

which finally evolves during ground-state solvent relaxation to U_g^{rel} . Direct consequences of the different solute-solvent interaction energies at different stages of absorption and fluorescence events are the spectral shifts in absorption (ΔU_{abs} and fluorescence (ΔU_{flu}) spectra (Figure 3):

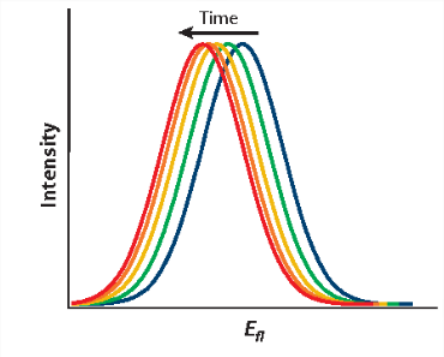

Figure 3: The typical time dependency of the fluorescence spectrum

which finally evolves during ground-state solvent relaxation to U_g^{rel} . Direct consequences of the different solute-solvent interaction energies at different stages of absorption and fluorescence events are the spectral shifts in absorption (ΔU_{abs}) and fluorescence (ΔU_{flu}) spectra:

$$\Delta U_{abs} = U_e^{FC} - U_g^{rel}$$
$$\Delta U_{flu} = U_g^{FC} - U_e^{rel}$$

Reorganization Energy

If we assume the stabilization energies in the excited and ground state are identical, we can assign them to the **reorganization energy** (λ) of the system:

$$U_g^{rel} = U_e^{rel} = \lambda$$

Reorganization energies are critical parameters in Marcus theory for charge transfer.

2.15: Breaking Symmetries

Local Symmetry

Small modification of the molecule that reduces symmetry will have small effects on the spectra (e.g. H_2CO to CH_3CHO).

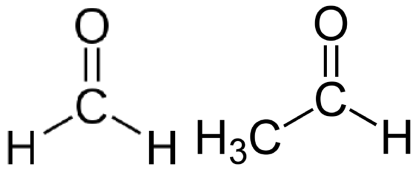

Figure 2.15.1: Formaldehyde (left) and acetaldehyde (right)

This gives same spectra patterns even though the point group of acetaldehyde is Cs, containing only two representations A' and A'' with x, y = A' and $z = A''$. Thus, *all transitions are symmetry allowed*. Because of this, the idea of **local symmetry** is important. Local symmetry is that associated with the **electronically active component** of the molecule only, which is the $C{=}O$ moiety.

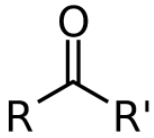

Independent of what R and R' are, provided that they not interact strongly with the C=O bond through conjugation etc. Hence this introduces the concept of a ”correlation or coherence length” of the excitation. Hence the UV-Vis spectra of all compounds of this type are similar: acetone, acetaldehyde, cyclopentanone, etc).

Acetone:

- $\pi \rightarrow \pi*$ with $\lambda_{max} = 188\, nm$ and $\varepsilon = 1860$
- $n \rightarrow \pi^*$ with $\lambda_{max} = 279\, nm$ and $\varepsilon = 15$

vs. formaldehyde

- $\pi \rightarrow \pi*$ with $\lambda_{max} = 185\, nm$ and $\varepsilon > 10,000$
- $n \rightarrow \pi^*$ with $\lambda_{max} = 270 nm$ and $\varepsilon = 100$

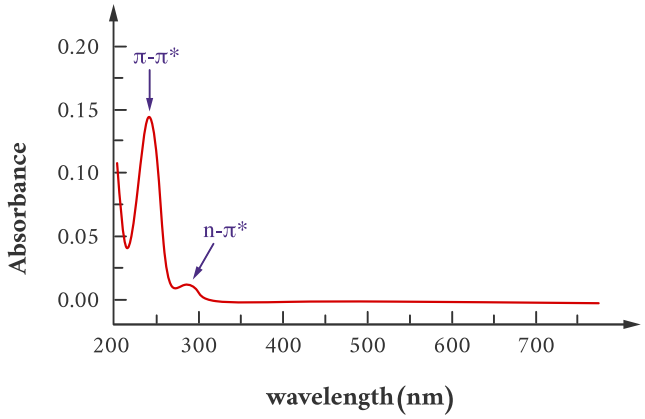

Figure 2.15.2: Electronic absorption spectrum of Formaldehyde in water. (CC BY-NC 4.0; Ümit Kaya via LibreTexts)

Vibronic Coupling

The ${}^1A_2 \leftarrow {}^1A_1$ transition is forbidden by symmetry selection rules for formaldehyde. Why do we see it in the H_2CO molecule at all? Answer= **Vibronic coupling.** The Born-Oppenheimer approximation is not absolute. There is always some interaction between vibrational and electronic motion in a molecule. This means that the separation

$$|q,r\rangle \approx |r;q\rangle_{el}|q\rangle_{vib}$$

is not always exact. Thus we must consider the transition moment integral in its entirety.

$$\langle q,r|\hat{M}|q,r\rangle^{ex}$$

Let's assume $|q,r\rangle$ is in its ground state for all vibrations (k_bT < all vibrational frequencies). The irreducible representation of all vibrations in non-excited state is A_1. Thus $|q,r\rangle$ has the symmetry of the electron wavefunction itself $|r\rangle$. In general, the symmetry is the direct product of the symmetry representations of $|r\rangle$ and $|q\rangle$.

Now, for the *excited* state wavefunction ($|q,r\rangle^{ex}$), the symmetry is that of the electronic wavefunction ($|r\rangle^{ex}$) **only** if the vibrational state is totally symmetric (i.e. $v'=0$) for all normal modes or only A_1 vibrations are excited. However, if one-quantum of a non-symmetric vibrational state is excited along with the electronic state (upon absorption of light), then the excited state representation will be:

$$\Gamma_{total} = \underbrace{\Gamma\left(|r\rangle^{rx}\right)}_{\text{vibration symmetry}} \otimes \underbrace{\Gamma\left(|q\rangle^{j^{ex}}\right)}_{\text{electronic symmetry}}$$

If Γ_{total} contains the same representation as a component of $\hat{M}$ then the transition becomes weakly allowed vibrationally. Important, the appropriate vibrational mode is exited simultaneously with electronic transition.

Example 2.15.1: Formaldehyde

$\hat{M}$ in the C_{2v} point group has the following representations for x, y, and z polarizations:

$$\begin{pmatrix} M_x \\ M_y \\ M_z \end{pmatrix} = \begin{pmatrix} B_1 \\ B_2 \\ A_1 \end{pmatrix}.$$

Hence, the ${}^1A_2\,(n,\pi^*) \leftarrow {}^1A_1$ transition in H_2CO transition can be vibronically coupled (allowed) if the quantum of a normal mode with symmetry:

- a_1 giving a z-polarization
- b_1 giving a y-polarization
- b_2, giving a x-polarization

is *simultaneously* excited by the absorption of the photon. We can use this to predict the symmetries of the normal modes of vibration that a molecule has. A mode active in inducing an electronic transition (vibronically) is called an **inducing mode** or **promoting mode**.

Symmetry

Assume the electronic (lowest vibrational level) ground state is totally symmetry (e.g., closed shell) is usually the case for organic molecules. A transition may be vibronically induced by exciting one quantum of a vibrational mode of symmetry, , provided the direct produce

$$\Gamma_q \otimes \Gamma_{\hat{M}} \otimes \Gamma_{ex} = A_1 \text{ or } A_{1g}$$

where $\Gamma_{\hat{M}}$ is the symmetry of the $\hat{M}$ operator and Γ_{ex} is the symmetry of the electronic excited state. Of course, the allowed vibrations must contain one of the symmetry Γ_{vib}.

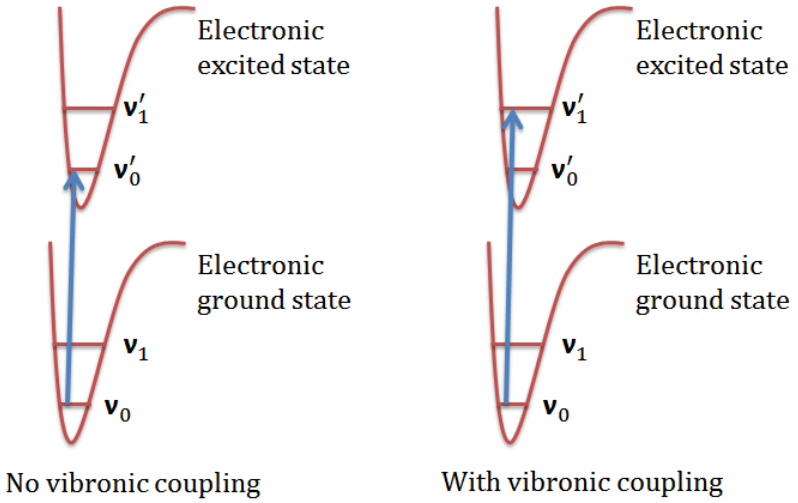

Figure 2.15.3: the 0-0 electronic transition (left) and the 0-1 electronic transition that is coupled with a vibrational transition (right)

The $0 \longrightarrow 0$ band does not appear in a vibrationally-induced electronic transition! This is one of its characteristics other than its reduced oscillator strength.

Possible vibrational modes for H_2CO

A nonlinear molecule has $3N-6$ internal degrees of vibrational freedom. These are these many vibrational frequencies, each of which has a symmetry of an irreducible representation for the molecular point group (https://www.chem.purdue.edu/jmol/vibs/form.html). For formaldehyde, with $N=4$, we have $3\times4-6=6$ vibrational degrees of freedom which are distributed as normal modes comprising of a superposition of local modes. These turn out to (we will discuss later) transform as: $3a_1, b_1, 2b_2$.

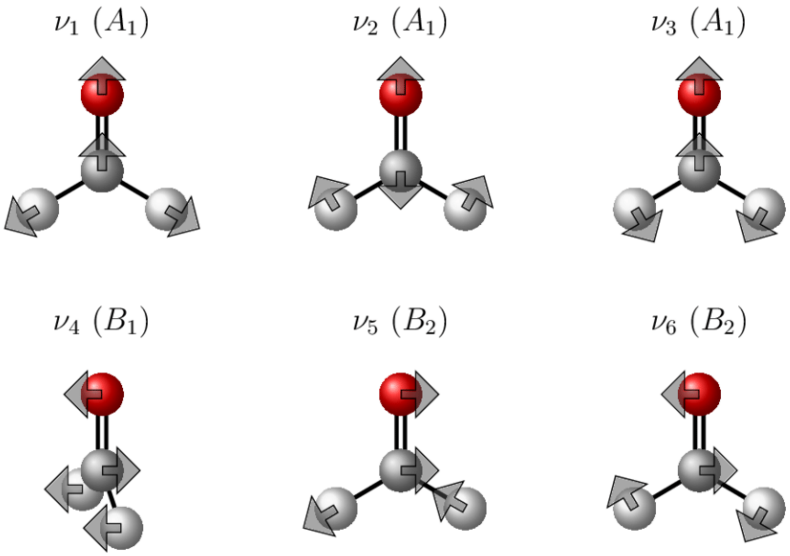

Thus only b_1 and b_2 unsymmetrical modes are possible? We can thus have no Z-polarized vibronic transitions (no a_2 mode in H_2CO), but we can have x- and y-polarized vibronic transition with b_2 and b_1 inducing modes, respectively. Hence, we can use polarization to identify inducing modes for vibronic transitions.

Example 2.15.1: Octahedral Transitions Metal Complexes

The $d \longrightarrow d$ transitions in octahedral complexes are electronically forbidden (Laporte forbidden since they are $g \longleftrightarrow g$), but they can be weakly allowed vibrationally by vibrations that remove the inversion center. Let's consider the $(NH_3)_6Co^{III}$ complex that has a d^6 configuration (loss of two 4s electrons and one d electron to make the ion).

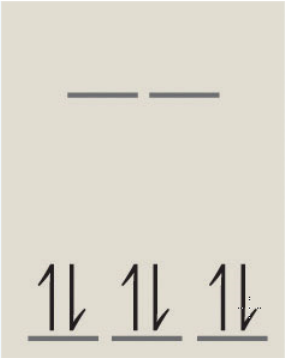

The ground state is t_{2g} and the excited state e_g. Is a d-d transition allowed?

The ground state symmetry is and has a O_h symmetry of ground state configuration due to the octahedral ligand field. Let's consider the potential electronic $\mathrm{d} \longrightarrow \mathrm{d}$ transition from the t_{2g} orbitals to the e_g orbitals. The excited electronic state symmetries are obtained from the orbital direct product:

$$\Gamma_{t_{2g}} \otimes \Gamma_{e_g} = T_{1g} + T_{2g}$$

(From direct product table for O_h)

Both ${}^1T_{2g} \leftarrow {}^1A_{1g}$ and ${}^1T_{1g} \leftarrow {}^1A_{1g}$ transitions are forbidden. Now, $\hat{M}$ or $\{x, y, z\}$ form the basis for a triply degenerate representation T_{1u} in O_h.

O_h	E	$8C_3$	$6C_2$	$6C_4$	$3C_2 = (C_4)^2$	i	$6S_4$	$8S_6$	$3\sigma_h$	$6\sigma_d$	linear functions, rotations	quadratic functions	cubic functions
A_{1g}	+1	+1	+1	+1	+1	+1	+1	+1	+1	+1	-	$x^2+y^2+z^2$	-
A_{2g}	+1	+1	-1	-1	+1	+1	-1	+1	+1	-1	-	-	-
E_g	+2	-1	0	0	+2	+2	0	-1	+2	0	-	$(2z^2-x^2-y^2, x^2-y^2)$	-
T_{1g}	+3	0	-1	+1	-1	+3	+1	0	-1	-1	(R_x, R_y, R_z)	-	-
T_{2g}	+3	0	+1	-1	-1	+3	-1	0	-1	+1	-	(xz, yz, xy)	-
A_{1u}	+1	+1	+1	+1	+1	-1	-1	-1	-1	-1	-	-	-
A_{2u}	+1	+1	-1	-1	+1	-1	+1	-1	-1	+1	-	-	xyz
E_u	+2	-1	0	0	+2	-2	0	+1	-2	0	-	-	-
T_{1u}	+3	0	-1	+1	-1	-3	-1	0	+1	+1	(x, y, z)	-	(x^3, y^3, z^3) $[x(z^2+y^2), y(z^2+x^2), z(x^2+y^2)]$

O_h	E	$8C_3$	$6C_2$	$6C_4$	$3C_2 = (C_4)^2$	i	$6S_4$	$8S_6$	$3\sigma_h$	$6\sigma_d$	linear functions, rotations	quadratic functions	cubic functions
T_{2u}	+3	0	+1	-1	-1	-3	+1	0	+1	-1	-	-	[x(z^2-y^2), y(z^2-x^2), z(x^2-y^2)]

For instance, for the purely electronic transition ${}^1T_{1g} \leftarrow {}^1A_{1g}$ component,

$$T_{1g} \otimes T_{1u} \otimes A_{1g} = A_{1u} + E_u + T_{1g} + T_{2u}$$

this **does not contain** the A_{1g} symmetry representation (i.e., Laporte forbidden) and is therefore, this is a forbidden electronic transition.

What vibrations will couple these two electronic states? An octahedral complex (7 atoms so there are $3 \times 7 - 6 = 15$ normal modes) has the following vibrational symmetries (discussed later):

$$\Gamma_{vib} = a_{1g} + e_g + 2t_{1u} + t_{2g} + t_{2u}$$

(15 modes here, count them up)

The potential promoting modes are the $2t_{1u}$ and t_{2u} normal modes. The t_{1u} mode will serve as a promoting mode provided

$$T_{1u} \otimes \{T_{1g} \otimes T_{1u} \otimes A_{1g}\} =$$
$$T_{1u} \otimes [A_{1u} + E_u + T_{1u} + T_{2u}] = A_{1g}$$

This turns out to contain A_{1g}, so the t_{1u}'s can serve as a promoting mode for a vibrationally allowed transition. So it turns out, also can the t_{2u} mode.

2.16: Charge Transfer Bands

Charge transfer (CT) transitions are important these days because they represent an interaction between light and energy in which an electron can be moved from one part of a molecule to another. Such processes are potentially important in solar energy conversion schemes, optical devices storage etc.

Charge Transfer Bands

If color is dependent on d-d transitions, why is it that some transition metal complexes are intensely colored in solution but possess no d electrons? In transition metal complexes a change in electron distribution between the metal and a ligand give rise to charge transfer (CT) bands.[1] CT absorptions in the UV/Vis region are intense (ε values of 50,000 L mole^{-1} cm^{-1} or greater) and selection rule allowed. The intensity of the color is due to the fact that there is a high probability of these transitions taking place. Selection rule forbidden d-d transitions result in weak absorptions. For example octahedral complexes give ε values of 20 L mol^{-1} cm^{-1} or less.[2] A charge transfer transition can be regarded as an internal oxidation-reduction process. [2]

Ligand to Metal and Metal to Ligand Charge Transfer Bands

Ligands possess σ, σ*, π, π*, and nonbonding (n) molecular orbitals. If the ligand molecular orbitals are full, charge transfer may occur from the ligand molecular orbitals to the empty or partially filled metal d-orbitals. The absorptions that arise from this process are called ligand-to-metal charge-transfer bands (LMCT) (Figure 2.16.1).[2] LMCT transitions result in intense bands. Ligand to metal charge transfer results in the reduction of the metal.

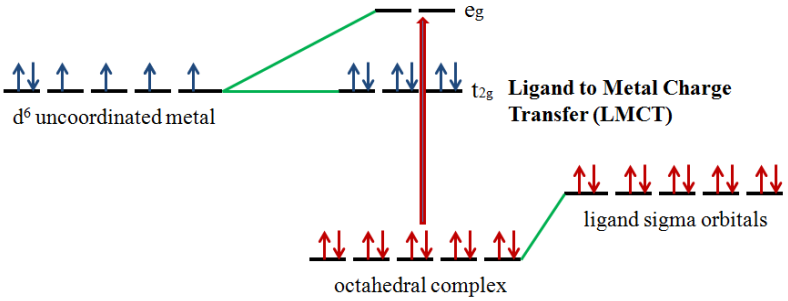

Figure 2.16.1: Ligand to Metal Charge Transfer (LMCT) involving an octahedral d^6 complex.

If the metal is in a low oxidation state (electron rich) and the ligand possesses low-lying empty orbitals (e.g., CO or CN^-) then a **metal-to-ligand charge transfer (MLCT)** transition may occur. LMCT transitions are common for coordination compounds having π-acceptor ligands. Upon the absorption of light, electrons in the metal orbitals are excited to the ligand π* orbitals.[2] Figure Figure 2.16.2 illustrates the metal to ligand charge transfer in a d^5 octahedral complex. MLCT transitions result in intense bands. Forbidden d – d transitions may also occur. This transition results in the oxidation of the metal.

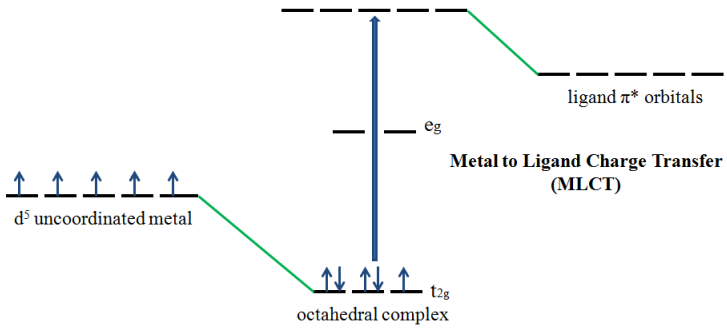

Figure 2.16.2. Metal to Ligand Charge Transfer (MLCT) involving an octahedral d^5 complex.

Effect of Solvent Polarity on CT Spectra

The position of the CT band is reported as a transition energy and depends on the solvating ability of the solvent. A shift to lower wavelength (higher frequency) is observed when the solvent has high solvating ability.

Polar solvent molecules align their dipole moments maximally or perpendicularly with the ground state or excited state dipoles. If the ground state or excited state is polar an interaction will occur that will lower the energy of the ground state or excited state by solvation. The effect of solvent polarity on CT spectra is illustrated in the following example.

Example 2.16.1

You are preparing a sample for a UV/Vis experiment and you decide to use a polar solvent. Is a shift in wavelength observed when:

Both the ground state and the excited state are neutral

When both the ground state and the excited state are neutral a shift in wavelength is not observed. No change occurs. Like dissolves like and a polar solvent won't be able to align its dipole with a neutral ground and excited state.

The excited state is polar, but the ground state is neutral

If the excited state is polar, but the ground state is neutral the solvent will only interact with the excited state. It will align its dipole with the excited state and lower its energy by solvation. This interaction will lower the energy of the polar excited state. (increase wavelength, decrease frequency, decrease energy)

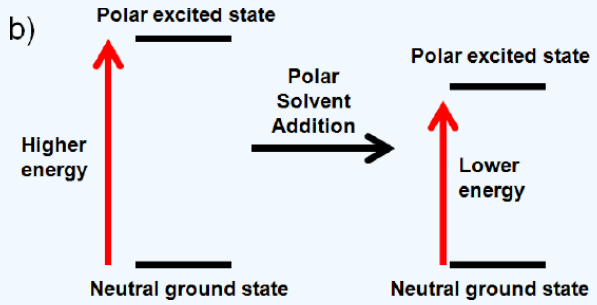

The ground state and excited state is polar

If the ground state is polar the polar solvent will align its dipole moment with the ground state. Maximum interaction will occur and the energy of the ground state will be lowered. (increased wavelength, lower frequency, and lower energy) The dipole moment of the excited state would be perpendicular to the dipole moment of the ground state, since the polar solvent dipole moment is aligned with the ground state. This interaction will raise the energy of the polar excited state. (decrease wavelength, increase frequency, increase energy)

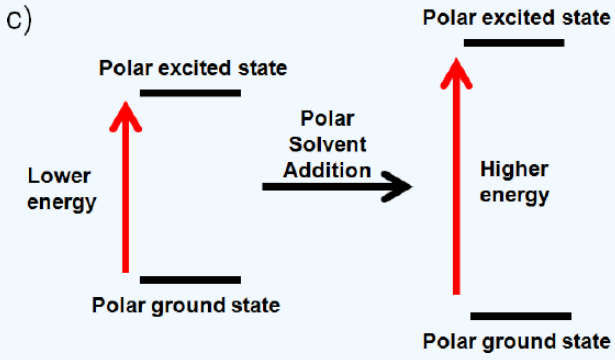

The ground state is polar and the excited state is neutral

If the ground state is polar the polar solvent will align its dipole moment with the ground state. Maximum interaction will occur and the energy of the ground state will be lowered. (increased wavelength, lower frequency, and lower energy). If the excited state is neutral no change in energy will occur. Like dissolves like and a polar solvent won't be able to align its dipole with a neutral excited state. Overall you would expect an increase in energy (Illustrated below), because the ground state is lower in energy (decrease wavelength, increase frequency, increase energy).[4]

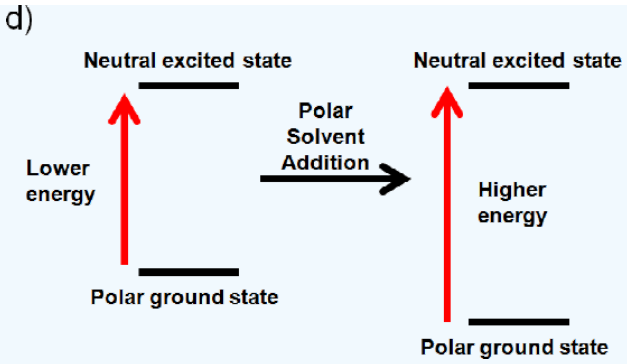

How to Identify Charge Transfer Bands

CT absorptions are selection rule allowed and result in intense (ε values of 50,000 L mole^{-1} cm^{-1} or greater) bands in the UV/Vis region.[2] Selection rule forbidden d-d transitions result in weak absorptions. For example octahedral complexes give ε values of 20 L mol^{-1} cm^{-1} or less.[2] CT bands are easily identified because they:

- Are very intense, i.e. have a large extinction coefficient
- Are normally broad
- Display very strong absorptions that go above the absorption scale (dilute solutions must be used)

Example 2.16.2: Ligand to Metal Charge Transfer

$KMnO_4$ dissolved in water gives intense CT Bands. The one LMCT band in the visible is observed around 530 nm.

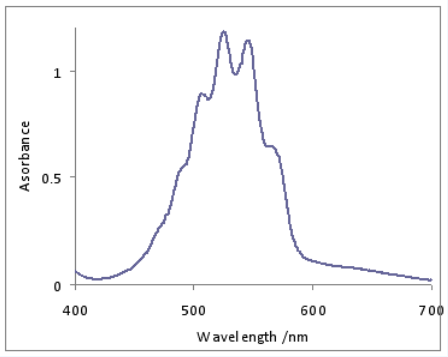

Figure 2.16.5: Absorption spectrum of an aqueous solution of potassium permanganate, showing a vibronic progression. (CC BY-SA 3; Petergans via Wikipedia)

The band at 528 nm gives rise to the deep purple color of the solution. An electron from a “oxygen lone pair” character orbital is transferred to a low lying Mn orbital.[1]

Example 2.16.3: Metal to Ligand Charge Transfer

Tris(bipyridine)ruthenium(II) dichloride (\ce{[Ru(bpy)3]Cl2}\)) is a coordination compound that exhbits a CT band is observed (Figure 2.16.6)

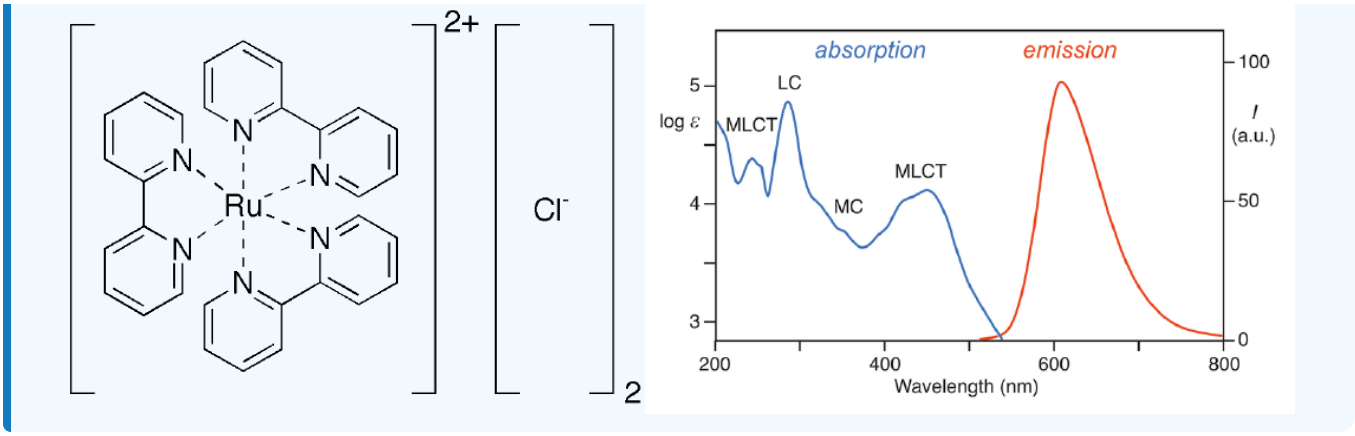

Figure 2.16.6: a) Structure of $[Ru(bpy)_3]Cl_2$, b) CT band observed in its V/Vis spectrum. (CC BY-SA 4.0; Albris via Wikipedia)

A d electron from the ruthenium atom is excited to a bipyridine anti-bonding orbital. The very broad absorption band is due to the excitation of the electron to various vibrationally excited states of the π* electronic state.[6]

2.17: Conjugation Length

Delocalization Length

Delocalized electrons are electrons that are not associated with a single atom or a covalent bond. Term delocalization is general and can have slightly different meanings in different fields. In organic chemistry, this refers to resonance in conjugated systems and aromatic compounds. In solid-state physics, this refers to free electrons that facilitate electrical conduction. In quantum chemistry, this refers to molecular orbital electrons that have extended over several adjacent atoms. Standard ab initio quantum chemistry methods lead to delocalized orbitals that, in general, extend over an entire molecule and have the symmetry of the molecule as discussed previously.

The Particle in a Box Model to decribe Delocalization Effects

In general, Molecular Orbitals may be delocalized over the entire length of the molecule. The Particle-in-a-box quantum model is useful in describing the impact of delocalization length on the electronic transition of the molecule.

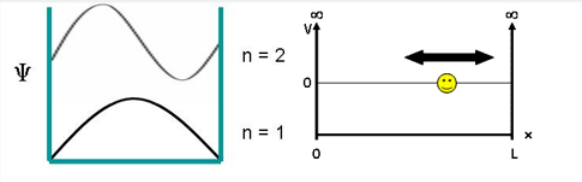

These PIB energies for an electron trapped in a box of length L goes as

$$E_n = \frac{n^2 h^2}{8mL^2} \tag{2.17.1}$$

The observed frequency for a transition is calculated from the change in energy using the following equalities,

$$\begin{aligned} \Delta E &= E_f - E_i \\ &= h\nu \end{aligned}$$

Then, for the specific case of the particle-in-a-box (via Equation 2.17.1):

$$\begin{aligned} \Delta E &= E_f - E_i \\ &= \frac{(n_f^2 - n_i^2)h^2}{8mL^2} \end{aligned} \tag{2.17.2}$$

where n_f is the quantum number associated with the final state and n_i is the quantum number for the initial state.

Equation 2.17.2 argues that the larger the box (i.e., the number of atoms the electron is delocalized over), the smaller the energy differences between quantum levels.

This is a simplistic model for bonding, compared to the molecular orbital approaches discussed so far, but guides general intuition around delocalization effects in comparing molecules with different sizes.

Molecular Orbitals from One double bond

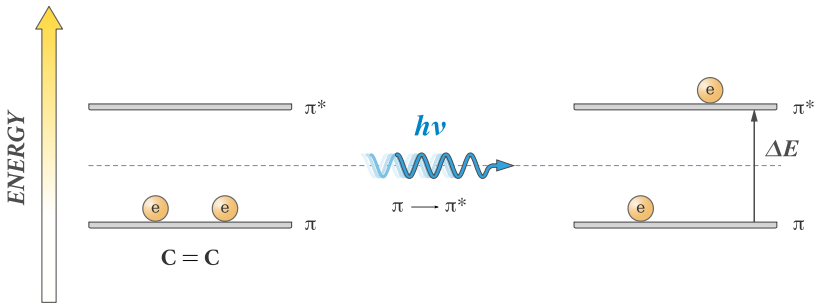

Figure 2.17.2: Scheme of electronic transition due to delocalization of molecular orbitals over two atoms (one double bond in a simple local bonding perspective). (CC BY-NC; Ümit Kaya via Libretexts)

Molecular Orbitals from Two double bonds

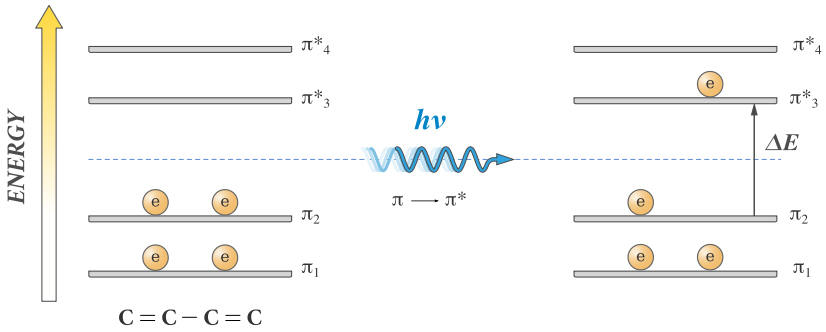

Figure 2.17.3: Scheme of electronic transition due to delocalization of molecular orbitals over found four atoms (two double bonds and one single bond in a simple local bonding perspective). (CC BY-NC; Ümit Kaya via Libretexts)

Molecular Orbitals from Three double bonds

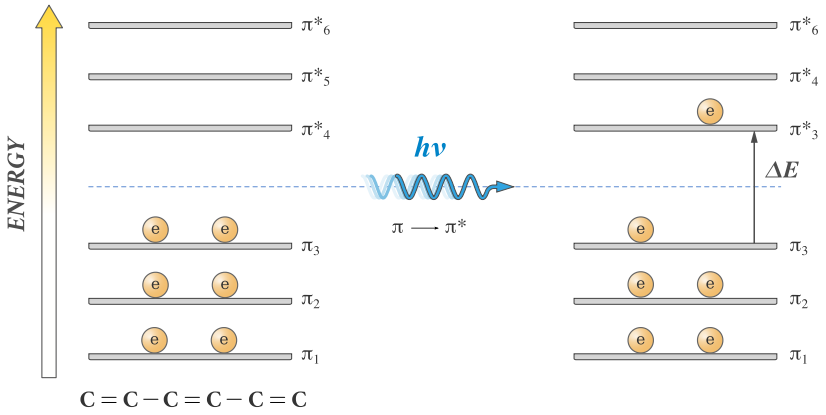

Figure 2.17.4: Scheme of electronic transition due to delocalization of molecular orbitals over found six atoms (three double bonds and two single bonds in a simple local bonding perspective). (CC BY-NC; Ümit Kaya via Libretexts)

For a more detailed overview of the the effect of delocalization on the ground state energies check Section 10.5 and Section 10.6 of the physical chemistry textbook.

The added conjugation in naphthalene (pink), anthracene (green) and tetracene (blue) causes bathochromic (red-shifts) shifts of these absorption bands, as displayed in the chart on the left below. All the absorptions do not shift by the same amount, so for anthracene (green shaded box) and tetracene (blue shaded box) the weak absorption is obscured by stronger bands that have

experienced a greater red shift. As might be expected from their spectra, naphthalene and anthracene are colorless, but tetracene is orange. *What break's conjugation lengths? Aliphatic bonding does.*

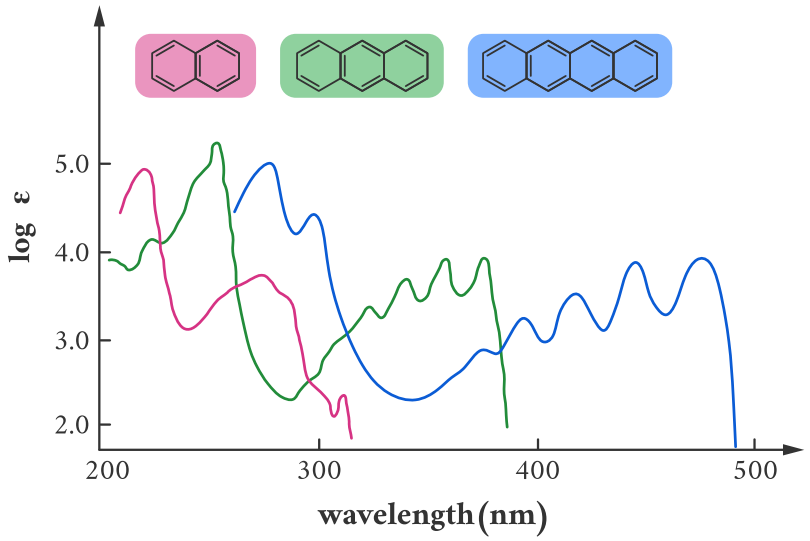

Figure 2.17.1: Conjugation effects for fused ring systems. As the molecular orbitals extend over more atoms, the electronic transitions shift red-shift (CC BY-NC; Ümit Kaya via Libretexts)

What about Oscillator Strength?

The greater the conjugation strength, the greater the molar The greater the conjugation strength, the greater the molar absortivity.

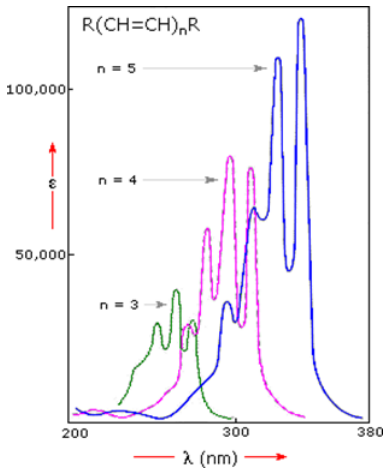

That is the end of Electronic Absorption Spectroscopy. We did not cover may interesting and powerful tweaks to this field, including ORD, CD, or MCD.

CHAPTER OVERVIEW

3: Vibrational Spectroscopy

Infrared spectroscopy is the measurement of the interaction of infrared radiation with matter by absorption, emission, or reflection. It is used to study and identify chemical substances or functional groups in solid, liquid, or gaseous forms. It can be used to characterize new materials or identify and verify known and unknown samples. The method or technique of infrared spectroscopy is conducted with an instrument called an infrared spectrometer (or spectrophotometer) which produces an infrared spectrum.

Raman spectroscopy is a spectroscopic technique typically used to determine vibrational modes of molecules, although rotational and other low-frequency modes of systems may also be observed. Raman spectroscopy is commonly used in chemistry to provide a structural fingerprint by which molecules can be identified.Raman spectroscopy relies upon inelastic scattering of photons, known as Raman scattering. A source of monochromatic light, usually from a laser in the visible, near infrared, or near ultraviolet range is used, although X-rays can also be used. The laser light interacts with molecular vibrations, phonons or other excitations in the system, resulting in the energy of the laser photons being shifted up or down. The shift in energy gives information about the vibrational modes in the system. Infrared spectroscopy typically yields similar yet complementary information.

3.1: Introduction to Vibrations
3.2: Polyatomic Molecules
3.3: Raman vs. IR Spectroscopies
3.4: Resonant Raman Spectroscopy
3.5: Classification of Normal Modes
3.6: IR and Raman Activity
3.7: Non-Fundamental Transations - Hot Bands, Combination Bands, and Fermi Resonances
3.8: Fourier Transform IR Spectroscopy
3.9: Spectra of Gases - Rovibronic Transitions

3.1: Introduction to Vibrations

We will begin with the vibrations of molecules since these are what we observed using IR and Raman spectroscopies. The vibrations of molecules can be modified by considering the atom as point mass that are attached to each other by massless springs (The electron pair bands). Thus for a simple diatomic molecules, we have only one vibration possible. The potential energy vs. internuclear distance, r, can be represented by a Morse curve (as discussed earlier).

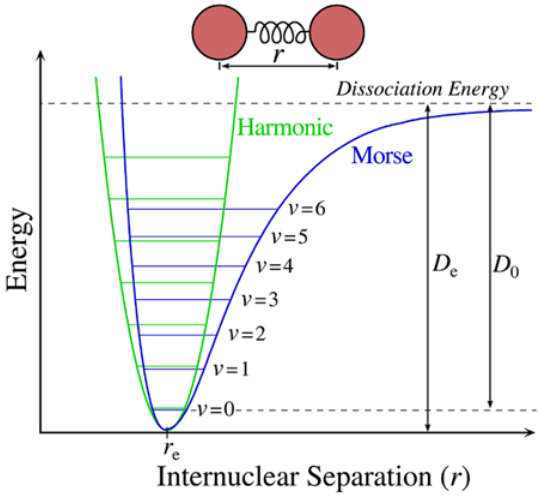

The Hooks law potential on the other hand is based on the ideal spring

$$F = -kx$$

with x as the displacement from equilibrium ($x = r - r_{eq}$). This leads to the harmonic oscillator or Hooks's law parabolic curve (green curve above) when integrating the definitions of the potential

$$F(x) = -\frac{dV(x)}{dx}$$

in one dimensional space. This integration results in

$$V(r) = \frac{1}{2}k(r - r_{eq})^2$$

The Harmonic and Morse potentials resemble each other for small displacements (x) from equilibrium. Solving the Schrödinger equation for the Harmonic Oscillator potentials results in the energy levels going as

$$E_v = \left(v + \frac{1}{2}\right) h\nu_e$$

with $v = 0, 1, 2, 3 \ldots \infty$ and

$$\nu_e = \frac{1}{2\pi}\sqrt{\frac{k}{\mu}}.$$

The Morse potential is an anharmonic potential that exhibits a more complicated expression for the vibrational energy levels.

$$E_v = h\left[\left(v + \frac{1}{2}\right) v_e - \left(v + \frac{1}{2}\right) \chi_e v_e\right] + \ldots \tag{3.1.1}$$

plus other smaller terms.

The second term in Equation 3.1.1 is the **anharmonic coupling** (deviations from the Harmonic Oscillator). The χ_e term is a parameter that depends on details of $V(r)$, D_e etc. Because of the 2nd term, the vibrational energy level spacing get closer together as v increases. For a Harmonic Oscillator, the spacings are equal.

Selection Rule for Vibrational Transitions

1. The vibrational molecule must interact with the oscillating electric field of the electromagnetic radiation, in order for a transition to take place. This means that there must be a change in the electric dipole moment for the particular transition.

$$\left(\frac{d\mu}{dr}\right)_{r_{eq}} \neq 0$$

   The derivative of the mode with respect to the displacement must not equal zero.
2. $\Delta v = +1$ (for absorption of radiation). This is rigorously true for a Harmonic Oscillator, but for any anharmonic oscillator (e.g. Morse Potential), then Δv=+2 (first overtone) transitions can occur. As well as the 2nd overtone Δv=+3. The frequencies of the 1st and 2nd overtones provides information about the potential surface (i.e. χ_e can be determined.
3. For a diatomic, since μ is known, measurement of ν_e provides a value for k, the force constant.

$$k = \left(\frac{d^2V(r)}{dr^2}\right)_{r_{eq}}$$

   The force constant is an **important parameter**, since it gives an indication of the strength of the bond.

Isotope Effects

Replacing of an atom with an isotope, had negligible effects on k, but will affect μ. The stretching vibrational of $\mathrm{H-Cl}$ will be reduced by ~1.3 to 1.4 in frequency when H is substituted with D. This is because μ is increased by a factor of 2 and thus ν_e is decreased by $\sqrt{2}$.

3.2: Polyatomic Molecules

These have many more ways to vibrate (vibrational degrees of freedom) than a diatomic that had only one. Each bond can vibrate **(stretch)**, and each pair of bonds attached to a common atom can **bend**. These motions are all described by their individual force constants., but these individual bonds stretches and bends are all coupled together so that all atoms vibration together in converted set of frequencies, call the normal modes frequencies. These group vibrations themselves are called normal modes. The normal modes and the force constants are not easy to find, but require a procedure called normal mode analysis.

Details behind normal mode analysis are beyond what we have time to develop in this course. Anyone who wants to really learn the mathematics behind this method should consult the classical textbook by Wilson, Decius and Corss, “Molecular Vibrations” or look at chapter 6 in Drago.

The gist is as follows: If we have a diatomic molecule, we can solve the force constant since we can measure the vibrations frequency and calculate the reduced mass, knowing the masses of the atoms. This is a principle problem which becomes more complicated in a polyatomic molecule. **We must task first, how many Normal Modes are there?** These normal modes are linear combinations of the possible Cartesian displacement of each atoms.

The normal modes of vibration are: asymmetric, symmetric, wagging, twisting, scissoring, and rocking for polyatomic molecules.

Symmetric Stretching	Asymmetric Stretching	Wagging
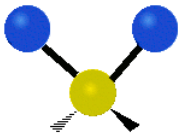	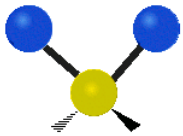	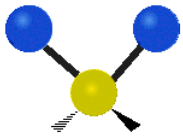
Twisting	**Scissoring**	**Rocking**
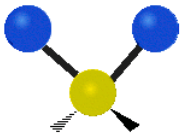	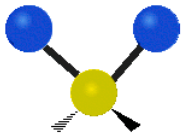	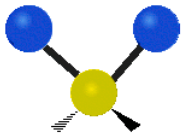

Figure 3.2.1: Six types of Vibrational Modes. Images used with permission (Public Domain; Tiago Becerra Paolini).

Calculate Number of Vibrational Modes

Degree of freedom is the number of variables required to describe the motion of a particle completely. For an atom moving in 3-dimensional space, three coordinates are adequate so its degree of freedom is three. Its motion is purely translational. If we have a molecule made of N atoms (or ions), the degree of freedom becomes 3N, because each atom has 3 degrees of freedom. Furthermore, since these atoms are bonded together, all motions are not translational; some become rotational, some others vibration. For non-linear molecules, all rotational motions can be described in terms of rotations around 3 axes, the rotational degree of freedom is 3 and the remaining 3N-6 degrees of freedom constitute vibrational motion. For a linear molecule however, rotation around its own axis is no rotation because it leave the molecule unchanged. So there are only 2 rotational degrees of freedom for any linear molecule leaving 3N-5 degrees of freedom for vibration.

The degrees of vibrational modes for **linear molecules** can be calculated using the formula:

$$3N-5 \tag{3.2.1}$$

The degrees of freedom for **nonlinear molecules** can be calculated using the formula:

$$3N-6 \tag{3.2.2}$$

n is equal to the number of atoms within the molecule of interest. The following procedure should be followed when trying to calculate the number of vibrational modes:

1. Determine if the molecule is linear or nonlinear (i.e. Draw out molecule using VSEPR). If linear, use Equation 3.2.1. If nonlinear, use Equation 3.2.2
2. Calculate how many atoms are in your molecule. This is your N value.
3. Plug in your N value and solve.

Each of the normal modes must preserve the *center of mass* of the molecule, but not the bond lengths and angles. Each has a characteristic frequency that MAY be measured by IR or Raman spectroscopy. These are assumed to be known. There is a lot more involved in constructing Normal Modes, but we will ignore it for now in this class.

IR Spectra

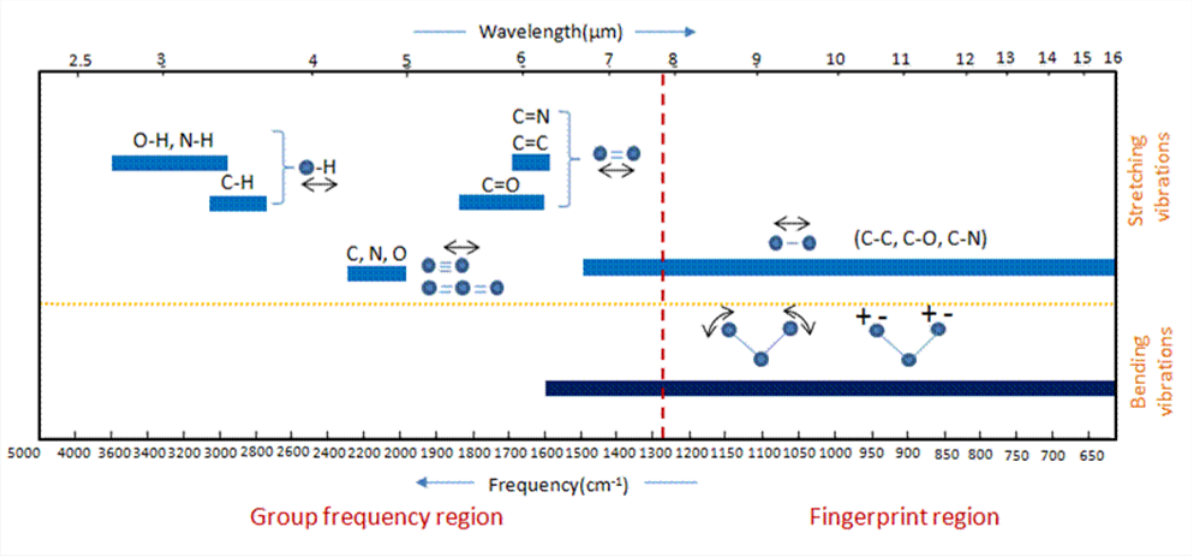

The region of the infrared spectrum from 1200 to 700 cm^{-1} is called the **fingerprint region**. This region is notable for the large number of infrared bands that are found there. Many different vibrations, including C-O, C-C and C-N single bond stretches, C-H bending vibrations, and some bands due to benzene rings are found in this region. The fingerprint region is often the most complex and confusing region to interpret, and is usually the last section of a spectrum to be interpreted. However, the utility of the fingerprint region is that the many bands there provide a fingerprint for a molecule.

Local vs. Normal modes

A useful tool for understanding vibrations is the concept of **normal modes**. These are patterns of vibration such that all components of a system move synchronously and with the same frequency, even if they do so in different directions. If a molecule is vibrating in a normal mode, its vibrational dynamics are straightforward: it continues to vibrate in the same pattern. More interesting is the situation where a polyatomic molecule vibrates in a pattern that is not a normal mode, e.g., when the vibration is localized on specific atomic positions or chemical bonds. These patterns are referred to as *local* modes, and their evolution in time is more challenging to predict and analyze.

- Water has three vibrational normal modes: the symmetric and asymmetric stretching modes, and a bending mode (below).
- These normal modes can be transformed to three local modes: two stretching modes describing the vibrations of the single OH bonds, and a bending mode.

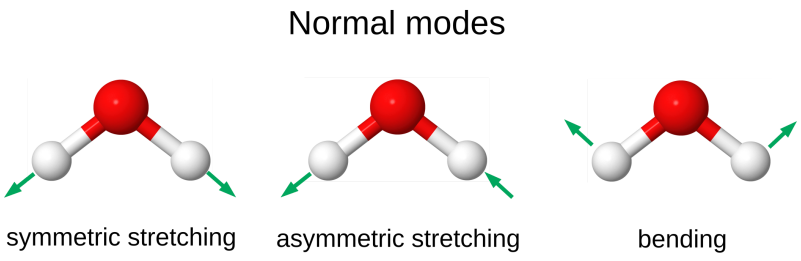

https://strawberryfields.ai/photonic..._dynamics.html

The idea of group vibrations has a certain usefulness attached to it – information about vibrational motions of a molecule can sometimes be obtained without having to resort to a full blown normal mode analysis. Can we pick a vibrational frequency out of a spectrum and assign it to a particular functional group e.g. CH_3-H, or CH_2=0 or -C=-H?

Often we can, and this is the basis for the IR analytical method of identifying substance and the present of functional group in molecules. An IR band is usually found near 1700 cm^{-1} in a molecule with a --C=0 group, that is assigned to the stretching vibration. But it varies by quite a bit, depending on the other features of the molecules (-+ 150 cm^{-1}).

If a particular group vibration involves largely a H, then deuteration will reduce the frequency of ~sqrt(2) confirming that the H is strongly involved. A good example of the interaction of group vibrations is the linear triatomic HCN. The displacement coordinate for the stretching are:

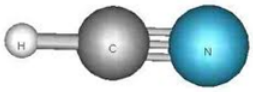

The individual force constants, F_{11} and F_{22} are such that the group frequencies are similar in the absence of coupling. In the absence of coupling, for L_{11}, imaging H and a rigid C=-N moving like a diatomic and for L_{22} imagine a rigid H-C and a N moving like a diatomic. The symmetry of these vibrations are the same, so they can interact. *Since the frequencies are similar, their interaction can be considerable.*

For HCN, the two stretching frequencies are found at **3313** and **2089 cm^{-1}**. For deuterated (D-CN), these are lower to **2629 cm^{-1}** and **1906 cm^{-1}**. If the 3313 cm^{-1} mode were a pure CH mode, it would have been reduced by sqrt(2) to **2360 cm^{-1}**; not quite as expected. But what of the 2089 cm^{-1} which could have been assigned as a “pure” CN stretch. It should have been reduced by only a minor factor about 2% (via reduced mass arguments). Actually, it was reduce by a factor of 1.1. This shows that the HC and the C-=N stretching vibrations are coupled in the normal modes and that the group vibration description is *oversimplified*. Since the deuteration has a larger effect on the higher frequency mode than the lower frequency, it is clear that the former has a larger contribution of C-H.

Chloroform

In chloroform ($CHCl_3$), the small peak at 3019 cm^{-1} has been assigned to the C–H stretching vibration. Below illustrates the isotope effect in this vibrational mode when hydrogen is replaced by deuterium. The heavier isotope lowers the frequency of the C–

H stretching vibration, which is well-described by the diatomic approximation (a local mode). The small Raman peak that appears just below 1205 cm^{-1} in the chloroform spectrum is attributed to the n_4 asymmetric-stretching vibration. This vibrational mode involves motion of the hydrogen atom and its vibrational frequency is also decreased as the result of deuterium substitution.

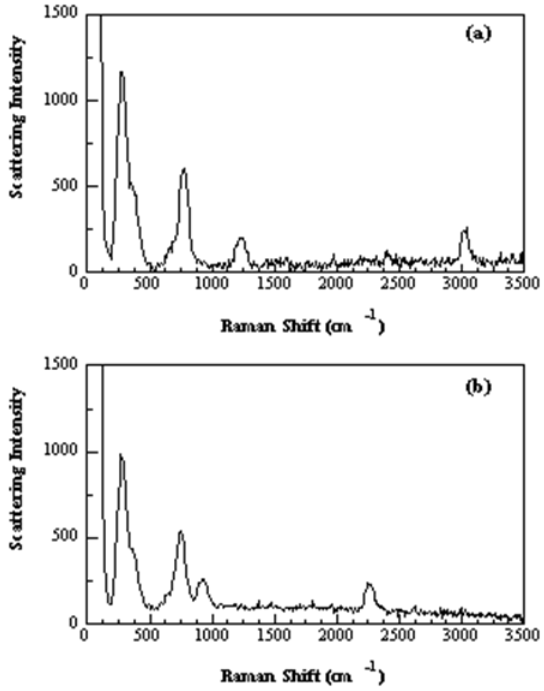

Figure 2. Raman spectra of neat chloroform (a) and deuterated chloroform (b).

3.3: Raman vs. IR Spectroscopies

IR spectra

The vibrations of molecules can either be detected by direct absorption, which requires that the change in the dipole moment with normal coordinate be not equal to zero.

$$\left(\frac{d\mu}{dq}\right)_{q_{eq}} \neq 0$$

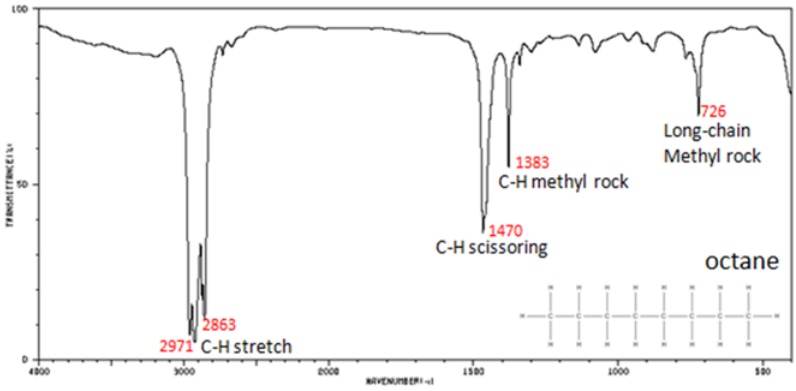

Infrared Spectrum of Octane

Raman

Or it can be detection by the Raman effect, which is the inelastic scattering of a high energy (visible or UV) photon. Vibrational frequencies can also be obtains by single level fluorescence (like vibronic features in the absorption spectrum).

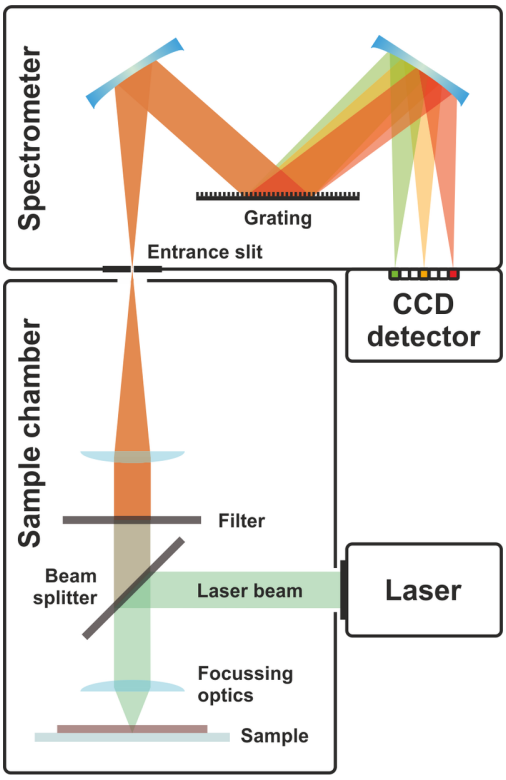

Schematic of one possible dispersive Raman spectroscopy setup. (CC BY-SA 4.0; Toommm via Wikipedia)

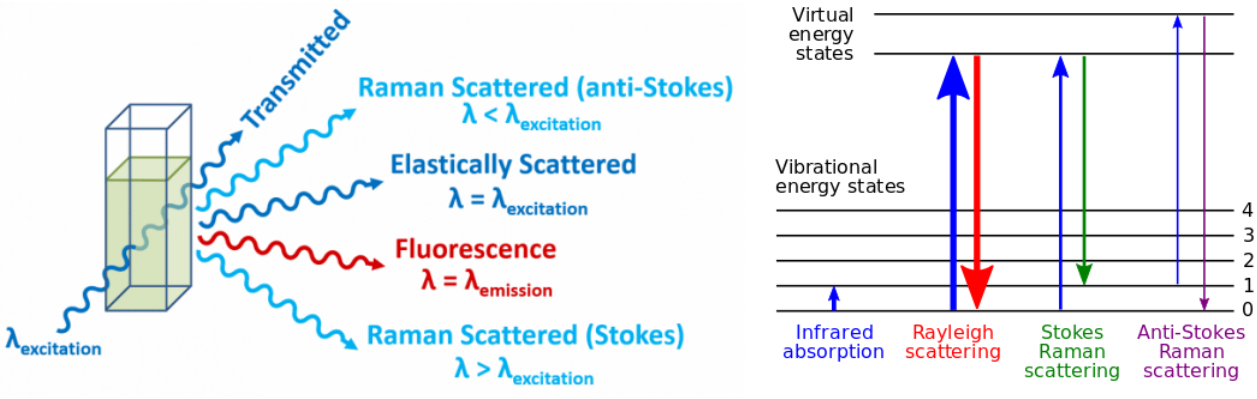

Energy-level diagram showing the states involved in Raman spectra. CC BY-SA 3.0; Moxfyre, via Wikipedia).

Energy level diagram showing the states involved in Raman signal. The line thickness is roughly proportional to the signal strength from the different transitions.

Requirement for Raman transition to be observed

The intensity of the light scatter from a molecule depends upon the size of the induced dipole moment, which depends on the oscillating electric fiends, *E* of the radiation and the polarizability α. We can write

$$\vec{D} = \alpha \vec{E}$$

where $\vec{D}$ is a vector and α is the **polarizability tensor** whose elements depends on the molecule (specifically the symmetry of the molecule).

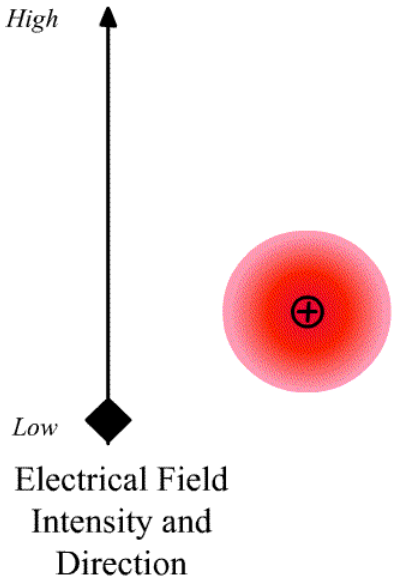

The polarizability tensor is defined:

$$\alpha = \begin{bmatrix} \alpha_{xx} & \alpha_{xy} & \alpha_{xz} \\ \alpha_{yx} & \alpha_{yy} & \alpha_{yz} \\ \alpha_{zx} & \alpha_{zy} & \alpha_{zz} \end{bmatrix}$$

The elements describing the response parallel to the applied electric field are those along the diagonal. A large value of {\displaystyle \alpha _{yx}}{\displaystyle \alpha _{yx}} here means that an electric-field applied in the {\displaystyle x}x-

direction would strongly polarize the material in the {\displaystyle y}y-direction. Explicit expressions for {\displaystyle \alpha }\alpha have been given for homogeneous anisotropic ellipsoidal bodies.

$\vec{D}$ is responsible for the Raleigh Scattering, which is the *elastic* scattering of the same frequency as the incident radiation. Raman (inelastic) scattering will occur at:

$$\nu - \nu_0$$

Where ν_o is the frequency of the normal mode q_o. If there is a change in the polarizability of the molecule for a small displacement around equilibrium (q_{eq}) with respect to the normal mode coordinate (q).

$$\alpha = \alpha_0 + \left(\frac{\partial \alpha}{\partial q}\right)_0 q + \ldots$$

where

- α_0 is the polarizability at the equilibrium position and
- $\left(\frac{\partial \alpha}{\partial q}\right)_0$ is the rate of change of the polarization wrt the coordinate evaluated at the equilibrium position

The Raman activity and Raman intensity of a particular normal mode are determined from the polarizability tensors for that mode, whereas infrared activity/intensity are determined from dipole moment tensors. These relationships are shown diagrammatically below, where α is the polarizability, μ is the dipole moment, and q is the motional coordinate associated with a particular normal mode. Note that the intensity, I of the transition, is proportional to:

- $(d\alpha/dq)_0$ for Raman
- and $(d\mu/dq)_0$ and infrared activity.

The zero subscript indicates that the derivative is evaluated at the equilibrium (ground state) condition of the motional coordinate.

Carbon Dioxide

Using the carbon dioxide molecule (a molecule with a center of inversion) as an example, the diagrams below show that the symmetric stretching mode of CO_2 has a non-zero $d\alpha/dq)_0$ but a zero value for $d\mu/dq)_0$, while the antisymmetric stretching mode has a non-zero $d\mu/dq$ but a zero value for $(d\alpha/dq)_0$.

For the symmetric stretch in $\mathrm{CO_2}$, the α increases along z axis.

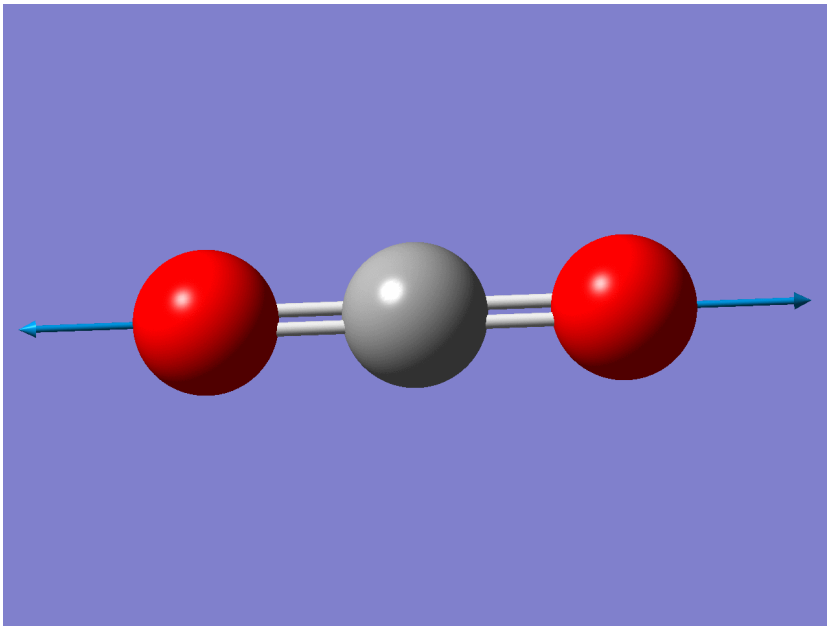

https://imgur.com/gallery/vnmaBrJ

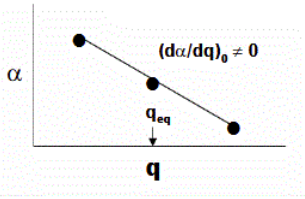

As the mode vibrates, the electron cloud changes and the polarization changes

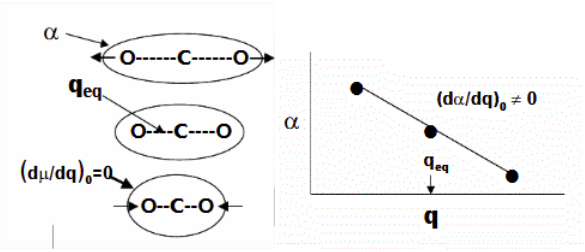

This a Raman Active mode since

$$\left(\frac{\partial \alpha}{\partial q}\right)_0 \neq 0$$

This a IR Inactive mode since

The dipole moment of the molecule does not change during the vibration due to symmetry.

$$\left(\frac{d\mu}{dq}\right)_o = 0$$

For the asymmetric stretch in CO_2, there is no change in α_{zz} (or any other components) *for small displacements*.

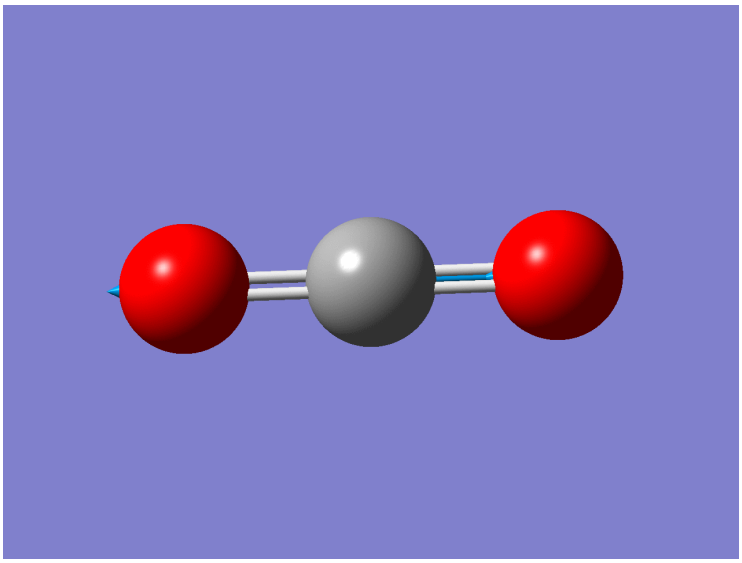

As the mode vibrates, the electron cloud changes and the polarization changes and the dipole moment.

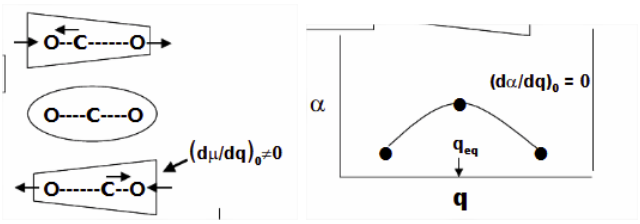

Raman Inactive

This a Raman Inactive mode since

$$\left(\frac{\partial \alpha}{\partial q}\right)_0 = 0$$

This a Raman Active mode since

The dipole moment of the molecule does not change during the vibration due to symmetry.

$$\left(\frac{d\mu}{dq}\right)_o \neq 0$$

In the actual spectra of CO_2, the symmetric stretch appears in the Raman spectrum but not in the infrared spectrum, and the antisymmetric stretch appears in the infrared but not the Raman. In a qualitative sense one can see that the polarizability ellipsoids in the stretched and compressed states of the symmetric stretch are not equivalent (in shape and volume), whereas they are for the antisymmetric stretch.

Comparison

We will see later how group theory helps us to decide about which transitions are *IR* active with

$$\left(\frac{d\mu}{dq}\right)_{q_{eq}} \neq 0$$

and which are *Raman* active with

$$\left(\frac{d\alpha}{dq}\right)_{q_{eq}} \neq 0$$

Unfortunately, a transition in a particular mode may be “Active" from a symmetry point of view, but the actual change in α or μ may be so small that the transition may not be observed. In IR and Raman, we often do not see all the predicted active vibrations.

3.4: Resonant Raman Spectroscopy

In the previous discussion of Raman spectroscopy, the incident laser wavelength is not in resonance with the electronic transition, hence it is often referred to as non-resonant Raman scattering like below.

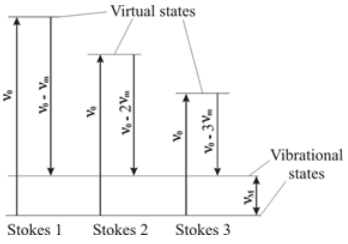

If ν_o is tuned close to ν_{el}, the frequency of an electronic transition, normal modes that are *vibronically active* in the electronic transition are intensified in the Raman scattering. This is called the resonance Raman effect, because ν_o comes close to being in resonance with ν_{el}. Because the laser photon can be absorbed by a real electronic state, and not a virtual state, the interaction of photons with vibrational is enhanced and there is a greater probability of the molecule being vibrationally excited after scattering. If the absorption is electronically allowed, mostly totally **symmetric modes** appear in the Raman spectrum.

Advantages

1. Intensity is enhanced – allows measurements of dilute samples (i.e., metal centers of metalloproteins)
2. Spectrum is simplified. Only a few vibrations are enhanced. Selects only vibrations that are associated with absorbing chromophores (or specifically the electronic transition).
3. Long progression of a vibration are the often observed enabling the vibrational potential energy to be specified over large range of ν. This enables a greater description of the vibrational potential energy surfaces for the probe molecule.

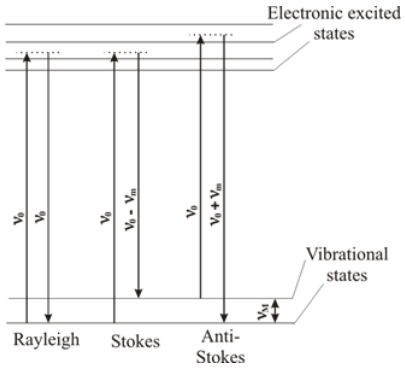

Disadvantage

- Local heating that perturbs the sample during Raman Probing!
- Also *fluorescence* can obscure signals

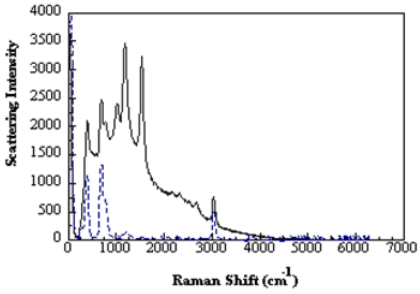

Solid line: Resonance Raman spectrum of *b*-carotene in chloroform. The emission envelope of a fluorescent impurity is visible underneath the spectrum. Dashed line: Non-resonant Raman spectrum of neat chloroform taken under the same conditions.

Inducing a Dipole via the Polarizability Tensor (simple math)

The simple undergraduate description of polarizability, α, is that it is a scalar whose amplitude describes the amplitude of the induced dipole moment on a molecule via an applied electric field, which is a vector oriented along its polarization (presuming linear polarization here). Hence:

$$\bar{\mu}_{ind} = \alpha \bar{E}$$

And the amplitude of the induced dipole moment is oriented directly along the **same orientation** as the polarization of the applied electric field. However, α is not really a scalar, but is a 2-rank tensor (matrix) consisting of **nine** elements:

$$\alpha = \begin{vmatrix} \alpha_{xx} & \alpha_{xy} & \alpha_{xz} \\ \alpha_{yx} & \alpha_{yy} & \alpha_{yx} \\ \alpha_{zx} & \alpha_{xx} & \alpha_{zz} \end{vmatrix}$$

Now a simplification, the tensor is symmetric (i.e., $\alpha_{ij} = \alpha_{ji}$), so there are only **six** independent elements. α can be separated into two tensors:

$$\begin{vmatrix} \alpha_{xx} & \alpha_{xy} & \alpha_{xz} \\ \alpha_{yx} & \alpha_{yy} & \alpha_{yx} \\ \alpha_{zx} & \alpha_{zx} & \alpha_{zz} \end{vmatrix} = \begin{vmatrix} \alpha_{xx} & 0 & 0 \\ 0 & \alpha_{yy} & 0 \\ 0 & 0 & \alpha_{zz} \end{vmatrix} + \begin{vmatrix} 0 & \alpha_{xy} & \alpha_{xz} \\ \alpha_{yx} & 0 & \alpha_{yx} \\ \alpha_{x} & \alpha_{zx} & 0 \end{vmatrix}$$

The first matrix is the isotropic contribution to α and the second is the anisotropic. Using vectors along the X, Y and Z axis you can confirm that using only the isotropic component of α the induced dipole moment, $\vec{\mu}_{Pind}$, will be oriented **only** along the direction of $\vec{E}$. The off-diagonal elements of α induce a dipole moment in one direction when the applied electric field it oriented in a normal orientation. Hence the term **anisotropic** to describe this component.

Polarization of Raman Bands

If a symmetric molecule with isotropic polarizability (i.e. no off axis non-zero elements) is irradiated by a polarized laser radiation along y, and the molecule is observed along x, we will observe z polarized Raleigh scattering only.

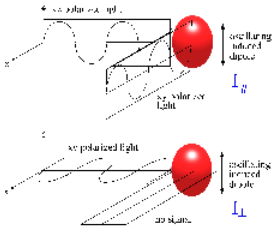

If α is **not** isotropic, induced dipole will have a component along y, and the scattering radiation is then partially or completely depolarized. **Generally, α is not isotropic and some depolarization is observed**. In Stokes Raman scattering, the polarization depends on the symmetry of the excited vibration. The following rules have been developed:

For liquid samples:

1. Even if α is isotropic, for a totally symmetric (e..g A_g) normal mode, the Raman scattered light is polarized.
2. For a non-totally symmetric normal mode, the scattered light is depolarized and we can construct a depolarization ratio:

$$\rho = \frac{I_y(\perp)}{I_x(\square)}$$

Depolarized means $\rho = 3/4$ (non-symmetric) and polarized mean $0 <= \rho <= ¾$ (only for totally symmetric modes).

Example 3.4.1: The Perchlorate Ion

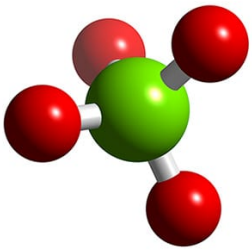

Below, we show the effect for the totally symmetric v_1 mode of the ClO_4^- ion. The figure shows the spectra obtained using both vertically polarized and horizontally polarized light. The large v_1 peak near 1000 cm^{-1} cannot be observed when the beam is horizontally polarized. The very small amount of scattered light observed at this wavelength in the horizontally polarized spectrum results from imperfect polarization of the laser beam.

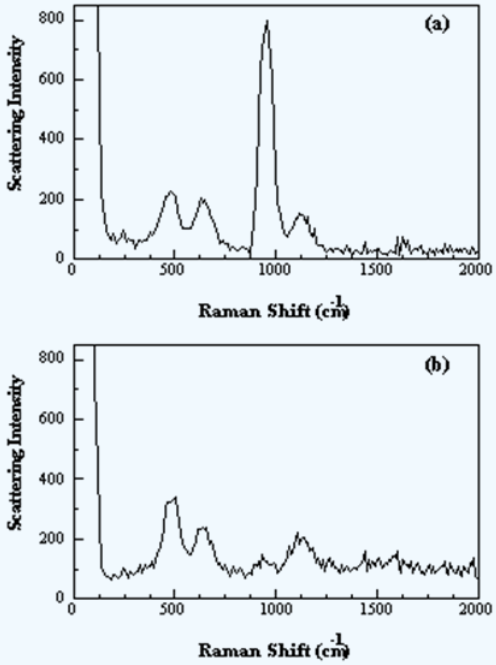

Figure 3. Raman spectra of a saturated solution of $NaClO_4$ with (a) vertically and (b) horizontally polarized light impinged on the sample. https://www.thevespiary.org/library/...10mW.Diode.pdf

3.5: Classification of Normal Modes

Normal modes are used to describe the different vibrational motions in molecules. Each mode can be characterized by a different type of motion and each mode has a certain symmetry associated with it. Group theory is a useful tool in order to determine what symmetries the normal modes contain and predict if these modes are IR and/or Raman active. Consequently, IR and Raman spectroscopy is often used for vibrational spectra.

The normal modes that come out of the normal mode analysis are grouped displacements (linear combination of displacement vectors). They have the characteristic that each has the symmetry of an irreducible representation of the point group of the molecule.

The linear combination of displacements vectors that describe a normal mode transform among themselves as irreducible presentation of the point group of the molecule

We will not review how these irreducible representations are formed for each normal mode. We begin with the primitive Cartesians vectors on each atom. There are thus 3N vectors in the basis. This produced a 3N-dimensional (reducible, normally) representation of the group. We need that X_{3N} for each group operation to use the reduction formula. Check out: https://sites.cns.utexas.edu/jones_c...odes-vibration

Water

Let's begin with an example: H_2O, which is a C_{2v} molecule.

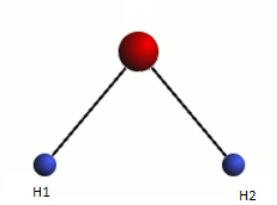

Water belongs to the C_{2v} symmetry group and has the following symmetry elements:

- $\hat{E}$
- $\hat{C}_2(z)$
- $\hat{\rho}_v(xy)$
- $\hat{\rho}_{v'}(yz)$

Its character table is shown below.

C_{2v}	E	C_2^z	σ_{xz}	σ_{yz}	h = 4
A_1	1	1	1	1	$z,\ x^2,\ y^2,\ z^2$
A_2	1	1	−1	−1	xy, R_z
B_1	1	−1	1	−1	x, xz, R_y
B_2	1	−1	−1	1	y, yz, R_x
Γ_{tot}	−9	−1	1	3	

The Cartesian vectors form the basis of a 9-dimensional representation (three dimensions on each atom).

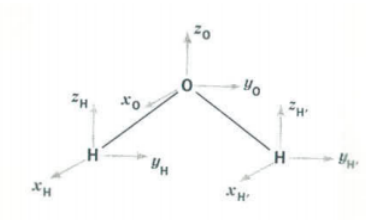

A symmetry analysis for water begins by determining how these 9 coordinates behave under the symmetry operations of the C_{2v} group. You should be able to show that this generates the reducible representation Γ_{tot}, which is given in the last row of the

character table shown above. Γ_{tot} can also be calculated as

$$\Gamma_{uma}\left(\Gamma_x+\Gamma_y+\Gamma_z\right),$$

where Γ_{uma} is the behavior of the atoms under the symmetry operations of the group. Of the 9 degrees of freedom possessed by the water molecule, three are for translation of the center of mass in the x-, y- and z-directions, and three are related to rotation about the x-, y-, and z-axes. This leaves three vibrational degrees of freedom. To determine the symmetry of the vibrational modes we decompose Γ_{tot} into the unit vectors or irreducible representations of the C_{2v} character table. This involves taking the dot product of Γ_{tot} with each of the irreducible representations of the C_{2v} symmetry.

$$\Gamma_{tot}\mathrm{A}_1=\frac{[(9)(1)+(-1)(1)+(1)(1)+(3)(1)]}{4}=3$$
$$\Gamma_{tot}\mathrm{A}_2=\frac{[(9)(1)+(-1)(1)+(1)(-1)+(3)(-1)]}{4}=1$$
$$\Gamma_{tot}\mathrm{B}_1=\frac{[(9)(1)+(-1)(-1)+(1)(1)+(3)(-1)]}{4}=2$$
$$\Gamma_{tot}\mathrm{B}_2=\frac{[(9)(1)+(-1)(-1)+(1)(-1)+(3)(1)]}{4}=3$$

This procedure has revealed the that the reducible representation, Γ_{tot}, is composed of the following irreducible representations:

$$\Gamma_{tot}=3\mathrm{A}_1+\mathrm{A}_2+2\mathrm{B}_1+3\mathrm{B}_2$$

From the right side of the character table we see that translation and rotation have the following symmetry properties:

$$\Gamma_{trans}=\mathrm{A}_1+\mathrm{B}_1+\mathrm{B}_2$$
$$\Gamma_{rot}=\mathrm{A}_2+\mathrm{B}_1+\mathrm{B}_2$$

From this information we can determine the symmetry properties of the vibrational modes of the water molecule.

$$\Gamma_{vib}=\Gamma_{tot}-\Gamma_{trans}-\Gamma_{rot}=2\mathrm{A}_1+\mathrm{B}_2$$

There are three vibrational fundamentals. And, since there are two bonds there will be two stretching vibrations and one bending vibration. To determine which symmetry classification the bend belongs to, examine how the H-O-H bond angle transforms under the symmetry operations of the C_{2v} group.

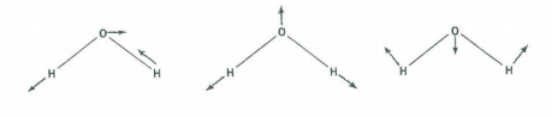

The vibrational modes are shown above. Convince yourself that their symmetry properties are captured in the table below.

C_{2v}	E	C_2^z	σ_{xz}	σ_{yz}	
Γ_{bend}	1	1	1	1	A_1
$\Gamma_{stretch}$	1	1	1	1	A_1
$\Gamma_{stretch}$	1	−1	−1	1	B_2

Therefore, the stretches have A_1 symmetry and the bend has B_2 symmetry.

Predict three vibrational normal modes, $2a_1+b_2$. The two totally symmetric normal coordinates are linear combinations of symmetric stretch and bend (https://people.chem.ucsb.edu/laverma...water_vib.html).

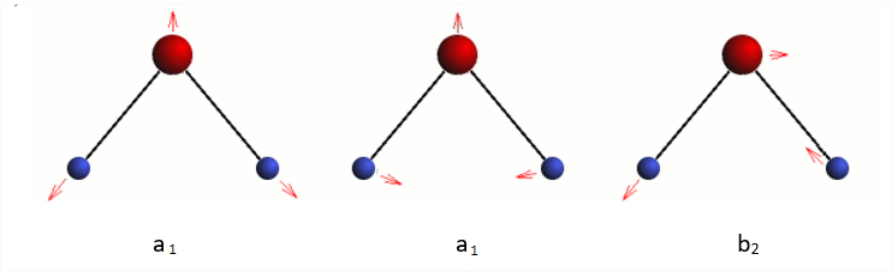

One of the two a_1 modes is mostly the stretch (high frequency), while the other is mostly the bend (lower frequency). The b_2 is the unsymmetrical stretch.

Other Molecules

Determination of normal modes becomes quite complex as the number of atoms in the molecule increases. Nowadays, computer programs that simulate molecular vibrations can be used to perform these calculations.

The example of $[PtCl_4]^{2-}$ shows the increasing complexity. The molecule has five atoms and therefore 15 degrees of freedom, 9 of these are vibrational degrees of freedom. The nine normal modes are exemplified below along with the irreducible representation the normal mode belongs to (D_{4h} point group).

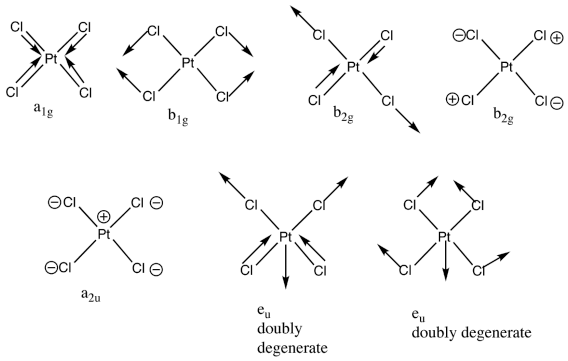

A_{1g}, b_{1g} and e_u are stretching vibrations whereas b_{2g}, a_{2u}, b_{2u} and e_u are bending vibrations.

3.6: IR and Raman Activity

Selection Rule for IR

Recall, that for IR activity, we require that

$$\left(\frac{d\mu}{dq}\right)_{q_{eq}} \neq 0$$

If motion along the normal coordinate does not change the dipole moment, the transition is forbidden. In order for μ to be changed by the normal coordinate, at lease on of the following must be non-zero!

$$\langle v=0|\hat{x}|v\neq 0\rangle$$

$$\langle v=0|\hat{y}|v\neq 0\rangle$$

$$\langle v=0|\hat{z}|v\neq 0\rangle$$

integrated over q, the normal coordinate. **This is since μ is a vector that transforms as x, y, z in the point group**. The polarization of the IR transition is determined by which transition integral is *non-zero*. This is very much like the criterion for an electronically allowed transition.

All $|v=0\rangle$ are a_1 (totally symmetric) and $|v=1\rangle$ has the same symmetry as the singly excited normal mode, q. Since

$$A_1 \otimes \Gamma_{x,y,z} \otimes \Gamma_q \supset A_1$$

The transition will be IR active if the normal mode symmetry belongs to the same irreducible representation as x, y, or z for the point group of the molecule. This can be applied immediately to H_2O.

Example 3.6.1: Water

Water has three vibrational modes.

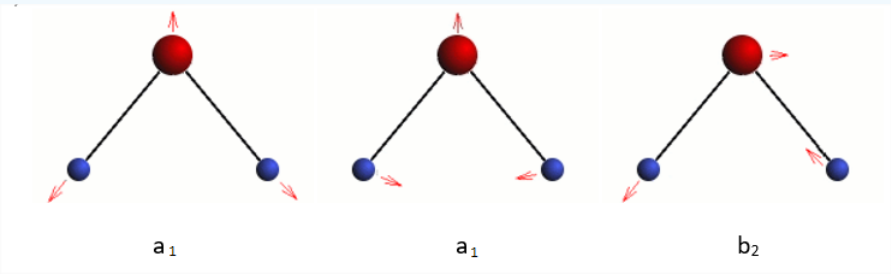

Three normal modes of water

Whether any of these modes is active in the infrared region of the spectrum is the question. This is determined by evaluating the quantum mechanical transition probability integral,

$$P = e\int \Psi^f(vib)\hat{q}\,\Psi^i(vib)d\tau$$

where q is the spatial coordinate and is either x, y, or z. If this integral is non-zero the transition is allowed. Group theory enables us to determine if the integral is non-zero as follows. We evaluate the direct product (note the similarity to the quantum mechanical transition probability integral) $\Gamma_{vib}{}^f\Gamma_q\Gamma_{vib}{}^i$ and if it turns out to be equal to, or contain, the irreducible representation A_1 then the transition is allowed. If the direct product isn't equal to or contain A_1 then the transition is forbidden.

$\Gamma_{vib}{}^i$, the representation for the ground state is always equal to A_1 and $\Gamma_{vib}{}^f$ is always equal to A_1 and $\Gamma_{vib}{}^f$ has the symmetry of the vibrational mode being excited, which in our case is either A_1 or B_2. Thus we can see that a vibrational mode will be infrared active if it belongs to the same symmetry species as one of the Cartesian coordinates. You should verify that this is correct and also be able to show that all three vibrational modes of the water molecule are infrared active.

Selection Rule for Raman

Recall, for Raman activity, there must be a change in the polarizability with respect to the normal mode.

The components of the polarizability transform as the quadratic functions of x,y,z. i.e. x^2, y^2, z^2, xy, xz, yz or combinations thereof (x^2-y^2). Thus we require that for the polarizability operator to transform as one of the quadratic terms e.g.

with

Thus since has the same symmetry as the singly excited normal mode, **q**. The transition integrals we know and love will be:

for at least one representation of polarization. At least one quadratic form transforms as each one of the irreducible representations. Therefore, all possible vibrations of any C_{2v} molecule will be Raman allowed. But what about other point groups?

Centrosymmetric molecules – exclusion rules

There are important examples for which the IR allowed and Raman allowed transitions are mutually exclusive. There are molecules having a center of inversion. In this case, there normal coordinates, q, must be either g or u, depending on their behavior toward the $\hat{i}$ operation. Thus $|v=1\rangle$ must be either g or u, while $|v=0\rangle$ will always be g.

In centrosymmetric molecules, the x,y,z operators are *u*-operators, while all components of $\hat{P}$ are *g*-operators (go look it up on the O_h point group character table!) i.e.

$$\hat{x}^2 = (-x)^2 \quad \therefore \text{ g symmetry}$$

$$\hat{x} = -(-x) \quad \therefore \text{ u symmetry}$$

This symmetry behavior leads to the rule for centrosymmetirc molecules. Excitation of g-normal modes are forbidden in the IR, while excitation of *u*-normal modes are forbidden in Raman.

Example 3.6.1

Carbon Dioxide is a linear triatomic molecule with 3N-5=4 normal modes:

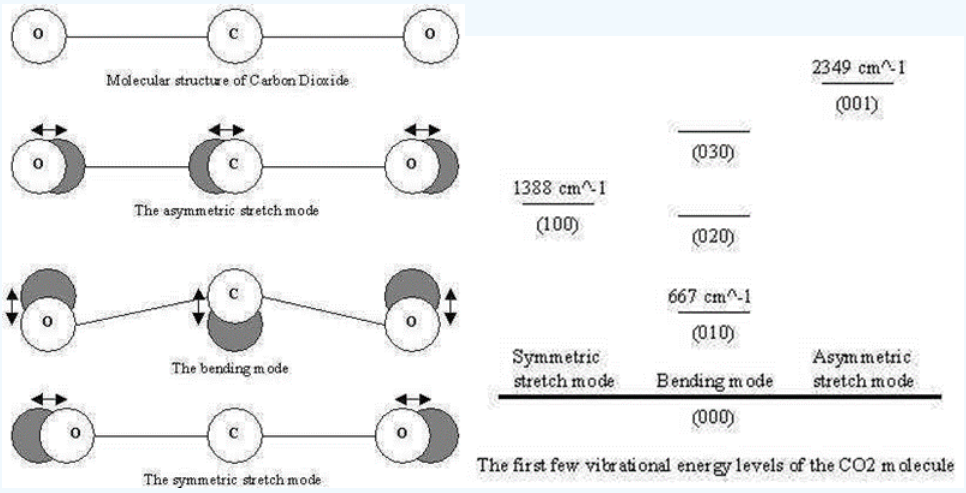

e.

The point group is $D_{\infty h}$ and the irreducible representations are Σ_g^+, \Sigma_{u}^{+}, and Π_u respectively. Thus only asymmetric stretch and bends are found in the IR, while only the symmetric stretch is found in Raman spectra.

The IR spectrum of CO_2 (4.0 kPa total pressure) is shown below. Note these extra bands: v_3+v_1=3610 cm^{-1} and v_3+2*v_2=3710 cm^{-1}

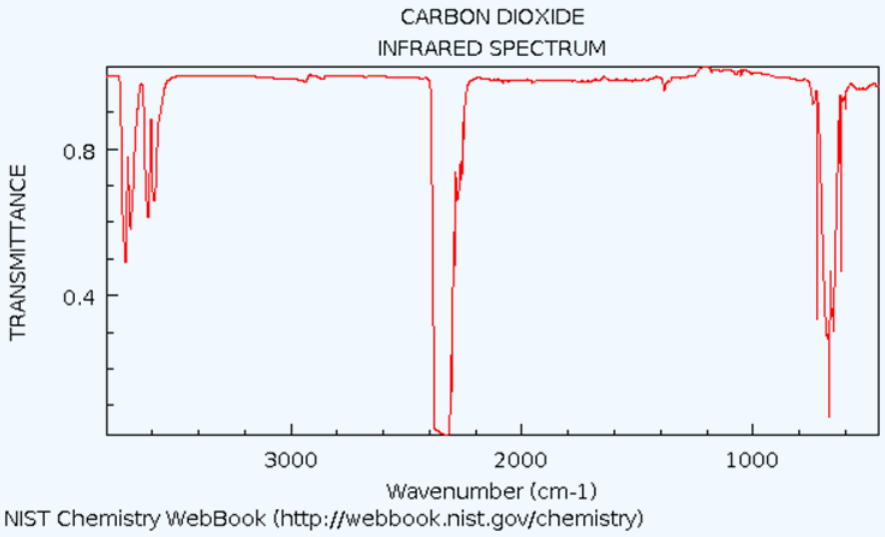

Vibrational frequency nomenclature

The $3N-5$ (5) fundamental frequencies are usually numbered sequentially, ν_1, ν_2, ν_3,.. ν_{3N-6}. The convention is that the highest frequencies of totally symmetric vibrations in ν_1 follow all other totally symmetric vibrations in order of *decreasing* frequency. Once all totally symmetric vibrations are numbers, the next number goes to the highest frequency non-symmetric vibration.

For H_2O:

- ν_1 is the “symmetric stretch”
- ν_2 is the “asymmetric stretch”
- ν_3 is the “symmetric bend”

Exception, the bending mode of a linear molecule is ν_2

For CO_2:

- ν_1 is the “symmetric stretch”
- ν_2 is the “symmetric bend”
- ν_3 is the “asymmetric stretch”

If IR and Raman spectra consisted only of fundamental and overtones, spectra would be easier to assign, but combinations bands, $\nu_1 \pm \nu_2$ and overtones $2\ \nu_1$ also appear, complicating the assignment of the fundamental frequencies.

3.7: Non-Fundamental Transations - Hot Bands, Combination Bands, and Fermi Resonances

Hot bands

Hot bands are observed when an already excited vibration is further excited. For example an v_1 to v_1' transition corresponds to a hot band in its IR spectrum. These transitions are temperature dependent, with lower signal intensity at lower temperature, and higher signal intensity at higher temperature. This is because at room temperature only the ground state is highly populated (kT ~ 200 cm^{-1}), based on the Boltzmann distribution. The Boltzmann distribution states that if molecules in thermal equilibrium occupy two states of energy ε_j and ε_i, the relative populations of molecules occupying these states will be,

$$\frac{n_j}{n_i} = \frac{e^{-\varepsilon_j/RT}}{e^{-\varepsilon_i/RT}} = e^{-\Delta\varepsilon/RT}$$

where k is the Boltzmann constant and T is the temperature in Kelvin.

In the harmonic oscillator model, hot bands are impossible to distinguished from fundamental transitions because the energy levels are equally spaced. Because the spacing between energy levels in the anharmonic oscillator decrease with increasing vibrational levels, the hot bands occur at lower frequencies than the fundamentals. Also, the transition moment integrals are slightly different since the ground state will not necessarily be totally symmetric since it is not in $v = 0$.

For a simple three vibration system, a hot band transition would look like this:

$$\psi^1(0)\,\psi^2(0)\,\psi^3(1) \rightarrow \psi^1(0)\,\psi^2(0)\,\psi^3(2)$$

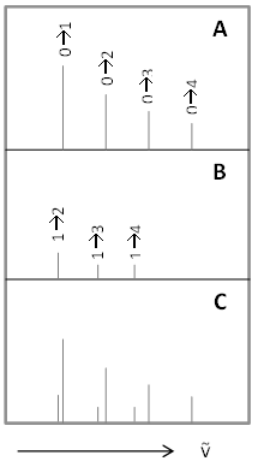

Example of hot bands in a vibrational line spectrum of a diatomic molecule: (A) harmonic frequencies; (B) hot band transitions; (C) combination of both spectra.

Combination Bands

It frequently occurs that particular fundamental may not occur for symmetry reason (above) , but it can be excited in combinations with a different normal mode, because the **doubly excited state** has a symmetry that is allowed by IR (or Raman) selection rules. This shares some similarity to vibronic coupling in electronic transitions.

For a simple three vibration system, A combination transition would look like this:

$$\psi^1(0)\,\psi^2(0)\,\psi^3(0) \rightarrow \psi^1(1)\,\psi^2(1)\,\psi^3(0)$$

The thing to keep in mind is that a doubly vibrationally excited state normal modes q_1 and q_2 have a wavefunction with symmetry

$$\Gamma_{q_1} \otimes \Gamma_{q_2}.$$

Example 3.7.1: Boron Trifluoride

BF_3 is of symmetry D_{3h} (see https://people.chem.ucsb.edu/laverma...e/BF3_vib.html).

- The symmetric stretch, ν_1, is of symmetry A_1' and is IR inactive (x, y transform a E', while z transforms as A_2").
- The ν_2 vibration of symmetry A_2" and double degenerate E' vibrations ν_3 (ν_4).

A combination band is formed at frequency ν_1 + ν_3. The symmetry of this doubly excited band is the direct product of constituent modes:

$$\Gamma_{v_1} \otimes \Gamma_{v_2} = A_1' \otimes E' = E'.$$

and the transition $\nu_1 + \nu_3$ is allowed and x, y-polarized. This ν_2 vibration is IR active since q_2 transforms as A_2" as does the $\hat{z}$ operator so the ν_2 vibration is z-polarized.

Overtones

The Harmonic Oscillator approximation predicts that there will be only one line the spectrum of a diatomic molecule, and while experimental data shows there is in fact one dominant line-the fundamental--there are also other, weaker lines. How can we account for these extra lines?

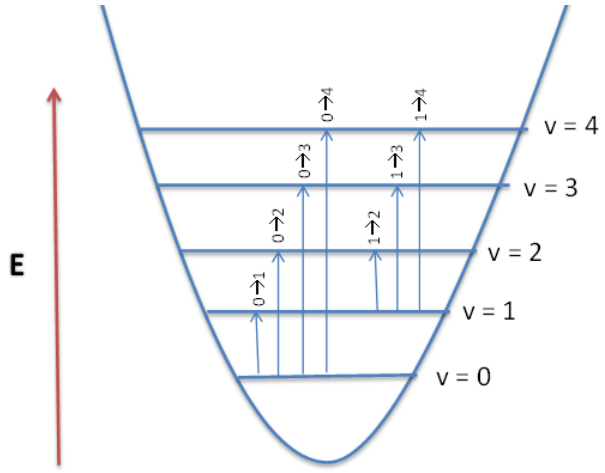

A diagram for a vibrating diatomic molecule. The levels denoted by vibrational quantum numbers v represent the potenital energy for the harmonic (quadratic) oscillator. The transition $0 \rightarrow 1$ is fundamental, transitions $0 \rightarrow n$ (n>1) are called overtones, and transitions $1 \rightarrow n$ (n<1) are called hot transitions (hot bands).

These transitions are called **overtones**. For a simple three vibration system, An overtone transition would look like this:

$$\psi^1(0)\,\psi^2(0)\,\psi^3(0) \rightarrow \psi^2(0)\,\psi^2(2)\,\psi^3(0)$$

In the IR spectrum, overtone bands are multiples of the fundamental absorption frequency. As you can recall, the energy levels in the Harmonic Oscillator approximation are evenly spaced apart. Energy is proportional to the frequency absorbed, which in turn is proportional to the wavenumber, the first overtone that appears in the spectrum will be twice the wavenumber of the fundamental. That is, first overtone $v = 1 \rightarrow 2$ is (approximately) twice the energy of the fundamental, $v = 0 \rightarrow 1$. This is demonstrated with the vibrations of the diatomic HCl in the gas phase.

Table 1: HCl vibrational spectrum.

Transition	Term	$\tilde{\nu}_{obs}$ [cm^{-1}]	$\tilde{\nu}_{Harmonic}$ [cm^{-1}]	$\tilde{\nu}_{Anharmonic}$ [cm^{-1}]
$0 \rightarrow 1$	fundamental	2,885.9	2,885.9	2,885.3
$0 \rightarrow 2$	first overtone	5,668.0	5,771.8	5,665.0
$0 \rightarrow 3$	second overtone	8,347.0	8,657.7	8,339.0
$0 \rightarrow 4$	third overtone	10,923.1	11,543.6	10,907.4

Transition	Term	$\tilde{\nu}_{obs}$ [cm^{-1}]	$\tilde{\nu}_{Harmonic}$ [cm^{-1}]	$\tilde{\nu}_{Anharmonic}$ [cm^{-1}]
$0 \rightarrow 5$	fourth overtone	13,396.5	14,429.5	13,370

We can see from Table 1, that the anharmonic frequencies correspond much better with the observed frequencies, especially as the vibrational levels increase.

Example 3.7.2: Boron Trifluoride II

BF_3 is of symmetry D_{3h} (see https://people.chem.ucsb.edu/laverma...e/BF3_vib.html).

- The symmetric stretch, ν_1, is of symmetry A_1' and is IR inactive (x, y transform a E', while z transforms as A_2").
- The ν_2 vibration of symmetry A_2" and double degenerate E' vibrations ν_3 (ν_4).

The first overtone of ν_2 ($2\nu_2$) is a state with symmetry

$$A_2'' \otimes A_2'' = A_1'$$

and is **not allowed** in the IR, but the next overtone

$$A_2'' \otimes A_2'' \otimes A_2'' = A_2''$$

is symmetry allowed with z-polarization. The A_1' fundamentals are allowed in Raman as is the first overtone of ν_2 .

Fermi Resonance

Fermi resonance is the shifting of the energies and intensities of absorption bands in an infrared or Raman spectrum. It is a consequence of quantum mechanical wavefunction mixing.

Requirements

Two conditions must be satisfied for the occurrence of Fermi Resonance:

- The two vibrational modes of a molecule transform according to the same irreducible representation in their molecular point group. In other words, the two vibrations must have the same symmetries (Mulliken symbols).
- The transitions coincidentally have very similar energies.

Sometime a vibrationally excited state can have a nearby same frequency; e.g. ν_1 + $2\nu_2$ in CO_2. Since ν_1 = 1340 cm^{-1} and ν_2= 2(667) = 1334 cm^{-1} these states can interact – **provided** a component of has the same symmetry as ν_1. This phenomenon is call a **Fermi Resonance**. The interaction, as expected, looks something like the splitting we observed in a MO's for the 1s atomic orbital in H_2.

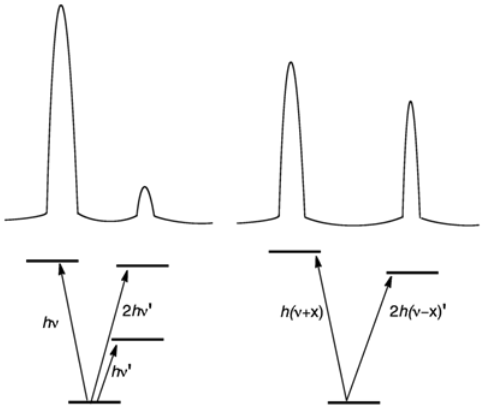

Figure 3.7.5: Fermi Resonance (Public Domain; Smokefoot via Wikipedia)

These state are mixture of $|1,0\rangle$ and $|0,2\rangle$ with $|v_1,v_2\rangle$ the as the wavefunction for the molecule (vib.). So mixing gives:

$$|up\rangle = a|10\rangle + b|02\rangle$$

$$|low\rangle = b'|10\rangle + a'|02\rangle$$

The for the linear CO_2 molecules, the symmetry so these states are

$$\Gamma_{10} = \Sigma_g^+$$

and

$$\Gamma_{02} = \Pi_u \otimes \Pi_u$$

which in the D_{3h} point group is

$$\Sigma_g^+ + \Sigma_g^- + \Delta_g$$

this **contains the totally symmetry** Σ_g^+ representation.

So

$$\Gamma_{02} = \Pi_u \otimes \Pi_u$$

contains the same symmetry as

$$\Gamma_{10} = \Sigma_g^+$$

thus a Fermi resonance is allowed (still the similarity in energies is naturally required).

The v_1 fundamental is allowed by Raman, as is $2v_2$ and, but the latter is expected to be weak being an overtone. However, both $|up\rangle$ and $|$ low $\rangle$ bands of the Fermi Resonance doublet are intense since they both contain a large amount of $|1,0\rangle$.

3.8: Fourier Transform IR Spectroscopy

The invention of the FFT algorithm lead to its practical application to IR Spectroscopy. Today, an inexpensive 4000-400 cm^{-1} FTIR can compute a spectrum in ~0.2s. In contrast to the frequency domain spectrometers discussed in class regarding, the FTIR measures the data in time and converts it to frequency. In mathematics, Fourier analysis is a subject area which grew out of the study of Fourier series. The subject began with trying to understand when it was possible to represent general functions by sums of simpler trigonometric functions. The attempt to understand functions (or other objects) by breaking them into basic pieces that are easier to understand is one of the central themes in Fourier analysis. http://www.newport.com/store/genContent.aspx/Introduction-to-FT-IR-Spectroscopy/405840/1033

Most often, the unqualified term Fourier transform refers to the transform of functions of a continuous real argument, such as time (t). In this case the Fourier transform describes a function f(t) in terms of basic complex exponentials of various frequencies. In terms of ordinary frequency ν, the Fourier transform is given by the complex number:

$$F(v) = \int_{-\infty}^{\infty} f(t) \cdot e^{-2\pi i v t}\, dt \tag{3.8.1}$$

The inverse FT is

$$f(t) = 2\pi \int_{-\infty}^{\infty} F(v) \cdot e^{+2\pi i v t}\, dt$$

There are differing expressions of this depending on how you want to normalize, or if you are talking in terms of angular frequency (ω or natural frequency ν, with $\omega = 2\pi\nu$).

The FT can be expanded into a sum of two functions: the cosine and the sine via the Euler equation:

$$e^{ix} = \cos(x) + i\sin(x) \tag{3.8.2}$$

Combining Equations 3.8.2 and 3.8.1 results in

$$\begin{aligned} F(v) &= \int_{-\infty}^{\infty} f(t) \cdot e^{-2\pi i v t} dt \\ &= \int_{-\infty}^{\infty} f(t) \cdot \cos(-2\pi v t) dt - i \int_{-\infty}^{\infty} f(t) \cdot \sin(-2\pi v t) dt \end{aligned}$$

This can be re-written using simple trig properties (to avoid unnecessary negative signs) to

$$F(v) = \int_{-\infty}^{\infty} f(t) \cdot \cos(2\pi v t) dt + i \int_{-\infty}^{\infty} f(t) \cdot \sin(2\pi v t) dt$$

What does this mean? The function $f(t)$ can be converted from a basis that is in localized δ functions (e.g. the value of y at the exact point x with no width associated with it) to a different basis set consisting of delocalized sinusoids sines and cosines). This is a transform and there are many other basis sets out there to transform data (e.g. Lorentz transform with exponential decays or wavelets which use localized trig functions etc.).

Now back to instrumentation. How do we measure IR spectra in time? With an interferometer with works as follows.

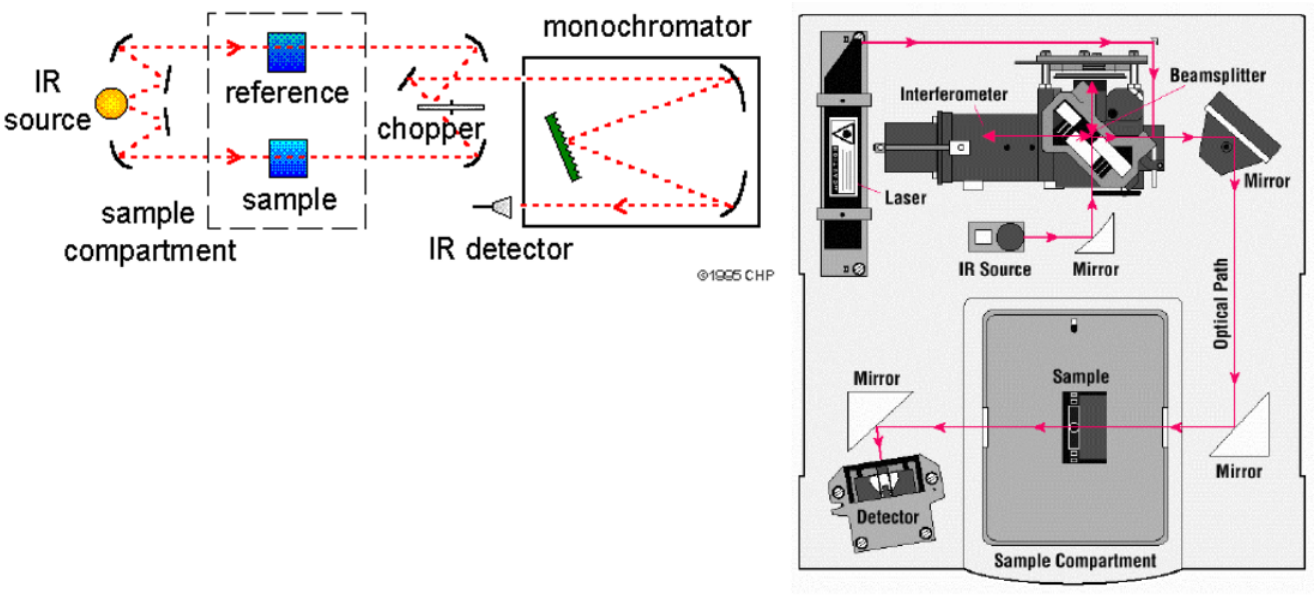

Figure 3.8.1: (left) A dispersive IR instrument and (right) A FTIR instrument

For example, a single wavelength, λ, from the source and the beam is split by a ½ reflection mirror (a beam splitter). ½ of the output goes to a stationary mirror and the other ½ goes to a moving mirror. Both halves are reflected back to the beam splitter resulting in some of the light going to the sample and detector.

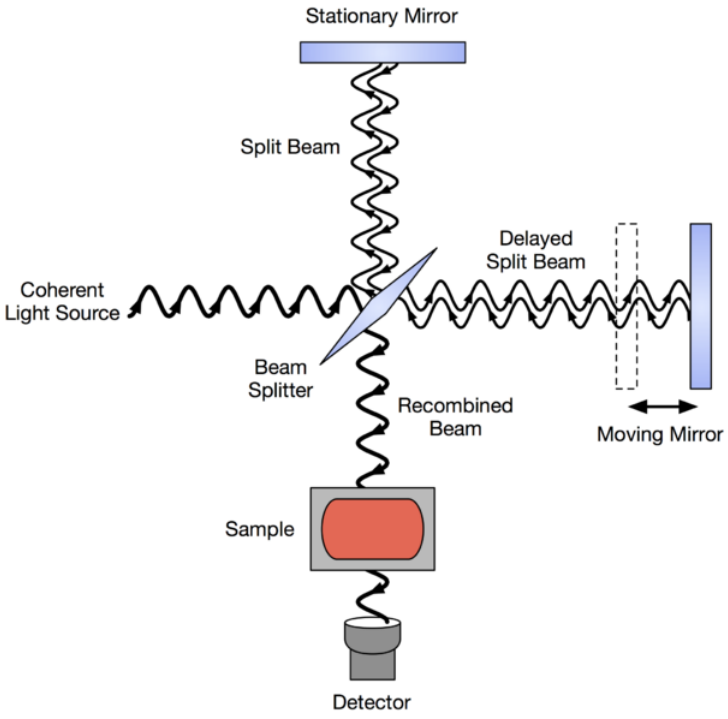

Interferometer for FTIR (Public Domain; Sanchonx via Wikipedia)

If the pathlength is equal (δ = retardation = optical phase difference (OPD) = 0), then the beams (or specifically the oscillating light from each path) recombine in phase and we have a maximum at the detector (ignoring the sample). If the movable mirror is displaced by $\lambda/4 = x$, then $\delta = 2x = \lambda/2$ and the beams are out of phase and no or little light is measured at the detector. When $\delta = \lambda$, we have constructive interference again, etc. If we plot $I(\delta)$, the intensity measured on the detector vs. δ we get a cosine plot of wavelength λ.

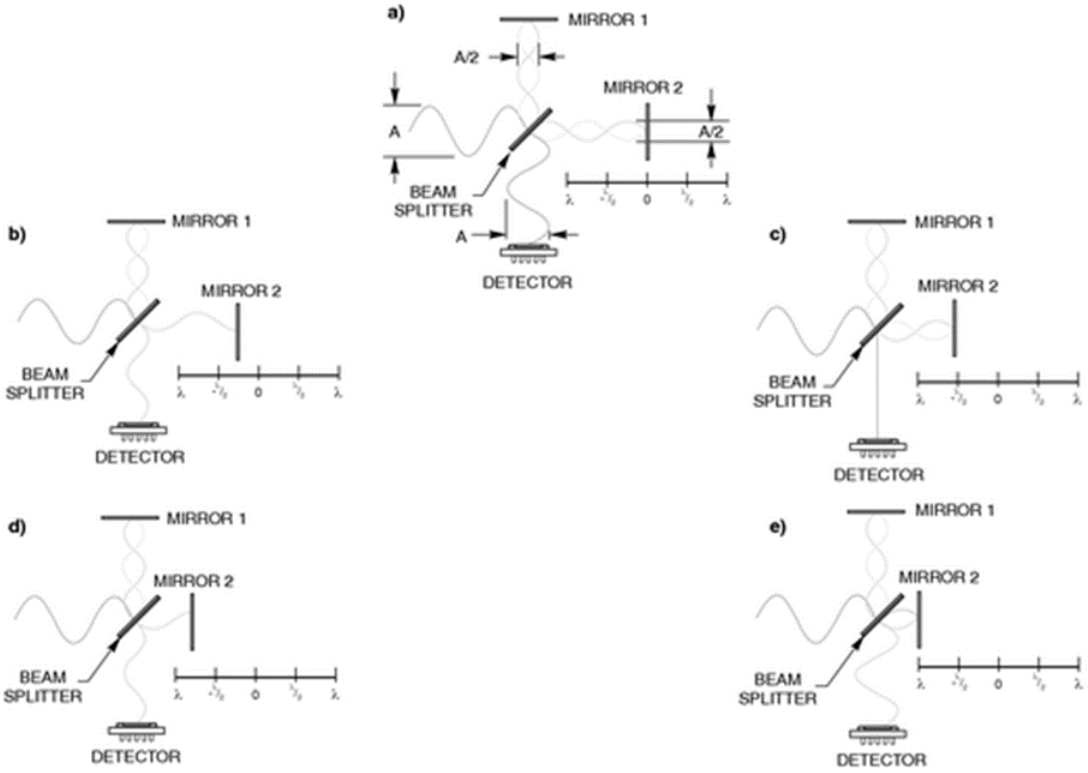

Figure 3.8.5: Schematic representation of waves and their phases, input, output, and the two arms of the interferometer as the scan goes from zero path difference condition to $\delta = \lambda$. (a) $\delta = 0$ case. (b) $\lambda/4\delta$ case. (c) $\lambda/2\delta$ case. (d) $3\lambda/4\delta$ case. (e) $1\lambda\delta$ case.

That was with one monochromatic light source, whereby physically moving the moving arm of the interferometer tells you about the wavelength of the incident light. Now what about more colors (wavelengths):

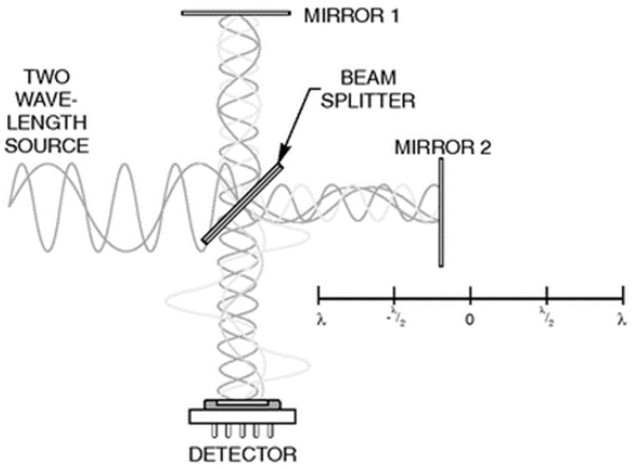

Figure 3.8.8: Two wavelength sources.

Now δ is the inverse of $\tilde{\nu}$, the wavenumber of the measured light, just as velocity and time are inverses of each other. The retardation and $\tilde{\nu}$ are relate by a **Fourier Transform**. Let $B\tilde{\nu}$ be the Fourier Transform of the interferogram $I(\delta)$. (https://www.colby.edu/chemistry/NMR/...erfourier.html)

A Dichromatic FTIR Spectrometer

Imagine a light source that emits only two discreet frequencies of light $\bar{u_1}$ and $\bar{u_2}$ of equal intensity (Figure 1).

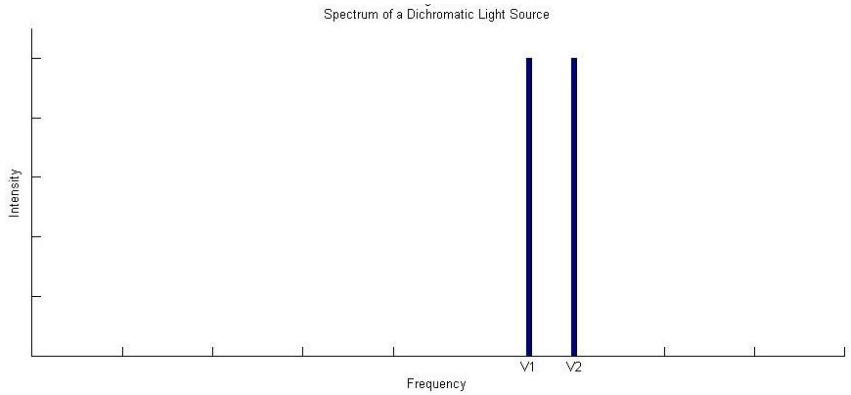

Figure 3.8.1: Dichromatic spectrum. $\bar{\nu_2} - \bar{\nu_1} = 0.1$. Passing these two frequencies through the Interferometer (without an absorbing sample), and measuring the interference with a light sensitive detector gives the intensity interferogram shown in red in Figure 2. The horizontal axis in Figure two is the delay of the movable mirror in the interferometer (z), and the vertical axis is arbitrary.

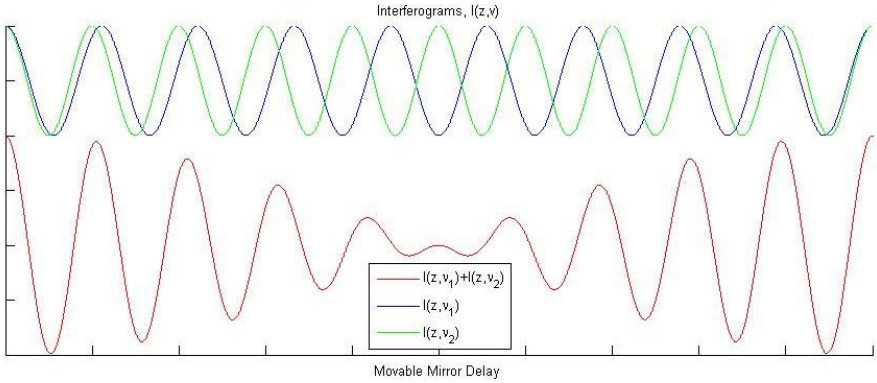

Figure 3.8.2: Interferogram (red), and the two frequencies (blue and green). The total distance on the movable mirror delay axis is $10\lambda_1$ or $(\lambda_2$.

Now imagine we place an absorbing sample in our interferometer, and that it absorbs light at either $\bar{\nu_1}$ or $\bar{\nu_2}$, although we do not know which one yet. The result on the measured interferogram is given in blue in Figure 3 (with the reference interferogram from Figure 2 given in green).

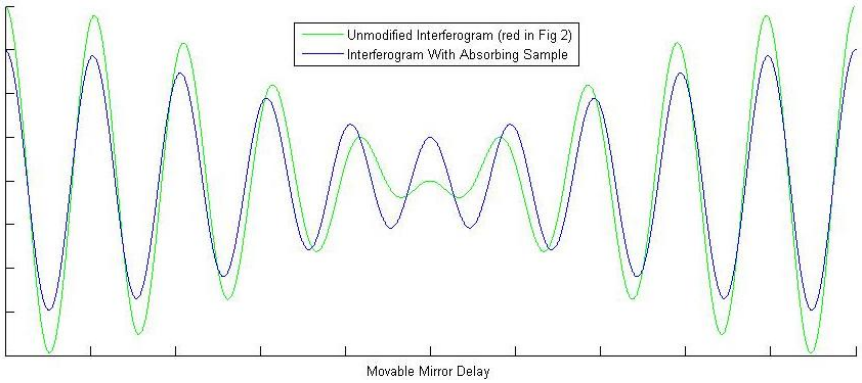

Figure 3.8.3: Interferogram with absorbing sample (blue), and background interferogram (green). Notice there is a clear difference when one of the frequencies is partially absorbed.

These two interferograms are all we need from the instrument! Now comes the FT of the FTIR. Fourier transforms will be covered in more detail in the next section. For now just think of it as a black box function in which you plug in an interferogram and get out a spectrum. Figure 1, therefore, is the Fourier transform of the red interferogram in Figure 2. Performing a Fourier transform on the measured blue interferogram in Figure 3 gives the spectrum in Figure 4.

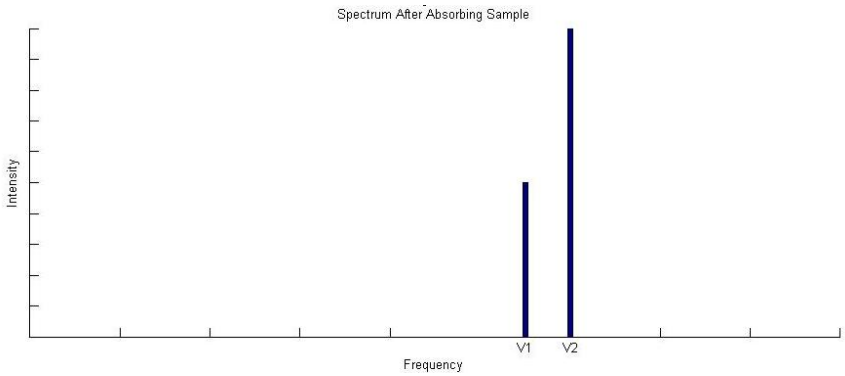

Figure 3.8.4: Spectrum that reached the detector after the absorbing sample. This spectrum is the Fourier transform of the blue curve in Figure 3. Comparing this spectrum to the one in Figure 1 shows a clear absorption at $\bar{u_1}$.

By comparing the spectrum in Figure 4 to Figure 1, we can immediately deduce that our absorbing sample absorbs light at frequency $\bar{u_1}$, and the FTIR spectrometer has done its job. Fundamentally thats all there is to it. The FTIR spectrometer takes light of various wavelengths, and measures an reference interferogram. You then place your absorbing sample into the interferometer and measure the interferogram again. Finally you Fourier transform both interferograms, and compare the spectra to determine what frequencies of light the sample is absorbing.

The next sections work on developing a more complete description of the the measured spectra, and the instrument nuances that factor into your data manipulation. To do this, however, we will need to open up the black box we put the Fourier transform in, and get an idea of how it works.

Fourier Transforms

From the previous section we saw that Fourier Transforms (in the context of FTIR) take an interferogram and produce a spectrum. The last section also implicitly presented the idea that the interferogram measured by an FTIR interferometer is just the sum of the interferograms of all the constituent frequencies present in the source. The Fourier transform, then, must break down the interferogram to reveal these constituent frequencies telling us which are present and in what amount.

To make this as easy on ourselves as possible, the first step we can take is to shift a maximum value of the interferogram to the origin. This ensures that it will be inherently cosine in nature (cos(0) = 1 vs sin(0)=0). As we will see in the phase error section below, this also assumes a symmetric interferogram, which you will not generally have.

Now that our interferogram is symmetric about the origin, all we need to do (all the Fourier transform does) is product it with a large variety of cosines to see which fit. The idea behind this is quite simple. If we luck out and hit our interferogram with a cosine that exactly matches one of our constituent frequencies, we will get a $\cos^2(x)$ which is positive for all values of x. If we add up our $\cos^2(x)$ over all values of x we will get a large positive value.

All other cosines not equal to a cosine present in the interferogram will be positive for some x and negative for the rest. Adding the positive and the negative together for all x will give zero. Lets look at the simple case of an $\cos(x)$ interferogram tried against three different cosines and one cosine that exactly matches (Figure 5):

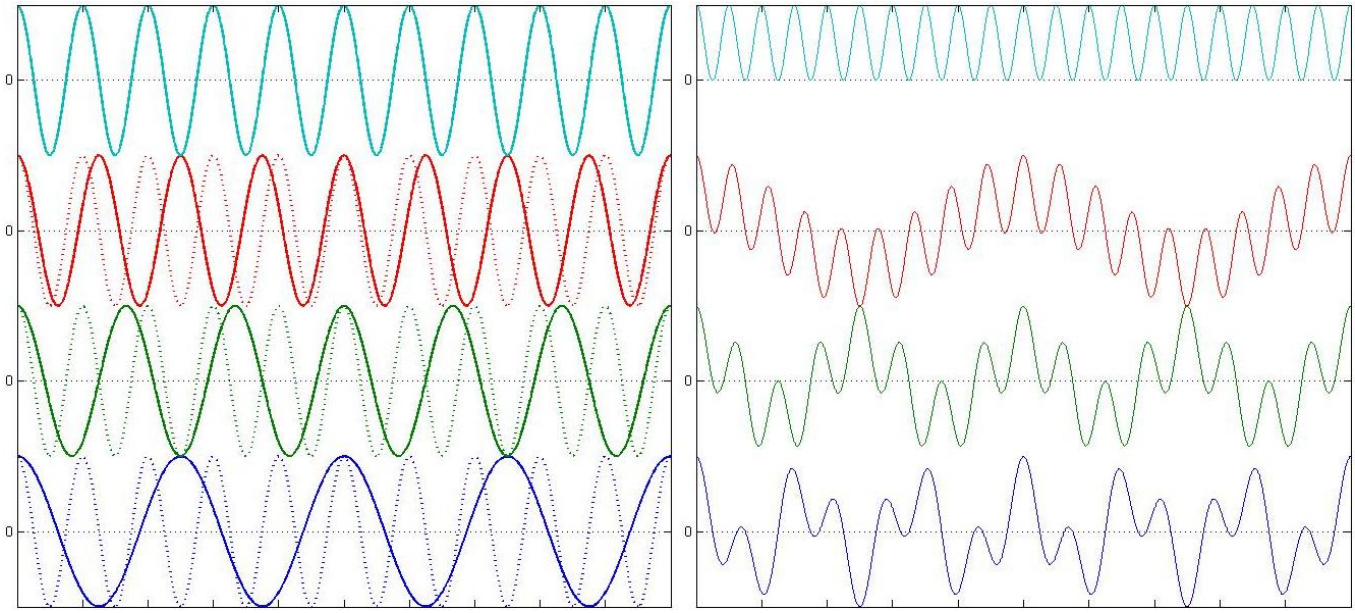

Figure 5a is shown. Notice that only the top (teal) curve has a large and positive area when measured over the entire window.

As you can see in 5b every cosine but the one that exactly matches the interferogram spends an equal amount of time above and below 0; such that if we were to add up the *area* under these curves, only the top (teal) one would be non-zero. We can also look at various test cosines against the interferogram from Figure 2, again ending in a cosine that matches one of the two frequencies present in that interferogram (Figure 6):

Polychromatic Light Sources

So far all we have considered are monochromatic and dichromatic FTIR spectrometers that have allowed us to use very simple interferograms. It might occur to you, however, that such instruments would not be terribly useful. We would need our samples to just happen to absorb at whatever frequency of light we selected for our interferometer. Real FTIR spectrometers don't use just two frequencies, but a whole continuum of light typically generated from a black body source (more on instrumentation here).

To get an idea of what this looks like for an interferogram lets see what happens when 5 and 50 frequencies of light interfere with equal intensities (Figure 7):

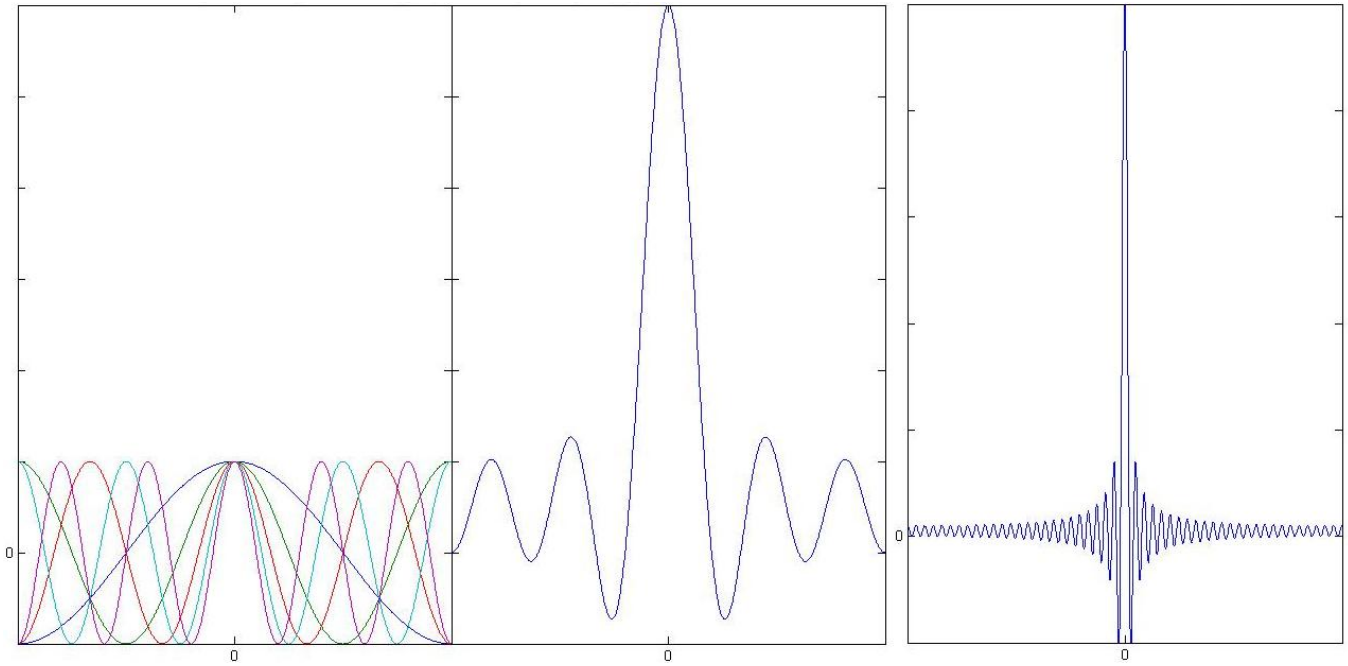

Figure 7b (right) shows the interference of 50 frequencies of with intensity.

Figure 7b already has the well defined centerburst of an actual interferogram. We have, however, left out a very important feature of blackbody sources. A blackbody source emits radiation in a continuous envelope described by Planks law, and this modifies our interferogram in a significant way (Figure 8).

If the source is continuous, as in a blackbody radiator, which is usually used, then we have the cosine transform of the Fourier Transform:

$$B(\tilde{v}) = \int_{-\infty}^{\infty} I(\delta) \cdot \cos(2\pi\tilde{v}\delta) d\delta$$

This is carried out by sampling the $I(\delta)$ through a sample window (range of δ). Then carry out the Fourier transform (or the cosine transform via the Fast Fourier Transform (FFT) algorithm.

$\Delta\tilde{v}$ is approximated by the FFT is the emission spectrum of the source. We then put in a sample, measure an interferogram – then do a FFT and subtract the two FT's to give the absorption spectrum by the difference.

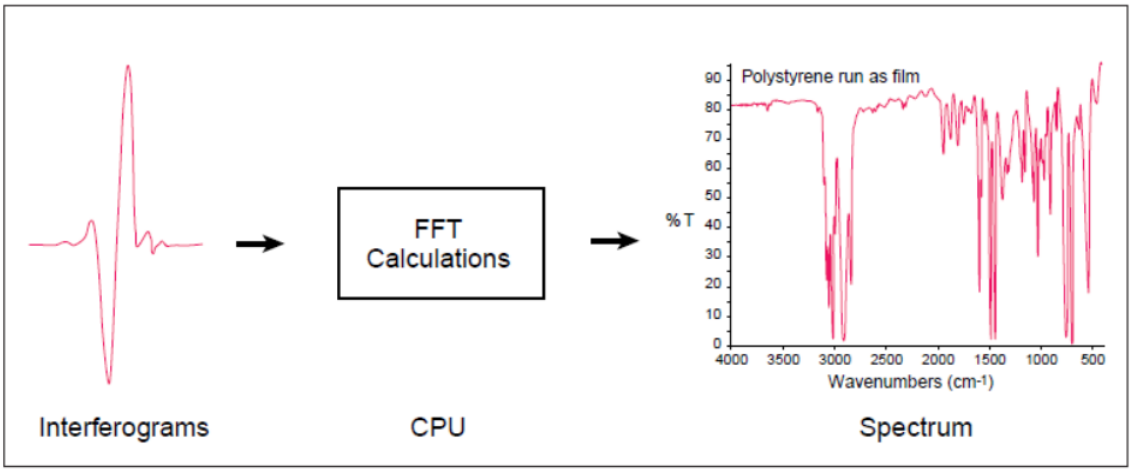

What is the maximum frequency measured in this setup? This in Fourier Analysis is called the **Nyquist wavenumber**, $\Delta\tilde{v}_n$ and is the highest frequency that you can measure in a FFT of a sample. This is given by

$$\tilde{v}_n = \frac{1}{2\Delta\delta}$$

where $\Delta\delta$ is the retardation sampling frequency (i.e. how often you sample).

? Exercise 3.8.1: Nyquist wavenumber

What is the ultimate resolution of $\Delta\tilde{v}$? Via Fourier analysis, this is giving via the length of the sampling window In this case,

$$\delta_{\max} = \Delta$$

And the best we can do is

$$\Delta\tilde{v} = 1/\Delta.$$

Recall that time à frequency Fourier Transform:

$$\Delta\tilde{v} \propto 1/ \text{ window lenth}$$

This is the instrumentation limit in FTIR.

✓ Example 3.8.1

If

$$\delta_{\max} = \frac{1}{2} \text{ cm}$$

and this is divided into 4096 (2^{12}) position slots, then

$$\delta = \frac{1}{8,000}\ \text{cm}$$

and therefore

$$\tilde{v}_n = 4000\ \text{cm}^{-1}.$$

The resolution is ~2 cm^{-1}.

3.9: Spectra of Gases - Rovibronic Transitions

IR spectroscopy of gases is special in that rotational fine structure contributes to the spectral lineshapes and can often be resolved – providing another layer of information to be obtained from the spectra about structure of the molecule. Rotational structure is not obtained in liquid and solids, because the molecules are not allowed to freely rotate by the intermolecular interactions (librations are hindered rotations in condensed phases) of the neighbors.

Just as the Born-Oppenheimer approximation allows us to separate electronic and nuclear motions, because electrons moves so much more rapidly than nuclear, the nuclear vibrations can be separated from molecular rotations, because their timescale is shorter. The Hamiltonian can be separated into two contributions:

$$H_{\text{tot}} = H_{\text{elect}} + H_{\text{rot}} + H_{\text{vib}}$$

Resulting in the nuclear energy being written as the sum of two contributions.

$$\varepsilon_{mc} = \varepsilon_{elect} + \varepsilon_{rot} + \varepsilon_{vib}$$

Let's consider only a diatomic for this discussion and ignoring electronic transitions (i..e, $\varepsilon_{elect} = 0$), so there is only one degree of vibrational freedom (a stretch) with a frequency of $\nu_\circ$, thus the

$$\varepsilon_{vib} = \left(v + \frac{1}{2}\right) h\nu_\circ$$

with $v = 0, 1, 2, 3 \ldots .$

Now, ε_{rot} can be obtained by considering that the diatomic is a pair of masses held together by a rigid bond (the rigid rotor approximation). The bond is not actually rigid, the atoms are vibrating naturally (with at least zero point motion), but because vibrations are fast, we can think of an "average" bond length. Solving the quantum mechanics for this system gives the following energy level manifold:

$$\varepsilon_{rot} = hBJ(J+1)$$

with $J = 0, 1, 2, \ldots$

where J is the rotational quantum number and B is the **rotational constant**, which depends on the moment of inertia, I.

$$B = \frac{h}{8\pi^2 I}$$

with

$$I = \mu \left\langle R^2 \right\rangle$$

μ is the reduced mass and $\left\langle R^2 \right\rangle$ is the mean square displacement of the bond length. Thus the total nuclear energy is

$$\varepsilon_{mc} = (v + 1/2)hv_0 + hBJ(J+1)$$

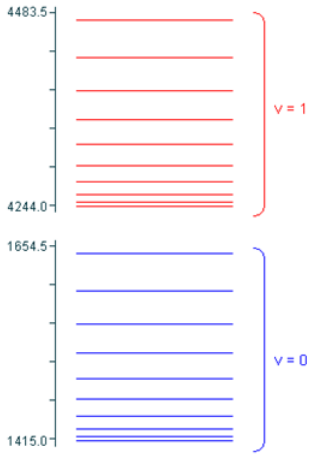

Occupations

The vibrational transitions from ground state vibration eigenstate to the next higher eigenstate is ($v = 0 \rightarrow v' = 1$), but the various rotational eigenstates are population thermally (far less than kT of 200 cm^{-1}), hence many different J state are initially populated in the sample. Now, a point of importance since we are going to do a little statistics. The eigenstates calculated from the harmonic oscillator are non-degenerate, meaning that each eigenstate corresponds to a signal energy and each energy (allowed) has only one eignestate. For the rotation rigid rotor, the eigenstates have a degeneracy of ($2J+1$). So while the ground rotational level has only one eigenstate (one vibrational and one rotation), the next higher energy ($V = 0$, $J = 1$) has three eigenstates associated with it.

✔ Example 3.9.1: Thermal population of rotational levels, a skirmish with statistical mechanics and the Boltzmann Distribution

A typical diatomic molecule might have $B\, 2 \times 10^{10}\ Hz$. What are the relative number of molecules in the $J = 5$ state?

Solution

This is just the application for the Boltzmann equations discussed before in class:

$$N_J = g_J e^{-\varepsilon_J / kT}$$

where g is the degeneracy for the J^{th} energy state and ε is the energy of that eigenstate. We can construct a ratio to answer this question

$$\frac{N_J}{N_{J=0}} = \frac{g_J e^{-\varepsilon_J / kT}}{g_{J=0}\, e^{-\varepsilon_{J-0} / kT}}$$

or

$$\frac{N_J}{N_{J=0}} = \frac{g_J}{g_{J=0}} e^{-(\varepsilon_J - \varepsilon_{J-0})/kT}$$

The energy for the $J = 5$ eigenstate is

$$\varepsilon_{rot} = hBJ(J+1) = hB5(5+1) = 30hB$$

For the $J = 0$, the energy is zero (note: there is no such thing as a zero point rotational energy)

So the different in energy between the two eigenstates is $30hB = 4 \times 10^{22}\ J/molecule$ or $240\ J/mole$. Now let's look at the degeneracy

$$g_{J=0} = 2J+1 = 1$$
$$g_{J=5} = 2J+1 = 11$$

So the relative population of the $J = 5$ level vs. the $J = 0$ level is

$$\frac{N_J}{N_{J=0}} = \frac{11}{1} e^{-(240)/8.34T} = \frac{11}{1}(0.9) = 10$$

So many rotational states are populated at room temperature, more so than non-rotating molecules.

Spectra

Three major types of transitions can be observed in this case (with a corresponding change in v):

1. $\Delta J = 0$. The photon initiates no change in the rotational quantum number. Transitions of this type are called **Q-branch** transitions
2. $\Delta J = +1$. The photon initiates an increase in the rotational quantum number. Transitions of this type are called **R-branch** transitions
3. $\Delta J = -1$. The photon initiates a decrease in the rotational quantum number. Transitions of this type are called **P-branch** transitions

These are the three major components of a vibrational transition of a molecule that has rotational levels in the vibrational transition (mostly gases).

Initial Approximation

B is the same for $v = 0$ and $v = 1$ (i.e., no change in the moment of inertia, hence average bond distance squared). What do the branches look like in this case?

Q-branch: $J' = J$ *Same Rotational Quantum number in the ground and vib. Excited state*

$$\begin{aligned} \Delta\varepsilon_{mc} &= h\nu_\circ + hB\left[J(J+1) - J'\left(J'+1\right)\right] \\ &= h\nu_\circ \end{aligned}$$

So all transitions will have same frequency regardless of initially population J levels!

R-branch: $J' = J+1$ *One more Rotational Quantum number in the vib. Excited state vs. the Ground state*

$$\begin{aligned} \Delta\varepsilon_{mc} &= h\nu_0 + hB\left[J(J+1) - J'\left(J'+1\right)\right] \\ &= h\nu_0 + hB[(J+1)(J+2) - J(J+1)] \\ &= h\nu_0 + 2hB(J+1) \end{aligned}$$

P-branch: $J' = J-1$ *One less Rotational Quantum number in the vib. Excited state vs. the Ground state*

$$\begin{aligned} \Delta\varepsilon_{mc} &= h\nu_\circ + hB\left[J(J+1) - J'\left(J'+1\right)\right] \\ &= h\nu_\circ + hB[J(J-1) - J(J+1)] \\ &= h\nu_\circ - 2hBJ \end{aligned}$$

As seen in Figure 1, the lines of the P-branch (represented by purple arrows) and R-branch (represented by red arrows) are separated by specific multiples of B (2B), thus the bond length can be deduced without the need for pure rotational spectroscopy.

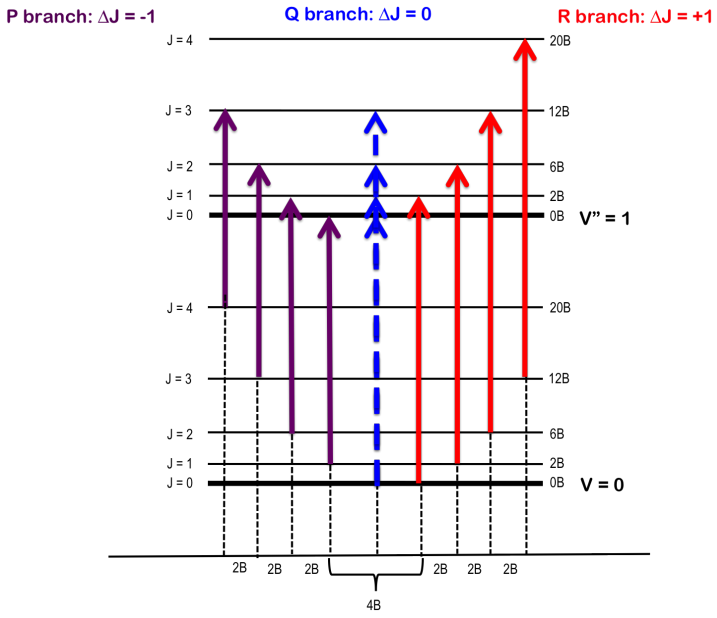

Figure 1: Cartoon depiction of rotational energy levels, J, imposed on vibrational energy levels, v. The transitions between levels that would result in the P- and R-branches are depicted in purple and red, respectively, in addition to the theoretical Q-branch line in blue.

Spectra

Ramp over all initially populated J rotational levels and exclude $J = 0$ (since that is the ground rotational state).

For frequencies divide by h to get:

- **P-branch**:

$$\begin{aligned} \frac{\Delta\varepsilon_{mc}}{h} &= v^P \\ &= v_0 - 2BJ \end{aligned}$$

  w/ $J = 1, 2, 3 \ldots .$
- **Q-Branch**:

$$\begin{aligned} \frac{\Delta\varepsilon_{mc}}{h} &= v^Q \\ &= v_\circ \end{aligned}$$

  for all J values
- **R-Branch**:

$$\begin{aligned} \frac{\Delta\varepsilon_{mc}}{h} &= v^R \\ &= v_\circ + 2BJ \end{aligned}$$

  w/ $J = 0, 1, 2, 3 \ldots .$

The Q-branch is a single frequency at ν_o and P-branch is a set of lines equally spaces ($2B$) to lower frequencies. R-branch is a set of lines equally spaces to higher frequencies. (https://scilearn.sydney.edu.au/spect...ce.php?res=low)

The spectrum we expect, based on the conditions described above, consists of lines equidistant in energy from one another, separated by a value of 2B. The *relative* intensity of the lines is a function of the rotational populations of the ground states, i.e. the intensity is proportional to the number of molecules that have made the transition. The *overall* intensity of the lines depends on the vibrational transition dipole moment.

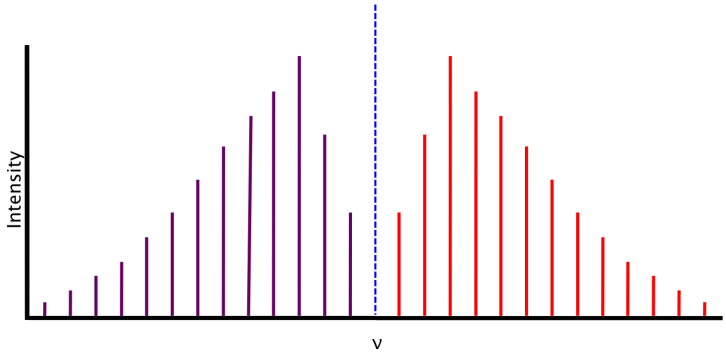

Figure 2: A cartoon depiction of an ideal rovibrational spectrum of a diatomic. Note the absence of the q-branch

Missing Q-branches

A diatomic molecule does not exhibits a Q-branch, in general, and only P and R braches. The diatomic molecules must have electronic angular momentum about the internuclear axis in order to exhibit ΔJ=0 transition. NO, a $^2\Pi$ molecule has Λ=1 and shows a Q-branch. Σ states (most ground state diatomics) do not.

Between P(1) and R(0) lies the zero gap, where the the first lines of both the P- and R-branch are separated by 4B, assuming that the rotational constant B is equal for both energy levels. The zero gap is also where we would expect the Q-branch, depicted as the dotted line, if it is allowed.

We find that real spectra do not exactly fit the expectations from above.

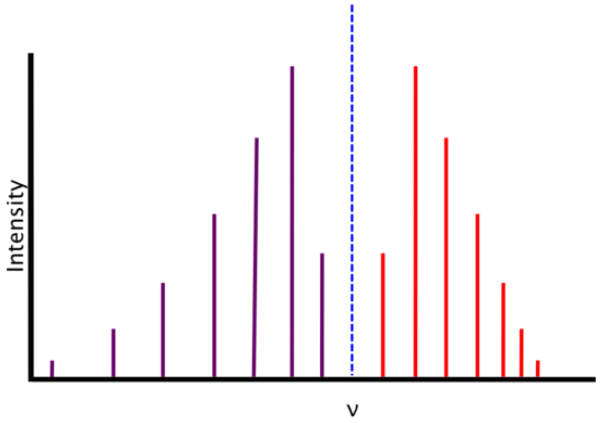

Figure 3: A cartoon depiction of a real rovibrational spectrum.

As energy increases, the R-branch lines become increasingly similar in energy (i.e., the lines move closer together) and as energy decreases, the P-branch lines become increasingly dissimilar in energy (i.e. the lines move farther apart). This is attributable to two phenomena:

1. **rotational-vibrational coupling** and
2. **centrifugal distortion**.

Rotational-Vibrational Coupling

As a diatomic molecule vibrates, its bond length changes. Since the moment of inertia is dependent on the bond length, it too changes and, in turn, changes the rotational constant B. We assumed above that B of $R(0)$ and B of $P(1)$ were equal, however they differ because of this phenomenon and B is given by

$$B_e = \left(-\alpha_e \nu + \frac{1}{2}\right)$$

Where B_e is the rotational constant for a rigid rotor and α_e is the **rotational-vibrational coupling constant**. The information in the band can be used to determine B_0 and B_1 of the two different energy states as well as the rotational-vibrational coupling constant, which can be found by the method of combination differences.

Centrifugal Distortion

Similarly to rotational-vibrational coupling, centrifugal distortion is related to the changing bond length of a molecule. A real molecule does not behave as a rigid rotor that has a rigid rod for a chemical bond, but rather acts as if it has a spring for a chemical bond. As the rotational velocity of a molecule increases, its bond length increases and its moment of inertia increases. As the moment of inertia increases, the rotational constant B decreases.

$$F(J) = BJ(J+1) - DJ^{2}(J+1)^{2}$$

Where D is the **centrifugal distortion constant** and is related to the vibration wavenumber, ω

$$D = \frac{4B^3}{\omega^2}$$

When the above factors are accounted for, the actual energy of a rovibrational state is

$$S(v, J) = \left(v + \frac{1}{2}\right)\nu_0 + B_e J(J+1) - \alpha_e \left(v + \frac{1}{2}\right) J(J+1) - D_e[J(J+1)]^2$$

Temperature Dependence

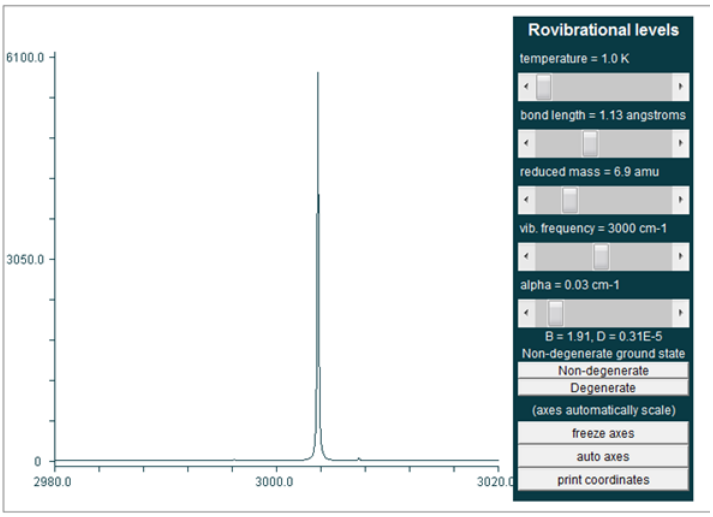

The rovibrational spectrum at 0K

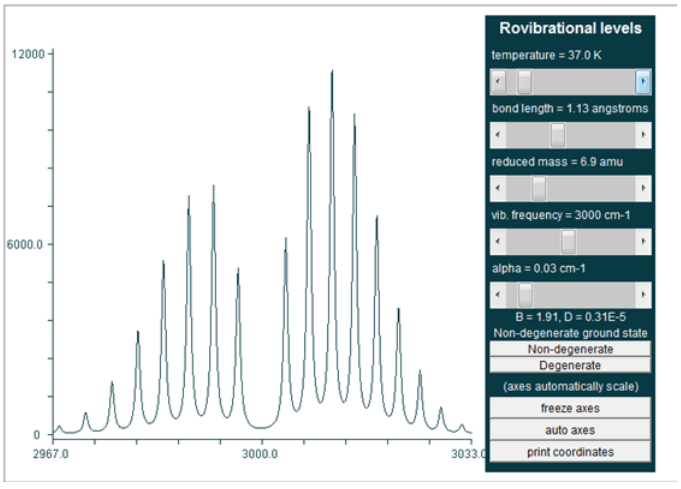

The rovibrational spectrum at 37K

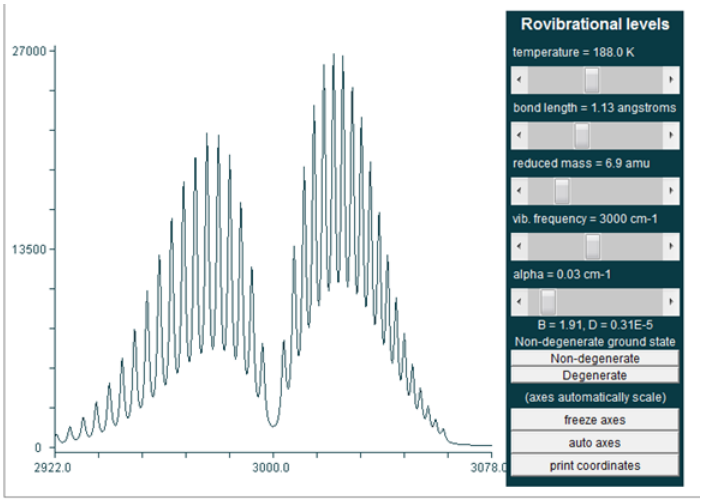

The rovibrational spectrum at 188K

Sometimes the individual rotational fine structure cannot be resolved an only the contour is observed. The relative intensities are controlled by the populations of the individual J rotational energy levels.

The ideal spectrum will NOT be observed because

1. B varies with ν because of anharmonicity. It will increase as ν increases, producing a decrease in B for ν=1 vs. ν=0.
2. Centrifugal stretching in the higher J states. The bond stretches (not a rigid rotor) causing B to decrease with increasing J .
3. Selection rules. **Q-branch may not occur and usually does not occur in diatomic molecules**.

This type of vibrational spectrum is formed for any vibrational transition in a polyatomic molecule, except that the rotational analysis is not a simple as in a diatomic. Generally, P, Q, and R branches are seen.

Linear Polyatomic Molecules (Not covered)

The shape of the rotational –vibrational transition depends on whether the vibration induces a dipole moment, μ, along the bond axis of perpendicular to it. If μ changes along the bond axis (as in a diatomic) we have a $\parallel$ band with the same selection rules, e.g. no Q-branch. This is the case for the asymmetric stretch, ν_3, of CO_2. So no Q-branch is observed in the high resolution rovibrational spectrum for this mode.

If μ changes $\perp$ to the bond axis, we have a $\perp$ band. This will carry P, Q, and R branches. For example the , ν_2 band (bends) of CO_2.

Key point!

Observation of pure rotational spectra ($\Delta J = \pm 1$) in the microwave region requires that the molecule possesses a permanent dipole moment. But, rotational structure is observed in a rovibrational band from which the rotational constants can be deduced. No permanent dipole moment is required in this case. Hence rotational features in molecules like CO_2.

Spin Statistics (Not covered)

In some molecules with equivalent sets of nuclear, certain rotational and vibrational states do not occur or occur with reduced statistical weights because of the fact that half integral spin nuclear obey Fermi statistics while 0 and integer spin nuclei obey Bose-Einstein statistics. We do not have the time here to discuss this aspect in more detail.

$$\hat{P}_{12}\Psi(1,2) = +\Psi(1,2)$$

Where the exchange operator switches the two equivalent nuclei (like in a rotation). This case the eigenvalue is positive and the wavefunction acts as a **Boson (*I*=integral)**

$$\hat{P}_{12}\Psi(1,2) = -\Psi(1,2)$$

Where the exchange operator switches the two equivalent nuclei (like in a rotation). This case the eigenvalue is negative and the wavefunction acts as a **Fermion (*I*=half integral)**

This has consequences on which rovibrational states occur and what their statistical weight is. This is only a consideration with molecules with equivalent nuclei.

CHAPTER OVERVIEW

4: X-ray Spectroscopy

XAS, or X-ray Absorption Spectroscopy, is a broadly used method to investigate atomic local structure as well as electronic states. Very generally, an X-ray strikes an atom and excites a core electron that can either be promoted to an unoccupied level, or ejected from the atom. Both of these processes will create a core hole. If the electron dissociates, this produces an excited ion as well as photoelectron and is studied by X-ray Photoelectron Spectroscopy (XPS).

4.1: Physical Principles
4.2: Photoelectron Spectroscopy - Valence Ionization
4.3: Back to Basics
4.4: Experimental Details
4.5: X-ray Photoelectron (XPS) Spectroscopy
4.6: X-ray Absorption Spectroscopies
4.7: Experimental modes and Data Analysis
4.8: Introduction to X-ray Absorption Spectroscopy (XAS)
4.9: X-Ray Absorption Near Edge Structure (XANES)
4.10: X-ray absorption fine structure (XAFS)

4.1: Physical Principles

Photoelectron spectroscopy utilizes photo-ionization and analysis of the kinetic energy distribution of the emitted photoelectrons to study the composition and electronic state of the surface region of a sample. Traditionally, when the technique has been used for surface studies it has been subdivided according to the source of exciting radiation into :

- **X-ray Photoelectron Spectroscopy (XPS)** - using soft x-rays (with a photon energy of 200-2000 eV) to examine core-levels.
- **Ultraviolet Photoelectron Spectroscopy (UPS)** - using vacuum UV radiation (with a photon energy of 10-45 eV) to examine valence levels.

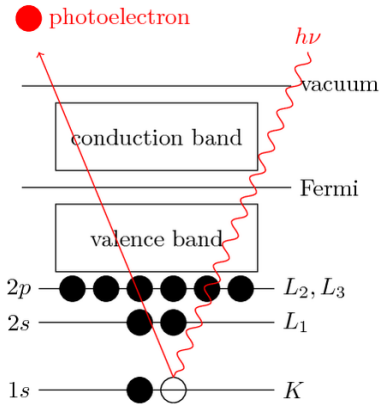

Figure 4.1.1: Principles of x-ray photoelectron spectroscopy (XPS) sometimes called photoelectron spectroscopy (PES). (CC BY 2.5; Kjell Magne Fauske via TeXample.net)

The development of synchrotron radiation sources has enabled high resolution studies to be carried out with radiation spanning a much wider and more complete energy range (5 - 5000+ eV) but such work remains a small minority of all photoelectron studies due to the expense, complexity and limited availability of such sources.

Physical Principles

Photoelectron spectroscopy is based upon a single photon in/electron out process and from many viewpoints. The energy of a photon of all types of electromagnetic radiation is given by the Einstein relation :

$$E = h\nu$$

where h is Planck constant ($6.62 \times 10^{-34}\ J \cdot s$) and ν is the frequency (Hz) of the radiation.

Photoelectron spectroscopy uses monochromatic sources of radiation (i.e. photons of fixed energy). In XPS, the photon is absorbed by an atom in a molecule or solid, leading to ionization and the emission of a core (inner shell) electron. By contrast, in UPS the photon interacts with valence levels of the molecule or solid, leading to ionization by removal of one of these valence electrons.

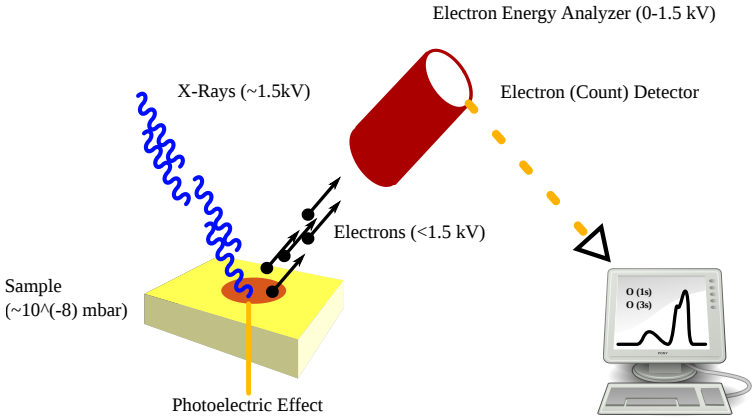

Figure 4.1.2: Shows the basic principle of XPS and the Photoelectric Effect. (CC BY-SA 4.0; Roland Siegbert via Wikipedia)

The kinetic energy distribution of the emitted photoelectrons (i.e. the number of emitted photoelectrons as a function of their kinetic energy) can be measured using any appropriate electron energy analyzer and a photoelectron spectrum can thus be recorded. The process of photoionization can be considered in several ways : one way is to look at the overall process as follows:

$$\mathrm{A} + \mathrm{h}\nu \rightarrow \mathrm{A}^{+} + \mathrm{e}^{-}$$

Conservation of energy then requires that :

$$\mathrm{E(A)} + h\nu = \mathrm{E(A^{+})} + \mathrm{E(e^{-})} \tag{4.1.1}$$

Since the electron's energy is present solely as kinetic energy (KE) this can be rearranged to give the following expression for the KE of the photoelectron:

$$\mathrm{KE} = \mathrm{h}\nu - [\mathrm{E(A^{+})} - \mathrm{E(A)}]$$

The final term in brackets, representing the difference in energy between the ionized and neutral atoms, is generally called the **binding energy** (BE) of the electron - this then leads to the following commonly quoted equation :

$$\mathrm{KE} = \mathrm{h}\nu - \mathrm{BE}$$

An alternative approach is to consider a one-electron model along the lines of the following pictorial representation ; this model of the process has the benefit of simplicity but it can be rather misleading.

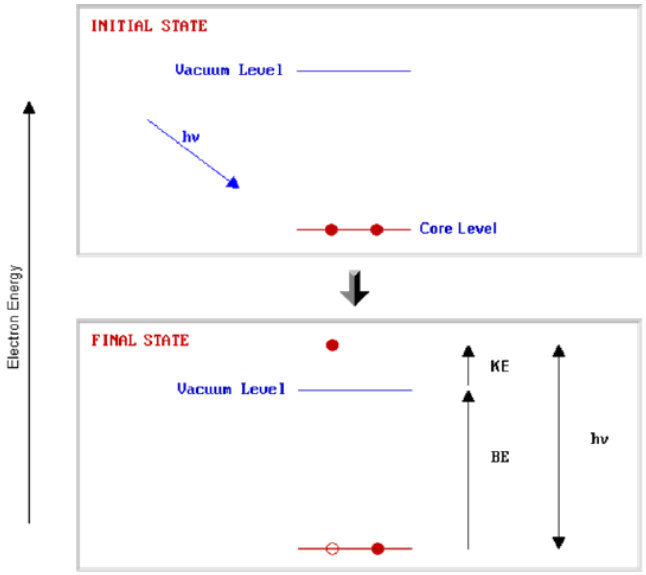

Figure 4.1.3

The BE is now taken to be a direct measure of the energy required to just remove the electron concerned from its initial level to the vacuum level and the KE of the photoelectron is again given by :

$$\mathrm{KE} = \mathrm{h}\nu - \mathrm{BE}$$

Binding Energies vs. Workfunctions

The binding energies (BE) of energy levels in solids are conventionally measured with respect to the Fermi-level of the solid, rather than the vacuum level. This involves a small correction to the equation given above in order to account for the *work function* (φ) of the solid.

At the most fundamental level ionization energies are well-defined thermodynamic quantities related to the **heats of protonation, oxidation/reduction chemistry, and ionic and covalent bond energies**. Ionization energies are closely related to the concepts of electronegativity, electron-richness, and the general reactivity of molecules. The energies and other characteristic features of the ionization bands observed in photoelectron spectroscopy provide some of the most detailed and specific quantitative information regarding the electronic structure and bonding in molecules. Photoelectron spectroscopy has served as a particularly important basis for the bonding models used to describe organic, inorganic, and organometallic molecules because the energetics of ion

formation from the neutral ground state are **directly related to orbital electron configurations, oxidation states, charge distributions, and covalency**.

The Orbital Model of Ionization

Ionization is explicitly defined in terms of transitions between the ground state of a molecule and ion states as shown in Equation ??? and as illustrated above. Information obtained from photoelectron spectroscopy is typically discussed in terms of the electronic structure and bonding in the ground states of neutral molecules, with ionization of electrons occurring from bonding molecular orbitals, lone pairs, antibonding molecular orbitals, or atomic cores. These descriptions reflect the relationship of ionization energies to the molecular orbital model of electronic structure.

Ionization energies are directly related to the energies of molecular orbitals by **Koopmans' theorem**, which states that *the negative of the eigenvalue of an occupied orbital from a Hartree-Fock* calculation is equal to the vertical ionization energy to the ion state formed by removal of an electron from that orbital, provided the distributions of the remaining electrons do not change. There are many limitations to Koopmans' theorem, but in a first order approximation each ionization of a molecule can be considered as removal of an electron from an individual orbital. The ionization energies can then be considered as measures of orbital stabilities, and shifts can be interpreted in terms of orbital stabilizations or destabilizations due to electron distributions and bonding. Koopmans' theorem is implicated whenever an orbital picture is involved, but is not necessary when the focus is on the total electronic states of the positive ions.

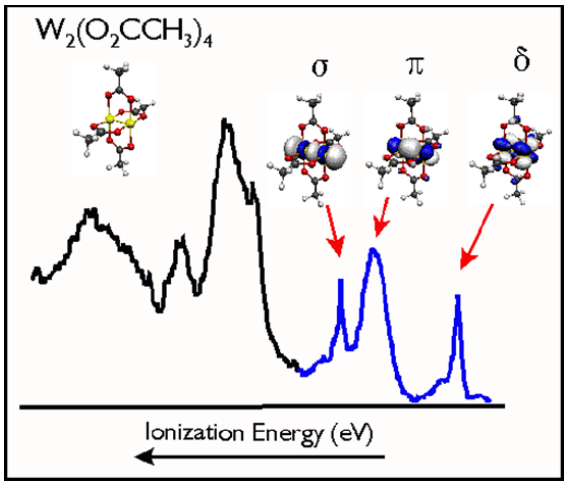

Figure 4.1.4: Direct connection of photoelectron bands to electronic states.

The direct ionization transition is not restricted by any symmetry selection rules because the ejected electron can carry any necessary angular momentum to make the process electric dipole allowed. Therefore, ionization to any excited positive ion state obtained by removal of a single electron and within range of the photon energy can be observed. That is, ionizations can be observed that correspond to removal of electrons from any of the occupied orbitals.

Photons with energies in the keV (X-ray) range are able to ionize down to the core electrons of atoms and molecules. Core ionizations of molecules are associated with the individual atoms present and fall in characteristic energy ranges related to the specific elements. The exact ionization energy of a core level is influenced by the charge potential around the atom and is useful for distinguishing between atoms in different chemical environments.

Information Content of Photoelectron Spectroscopy: While the energy information that is contained in a photoelectron spectrum is surely the most important information, further insight into the electronic structure of molecules is contained in other information within the spectrum. This includes **Ionization Band Shape**:

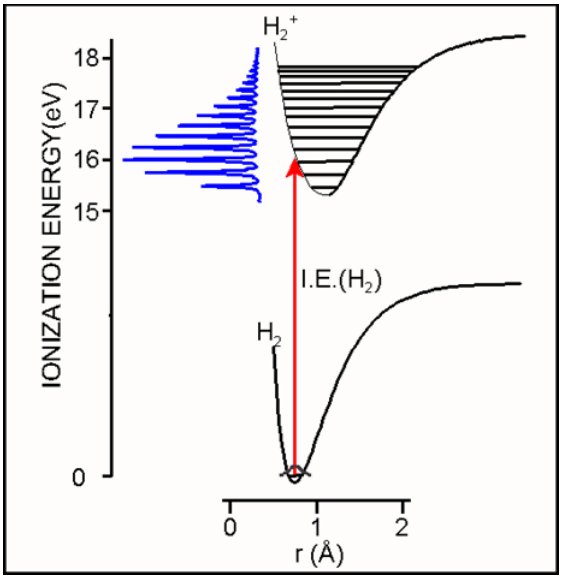

Figure 4.1.5: Photoionization of H_2 results in the formation of H_2^+ cation. This has

Removal of an electron changes the electronic structure and bonding in the molecule and results in a shift of the equilibrium internuclear separations. If the geometry changes are sufficiently great, the most probable (vertical) transitions from the neutral ground state to excited vibrational levels of the final ion state. When these vibrational levels are resolved, the change in **vibrational spacing from the initial state to the final state gives a measure of the change in vibrational frequencies and force constants associated with the excitation**, and the intensity pattern of the transitions to the excited vibrational levels (the Franck-Condon factors) gives a measure of the change in equilibrium bond distances.

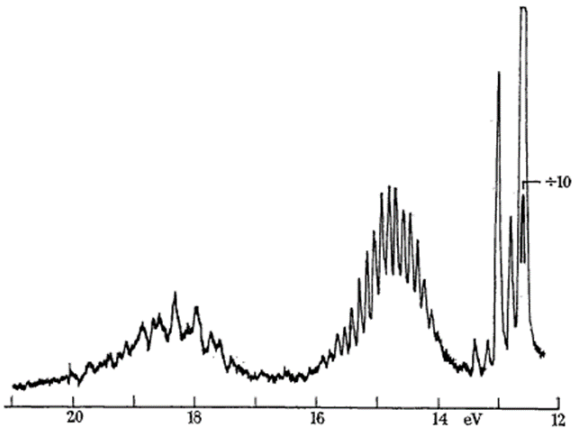

FIGURE 1. The photoelectron spectrum of H_2O using the helium 584 Å line.

Figure 4.1.6: The photoelectron spectrum of H_2O using the helium $58.4nm$ line.

The two bands for water above indicated three orbital energies. Now, look at the MO for water, derived as a linear combination of SALC (for Hydrogens)

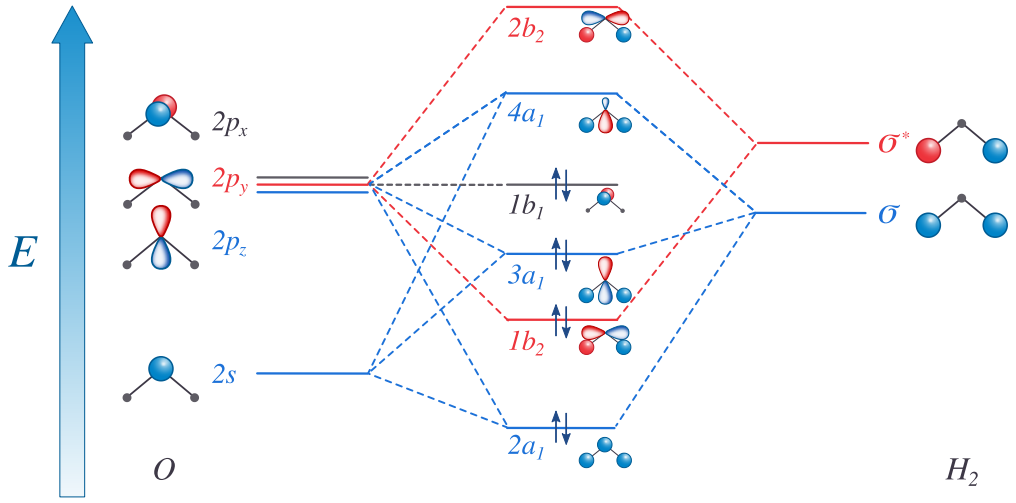

Figure 4.1.7: Molecular Orbitals of Water with irreducible representations. (CC BY-NC; Ümit Kaya via LibreTexts)

The oxygen atomic orbitals are labeled according to their symmetry as a_1 for the $2s^2$ orbital and b_2, a_1 and b_2 for 4 electrons in the 2p orbital. The two hydrogen 1s orbitals are premixed to form a A_1 (bonding) and B_2 (antibonding) MO.

- Notice that the O 1s orbital does not mix with the others - this is because it is much lower in energy than them.
- Notice also that the O $2p_x$ orbital does not mix with any others - this is because it is the only AO belonging to the b_2 irrep.

Electronic configuration of H_2O:

$$1\,a_1^{22}a_1^{21}b_1^{23}a_1^{21}b_2^2$$

Figure 4.1.8: Occupied (top) and selected virtual (bottom) HF molecular orbitals of water

In agreement with this description the photoelectron spectrum for water shows two broad peaks for the $1b_2$ MO (18.5 eV) and the $2a_1$ MO (14.5 eV) and a sharp peak for the nonbonding $1b_2$ MO at 12.5 eV. This MO treatment of water differs from the orbital hybridization picture because now the oxygen atom has just one lone pair instead of two.

Lone Pairs

In this sense, water does not have two equivalent lone electron pairs as VSEPR suggests from general chemistry.

4.2: Photoelectron Spectroscopy - Valence Ionization

Learning Objectives

- Demonstrate how photoelectron spectroscopy can be used to resolve the absolute energies of molecular orbitals.

Photoelectron spectroscopy (PES) utilizes photo-ionization and analysis of the kinetic energy distribution of the emitted photoelectrons to study the composition and electronic state of the surface region of a sample.

- **X-ray Photoelectron Spectroscopy** (XPS) uses soft x-rays (with a photon energy of 200-2000 eV) to examine electrons in *core*-levels.
- **Ultraviolet Photoelectron Spectroscopy** (UPS) using vacuum UV radiation (with a photon energy of 10-45 eV) to examine electrons in *valence* levels.

Both photoelectron spectroscopies are based upon a single photon in/electron out process. The energy of a photon of all types of electromagnetic radiation is given by the Planck–Einstein relation:

$$E = h\nu \tag{4.2.1}$$

where h is Planck constant and ν is the frequency (Hz) of the radiation. UPS is a powerful technique to exam molecular electron structure since we are interested in the molecular orbitals from polyatomic molecules (especially the valence orbitals) and is the topic of this page.

Photoelectron spectroscopy uses monochromatic sources of radiation (i.e. photons of fixed energy). In UPS the photon interacts with valence levels of the molecule or solid, leading to ionization by removal of one of these valence electrons. The kinetic energy distribution of the emitted photoelectrons (i.e. the number of emitted photoelectrons as a function of their kinetic energy) can be measured using any appropriate electron energy analyzer and a photoelectron spectrum can thus be recorded.

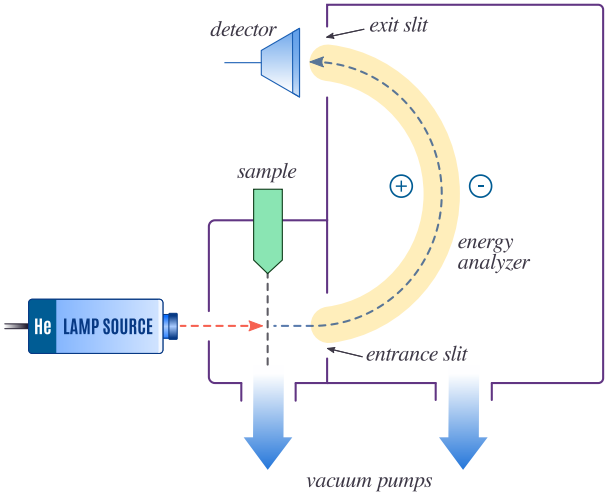

Figure 10.4.1 : Diagram of a basic, typical PES instrument used in UPS, where the radiation source is an UV light source. When the sample is irradiated, the released photoelectrons pass through the lens system which slows them down before they enter the energy analyzer. The analyzer shown is a spherical deflection analyzer which the photoelectrons pass through before they are collected at the collector slit. (CC BY-NC; Ümit Kaya via LibreTexts)

The process of photoionization can be considered in several ways. One way is to look at the overall process for a species A:

$$A + \text{photon} \rightarrow A^+ + e^- \tag{4.2.2}$$

Conservation of energy then requires that (after using Equation 4.2.1):

$$E(A) + h\nu = E(A^+) + E(e^-) \tag{4.2.3}$$

Since the free electron's energy is present solely as kinetic energy (KE) (i.e., there is no internal energy in a free electron)

$$E(e^-) = KE$$

Equation 4.2.3 can then be rearranged to give the following expression for the KE of the photoelectron:

$$KE = h\nu - \left[E(A^+) - E(A)\right] \tag{4.2.4}$$

The final term in brackets represents the difference in energy between the ionized and neutral species and is generally called the **vertical ionization energy** (IE) of the ejected electron; this then leads to the following commonly quoted equations:

$$KE = h\nu - IE \tag{4.2.5}$$

or

$$IE = h\nu - KE \tag{4.2.6}$$

The vertical ionization energy is a direct measure of the energy required to just remove the electron concerned from its initial level to the vacuum level (i.e., a free electron). Photoelectron spectroscopy measures the relative energies of the ground and excited positive ion states that are obtained by removal of single electrons from the neutral molecule.

Note

Equation 4.2.5 may look familiar to you as it the same equation Einstein used to describe the photoelectric effect except the vertical ionization energy (IE) is substituted for workfunction Φ. Both vertical ionization energy and workfunctions are metrics for the binding energy of an electron in the sample.

At a fundamental level, ionization energies are well-defined thermodynamic quantities related to the heats of protonation, oxidation/reduction chemistry, and ionic and covalent bond energies. Ionization energies are closely related to the concepts of electronegativity, electron-richness, and the general reactivity of molecules. The energies and other characteristic features of the ionization bands observed in photoelectron spectroscopy provide some of the molecular orbitals detailed and specific quantitative information regarding the electronic structure and bonding in molecules.

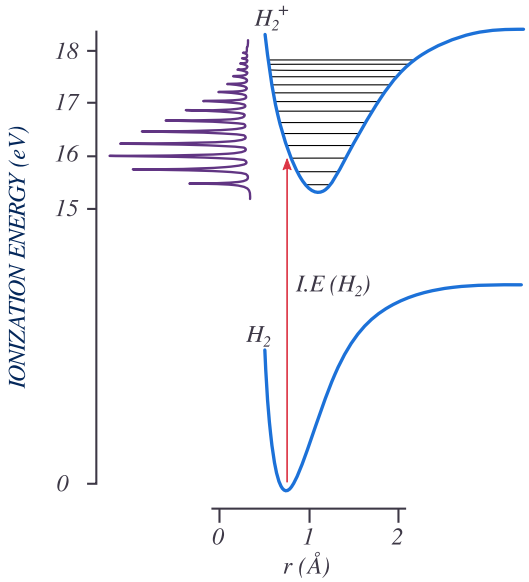

Figure 10.4.2 : Vertical ionization process for molecular hydrogen. (CC BY-NC; Ümit Kaya via LibreTexts)

Ionization is explicitly defined in terms of transitions between the ground state of a molecule and ion states as shown in Equation 4.2.6 and as illustrated in the Figure 10.4.2 . Nonetheless, the information obtained from photoelectron spectroscopy is typically discussed in terms of the electronic structure and bonding in the ground states of neutral molecules, with ionization of electrons occurring from bonding molecular orbitals, lone pairs, antibonding molecular orbitals, or atomic cores. These descriptions reflect the relationship of ionization energies to the molecular orbital model of electronic structure.

Ionization energies are directly related to the energies of molecular orbitals by Koopmans' theorem, which states that the negative of the eigenvalue of an occupied orbital from a Hartree-Fock calculation is equal to the *vertical ionization energy* to the ion state formed by removal of an electron from that orbital (Figure 10.4.3), provided the distributions of the remaining electrons do not change (i.e., frozen).

$$I_j = -\epsilon_j \tag{4.2.7}$$

There are many limitations to Koopmans' theorem, but in a first order approximation each ionization of a molecule can be considered as removal of an electron from an individual orbital. The ionization energies can then be considered as measures of orbital stabilities, and shifts can be interpreted in terms of orbital stabilizations or destabilizations due to electron distributions and bonding. Koopmans' theorem is implicated whenever an orbital picture is involved, but is not necessary when the focus is on the total electronic states of the positive ions.

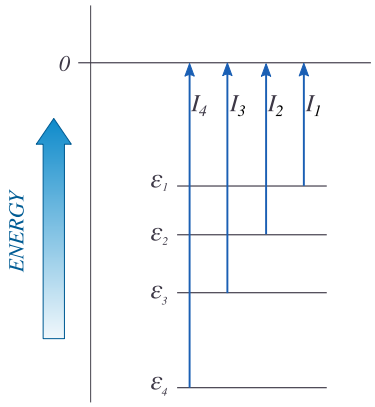

Figure 10.4.3 : Within Koopmans' Theorem, the energies of the orbitals (\epsilon\) have an attractively simple physical interpretation: they give the amount of energy necessary to remove (ionize) the electron out of the molecular orbital, which corresponds to the negative of the experimentally observable ionization potential (I). (CC BY-NC; Ümit Kaya via LibreTexts)

Koopmans' Theorem

Koopmans' theorem argues that the negative of the eigenvalue of an occupied orbital from a Hartree-Fock calculation is equal to the vertical ionization energy to the ion state formed by removal of an electron from that orbital.

Several different ionization energies can be defined, depending on the degree of vibrational excitation of the cations. In general, the following two types of ionization energies are considered (Figure 10.4.4):

- Adiabatic ionization energy corresponds to the ionization energy associated with this transition

  $$M(X, v" = 0) + h\nu \rightarrow M^+(x, v' = 0) + e^-$$

  Adiabatic ionization energy that is, the minimum energy required to eject an electron from a molecule in its ground vibrational state and transform it into a cation in the lowest vibrational level of an electronic state x of the cation.
- Vertical ionization energy corresponds to the ionization energy associated with this transition

  $$M(X, v" = 0) + h\nu \rightarrow M^+(x, v' = n) + e^-$$

  where, the value n of the vibrational quantum number v' corresponds to the vibrational level whose wavefunction gives the largest overlap with the v" = 0 wavefunction. This is the most probable transition and usually corresponds to the vertical transition where the internuclear separations of the ionic state are similar to those of the ground state.

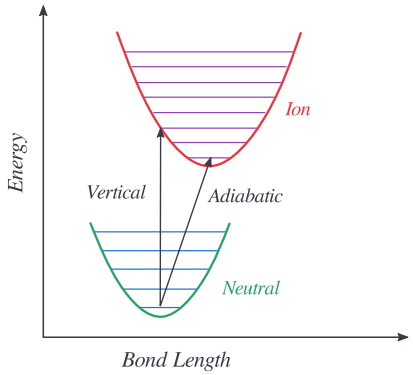

Figure 10.4.4 : Difference between vertical and adiabatic ionization energies for a simple harmonic oscillator system. (CC BY-NC; Ümit Kaya via LibreTexts)

The geometry of an ion may be different from the neutral molecule. The measured ionzation energy in a PES experiment can refer to the vertical ionization energy, in which case the ion is in the same geometry as the neutral, or to the adiabatic ionzaiton energy, in which case the ion is in its lowest energy, relaxed geometry (mostly the former though). This is illustrated in the Figure 10.4.4 . For a diatomic the only geometry change possible is the bond length. The figure shows an ion with a slightly longer bond length than the neutral. The harmonic potential energy surfaces are shown in green (neutral) and red (ion) with vibrational energy levels. The vertical ionzation energy is **always greater** than the adiabatic ionzation energy.

Differing Ionization Energies

You have been exposed to three metrics of ionization energies already, which are similar, but with distinct differences:

- The *ionization energy* (also called *adiabatic ionization energy*) is the lowest energy required to effect the removal of an electron from a molecule or atom, and corresponds to the transition from the lowest electronic, vibrational and rotational level of the isolated molecule to the lowest electronic, vibrational and rotational level of the isolated ion.
- The *binding energy* (also called *vertical ionization energy*) is the energy change corresponding to an ionization reaction leading to formation of the ion in a configuration which is the same as that of the equilibrium geometry of the ground state neutral molecule.
- The *workfunction* is the minimum energy needed to remove an electron from a (bulk) solid to a point in the vacuum.

Example 10.4.1 : Molecular Hydrogen

As you remember, the molecular orbital description of hydrogen involves two $|1s\rangle$ atomic orbitals generating a bonding $1\sigma_g$ and antibonding $2\sigma_u^*$ molecular orbitals. The two electrons that are responsible for the H_2 bond are occupied in the $1\sigma_g$.

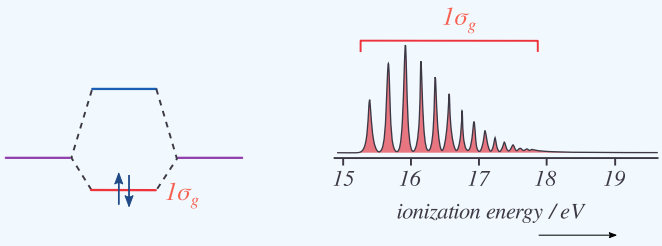

MO diagram and PES spectrum of H_2. (CC BY-NC; Ümit Kaya via LibreTexts)

The PES spectrum has a single band that corresponds to the ionization of a $1\sigma_g$ electron. The multiple peaks are due to electrons ejecting from a range of stimulated vibrational energy levels. When extensive vibrational structure is resolved in a PES molecular orbital, then the removal of an electron from that molecular orbital induces a significant change in the bonding (in this case an increase in the bond length since the bond order has been reduced).

Example 10.4.2 : Molecular Nitrogen

Diatomic nitrogen is more complex than hydrogen since multiple molecular orbitals are occupied. Four molecular orbitals are occupied (the two $1\pi_u$ orbitals are both occupied). The UV photoelectron spectrum of N_2, has three bands corresponding to $3\sigma_g$, $1\pi_u$ and $2\sigma_u$ occupied molecular orbitals. Both $3\sigma_g$ and $2\sigma_u$ are weakly bonding and antibonding. The $1\sigma_g$ orbital is not resolved in this spectrum since the incident light $h\nu$ used did not have sufficient energy to ionize electrons in that deeply stabilized molecular orbital.

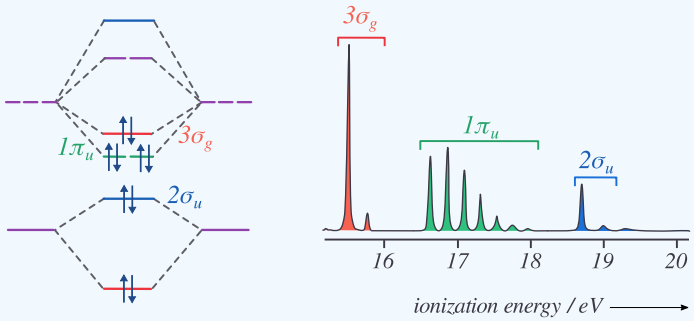

MO diagram and PES spectrum of N_2. (CC BY-NC; Ümit Kaya via LibreTexts)

Note that extensive vibrational structure for the $1\pi_u$ band indicates that the removal of an electron from this molecular orbital causes a significant change in the bonding.

Hydrogen Chloride

The molecular energy level diagram for HCl is reproduced in Figure 10.4.5

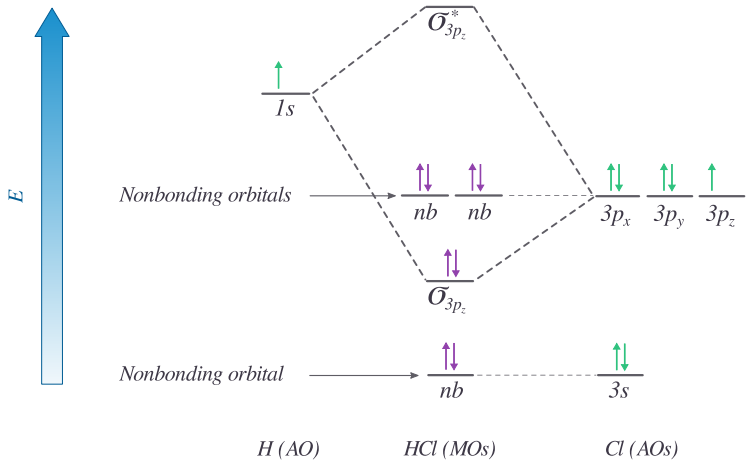

Figure 10.4.5 : Molecular Orbital Energy-Level Diagram for HCl. The hydrogen 1s atomic orbital interacts molecular orbitals strongly with the $3p_z$ orbital on chlorine, producing a bonding/antibonding pair of molecular orbitals. The other electrons on Cl are best viewed as nonbonding. As a result, only the bonding σ orbital is occupied by electrons, giving a bond order of 1. (CC BY-NC; Ümit Kaya via LibreTexts)

Important aspects of molecular orbital diagram in Figure 10.4.5 :

- The H 1*s* energy lies well above the Cl 2*s* and 2*p* atomic orbitals;
- The valence electron configuration can be written $3\sigma^2 1\pi^4$;
- The H 1*s* orbital contributes only to the σ molecular orbitals, as does one of the Cl 2*p* orbitals (hence the lines in Figure 10.4.5 connecting these atomic orbitals and the 3σ and 4σ molecular orbitals);

- The remaining Cl 2*p* orbitals (ie those perpendicular to the bond axis) are unaffected by bonding, and these form the 1π molecular orbitals;
- The 1π orbitals are nonbonding - they are not affected energetically by the interaction between the atoms, and are hence neither bonding nor antibonding;
- The 3σ orbital is weakly bonding, and largely Cl 2*p*;
- The 3σ* orbital is antibonding, and primarily of H 1*s* character;

Figure 10.4.6 shows the analogous MO diagram and photoelectron spectrum for HCl. The spectrum has two bands corresponding to non-bonding 1*p* (or 1π) molecular orbitals (with negligible vibrational structure) and the 3*s* bonding molecular orbital (vibrational structure).

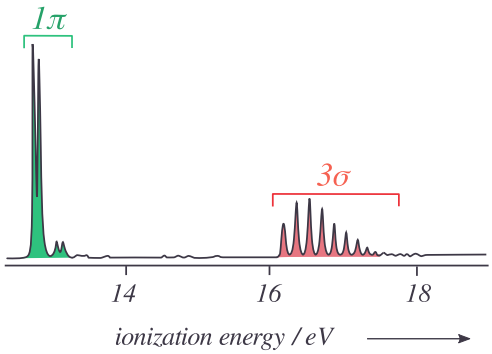

Figure 10.4.6 : Photoelectron spectrum HCl. (CC BY-NC; Ümit Kaya via LibreTexts)

The higher energy (more stabilized) core molecular orbitals are not observed since the incident photon energy $h\nu$ is below their ionization energies.

Water

In the simplified valence bond theory perspective of the water molecule, the oxygen atom form four sp^3 hybrid orbitals. Two of these are occupied by the two lone pairs on the oxygen atom, while the other two are used for bonding. Within the molecular orbital picture, the electronic configuration of the H_2O^+ molecule is $(1a_1)^2(2a_1)^2(1b_2)^2(3a_1)^2(1b_1)^2$ where the symbols a_1, b_2 and b_1 are orbital labels based on molecular symmetry that will be discussed later (Figure 10.4.7). Within Koopmans' theorem:

- The energy of the $1b_1$ HOMO corresponds to the ionization energy to form the H_2O^+ ion in its ground state $(1a_1)^2(2a_1)^2(1b_2)^2(3a_1)^2(1b_1)^1$.
- The energy of the second-highest molecular orbitals $3a_1$ refers to the ion in the excited state $(1a_1)^2(2a_1)^2(1b_2)^2(3a_1)^1(1b_1)^2$.

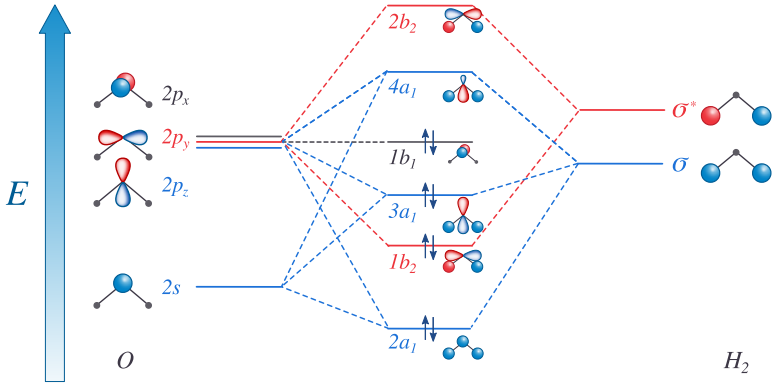

Figure 10.4.7 : MO diagram for water. (CC BY-NC; Ümit Kaya via LibreTexts)

The Hartree–Fock orbital energies (with sign changed) of these orbitals are tabulated below and compared to the experimental ionization energies.

Molecular orbital	Hartree–Fock orbital Energies (eV)	Experimental Ionization Energies (eV)
$2a_1$	36.7	32.2
$1b_2$	19.5	18.5
$3a_1$	15.9	14.7
$1b_1$	13.8	12.6

As explained above, the deviations between orbital energy and ionization energy is small and due to the effects of orbital relaxation as well as differences in electron correlation energy between the molecular and the various ionized states.

The molecular orbital perspective has the lone pair in different orbitals (one in a non-bonding orbital ($1b_1$ and one in the bonding orbitals). We tern to the photoelectron spectroscopy to help identify which theory is more accurate (i.e., describes reality better). The photoelectron spectrum of water in Figure 10.4.6 can be interpreted as having three major peaks with some fine structure arises from vibrational energy changes. The light source used in this experiment is not sufficiently energetic to ionize electrons from the lowest lying molecular orbitals.

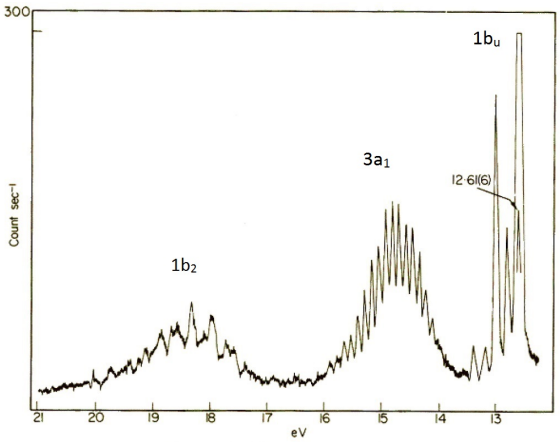

Figure 10.4.8 : Photoelectron spectrum of water. Note the energy axes is flipped compared to other spectra on this page.his spectrum does not go to high enough energy to show the deep $2a_1$ molecular orbital.

If water was formed two identical O-H bonds and two lone pairs on the oxygen atom line valence bond theory predicts, then the PES in Figure 10.4.8 would have two (degenerate) peaks, one for the two bonds and one for the two lone pairs. The photoelectron spectrum clearly shows three peaks in the positions expected for the molecular orbitals in Figure 10.4.8 .

If the molecular orbitals in Figure 10.4.7 represent the real electronic structure, how do we view the bonding? These molecular orbitals are delocalized and bare little relationship to the familiar 2-center bonds used in valence bond theory. For example, the $2a_1$ $1b_1$ and $3a_1$ molecular orbitals all have contributions from all three atoms, they are really 3-centered molecular orbitals. The bonds however can be thought of as representing a build up of the total electron density which loosely put is a total of all the orbital contributions. Despite this, we keep the ideas of hybridization and 2-center bonds because they are useful NOT because they represent reality

Summary

A photoelecton spectrum can show the relative energies of occupied molecular orbitals by ionization. (i.e. ejection of an electron). A photoelectron spectrum can also be used to determine energy spacing between vibrational levels of a given electronic state. Each orbital energy band has a structure showing ionization to different vibrational levels.

Contributors and Attributions

- Roger Nix (Queen Mary, University of London)

4.3: Back to Basics

As energy of the x-ray is increased, progressively more core electrons are excited and a more atomic picture can be constructed. Terminology:

Sub-shells (connected to the angular Momentum Quantum Number): An atom's electron shells are filled according to the following theoretical constraints:

- Each s subshell holds at most 2 electrons
- Each p subshell holds at most 6 electrons
- Each d subshell holds at most 10 electrons
- Each f subshell holds at most 14 electrons
- Each g subshell holds at most 18 electrons

Shells (principal quantum number): Electron shells are labeled K, L, M, N, O, P, and Q; or 1, 2, 3, 4, 5, 6, and 7; going from innermost shell outward:

Shells	s	p	d	f	g	Total
K	2					2
L	2	6				8
M	2	6	10			18
N	2	6	10	14		32
O	2	6	10	14	18	50

As you tune the applied x-ray photons, resonances with different ionization thresholds for electrons will occur resulting in progressively higher energy (higher energy = higher binding energy) electrons being ejected. This is a signature of the nature of the element.

Table 1-1. *Electron binding energies, in electron volts, for the elements in their natural forms.*

Element	K 1s	L_1 2s	L_2 $2p_{1/2}$	L_3 $2p_{3/2}$	M_1 3s	M_2 $3p_{1/2}$	M_3 $3p_{3/2}$	M_4 $3d_{3/2}$	M_5 $3d_{5/2}$	N_1 4s	N_2 $4p_{1/2}$	N_3 $4p_{3/2}$
1 H	13.6											
2 He	24.6*											
3 Li	54.7*											
4 Be	111.5*											
5 B	188*											
6 C	284.2*											
7 N	409.9*	37.3*										
8 O	543.1*	41.6*										
9 F	696.7*											
10 Ne	870.2*	48.5*	21.7*	21.6*								
11 Na	1070.8†	63.5†	30.65	30.81								
12 Mg	1303.0†	88.7	49.78	49.50								
13 Al	1559.6	117.8	72.95	72.55								
14 Si	1839	149.7*b	99.82	99.42								
15 P	2145.5	189*	136*	135*								
16 S	2472	230.9	163.6*	162.5*								
17 Cl	2822.4	270*	202*	200*								
18 Ar	3205.9*	326.3*	250.6†	248.4*	29.3*	15.9*	15.7*					
19 K	3608.4*	378.6*	297.3*	294.6*	34.8*	18.3*	18.3*					
20 Ca	4038.5*	438.4†	349.7†	346.2†	44.3 †	25.4†	25.4†					
21 Sc	4492	498.0*	403.6*	398.7*	51.1*	28.3*	28.3*					
22 Ti	4966	560.9†	460.2†	453.8†	58.7†	32.6†	32.6†					

Orbital energy levels

Assume there is one electron in a given atomic orbital in a **hydrogen-like** atom (ion). The energy of its state is mainly determined by the electrostatic interaction of the (negative) electron with the (positive) nucleus. The energy levels of an electron around a nucleus are given by :

$$E_n = -hcR_\infty \frac{Z^2}{n^2}$$

(typically between 1 eV and 10^3 eV), where R_∞ is the Rydberg constant, Z is the Atomic number, n is the principal quantum number, h is Planck's constant, and c is the speed of light. For hydrogen-like atoms (ions) only, the Rydberg levels depend only on the principal quantum number n.

For multi-electron atoms, interactions between electrons cause the preceding equation to be no longer accurate as stated simply with Z as the atomic number. Instead an approximate correction may be used where Z is substituted with an **effective nuclear charge** symbolized as Z_{eff}.

$$E_{n,l} = -hcR_\infty \frac{Z_{eff^2}}{n^2} \tag{4.3.1}$$

Hence, different atoms (higher Z) will have different effective Z_{eff} that couple into Equation 4.3.1 to result in different energies for the electrons. Note chance in energies for the S electrons below:

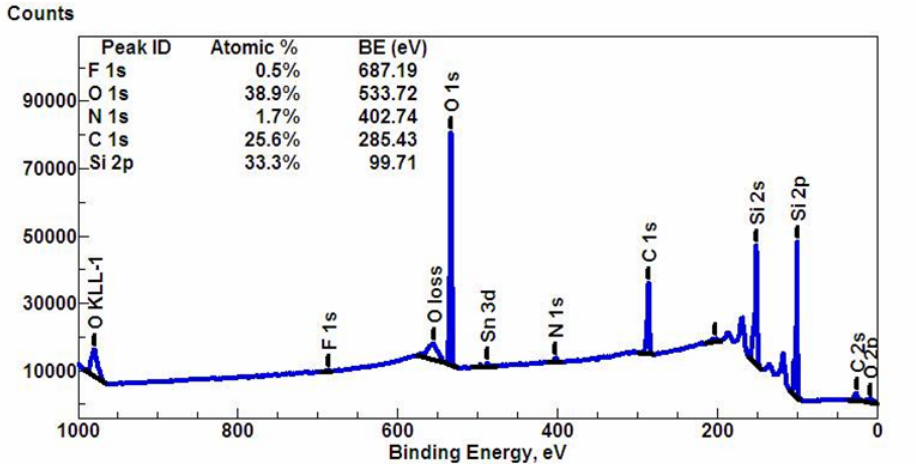

Figure 4.3.1: Wide-scan or survey spectrum of a somewhat dirty silicon wafer, showing all elements present. A survey spectrum is usually the starting point of most XPS analyses. It allows one to set up subsequent high-resolution XPS spectra acquisition. The inset shows a quantification table indicating the atomic species, their atomic percentages and characteristic binding energies. (CC BY-SA 3.0; ; Bvcrist via Wikipedia)

Hence, XPS can be used for elemental analysis of unknown compounds, by measuring and check to known values for the electronic energy levels of elements

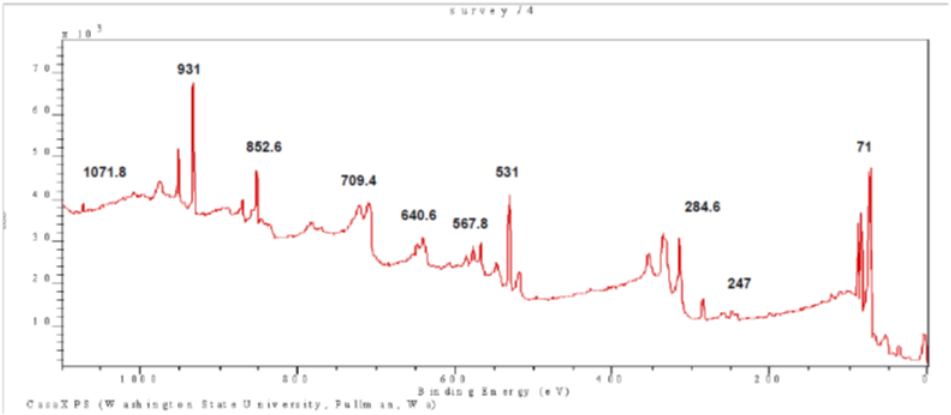

Position	FWHM	Raw Area	Library RSF	%At Conc
531.0	2.627	59285	0.736	27.61
284.6	2.410	12081.5	0.318	13.02
1071.8	1.924	2550.56	1.378	0.63
852.6	2.433	39781.1	3.845	3.55
931.8	2.234	112227	4.871	7.90
709.4	9.695	166995	2.947	19.42
71.0	2.227	193937	6.115	10.87
567.8	2.893	53803.5	2.491	7.40
247.0	8.855	13069.7	1.244	3.60
640.6	6.262	47149.5	2.693	6.00

BE Lookup Table for Signals from Elements and Common Chemical Species

1.0	Bi	6p1	3.9	Pt	5d	10.0	P	3p	18.0	At	6s	24.0	Kr	4s	34.0	K	3s	44.0	Ra	6s	52.0	Tm	5s	65.7	V	3s
1.0	Ce	4f	4.0	Ir	5d	10.0	Ti	4s	18.0	Ce	5p	24.0	Sn	4d	35.0	Re	5p3	44.0	U	6s	52.3	Yb	5s	66.0	Ni	3p
1.0	Co	3d	4.0	Pm	4f	10.0	V	4s	18.0	Pr	5p	25.0	Th	6p1	35.2	Mo	4p	44.4	Y	4s	52.6	Fe	3p	66.0	Pt	5p1
1.0	Cr	3d	4.5	Ag	4d	10.0	Zr	5s	18.1	Hf	Ntv Ox	26.0	Bi	5d3	35.2	W	Na2WO4	45.0	Ta	5p1	53.0	Sn	loss	67.8	Ta	5s
1.0	Fe	3d	4.8	Dy	5d	10.5	Bi	6s	18.2	C	2s	26.0	He	1s	35.3	Y	loss	45.1	As	2O3	53.4	Os	4f5	68.0	Ra	5d
1.0	Ga	4p	5.0	B	2p	10.7	Cd	4d5	18.4	Sr	4p	26.0	Rn	6s	35.8	W	O3	45.5	As	Ntv Ox	54.0	Os	5p1	68.0	Tc	4s
1.0	Hf	5d	5.0	Br	4p	11.0	Kr	4p	18.7	Ga	3d5	26.1	Lu	5p	36.0	Ce	5s	45.7	Ge	loss	54.2	Se	CdSe	68.5	Br	3d5
1.0	In	5p	5.0	Ca	3d	11.0	Rn	6p	18.8	Ga	3d	26.8	Ta	2O5	36.0	Gd	5s	46.0	Re	5p1	54.5	Se	GeSe	68.5	Br	KBr
1.0	Na	3s	5.0	Er	4f	11.0	Sc	4s	18.9	Ga	3d3	26.8	Zr	4p	36.6	Sr	4s	46.3	Ga	loss	54.9	Se	3d5	68.8	Cd	4p
1.0	Os	5d	5.0	Po	6p	11.1	Cs	5p3	19.0	Eu	5p	27.0	Br	4s	36.7	V	3p	46.8	Re	2O7	54.9	Li	1s	69.0	Br	3d
1.0	Pb	6p	5.3	Se	4p	11.6	Cd	4d3	19.0	Nd	5p	28.2	Sc	3p	37.0	W	5p3	46.8	W	5p1	54.9	Li	OH	69.5	Br	3d3
1.0	Sn	5p	5.5	Cl	3p	12.0	Cs	5p	19.0	Pb	5d5	28.6	In	loss	37.5	Hf	5p1	47.0	Mn	3p	54.9	Se	3d	70.0	Re	loss
1.2	Yb	4f7	5.8	Au	5d	12.0	Po	6s	19.0	Ra	6p	28.8	Rb	4s	38.0	Pm	5s	47.0	Rh	4p	55.2	Se	GeSe2	71.0	Pt	4f7
1.4	Pd	4d	6.0	Ta	5d	12.0	Te	5s	19.0	Sm	5p	29.0	Dy	5p1	38.0	Pr	5s	47.9	Ru	4p	55.3	Li	CO3	71.8	Mg	loss
1.4	Rh	4d	6.0	Y	4d	12.0	Tl	5d5	19.1	Ga	Sb fract	29.0	Er	5p	38.3	Sn	loss	48.0	Dy	5s	55.6	Nb	4s	72.6	Pt	4f
2.0	Cd	5p	6.2	Hg	5d	12.6	Cs	5p1	19.4	Ga	AlAs etch	29.0	Lu	5p	39.0	Eu	5s	48.0	Rn	5d	55.7	Se	3d3	72.7	Al	2p3
2.0	Mg	3s	6.9	Eu	4f	13.0	Tl	5d	19.5	N	2s	29.1	Ge	3d5	39.0	Nd	5s	48.0	Sb	loss	56.8	Au	5p3	72.9	Al	2p
2.0	Mo	4d	7.0	O	2p	13.2	Rb	4p	19.7	Ga	P fract	29.2	F	2s	39.0	Tc	4p	48.5	I	4d	56.8	Lu	5s	73.1	Tl	5p3
2.0	Nb	4d	7.0	Sm	4f	13.2	Rb	4p	19.7	Ga	As fract	29.4	Ge	3d	39.5	Tm	5p	49.5	Ho	5s	57.4	Er	5s	73.2	Al	2p1
2.0	Nd	4f	7.0	Sn	5s	14.0	Ne	2p	20.0	U	6p	29.5	Ho	5p1	40.0	At	5d	49.5	Mg	CO3	58.0	Ag	4p	73.8	Al	N
2.0	Ni	3d	7.0	Xe	5p	14.0	Sc	3d	20.2	Zn	loss	29.7	Ge	3d3	40.0	Ba	5s	49.6	Mg	(OH)2	58.0	Fr	5d	74.0	Au	5p1
2.0	Pr	4f	7.1	Lu	4f7	14.2	Hf	4f7	20.5	Gd	5p	30.2	Ge	Se	40.0	In	loss	49.6	Mg	2p3	58.0	Hg	5p3	74.2	Cr	3s
2.0	Sb	5p	7.1	Tb	4f	15.0	Fr	6p	20.7	Ga	2O3	30.3	Na	2p	40.0	Tb	5s	49.7	Mg	O	58.1	W	loss	74.3	Al	2O3
2.0	Sc	4p	7.7	Gd	4f	15.0	H	1s	21.0	Pb	5d3	30.9	Nb	4p	40.1	Te	4d	49.8	Mg	2p	58.2	Ti	3s	74.3	Al	2O3-nH2O
2.0	Tc	4d	7.8	Dy	4f	15.0	Hf	4f	21.6	Ta	4f7	30.9	Pb	loss	40.2	Re	4f7	49.9	Mg	2p1	58.3	Te	loss	74.4	Pt	4f5
2.0	Ti	3d	8.0	At	6p	15.0	Rb	4p1	21.8	Tb	5p	31.0	Hf	5p3	41.0	Ne	2s	50.0	Mg	CO3	58.6	Ag	4p	74.4	Al	(OH)3
2.0	V	3d	8.0	S	3p	15.0	Tl	5d3	22.0	Dy	5p3	31.0	Po	5d	41.0	Sm	5s	50.0	Sr	loss	58.9	Y	loss	74.9	Cu	3p
2.0	Yb	4f	8.3	Ho	4f	15.7	Cl	3s	22.0	Pm	5p	31.3	W	4f7	41.2	Re	4f	50.3	Zr	4s	59.0	Co	3p	74.9	Se	loss
2.0	Zr	4d	8.3	Lu	5d	15.9	Hf	4f5	22.3	Ar	3s	31.5	Ge	Se2	41.4	Re	Ntv Ox	50.4	Mg	NtvOx1	59.2	As	loss	75.0	Cs	4d5
2.5	Yb	4f5	8.4	Lu	2O3	15.9	I	5s	22.7	Ta	4f	31.7	Sb	4d	41.5	As	3d5	50.7	Os	4f7	60.8	Ir	4f7	75.1	Pt	O2-nH2O
2.6	Te	5p	8.5	Tm	4f7	16.0	K	3p	23.0	Cs	5s	32.1	Ga	loss	41.8	As	3d	50.7	Pd	4p	61.0	Mg	loss	75.1	W	5s
2.8	Cu	3d	8.6	Lu	4f5	16.0	P	3s	23.1	O	2s	32.3	W	4f	42.0	As	S	50.7	Sc	3s	62.0	Ir	4f	75.5	Al	Ntv Ox
2.8	Mn	3d	8.9	Ar	3p	16.0	S	3s	23.3	Ho	5p3	32.4	Ti	3p	42.0	Th	6s	50.9	Mg	reoxid	62.0	Ir	O2	76.0	Cs	4d
2.8	Re	5d	9.0	F	2p	16.9	In	4d	23.3	Y	4p	32.6	Ta	5p3	42.1	Ca	3s	51.0	Ir	5p3	62.0	Ir	5p1	77.8	Ni	loss
2.8	Si	3p	9.0	Ru	4d	17.0	La	5p	23.4	Ta	S2	33.0	La	5s	42.1	Cr	3p	51.0	Mg	NtvOx2	62.0	Mo	4s	78.3	In	4p
2.8	W	5d	9.0	Sb	5s	17.0	Th	6p3	23.5	Ca	3p	33.2	Ge	O2	42.2	As	3d3	51.4	Os	4f	62.0	Xe	4d	79.0	Cs	4d3
3.0	Ge	4p	9.0	Si	3s	17.0	Xe	5s	23.5	Yb	5p	33.4	Lu	5p	42.7	Re	4f5	51.5	Pt	5p3	62.3	Hf	5s	80.0	Ru	4s
3.0	I	5p	9.1	As	4p	17.1	Hf	O2	23.8	Bi	5d	33.5	W	4f5	42.7	Ta	loss	51.5	Mg	reoxid	62.7	Ir	Ntv Ox	80.7	Rh	4s
3.0	Pb	6s	9.7	Zn	3d	17.7	Pb	5d	24.0	Ta	4f5	33.8	Ge	Ntv Ox	43.0	As	2S3	51.7	Re	loss	63.3	Na	2s	81.0	Hg	5p1
3.2	Bi	6p3	10.0	Ba	5p	17.9	Ga	InAs (ar)	24.0	Bi	5d5	34.0	Fr	6s	44.0	Os	5p3	51.9	Mg	NtvOx3	63.8	Ir	4f5	81.8	Re	5s

Handbook of The Elements and Native Oxides

4.4: Experimental Details

The basic requirements for a photoemission experiment (XPS or UPS) are:

1. a source of fixed-energy radiation (an x-ray source for XPS or, typically, a He discharge lamp for UPS)
2. an electron energy analyzer (which can disperse the emitted electrons according to their kinetic energy, and thereby measure the flux of emitted electrons of a particular energy)
3. a high vacuum environment (to enable the emitted photoelectrons to be analyzed without interference from gas phase collisions)

Such a system is illustrated schematically below for a solid sample:

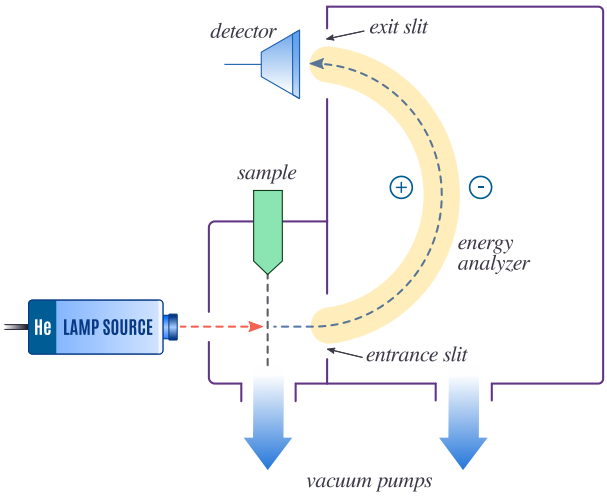

Figure 4.4.1: Diagram of a basic, typical PES instrument used in UPS, where the radiation source is an UV light source. When the sample is irradiated, the released photoelectrons pass through the lens system which slows them down before they enter the energy analyzer. The analyzer shown is a spherical deflection analyzer which the photoelectrons pass through before they are collected at the collector slit. (CC BY-NC; Ümit Kaya via LibreTexts)

There are many different designs of electron energy analyzer but the preferred option for photoemission experiments is a concentric hemispherical analyzer (CHA) which uses an electric field between two hemispherical surfaces to disperse the electrons according to their kinetic energy.

Radiation Sources

X-ray tubes

Aside from high-tech synchrotron facilities, most laboratory XAS work is done using X-ray (Coolidge) tube sources. Essentially, this is a high-vacuum tube containing a hot cathode filament (usually tungsten) and an anode surface.

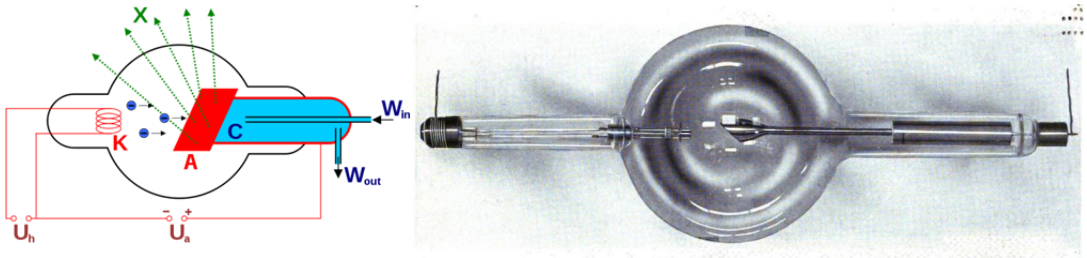

Figure 4.4.1: Coolidge X-ray tube, from around 1917. The heated cathode is on the left, and the anode is right. The X-rays are emitted downwards. (Public Domain; via Wikipedia)

Bremsstrahlung is electromagnetic radiation produced by the deceleration of a charged particle, such as an electron, when deflected by another charged particle, such as an atomic nucleus. The term is also used to refer to the process of producing the radiation. Bremsstrahlung has a continuous spectrum. Brehmsstrahlung is German for “braking radiation”, generated when fast-moving electrons closely approach atomic nuclei and are deflected off their incident trajectory by electrostatic forces. The energy

lost to this deflection is emitted in the form of radiation. Since the ΔE due to deflection differs depending on the path of the incident electron, brehmsstrahlung produces an essentially continuous spectrum.

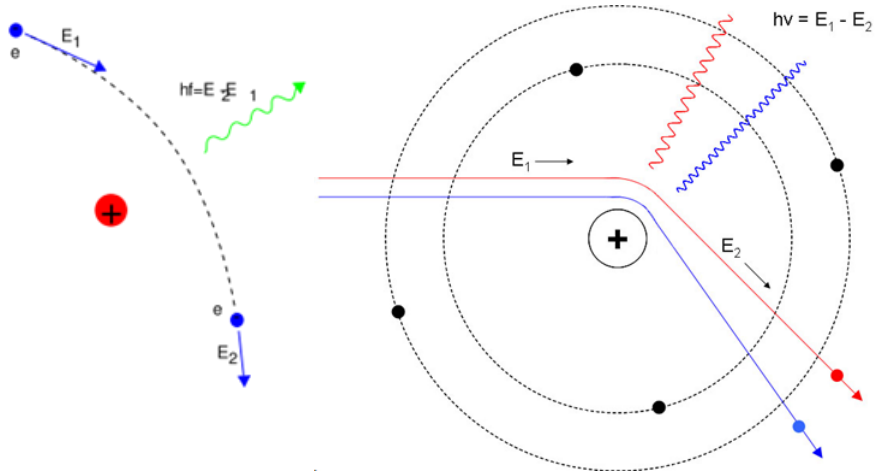

Figure 4.4.1: Bremsstrahlung radiation

Types of radiation from this: Characteristic output (Resonant transitions from one electron energy level to another) and Bremsstrahlung (inelastic scattering). The former is narrow and the latter is broadband.

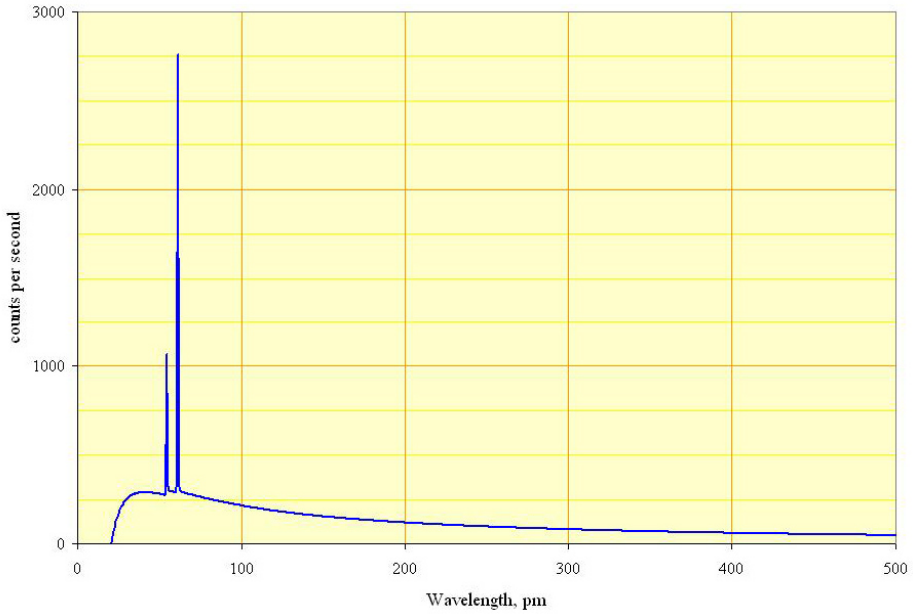

Figure 4.4.1: Spectrum of the X-rays emitted by an X-ray tube with a rhodium target, operated at 60 kV. The smooth, continuous curve is due to bremsstrahlung, and the spikes are characteristic K lines for rhodium atoms. (Public Domain; via Wikipedia). See https://xdb.lbl.gov/Section1/Periodi...h_Web_data.htm

Synchrotron radiation

Synchrotron radiation is, very simply, radiation from relativistic charged particles moving in a uniform magnetic field. It is the relativistic equivalent of cyclotron radiation and is named after the relativistic accelerators. Cyclotron radiation is electromagnetic radiation emitted by moving charged particles deflected by a magnetic field. The Lorentz force on the particles acts perpendicular to both the magnetic field lines and the particles' motion through them, creating an acceleration of charged particles that causes them to emit radiation (and to spiral around the magnetic field lines).

Figure 4.4.1: Left: The Advanced Photon Source at Argonne is the nation's most brilliant source of X-rays for research in physics, chemistry, biology, geosciences, materials science and environmental science. Right: ESRF at Grenoble (FRANCE)

Detectors

X-radiation, upon contact with an inert gas atom, can collide with and transfer a massive amount of kinetic energy to an outer electron of the shell, ionizing the gas. The ejected electron, known as a photoelectron, releases its excess kinetic energy by subsequent collisions with other outer shell electrons, causing an ionization cascade. Gas-filled transducers take advantage of this interaction by counting the number of electrons produced and correlating this with the kinetic energy of the original photon.

A general schematic of a gas-filled transducer is shown below. In this case, X-rays enter through a low-absorbance window on the side to ionize argon gas. Argon anions migrate towards the wall of the transducer tube, whereas ejected electrons migrate to the central wire anode. The electrical signal from the anode may then be measured and quantified by the signal processor.

X-radiation, upon contact with an inert gas atom, can collide with and transfer a massive amount of kinetic energy to an outer electron of the shell, ionizing the gas. The ejected electron, known as a photoelectron, releases its excess kinetic energy by subsequent collisions with other outer shell electrons, causing an ionization cascade. Gas-filled transducers take advantage of this interaction by counting the number of electrons produced and correlating this with the kinetic energy of the original photon.

A general schematic of a gas-filled transducer is shown below. In this case, X-rays enter through a low-absorbance window on the side to ionize argon gas. Argon anions migrate towards the wall of the transducer tube, whereas ejected electrons migrate to the central wire anode. The electrical signal from the anode may then be measured and quantified by the signal processor.

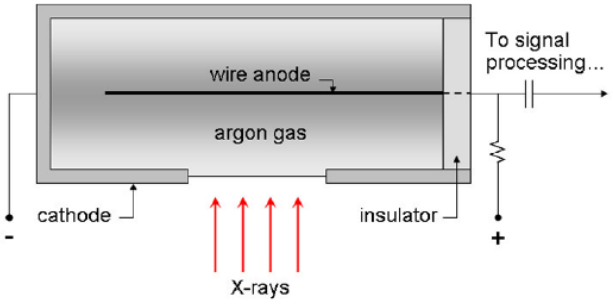

Scintillators are materials which fluoresce (or phosphoresce) in the presence of ionizing radiation. Scintillation counters combine this property with another well-known phenomenon — the photoelectric effect — to convert incident X-radiation into an electrical signal and quantify it.

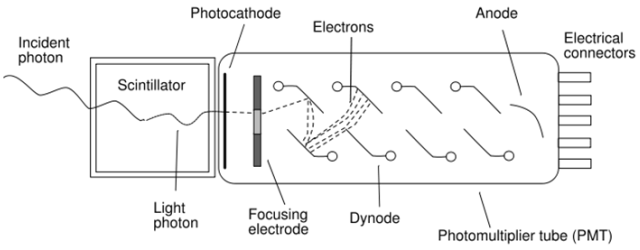

When an X-ray photon hits the scintillator, its energy is absorbed and promptly reemitted at a different wavelength. The emitted photons are gathered and focused towards the photocathode, where they are absorbed and their energy is used to emit electrons via the photoelectric effect. The photoelectrons are in turn focused towards a series of metal electrodes known as dynodes. When a photoelectron hits the first dynode, its kinetic energy is sufficient to knock several more electrons off the dynode surface via the Auger effect. These Auger electrons proceed through the rest of the dynode series, producing more and more electrons with each impact. Finally, the amplified electron signal is absorbed at the anode, measured, and quantified.

4.5: X-ray Photoelectron (XPS) Spectroscopy

X-Ray photoelectron spectroscopy (XPS), also known as electron spectroscopy for chemical analysis (ESCA), is one of the most widely used surface techniques in materials science and chemistry. It allows the determination of atomic composition of the sample in a non-destructive manner, as well as other chemical information, such as binding constants, oxidation states and speciation. The sample under study is subjected to irradiation by a high energy X-ray source. The X-rays penetrate only 5 – 20 Å into the sample, allowing for surface specific, rather than bulk chemical, analysis.

Figure 4.5.1 Excitation of an electron from an atom's K-shell.

As an atom absorbs the X-rays, the energy of the X-ray will cause a K-shell electron to be ejected, as illustrated by Figure 4.5.1. The K-shell is the lowest energy shell of the atom. The ejected electron has a kinetic energy (KE) that is related to the energy of the incident beam (hv), the electron binding energy (BE), and the work function of the spectrometer (φ) (4.5.1). Thus, the binding energy of the electron can be calculated.

$$BE = h\nu - KE - \psi_s \tag{4.5.1}$$

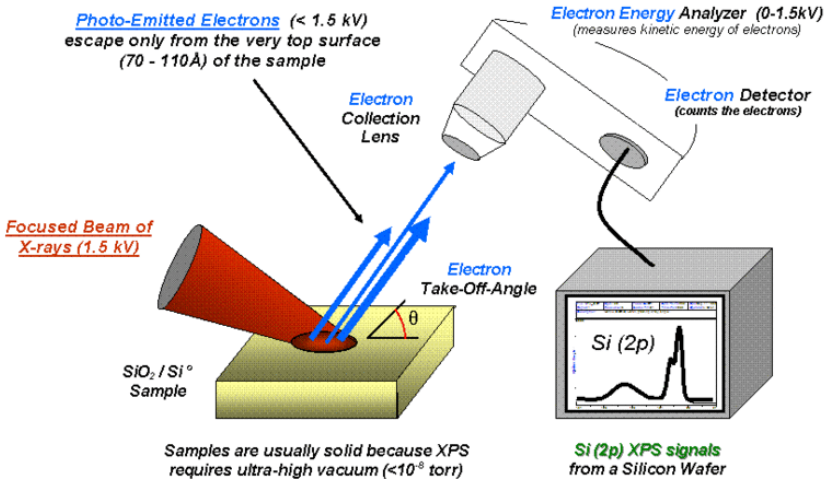

Figure 4.5.1: XPS Instrument. (Public Domain; **Bvcrist** via Wikipedia)

Table 4.5.1 shows the binding energy of the ejected electron, and the orbital from which the electron is ejected, which is characteristic of each element. The number of electrons detected with a specific binding energy is proportional to the number of corresponding atoms in the sample. This then provides the percent of each atom in the sample.

Table 4.5.1: Binding energies for select elements in their elemental forms.

Element	Binding Energy (eV)
Carbon (C) (1s)	284.5 - 285.1
Nitrogen (N) (1s)	396.1 - 400.5
Oxygen (O) (1s)	526.2 - 533.5
Silicon (Si) (2p)	98.8 - 99.5
Sulfur (S) ($2p_{3/2}$)	164.0 - 164.3
Iron (Fe) ($2p_{3/2}$)	706.8 - 707.2
Gold (Au) ($4f_{7/2}$)	83.8 - 84.2

The chemical environment and oxidation state of the atom can be determined through the shifts of the peaks within the range expected (Table 4.5.2). If the electrons are shielded then it is easier, or requires less energy, to remove them from the atom, i.e., the binding energy is low. The corresponding peaks will shift to a lower energy in the expected range. If the core electrons are not

shielded as much, such as the atom being in a high oxidation state, then just the opposite occurs. Similar effects occur with electronegative or electropositive elements in the chemical environment of the atom in question. By synthesizing compounds with known structures, patterns can be formed by using XPS and structures of unknown compounds can be determined.

Table 4.5.2 Binding energies of electrons in various compounds.

Compound	Binding Energy (eV)
COH (C 1s)	286.01 - 286.8
CHF (C 1s)	287.5 - 290.2
Nitride (N 1s)	396.2 - 398.3
Fe_2O_3 (from O, 1s)	529.5 - 530.2
Fe_2O_3 (from Fe, $2p_{3/2}$)	710.7 - 710.9
FeO (from Fe $2p_{3/2}$)	709.1 - 709.5
SiO_2 (from O, 2s)	532.5 - 533.3
SiO_2 (from Si, 2p)	103.2 - 103.9

Sample preparation is important for XPS. Although the technique was originally developed for use with thin, flat films, XPS can be used with powders. In order to use XPS with powders, a different method of sample preparation is required. One of the more common methods is to press the powder into a high purity indium foil. A different approach is to dissolve the powder in a quickly evaporating solvent, if possible, which can then be drop-casted onto a substrate. Using sticky carbon tape to adhere the powder to a disc or pressing the sample into a tablet are an option as well. Each of these sample preparations are designed to make the powder compact, as powder not attached to the substrate will contaminate the vacuum chamber. The sample also needs to be completely dry. If it is not, solvent present in the sample can destroy the necessary high vacuum and contaminate the machine, affecting the data of the current and future samples.

4.6: X-ray Absorption Spectroscopies

Originally discovered by Wilhelm Roentgen in the nineteenth century, X-rays have become one of the most useful applications of spectroscopy in both science and medicine. X-ray spectroscopy is a common analytical technique with a broad range of applications, particularly in determining crystal structure and elemental analysis of solid samples. X-rays are a form of electromagnetic radiation with a much higher degree of energy than UV radiation. This extra energy allows X-rays to be absorbed by core electrons within atoms. Also, X-rays can penetrate crystal structures more than other forms of EM radiation, having a wavelength on the same order of magnitude as interatomic distances. This allows the X-rays to be diffracted, producing diffraction patterns of the crystal. The most common means of generating X-ray for these analyses is with an **X-ray Tube**, but a synchrotron can work also.The electromagnetic radiation resulting from inner orbital electron transitions or deceleration of high-energy electrons is referred to as X-rays. The absorption, diffraction, emission, fluorescence and scattering of X-rays is exploited in a variety of X-Ray spectroscopic techniques. There are three basic applications of X-ray analysis (Figure 4.6.1):

1. Diffraction of X-rays on crystalline materials to obtain their crystal structure (X-ray Diffraction (XRD)),
2. Measurement of the energy of emitted X-rays during SEM imaging (X-ray Fluorescence (XRF) or x-ray emission spectroscopy (XES)) to give elemental information from the sample surface,
3. Using X-rays to knock out core electrons of atoms to provide surface chemical information from samples (X-ray Photoelectron Spectroscopy (**XPS**, also known as ESCA))

These techniques reveal useful information about the structure and composition of matter. The three main techniques that we are focusing on are X-ray Fluorescence (XRF), X-ray Photoelectron Spectroscopy (XPS or ESCA) and Auger, Electron Spectroscopy (AES). The subtle differences between these three techniques are shown below.

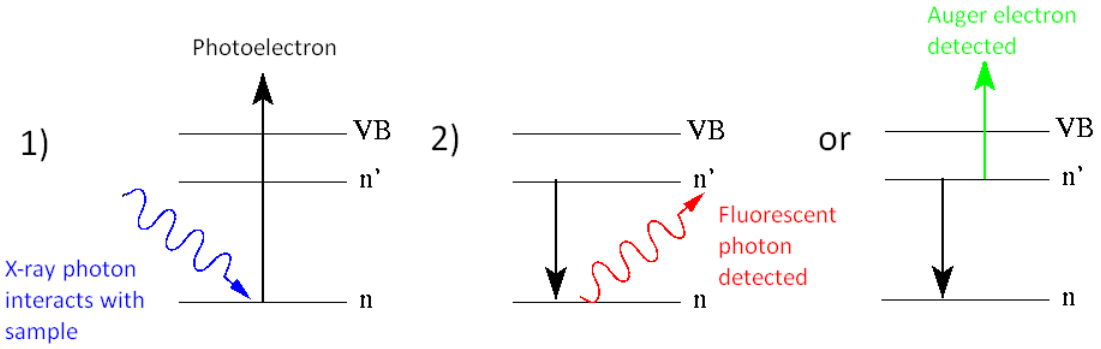

Figure 4.6.1: The fundamental processes which contribute to XANES spectra: 1) photoabsorption of an x-ray into a core level followed by photoelectron emission, followed by either 2) (left) filling of the core hole by an electron in another level, accompanied by fluorescence; or (right) filling of the core hole by an electron in another level followed by emission of an Auger electron. (CC BY-SA 3.0; Alison Chaiken via Wikipedia)

X-ray Photoelectron Spectroscopy (XPS)

XPS was discussed in the previous section and is in many ways the complete reverse of XRF in that an incoming X-ray photon causes the removal of a core or valence electron, although core electrons are more easily removed. These escaping electrons have a kinetic energy which is determined by the original photon and the binding energy of the atom. We can measure the kinetic energy of the electron and find out how tightly the electron was held in the atom. This is then used to find such information as oxidation state and bonding information. Like all X-ray techniques however, the information relates only to the top 100 Angstroms of the sample surface, making it useful for surface science techniques.

Auger Electron Spectroscopy

One of the two principal processes for the relaxation of an inner-shell electron vacancy in an excited or ionized atom. The **Auger effect** is a two-electron process in which an electron makes a discrete transition from a less bound shell to the vacant, but more tightly bound, electron shell. The energy gained in this process is transferred, via the electrostatic interaction, to another bound electron which then escapes from the atom. This outgoing electron is referred to as an Auger electron and is labeled by letters corresponding to the atomic shells involved in the process. For example, a KL_IL_{III} Auger electron corresponds to a process in which

an L_I electron makes a transition to the K shell and the energy is transferred to an L_{III} electron (illus. *a*). By the conservation of energy, the Auger electron kinetic energy E is given by

$$E = E(K) - E(L_I) - E(L_{III})$$

where $E(K, L)$ is the binding energy of the various electron shells. **Since the energy levels of atoms are discrete and well understood, the Auger energy is a signature of the emitting atom.**

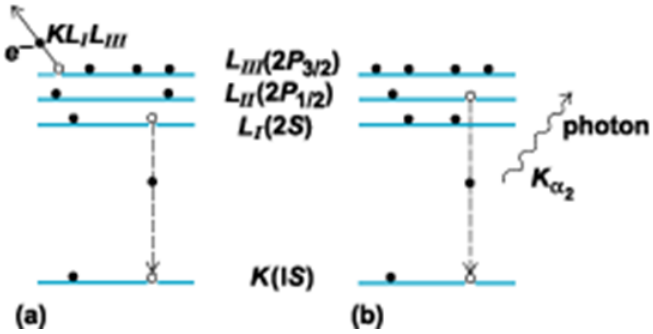

Figure 4.6.1: Radiative process in which an L_{II} electron fills the K-shell vacancy with the emission of a $K_{\alpha 2}$ photon. Two principal processes for the filling of an inner-shell electron vacancy. (a) Auger emission; a KL_IL_{III} Auger process in which an L_I electron fills the K-shell vacancy with the emission of a KL_IL_{III} Auger electron from the L_{III} shell. (b) Photon emission; a radiative process in which an L_{II} electron fills the K-shell vacancy with the emission of a $K_{\alpha 2}$ photon.

Auger spectroscopy is complimentary with XPS and most instruments allow both types of measurement to be made on a sample. The Auger process occurs in excited atoms which have a core electron removed. As in XRF, an upper electron drops to fill the vacancy, although instead of emitting a photon to release the excess energy, it transfers its energy to a neighboring electron which is then emitted from the atom. Auger electrons are of very low energy and are only emitted from the extreme surface of the sample. This is exploited by etching the surface of the sample with an ion beam, exposing progressively deeper layers into the sample. An electron beam is then directed onto the exposed regions. The Auger electrons produced by the beam come from each new layer exposed, allowing depth profiling to be achieved.

X-ray Fluorescence (XFS) or X-ray emission spectroscopy (XES)

X-ray Fluorescence (XFS) like other fluorescent techniques culminate with the emission of a photon. An atom which is induced into an excited state, usually by an electron beam causing the removal of a core electron from the atom, causes relaxation of the excited state. This relaxation occurs by an electron in a higher energy state dropping to fill the core level vacancy. The large energy decrease required to allow this to occur produces the release of an X-ray photon.

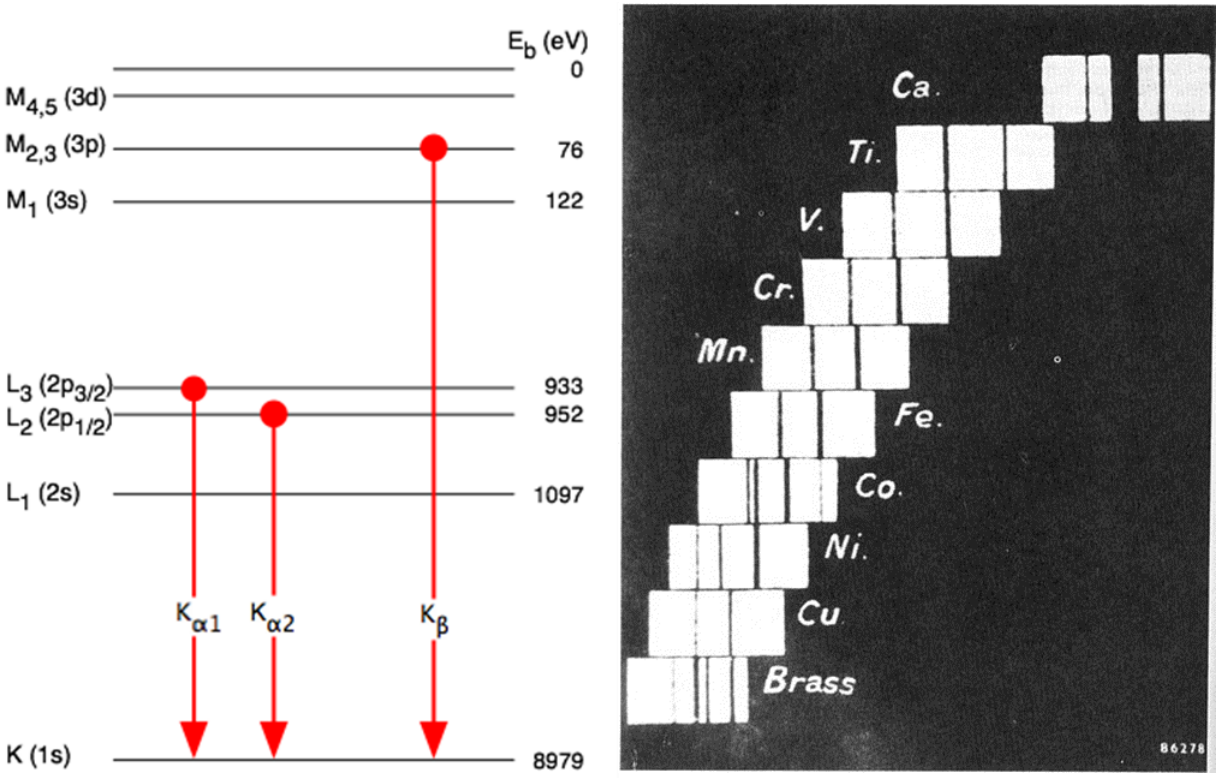

Figure 4.6.1: **Left**: A diagram displaying the nomenclature of the allowed energy levels and the allowed electron transitions of a generic atom. The red circles represent electrons. In X-ray spectroscopy, K-alpha emission lines result when an electron transitions to the innermost "K" shell (principal quantum number 1) from a 2p orbital of the second or "L" shell (with principal quantum number 2). The line is actually a **doublet**, with slightly different energies depending on *spin-orbit* interaction energy between the electron spin and the orbital momentum of the 2p orbital. K-alpha is typically by far the strongest X-ray spectral line for an element bombarded with energy sufficient to cause maximally intense X-ray emission. **Right**: Moseley was able to show that the frequencies of certain characteristic X-rays emitted from chemical elements are proportional to the square of a number which was close to the element's atomic number; a finding which supported van den Broek and Bohr's model of the atom in which the atomic number is the same as the number of positive charges in the nucleus of the atom.

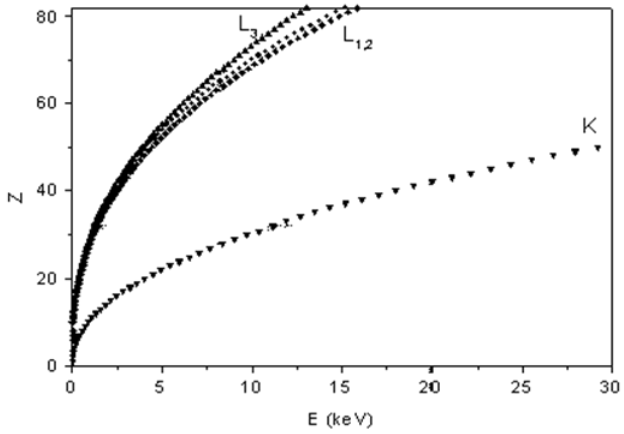

The relation between the atomic number Z of an element and the energy of its K and L x-ray absorption edges (Moseley law).

4.7: Experimental modes and Data Analysis

Designing the experiment requires an understanding of the four primary detection methods in X-ray Absorption Spectroscopies (XAS): (1) Transmission, (2) Fluorescence, (3) "Auger" Electron yield and (4) Total Electron Yield.

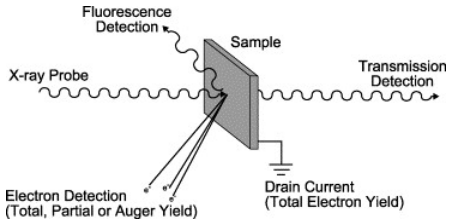

Figure 4.7.1: Schematic of the possible measurement techniques for XAS. The absorption process depicted in Fig. cannot be detected directly and so the signal must be detected through either the absence of the absorbed photons in the transmitted X-rays (transmission detection) or through the particles ejected during the relaxation process that follows (fluorescence detection or electron detection). Energy discrimination allows the electron detection technique to be broken down into total (TEY), partial (PEY) and Auger (AEY) electron yield detection schemes. ()

Transmission Mode

Absorption Length = distance over which x-ray intensity sets the fundamental length scale for choosing sample thickness, particle size, and sample homogeneity. This is often about 10 microns but varies depending on density and element that is probed. Sample cannot be significantly larger or it absorbs all the x-ray light.

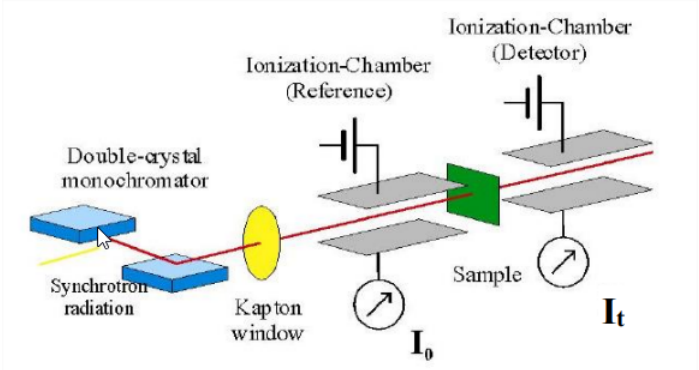

Figure 4.7.2: Experimental XAS setup transmission mode. (Copyright; author via source)

The XAS technique is *insensitive* and higher concentrations of metal will provide higher quality data (up to around 5 mM or so). Sample cuvets are commonly made out of machined polycarbonate or Lucite with one X-ray transparent (e.g., Mylar) window. Minimum volumes useful on current generation beamlines are dictated by the cross section of the beam and usually one needs at least 50 microliters. One major limitation to the use of this technique is its inability to distinguish multiple site structures within a given sample. If the sample has heterogeneous metal environments, the resulting XAS-derived structure would simply be the weighted sum of all the structures contained in the sample. Thus, many EXAFS reports describe an ”average” structure. It is usually helpful to have some independent measurement that suggests that all of the metal being probed exists in a homogeneous type of site.

This schematic of an X-ray absorption spectrometer shows that the essential components are analogous to those required for any spectroscopic technique. However, operating in the X-ray region of the electromagnetic spectrum requires that each component be designed differently than their analogs in the UV, visible, or IR regions.

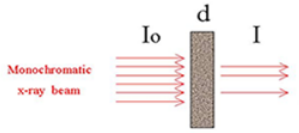

Figure 4.7.2B: A schematic representation of x-ray absorption spectroscopic measurements in transmission mode.

X-ray detectors are either gas ionization chambers (X-rays ionize an inert gas and charged plates collect and record the microcurrent generated) or fluorescence photon-counting detectors (scintillation counters, solid-state detectors). X-ray

monochromators are two parallel single crystals of silicon (usually) that take advantage of Bragg diffraction to monochromate the Xrays. Tuning occurs by simply rotating the crystals to different incident angles. A light bulb is *not* a good source of X-rays, so instead all biological XAS is performed using synchrotron radiation generated by a storage ring.

You measure absorption just like in UV-VIS and IR (dispersive):

$$\frac{I}{I_0} = e^{-\mu(E)x}$$

which can be converted to

$$\mu(x)x = \ln\left(\frac{I}{I_0}\right)$$

Fluorescence Mode

X-ray fluorescence or XRF is the emission of characteristic "secondary" (or fluorescent) X-rays from a material that has been excited by bombarding with high-energy X-rays. X-ray fluorescence. If the electron has enough energy it can knock an orbital electron out of the inner shell of a metal atom, and as a result electrons from higher energy levels then fill up the vacancy and X-ray photons are emitted. This process produces a discrete spectrum of X-ray frequencies, called spectral lines. The spectral lines generated depends on the target (anode) element used and thus are called characteristic lines. Usually these are transitions from upper shells into K shell (called K lines), into L shell (called L lines) and so on.

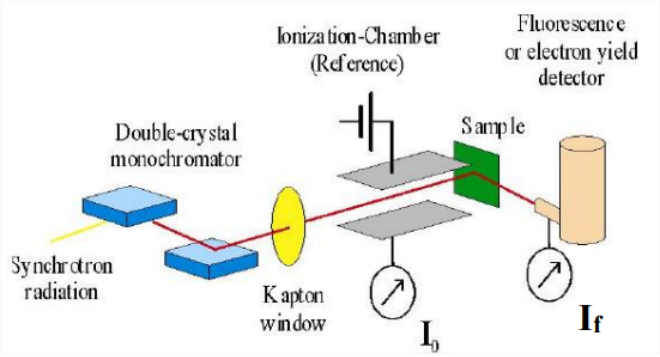

Figure 4.7.3: Experimental XAS setup fluorescence mode. (Copyright; author via source)

"Auger" Electrons

When an electron is removed from a core level of an atom, leaving a vacancy, an electron from a higher energy level may fall into the vacancy, resulting in a release of energy. Although sometimes this energy is released in the form of an emitted photon (XRF), the energy can also be transferred to another electron, which is ejected from the atom. This second ejected electron is called an **Auger electron.**

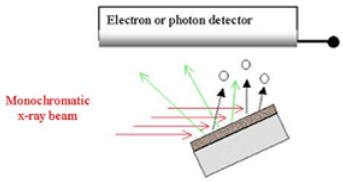

$I \propto I_0 \varepsilon \omega \Omega x \mu$

with

- μ-absorption coefficient
- x-layer thickness
- ω-radiative or nonradiative yield
- Ω-solid angle of collection
- ε-detection efficiency

Upon ejection the kinetic energy of the Auger electron corresponds to the difference between the energy of the initial electronic transition and the ionization energy for the electron shell from which the Auger electron was ejected. These energy levels depend on the type of atom and the chemical environment in which the atom was located.

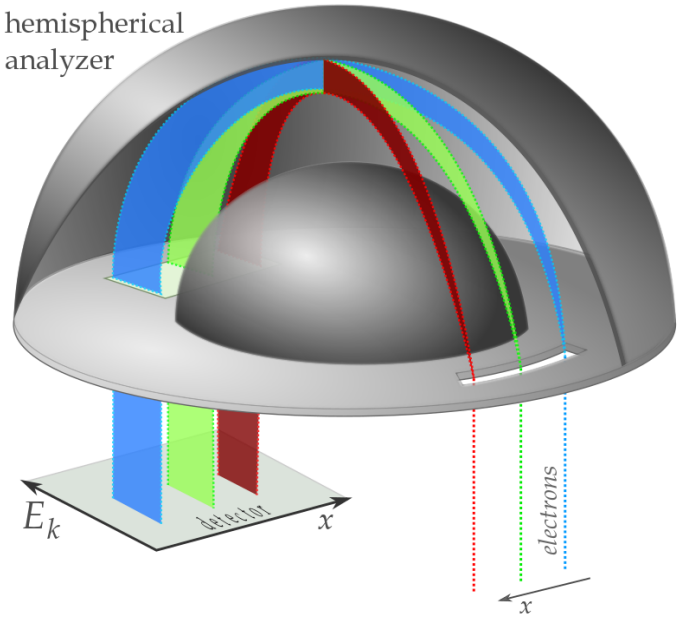

Figure 4.7.4: Hemispherical electron energy analyzer. Electron of different energies are dispersed to different channels of the detector in the direction perpendicular to the entrance slit.. (CC BY-SA 4.0; Ponor via Wikipedia)

Total Electron yield

In the total electron yield detection mode, a solid is illuminated with a monochromatic beam of x-rays. Core electrons are excited into the conduction band of the solid, and the resulting current measured in the variant known as **total electron yield**. The intensity of the emitted primary Auger electrons is a direct measure of the x- ray absorption process are highly surface sensitive, similar to XPS. As they leave the sample, the primary Auger electrons create scattered secondary electrons (Figure 4.7.4) which dominate the total electron yield (TEY) intensity. The TEY cascade involves several scattering events and originates from an average depth, the electron sampling depth L.

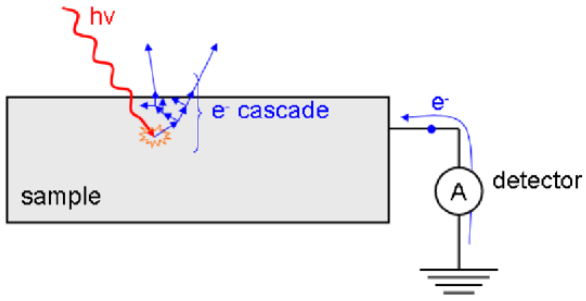

Figure 4.7.5: Principle of total electron yield XAS measurement. (all rights reserved)

This detection scheme has significantly limitations for non-conducting samples.

4.8: Introduction to X-ray Absorption Spectroscopy (XAS)

Definitions

- **XAS: X-Ray Absorption Spectroscopy:** Generic term for various techniques involving absorption of x-rays
- **XAFS: X-Ray Absorption Fine Structure:** Alternate generic term for following two techniques
  - **XANES: X-Ray Absorption Near Edge Structure:** Structure in x-ray absorption spectrum just before and after edge and its analysis – a spectroscopic technique
  - **EXAFS: Extended X-Ray Absorption Fine Structure:** Structure in x-ray absorption spectrum after edge and its analysis – a structural technique

The X-ray absorption spectra show a steep rise at the core-level binding energy of X-ray-absorbing atoms and attenuates gradually with the X-ray energy. The XAS spectra are usually divided in two energy regions:

1. the X-ray Absorption Near Edge Structure (XANES)
2. the extended X-ray absorption fine structure (EXAFS)

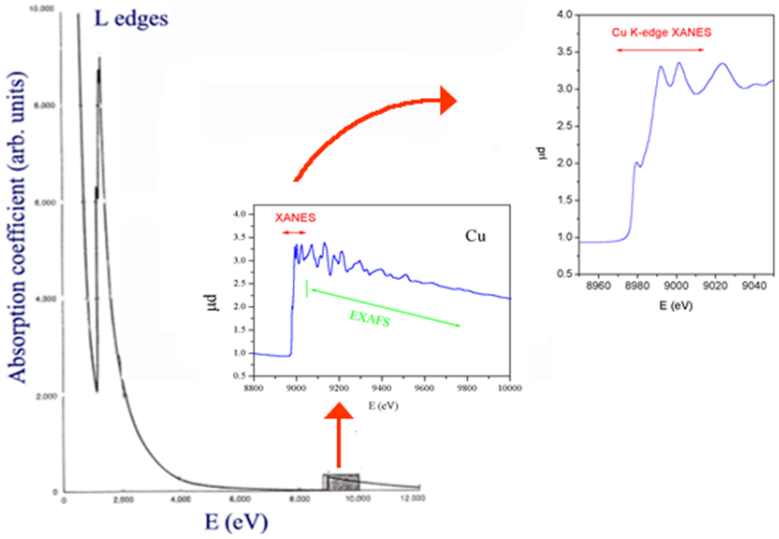

Figure 4.8.1: X-ray absorption coefficient of copper in the region of L and K edges. The box area is expanded in the inset to show EXAFS and XANES signal.

Spectroscopy (XANES)

Analysis of the edge region (XANES) provides information (i.e., position of the edge and the assignment of peaks near or on the edge) about oxidation state, covalency (e..g, increasing ligand character of metal d orbitals), molecular symmetry of the site, including coordination numbers.

- Oxidation State
- Covalency
- Site Symmetry
- Coordination Number

Structure (EXAFS)

The EXAFS provides direct, local structural information about the atomic neighborhood of the element being probed (usually a metal). The information content consists of numbers of ligands (coordination number), the identity of the ligand atoms, and precise radial distances. It can be particularly informative when there are other metals in the atomic neighborhood of the metal being probed (as in clusters).

- Radial Distances
- Coordination Numbers
- Types of Ligands

Band Edge Transitions

Absorption edge energies are characteristic of the absorbing element. XAFS allows you to tune into different types of atoms by selecting the energy:

$$E_{n,l} = -hcR_{\infty}\frac{Z_{eff}^2}{n^2}$$

R is the Rydberg constant for this element; ***Z* is the atomic number**, i.e. the number of protons in the atomic nucleus of this element. X-ray absorption probability can be calculated using standard quantum theory. As in optical spectroscopy discussed earlier, the absorption coefficient is proportional to the square of the transition matrix element, here shown in dipole approximation.

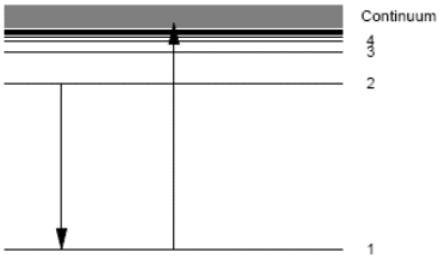

$$\mu \propto |\langle f|\vec{\varepsilon}\cdot\vec{r}|i\rangle|^2$$

with the **dipole approximation selection rule** $\Delta l = \pm 1$.

Absorption edges

The K-edge is a sudden increase in x-ray absorption occurring when the energy of the X-rays is just above the binding energy of the innermost electron shell of the atoms interacting with the photons. The term is based on X-ray notation, where the innermost electron shell is known as the K-shell. Physically, this sudden increase in attenuation is caused by the photoelectric absorption of the photons. For this interaction to occur, the photons must have more energy than the binding energy of the K-shell electrons (K-edge). A photon having an energy just above the binding energy of the electron is therefore more likely to be absorbed than a photon having an energy just below this binding energy or significantly above it.

- K: $1s \leftarrow p$
- L_3: $2p_{3/2} \leftarrow s, d$
- L_2: $2p_{1/2} \leftarrow s, d$
- L_1: $2s \leftarrow p$

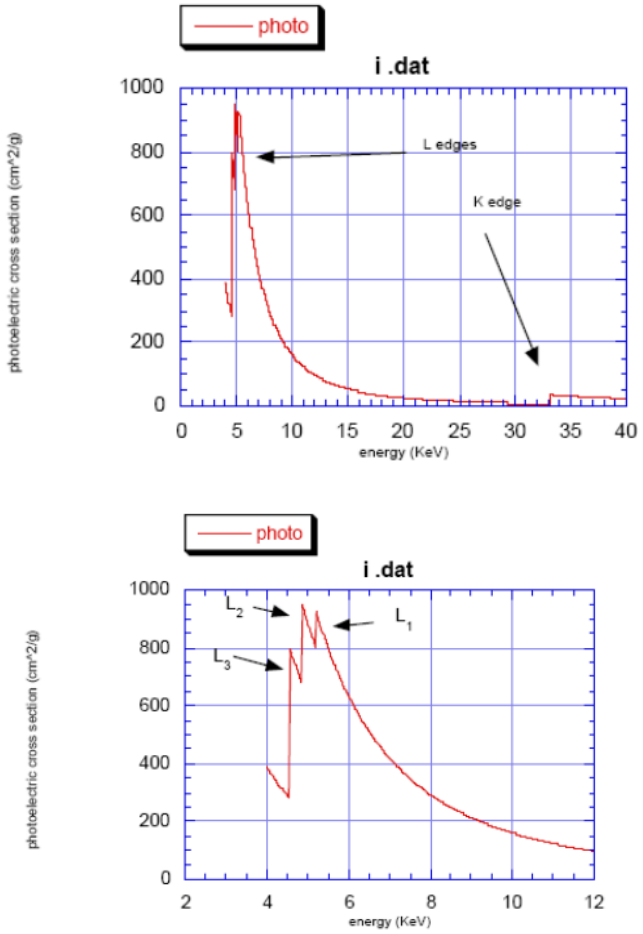

Figure 4.8.4: A schematic representation of x-ray absorption spectroscopic measurements in fluorescence and electron detection mode.

4.9: X-Ray Absorption Near Edge Structure (XANES)

The X-ray photon absorbed results in transitions within the atomic energy levels of the absorbing atom. During the spectroscopic scan , no absorption occurs until the photon has an energy equal to the ionization energy of core electrons. At lower X-ray energies, X-ray induced ionization of 2p or 2s electrons gives rise to what are called L_{III}, L_{II}, and L_I absorption edges. At significantly higher X-ray energies, photoionization of a 1s electron gives rise to the K X-ray absorption edge. The photon energies required for these edges of several selected elements are summarized above. X-ray sources provide a spectral distribution between 2 - 25 keV, giving access to K edges of elements through the second transition series. For elements in the remainder of the periodic table, these X-ray sources can access their L edges. Thus, all elements from ca. S throughout the periodic table can be probed.

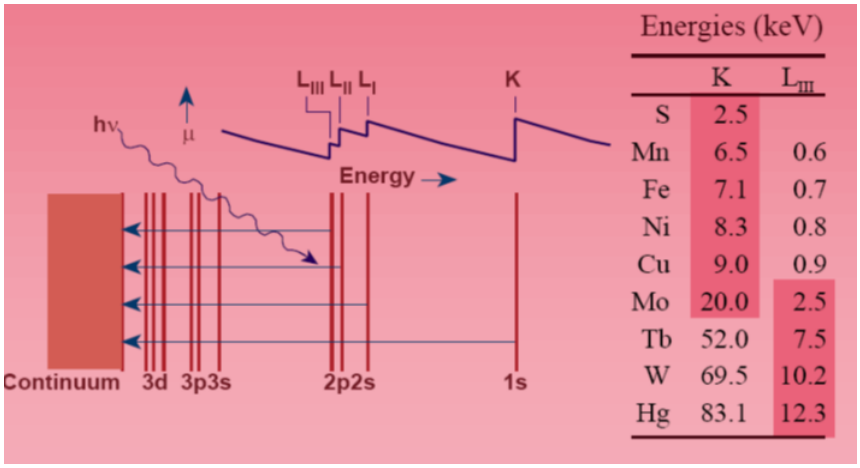

Energies (keV)

	K	L_{III}
S	2.5	
Mn	6.5	0.6
Fe	7.1	0.7
Ni	8.3	0.8
Cu	9.0	0.9
Mo	20.0	2.5
Tb	52.0	7.5
W	69.5	10.2
Hg	83.1	12.3

For a given element, K edge energies depend slightly (± a few eV) on the chemical environment of the element. For example, higher oxidation state metals have higher positive charge, making it slightly more difficult to photodissociate a 1s electron, shifting the K edge to higher energy. Shifts of 1-2 eV per oxidation state are typical for first-row transition metals. **Also, spectroscopic transitions from the 1s orbital to orbitals just below the continuum (Fermi level), such as 3d, 4s, 4p, etc., obey electric dipole selection rules like any other electronic transition and assignments of such features can provide information about molecular symmetry.**

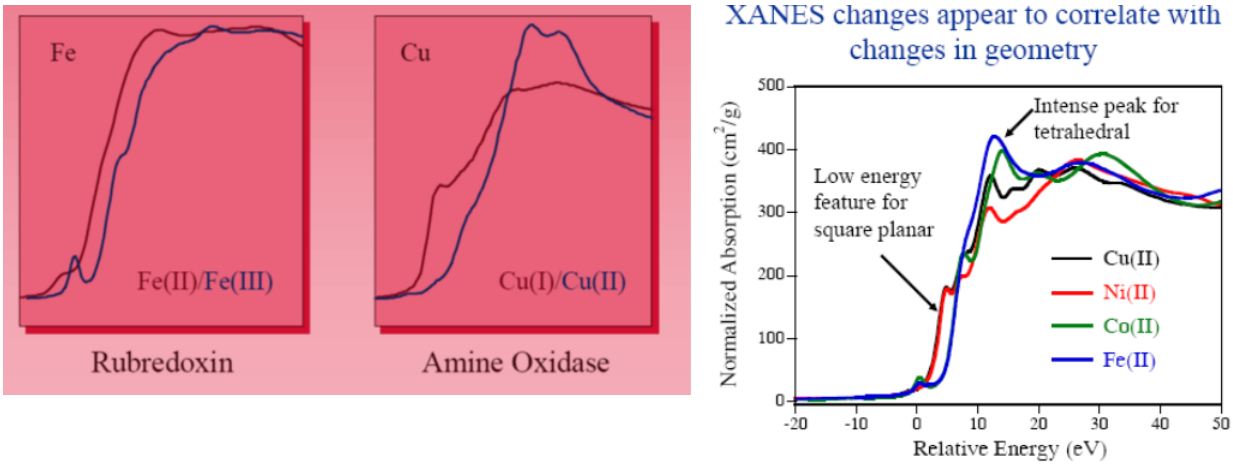

Figure 4.9.1: XANES sensitivity to oxidation state and geometry

The shape of the edge and the pre-edge resonances are characteristic for the local symmetry of the investigated atom sites and can be used as fingerprints in identification of its local structure. Tetrahedrally coordinated Cr materials, lacking an inversion center, exhibit a single intense pre-edge peak which can be assigned to a dipole allowed transition of 1s electron to an unoccupied anti-bonding t_2* tetrahedral orbital.

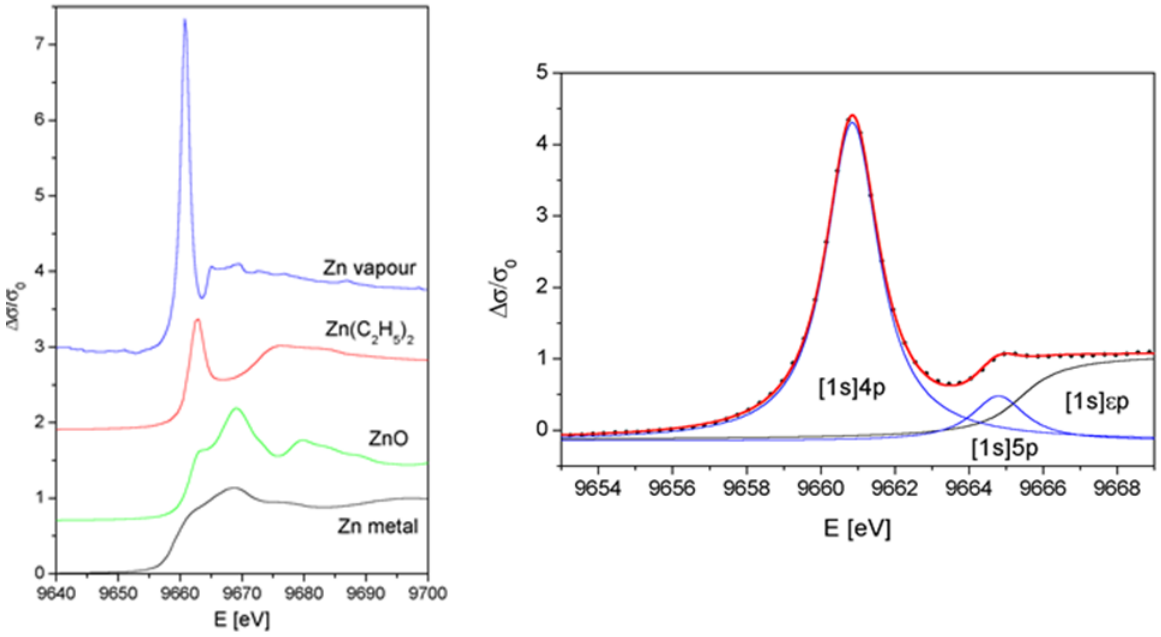

Figure 4.9.1: **Left**: Zn K-edge XANES measured on free and bound Zn atoms. Contains information on the unoccupied valence orbitals. **Right**: Atomic XANES can be described by pre-edge resonances due to transitions from 1s initial state to Rydberg final states below 1s ionization threshold and absorption edge due to transitions into continuum states above 1s ionization threshold.

Determining Oxidation state from XANES

The binding energies of the valence orbitals and therefore the energy position of the edge and the pre-edge features are correlated with **the valence state** of the absorbing atom in the sample. With increasing oxidation state each absorption feature in the XANES spectrum is shifted to higher energies.

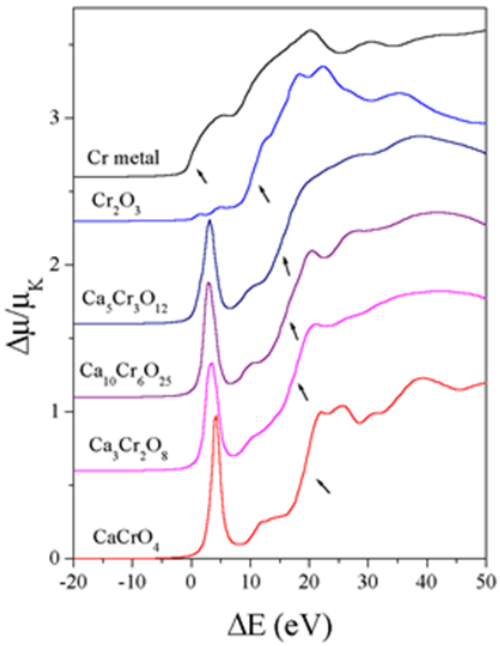

Normalized Cr K-edge profiles, displaced vertically, for the calcium chromate samples and Cr_2O_3, $CaCrO_4$, and Cr metal. Energy scale is relative to the Cr K-edge in metal (5989.0 eV). These spectra were measured at EXAFS 2 beamline in HASYLAB at DESY

in Hamburg.

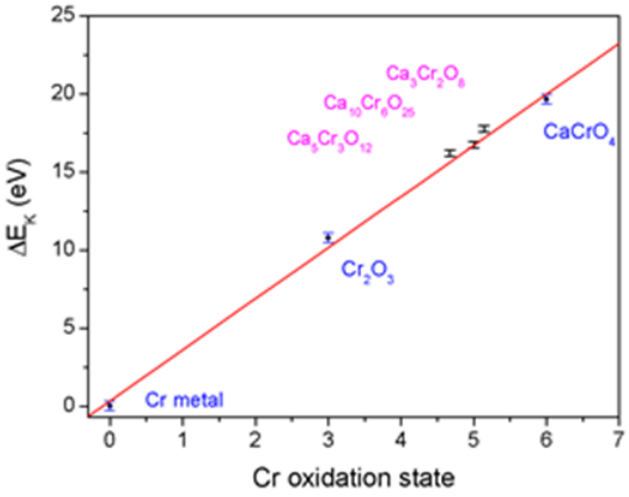

Energy positions of the Cr K-edge in chromates (|) and reference samples (o) vs. Cr oxidation state. Linear dependence based on the reference samples is shown by solid line

The energy shifts vary linearly with the valence of the absorbing atom. The largest shifts, up to a few eV per oxidation state, are observed at the edge position. Shifts of the pre-edge peaks are considerably smaller, of the order of a few tenths of eV.

The Take-home lesson about EXAFS utility

XANES tell Researchers what types of atoms and their oxidation states in a sample?

4.10: X-ray absorption fine structure (XAFS)

X-ray absorption fine structure (XAFS) spectroscopy is one of the most powerful tools we have for mapping local structure. In this technique, we probe a sample with x-rays that are tuned to the energy of a core electron shell in the element we wish to study. We monitor how many x-rays are absorbed as a function of their energy. If taken with sufficient accuracy, the spectrum exhibits small oscillations that are the result of the local environment's influence on the target element's basic absorption probability. From the spectrum, we can extract the distances between the absorber and its near-neighbor atoms, the number and type of those atoms, and the oxidation state of the absorbing element-all parameters that determine local structure. By selecting a different x-ray energy, we can obtain this information for any element in the sample.

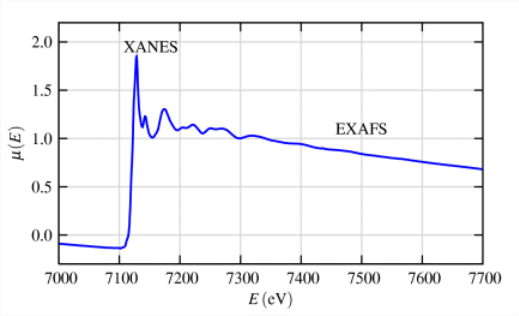

Figure 4.10.1: XAFS spectrum μ(E) for FeO. On top, the measured XAFS spectrum is shown with the XANES and EXAFS regions identified. (CARS)

EXAFS arises from photoelectron scattering, making it a spectroscopically detected scattering method. EXAFS spectra contain structural information comparable to that obtained from single-crystal x-ray diffraction. The principal advantage of EXAFS in comparison with crystallography is that EXAFS is a local structure probe and does not require the presence of long-range order. This means that EXAFS can be used to determine the local structure in noncrystalline samples.

Origin of the EXAFS Oscillations

We'll now develop the XAFS equation using a slightly more formal description of this simple physical picture. Since x-ray absorption is a transition between two quantum states (from an initial state with an x-ray, a core electron, and no photo-electron to a final state with no x-ray, a core hole, and a photo-electron), we describe μ(E) with Fermi's Golden Rule:

$$\mu(E) \propto |\langle i|\mathcal{H}|f\rangle|^2$$

where $\langle i|$ represents the initial state (an x-ray, a core electron, and no photo-electron), $|f\rangle$ is the final state (no x-ray, a core-hole, and a photo-electron), and H is the interaction term (which we'll come back to shortly). Since the core-level electron is very tightly bound to the absorbing atom, the initial state will not be altered by the presence of the neighboring atom. The final state, on the other hand, will be affected by the neighboring atom because the photo-electron will be able to see it.

The EXAFS phenomenon results from the sensitivity of the X-ray absorption coefficient to photoelectron-electron scattering with electron density surrounding neighboring atoms. Considering an absorbing atom a and a scattering atom s, photon-induced dissociation of a 1s electron creates a photoelectron that can be considered a **de Broglie wave with its origin at atom**. The excess energy from the photon is conserved as kinetic energy of the photoelectron, determining the wavelength.

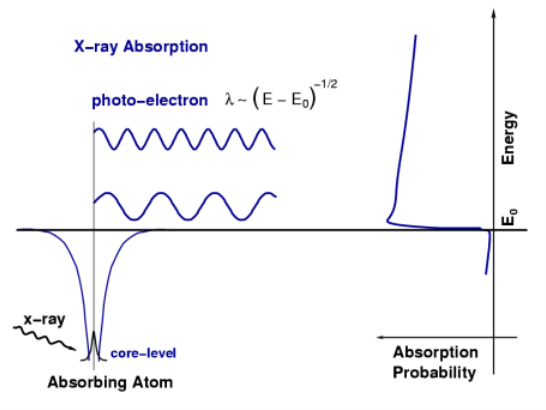

Figure 4.10.2: Cartoon of x-ray absorption through the photoelectric process. When an x-ray has the energy of a tightly bound core electron level, E0, the probability of absorption has a sharp rise. In the absorption process, the tightly bound core-level is destroyed, and a photo-electron is created. (CARS)

The wavefront of the ejected electron “propagates” out from atom the and backscatter from an nearby atom (Figure 4.10.3). The quantum mechanical formulation of the X-ray transition moment suggests that the X-ray absorption coefficient is dependent on the magnitude of the backscattered photoelectron at atom a.

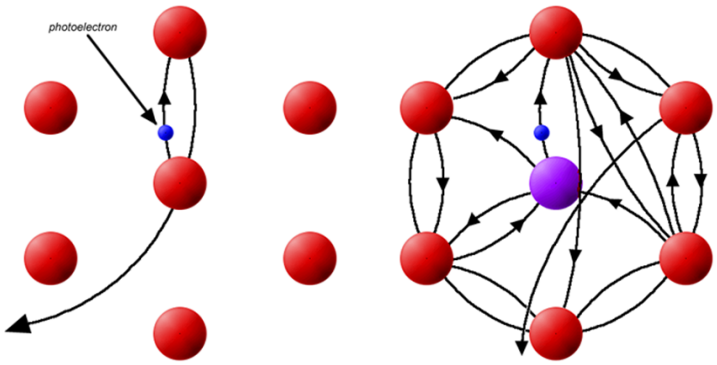

Figure 4.10.3: Schematic view of photoelectron scattering on neighbor atoms that determining the EXAFS oscillations.

At a given photon energy (E1), this backscattering amplitude will be a maximum due to constructive interference of outgoing and backscattered photoelectron waves. This yields a local maximum in the absorption coefficient. A higher photon energy results in a shorter photoelectron wavelength, eventually causing a minimum in the backscattered wave (destructive interference of outgoing and backscattered waves) at atom a and a local minimum in the absorption coefficient. This behavior repeats, resulting in a periodic modulation of the absorption coefficient, which contain information about the relationship of atom a and atom s, i.e., the atomic neighborhood of atom a.

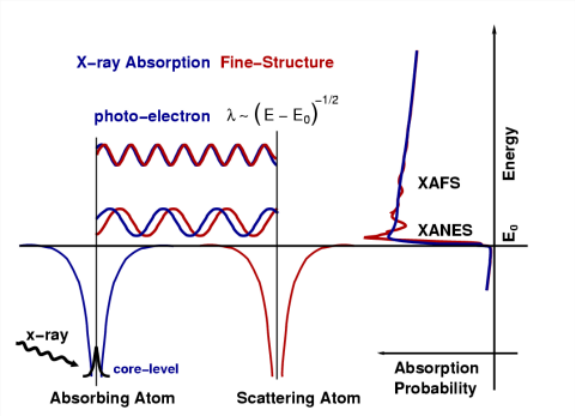

Figure 4.10.4: XAFS occurs because the photo-electron can scatter from a neighboring atom. The scattered photo-electron can return to the absorbing atom, modulating the amplitude of the photo-electron wave-function at the absorbing atom. This in turn modulates the absorption coefficient μ(E), causing the EXAFS. (CARS)

The different frequencies apparent in the oscillations in χ(k) correspond to different near-neighbor coordination shells which can be described and modeled according to the EXAFS Equation

$$\chi(k) = \sum_j \frac{N_j f_j(k) e^{-2k^2\sigma_j^2}}{kR_j{}^2} \sin[2kR_j + \delta_j(k)] \tag{4.10.1}$$

where $f(k)$ and $\delta(k)$ are scattering properties of the atoms neighboring the excited atom, N is the number of neighboring atoms, R is the distance to the neighboring atom, and σ^2 is the disorder in the neighbor distance. Though somewhat complicated, Equation 4.10.1 allows us to determine N, R, and σ^2 knowing the scattering amplitude $f(k)$ and phase-shift $\delta(k)$. Furthermore, since these scattering factors depend on the Z_{eff} of the neighboring atom, EXAFS is also sensitive to the atomic species of the neighboring atom.

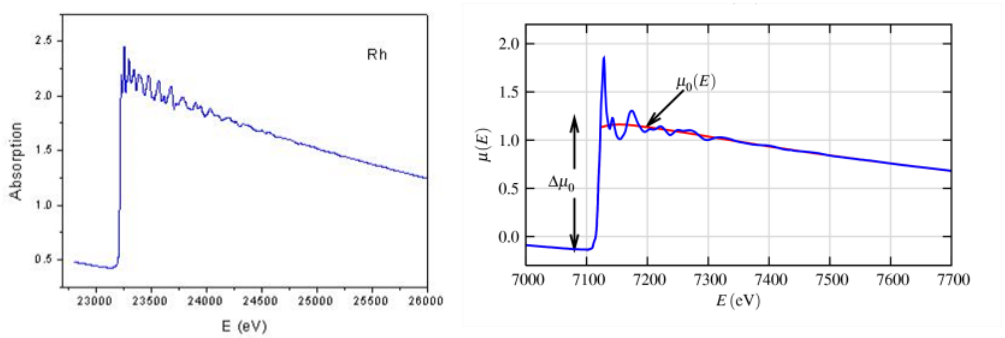

Figure 4.10.5: (left) XAFS spectrum μ(E) for FeO. On top, the measured XAFS spectrum is shown with the XANES and EXAFS regions identified. (right) μ(E) is shown with smooth background function μ0(E) and the edge-step Δμ0(E0)(CARS)

Data Reduction in EXAFS

The interference pattern of the photoelectron wavelets modifies the probability of the photoeffect. When the absorption spectrum is scanned by changing the photon energy, the energy of the photoelectron changes. Consequently, its wavelength varies, and the interference of the wavelets changes from constructive to destructive and back again. Each atom scattering contributes a harmonic oscillatory mode, together they form a complex quasiperiodic EXAFS signal: **Fourier analysis** of the signal resolves the harmonic components into a probability vs distance diagram.

Extraction of the EXAFS (the quasi-periodic modulations of the X-ray absorption coefficient above the edge) consists of several steps, pictorially represented above.

1. The raw XAS data are illustrated in maroon at the top of the left frame. The first step is to simulate (by fitting) and subtract the pre-edge absorbance (blue line) to isolate the contribution from only the element of interest.
2. The pre-edge subtracted data are illustrated in maroon in the center of the left frame and the modulations above the edge are isolated by fitting a smooth curve (usually a three-region cubic or quartic spline), represented by the blue line.
3. The resulting data (after spline subtraction and normalization) are defined as the EXAFS and are shown as a function of energy in the bottom of the left frame.
4. Conversion to k (wave vector)-space results in the EXAFS as it is more typically used (top of right top frame). To avoid underestimating the value of the EXAFS oscillations at high k, it is common to multiply the raw EXAFS by a weighting function (k^3 is almost universal) to emphasize the high-k oscillations (bottom of upper right frame).
5. Finally, a Fourier transform of the k^3-weighted EXAFS yields what appears to be a **radial distribution function** of electron density around the absorbing atom.

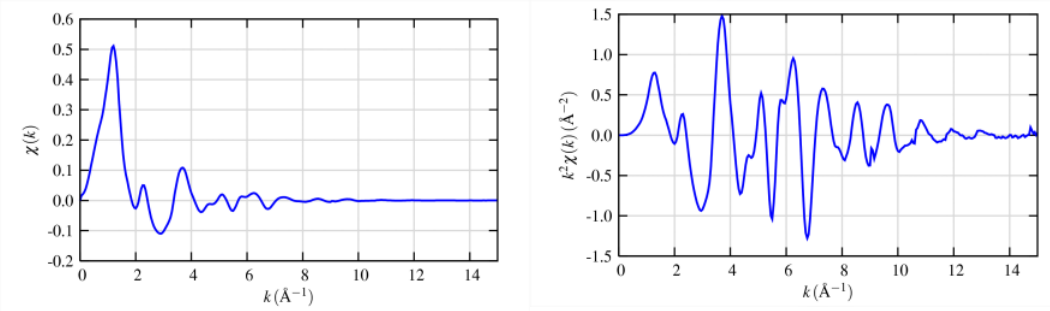

Figure 4.10.6: (left) Isolated EXAFS $\chi(k)$ for FeO (top), and (right) the k-weighted XAFS, $k^2\chi(k)$. (CARS)

Essential Information from EXAFS

How many of what type of ligands are at what distance from metal? To simplify, each scattering atom generates a quasi-sinusoidal modulation of the X-ray absorption coefficient in the EXAFS. These sine waves are completely defined by three observables, **Frequency**, **Phase Shift**, and **Amplitude**.

#1 Frequency ⇒ Distance

From these three observables, analysis of the EXAFS can extract molecular level information. Frequency yields direct information about the Distance between atoms a and s.

#2 Phase Shift ⇒ Type of Atom (affects amplitude also)

The Phase Shift is determined by the type of atom s (it also depends on atom a, but this is constant for a given sample).

#3 Amplitude ⇒ # of Atoms

The Amplitude is directly proportional to the number of atoms (in a given shell). Also, since the scattering Amplitude depends on the electron density around atom s, the Amplitude also contains information about the type of atom

? Exercise 4.10.1: Questions XAS Can Address

- What types of atoms are in the first coordination sphere of a metal site?
- What is the molecular symmetry of this metal site?
- How covalent are the metal ligand bonds?
- Does a particular treatment generate…
  - a redox change at this metal site?
  - result in a structural change at this metal site?
  - Is this metal part of a metal cluster?

The Take-home lesson about EXAFS utility

EXAFS tell Researchers how **many** of **what** type of ligands are at **what** distance from the metal?

EXAFS Accuracy

- Distances: ± 0.02 Å
- Coordination Numbers: ± 20-25 %
- Scattering Atoms: $\Delta Z \pm 1$ (for Z=6-17) & $\Delta Z \pm 3$ (for Z=20-35)

Examining the accuracy of the three pieces of information available from analysis of the EXAFS data (distance, coordination number, type of scattering atom) gives a good indication of the limitations of the EXAFS-derived structural information.

- Since the frequency of the sinusoidal oscillations is relatively easy to measure accurately, the absorber-scatterer **distances** are measured quite accurately. This accuracy **rivals** that obtainable from small molecule crystallography, and is much better than what is available from macromolecular (protein) crystallography. This provides the useful complementarity with

crystallography; the use of accurate metal-ligand distances from EXAFS can aid the refinement of metal sites in X-ray diffraction studies.

- **Coordination number** determinations are much less accurate. Since there is no good independent determination of the latter, we cannot accurately determine the former.
- **Scattering atom identification** is equally imprecise. Elements that are next to each other in the periodic table have barely distinguishable photoelectron scattering characteristics (much like they have similar X-ray scattering characteristics which makes elements hard to identify exactly in X-ray diffraction). This distinction becomes even harder at higher atomic no. (Z). Thus, C, N, and O, are impossible to distinguish, as are P, Cl, and S. Metal scatterers can only be placed in the proper row of the periodic table.

Case Study: Fe-S complexes

Historically, the characterization of metal clusters in biology has benefited from the use of EXAFS (in addition to many other techniques). A good example is the characterization of Fe-S clusters by the observation of Fe…Fe scattering in the Fe EXAFS. Displayed above are the "canonical" Fe-S sites observed in biology.

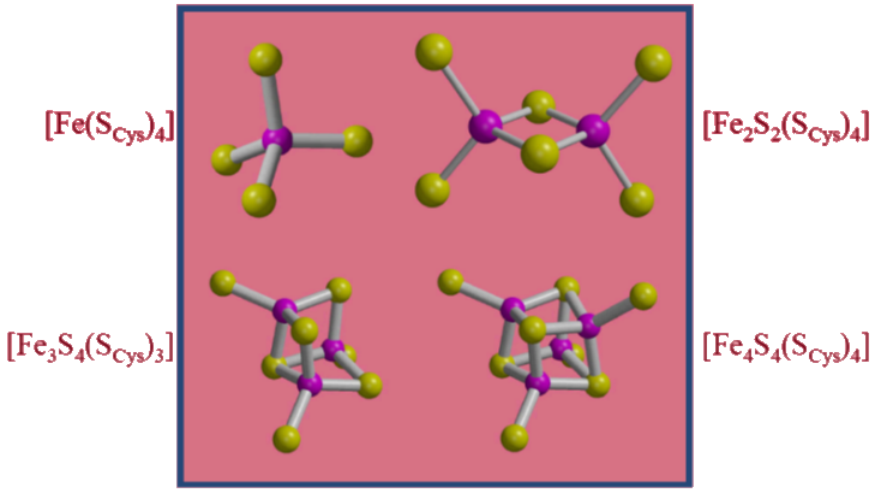

The Fourier transform of the Fe EXAFS of a simple Fe_2S_2 cluster in a [2Fe] ferredoxin provides a characteristic signature of the existence of a cluster. The raw EXAFS data display a beat pattern which implies a resolution of at least two FT peaks. In the FT, the peaks are color coded with the individual EXAFS component sine waves and the bonds (or non-bonded interactions) in the molecular model. The main (green) peak is associated with the Fe–S bonds, whereas the smaller, higher-R (blue) peak is associated with the Fe…Fe interaction.

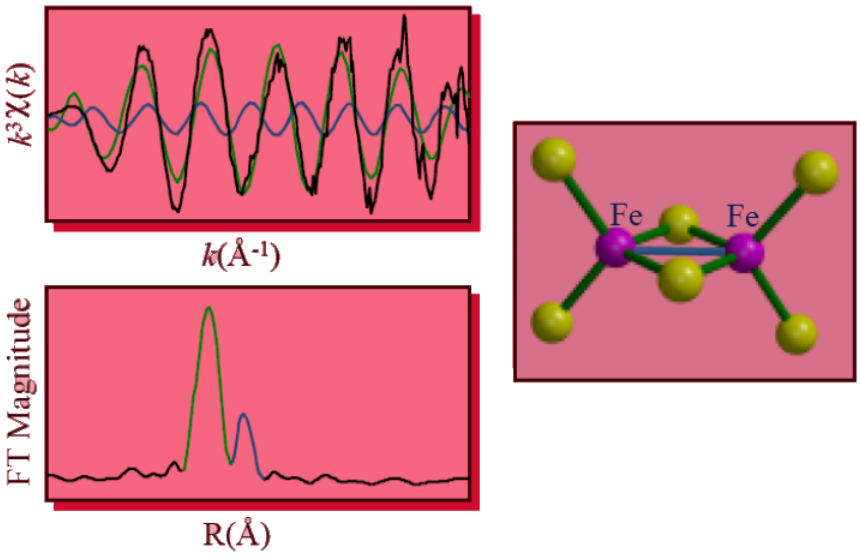

As the cluster size increases, each Fe should see 1 (2Fe cluster), 2 (3Fe cluster), or 3 (4Fe cluster) Fe scatterers, increasing the size of the 2.7-Å FT peak, while the main Fe–S peak remains unchanged.

- See: https://www.ncbi.nlm.nih.gov/pmc/articles/PMC4167288/

CHAPTER OVERVIEW

5: Magnetic Resonance Spectroscopies

5.1: Nuclear Magnetic Resonance (NMR) - Intrinsic Spins
5.2: Nuclear Magnetic Resonance (NMR) - Turning on the Field
5.3: Spin 1/2 Spectra
5.4: Chemical Shifts
5.5: Boltzmann Statistics
5.6: Larmour Frequency
5.7: Ensemble Effects
5.8: Precession and Relaxation
5.9: Chemical Shifts
5.10: Fourier Transform (pulsed) NMR - The way things are really done these days
5.11: Spin-Spin, J-Coupling or indirect dipole-dipole coupling (all the same phenomenon)
5.12: 13-C NMR Spectroscopy
5.13: Nuclear Overhauser Effect (NOE) and 2-D NMR
5.14: Electron Paramagnetic Resonance
5.15: EPR Instrumentation
5.16: EPR Signals
5.17: EPR - Hyperfine Structure

5.1: Nuclear Magnetic Resonance (NMR) - Intrinsic Spins

Proton Nuclear Magnetic Resonance (^{1}H NMR) Spectroscopy is a powerful method used in the determination of the structure of unknown compounds. Many useful properties can be extracted from NMR techniques and only a few are discussed here:

For example, from organic chemistry, we learned that ^{1}H NMR spectrum gives:

- the # of different types of hydrogens present in the molecule
- the relative #'s of the different types of hydrogens
- the electronic environment of the different types of hydrogens
- the number of hydrogen "neighbor" a hydrogen has

Many types of information can be obtained from an NMR spectrum. Much like using infrared spectroscopy (IR) to identify functional groups, analysis of a NMR spectrum provides information on the number and type of chemical entities in a molecule. However, NMR provides much more information than IR. The impact of NMR spectroscopy on the natural sciences has been substantial. It can, among other things, be used to study mixtures of analytes, to understand dynamic effects such as change in temperature and reaction mechanisms, and is an invaluable tool in understanding protein and nucleic acid structure and function. It can be applied to a wide variety of samples, both in the solution and the solid state.

Spins

The concept of spin is regularly addressed in subatomic particle physics. However, to most people spin seems like an abstract concept. This is due to the fact there is no macroscopic equivalent of what spin is. However, for those people who have taken an introduction to chemistry course have seen the concept of spin in electrons. Electrons are subatomic particles which have spin intrinsic to them.

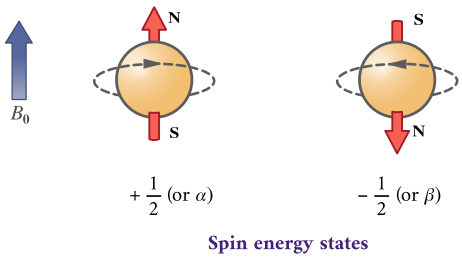

Figure 5.1.1: "Spinning" electrons. (CC BY-SA-ND; Reusch)

The nucleus is not much different. Spin is just another form of angular momentum. The nucleus consists of protons and neutrons and neutrons and protons are comprised of subatomic particles known as quarks and gluons. The neutron has 2 quarks with a -e/3 charge and one quark with a +2e/3 charge resulting in a total charge of 0. The proton however, has 2 quarks with +2e/3 charge and only one quark with a -e/3 charge giving it a net positive charge. Both protons and neutrons are spin=1/2.

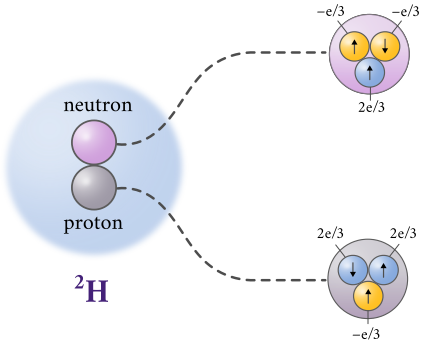

Figure 5.1.2: The atomic nucleus (black) of ^{2}H. The proton (green) and neutron (red) are composed of quarks (purple and teal) which have a charge and spin (arrow).

For any system consisting of n multiple parts, each with an angular momentum the total angular momentum can be described by J where

$$J = |J_1 + J_2 + \ldots + J_n|, |J_1 + J_2 + \ldots + J_n| - 1, \ldots |J_1 - J_2 - \ldots - J_n|$$

Here are some examples using the isotopes of hydrogen

- ^1H = 1 proton so J=1/2
- ^2H= 1 proton and 1 neutron so $J = 1$ or 0.

For larger nuclei, it is not immediately evident what the spin should be as there are a multitude of possible values. For the remainder of the discussion we will attribute the spin of the nucleus, I, to be an intrinsic value. There are some rules that the nuclei do follow with respect to nuclear spin. They are summarized in the table below.

Table 1. General rules for determination of nuclear spin quantum numbers

Mass Number	Number of Protons	Number of Neutrons	Spin (I)	Example
Even	Even	Even	0	^{16}O
	Odd	Odd	Integer (1,2,...)	^2H
Odd	Even	Odd	Half-Integer (1/2, 3/2,...)	^{13}C
	Odd	Even	Half-Integer (1/2, 3/2,...)	^{15}N

General Rule

Nuclei with even Z and even A have $I = 0$. Confirm with the examples above.

The interaction of with an external magnetic field, $\vec{H}$ (or $\overrightarrow{B_0}$) comprises the spectroscopy we call **NMR**. Most nuclei of greatest interest in NMR have I=1/2, for example, ^{1}H, ^{13}C, ^{19}F, ^{31}P. However, many nuclei are non-magnetic, I=0 and cannot be studied by NMR: ^{4}He, ^{12}O, ^{32}S, ^{12}C. NMR can only be performed on isotopes whose natural abundance is high enough to be detected. Some of the nuclei routinely used in NMR are listed below.

Nuclei	Unpaired Protons	Unpaired Neutrons	Net Spin
^{1}H	1	0	1/2
^{2}H	1	1	1
^{31}P	1	0	1/2
^{23}Na	1	2	3/2
^{14}N	1	1	1
^{13}C	0	1	1/2
^{19}F	1	0	1/2

$\vec{J}$ is the angular momentum of the nucleus and has dimensions of $\hbar$. For convenience, let's define a vector $\vec{I}$ that is parallel to $\vec{J}$, but is dimensionless:

$$\vec{J} = \hbar\vec{I}$$

The magnetic moment is also proportional to $\vec{J}$ and is collinear. We can introduce the proportionality constant, γ (also called the **magnetogyric ratio** or **gyromagnetic ratio**)

$$\vec{\mu}_N = \gamma\vec{J} = \gamma\hbar\vec{I}$$

For most nuclei, γ is positive, so $\overrightarrow{\mu_N}$ and are $\vec{I}$ parallel. But for some (^{15}N and ^{17}O), is negative, so and are *antiparallel* for these nuclei.

Nucleus	γ (10^6 rad.s^{-1}.T^{-1})	$\gamma/2\pi$ (MHz.T^{-1})
^{1}H	267.513	42.576
^{2}H	41.065	6.536
^{3}He	-203.789	-32.434
^{7}Li	103.962	16.546
^{13}C	67.262	10.705
^{14}N	19.331	3.077
^{15}N	-27.116	-4.316
^{17}O	-36.264	-5.772
^{19}F	251.662	40.053
^{23}Na	70.761	11.262
^{31}P	108.291	17.235
^{129}Xe	-73.997	-11.777

By the way

For electron gyromagnetic ratio is much, much bigger (addressed with EPR - electron paramagnetic resonance)

$$\gamma_e = -1.760859770(44) \times 10^{11} \text{rads}^{-1}\ \text{T}^{-1}$$

Bulk Magnetization

The net or bulk magnetization of the sample is given by M and is the sum of each individual magnetic vector, or

$$\vec{M} = \sum \vec{\mu}_i$$

since these magnetic moments are vectors and are randomly aligned, the bulk magnetization arising from the nucleus is zero in the absence of an external magnetic field. There may be unpaired electrons which give rise to paramagnetic, anti ferromagnetic, or ferromagnetic properties. However, if an external magnetic field is applied, the nuclei will align either with or against the field and result in a non-zero bulk magnetization.

5.2: Nuclear Magnetic Resonance (NMR) - Turning on the Field

Spin is a type of angular momentum. Nuclear spin angular momentum was first reported by Pauli in 1924 and will be described here. Analogous to the angular momentum commonly encountered in electron, the angular momentum is a vector which can be described by a magnitude L and a direction, m. The magnitude is given by

$$L = \hbar\sqrt{I(I+1)}$$

The projection of the vector on the z axis (arbitrarily chosen), takes on one of $2I+1$ discretized values according to m, where

$$m_I = -I, -I+1, -I+2, \ldots +I$$

The angular momentum along the z-axis is now

$$I_z = m\hbar$$

Pictorially, this is represented in Figure $5.2.1$ for three values of I.

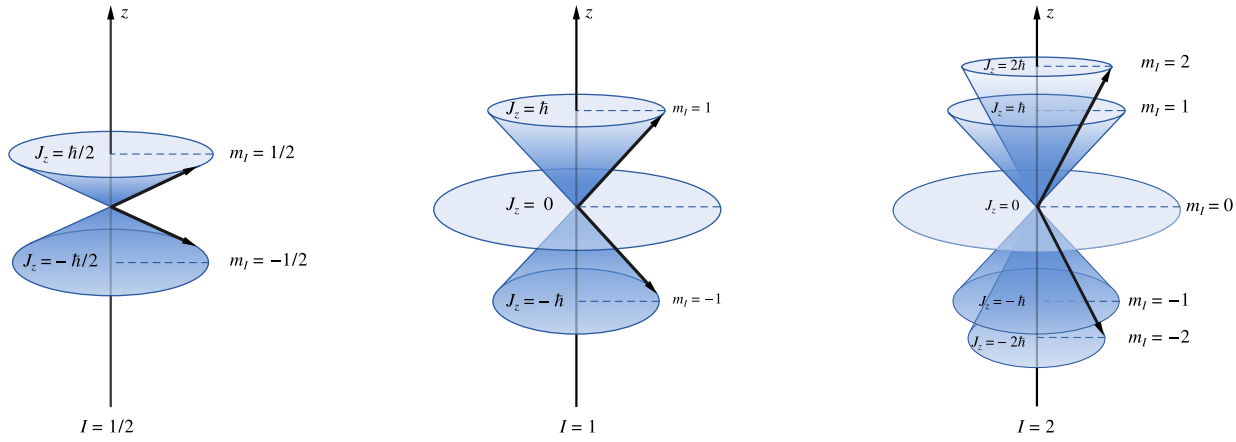

Figure 5.2.1: The quantized angular momentum values for a I=1/2 (left) I=1(middle) and I=2 (right). The magnitude is denoted by the arrow while the projection along the z-axis is denoted by the circle.

The quantum numbers of the nucleus are denoted below.

Interaction	Symbol	Quantum Numbers
Nuclear Spin Angular Momentum	I	$0 < I < 9/2$ by unites of $1/2$
Spin Angular Momentum Magnitude	L	$L = \hbar\sqrt{I(I+1)}$
Spin Angular Momentum Direction	m	$m = -I, -I+1, -I+2, \ldots +I$

Field Effects

The absence of external fields, there is no preferred orientation for a magnetic moment. That is, the different m values of the orientation of the spin are degenerate. However, since a nucleus is a charged particle in motion, it will develop a magnetic field. Randomly oriented nuclear spins are aligned when a magnetic field applied on it. Hence, in the presence of a magnetic field, the energy of a magnetic moment depends on its orientation relative to the applied field lines. Classically, this is the Zeeman interaction:

$$E = -\vec{\mu}\cdot\vec{B}_o \tag{5.2.1}$$

where B_0 is the external magnetic field.

The Zeeman interaction is the physical phenomenon underlying the coupling of magnetic moments to magnetic fields. Apply an external magnetic field to nuclei with $I = 1/2$ spin, and the different orientations split into **two** depending on if the nuclei are parallel or antiparallel with the applied field ($\vec{B}_o$ or $\vec{H}$).

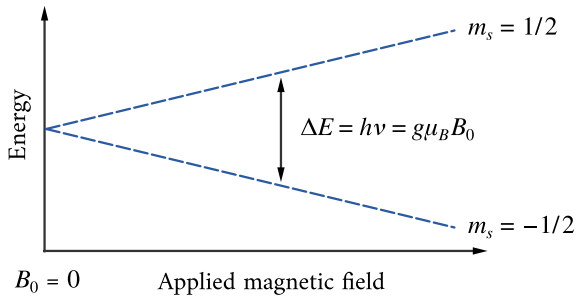

Figure 5.2.2: Energy levels for a I = -1/2 in an applied magnetic field B_o.

We now understand why the nucleus has a magnetic moment associated with it. Now we are getting to the crux of NMR, the use of an external magnetic field. Initially, the nucleus is in the nuclear ground state which is degenerate. The degeneracy of the ground state is $2I+1$. The application of a magnetic field splits the degenerate $2I+1$ nuclear energy levels via Equation 5.2.1, which we will simplify assuming the magnetic field is aligned with the z-direction, so Equation 5.2.1 becomes

$$E = -\mu B_0$$

by substitution with the definition of magnetic moment μ

$$E = -m\hbar\gamma B_0$$

The magnitude of the splitting therefore depends on the size of the magnetic field. In most labs this magnetic field is somewhere between 1 and 21T. Those spins which align with the magnetic field are lower in energy, while those that align against the field are higher in energy.

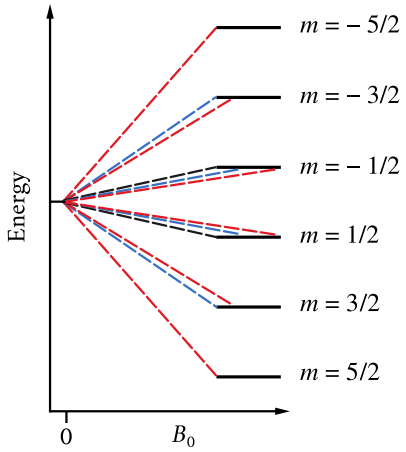

Figure 5.2.3: Splitting of the energy levels for a I=1/2 (black dashed lines), I= 3/2 (blue dashed lines), and I=5/2 (red dashed lines). Note how the energy level is dependent on the applied magnetic field. The offset of the red and blue lines is for illustrative purposes only.

Selection Rules

The selection rule in NMR is

$$\Delta m = \pm 1$$

For a nucleus with $I = 1/2$ there is only one allowed transition since there are only two states. However, for nuclei with $I > 1/2$, multiple transitions may take place. Consider the case of $I = 3/2$. The following transitions can take place

$$-\frac{3}{2} \leftrightarrow -\frac{1}{2}$$

$$-\frac{1}{2} \leftrightarrow \frac{1}{2}$$

$$\frac{1}{2} \leftrightarrow \frac{3}{2}$$

which is illustrated below.

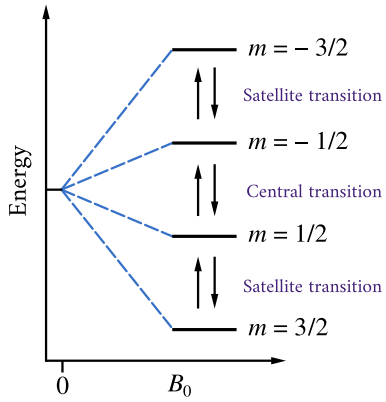

The transition from

$$-\frac{3}{2} \leftrightarrow -\frac{1}{2}$$

$$\frac{1}{2} \leftrightarrow \frac{3}{2}$$

are known as satellite transitions, while the

$$-\frac{1}{2} \leftrightarrow \frac{1}{2}$$

transition is known as the central transition. The central transition is primarily observed in an NMR experiment. For more information about satellite transitions please look at quarupole interactions.

The NMR Experiment

During the NMR experiment several things happen to the nucleus, the bulk magnetization is rotated from the z axis into the xy plane and then allowed to relax back along the z-axis. A full theoretical explanation for a single atom was developed by Bloch into a set of equations known as the Bloch equations. From the NMR experiment chosen a variety of information can be gleaned by studying different interactions.

References

1. Claude H. Yoder, Charles D. Schaeffer,Introduction to multinuclear NMR : theory and application, Benjamin/Cummings Pub. Co., Menlo Park, Calif., 1987.
2. Robin K. Harris, Nuclear magnetic resonance spectroscopy : a physicochemical view, Pitman, Marshfield, Mass., 1983.

3. Jeremy K.M. Sanders and Brian K. Hunter, Modern NMR spectroscopy : a guide for chemists, Oxford University Press, New York, 1993.
4. David A.R. Williams ; editor, David J. Mowthorpe, Nuclear magnetic resonance spectroscopy, Published on behalf of ACOL, London, by J. Wiley, New York, 1986.
5. Frank A. Bovey, Lynn Jelinski, Peter A. Mirau, Nuclear magnetic resonance spectroscopy, Academic Press, San Diego, 1988.
6. R.J. Abraham, J. Fisher and P. Loftus, Introduction to NMR spectroscopy, Wiley, New York, 1988.
7. J.W. Akitt, NMR and chemistry : an introduction to modern NMR spectroscopy, Chapman & Hall, London; New York, 1992.

5.3: Spin 1/2 Spectra

But for ^{1}H, ^{13}C, ^{15}N and other nuclei, we only have to deal with **two** orientations. The energy difference between the two spin states at a given magnetic field strength will be proportional to their magnetic moments. For the four common nuclei noted above, the magnetic moments are: ^{1}H μ = 2.7927, ^{19}F μ = 2.6273, ^{31}P μ = 1.1305 & ^{13}C μ = 0.7022. These moments are in **nuclear magnetons**, which are $5.05078 \cdot 10^{-27}$ JT^{-1}. The following diagram gives the approximate frequencies that correspond to the spin state energy separations for each of these nuclei in an external magnetic field of 2.35 T. The formula in the colored box shows the direct correlation of frequency (energy difference) with magnetic moment (h = Planck's constant = $6.626069 \cdot 10^{-34}$ Js) for a specific applied magnetic field.

A typical CW-spectrometer is shown in the following diagram. A solution of the sample in a uniform 5 mm glass tube is oriented between the poles of a powerful magnet, and is spun to average any magnetic field variations, as well as tube imperfections. Radio frequency radiation of appropriate energy is broadcast into the sample from an antenna coil (colored red). A receiver coil surrounds the sample tube, and emission of absorbed radiofrequency (RF) energy is monitored by dedicated electronic devices and a computer. An NMR spectrum is acquired by varying or sweeping the magnetic field over a small range while observing the RF signal from the sample. An equally effective technique is to vary the frequency of the radiofrequency radiation while holding the external field constant.

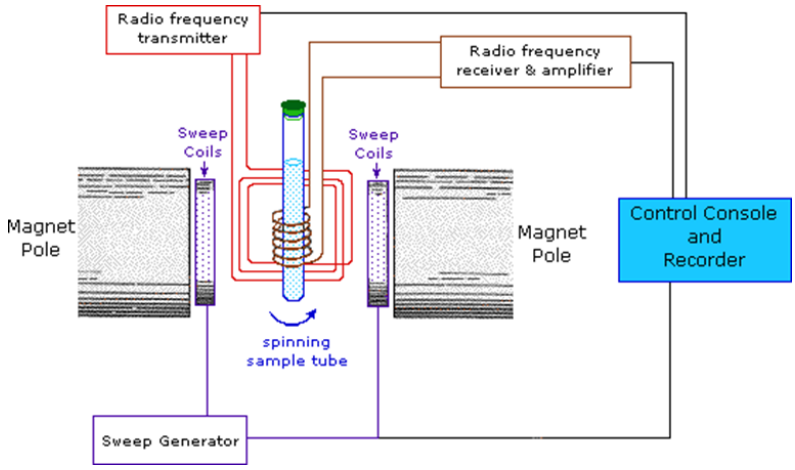

The energy of the two spin states can be represented by an energy level diagram. We have seen that $\nu = \gamma B$ and $E = h\nu$, therefore the energy of the photon needed to cause a transition between the two spin states is

$$E = h\gamma B_o$$

When the energy of the photon matches the energy difference between the two spin states an absorption of energy occurs.

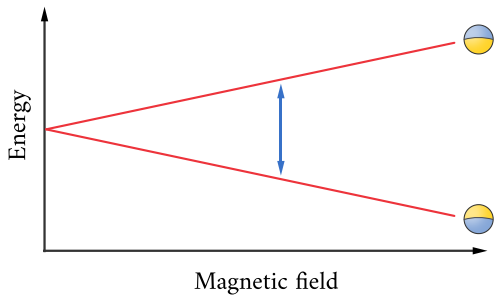

Figure 5.3.1: Absorption of a RF photon between two spin states split by the applied magnetic field.

In the NMR experiment, the frequency of the photon is in the radio frequency (RF) range. In NMR spectroscopy, ν is between 60 and 800 MHz for ^{1}H nuclei. In clinical MRI, ν is typically between 15 and 80 MHz for hydrogen imaging.

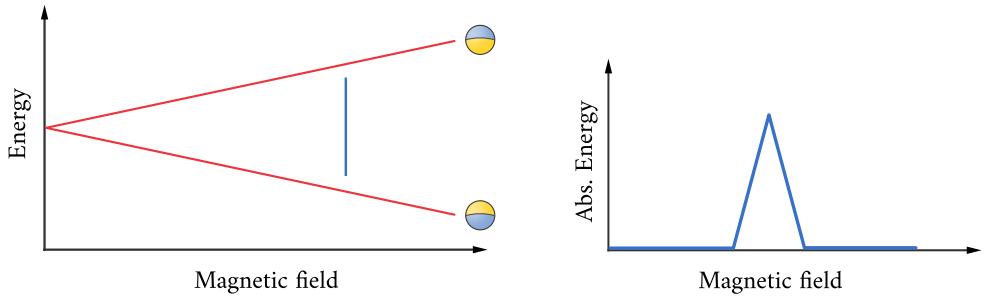

Figure 5.3.2: Continuous wave NMR by varying magnetic field with a fixed RF frequency.

The simplest NMR experiment is the continuous wave (CW) experiment. There are two ways of performing this experiment. In the first, a constant frequency, which is continuously on, probes the energy levels while the magnetic field is varied. The energy of this frequency is represented by the blue line in the energy level diagram. The CW experiment can also be performed with a **constant** magnetic field and a frequency which is **varied**. The magnitude of the constant magnetic field is represented by the position of the vertical blue line in the energy level diagram.

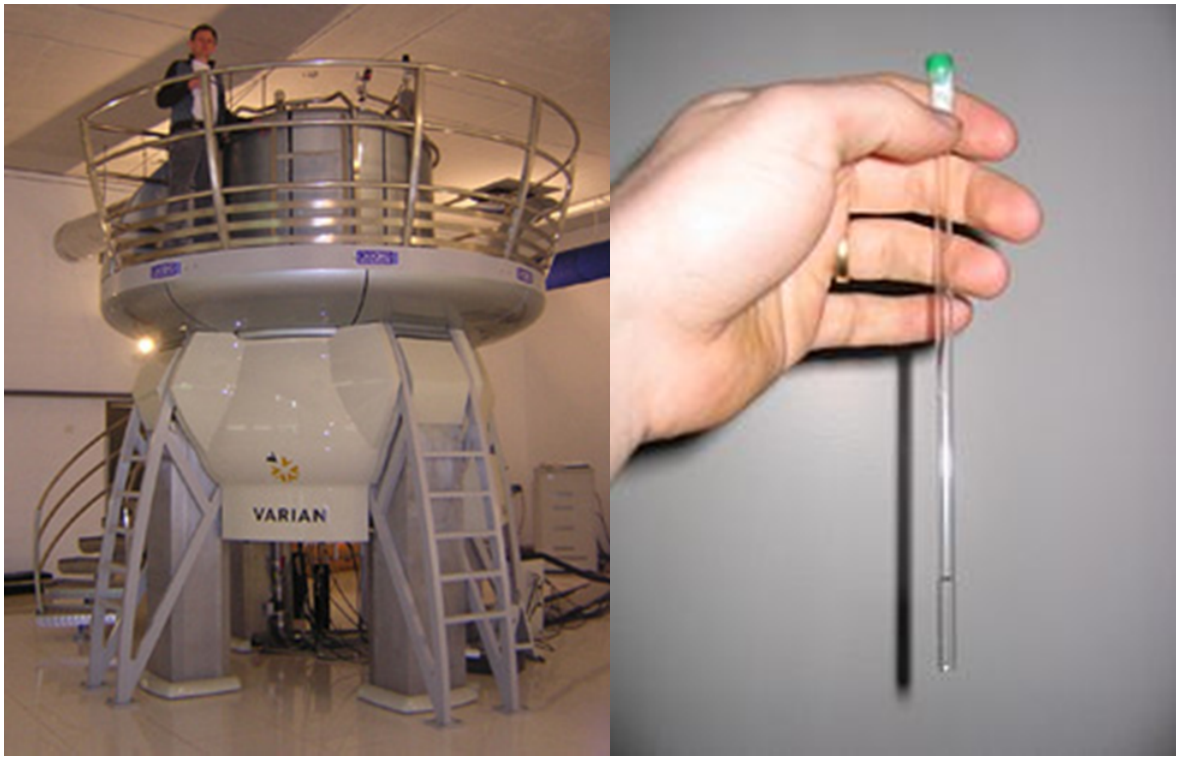

Figure 5.3.2: A 900MHz NMR instrument with a 21.2 T magnet at HWB-NMR, Birmingham, UK (left). The NMR sample is prepared in a thin-walled glass tube (right)

5.4: Chemical Shifts

Different nuclei of the same type in different environments have different frequencies in the same magnetic field

Since protons all have the same magnetic moment, we might expect all hydrogen atoms to give resonance signals at the same field / frequency values. Fortunately for chemistry applications, this is not true. By clicking the **Show Different Protons** button under the diagram, a number of representative proton signals will be displayed over the same magnetic field range. It is not possible, of course, to examine isolated protons in the spectrometer described above; but from independent measurement and calculation it has been determined that a naked proton would resonate at a lower field strength than the nuclei of covalently bonded hydrogens. With the exception of water, chloroform and sulfuric acid, which are examined as liquids, all the other compounds are measured as gases.

Remember when we were discussion polarizability with Raman scattering and the Z_{eff} in X-ray spectroscopy. These were products of the material that reduce the effective **electric** fields. The same thing occurs with externally applied **magnetic** fields. The net effect can be described using a quality called the shielding constant or screening constant σ, sothe nuclear shielding resonance condition can be expressed as:

Differences in the electronic environments cause the protons to experience slightly different applied magnetic fields owing to the shielding/deshielding effects of the induced electronic magnetic fields.

The Chemical Shift

Let's make things simple for people. Unlike infrared and uv-visible spectroscopy, where absorption peaks are uniquely located by a frequency or wavelength, the location of different NMR resonance signals is dependent on both the external magnetic field strength and the RF frequency. Since no two magnets will have exactly the **same** field, resonance frequencies will **vary** accordingly and an alternative method for characterizing and specifying the location of NMR signals is needed. This problem is illustrated by the eleven different compounds shown in the following diagram. Although the eleven resonance signals are distinct and well separated, an unambiguous numerical locator cannot be directly assigned to each.

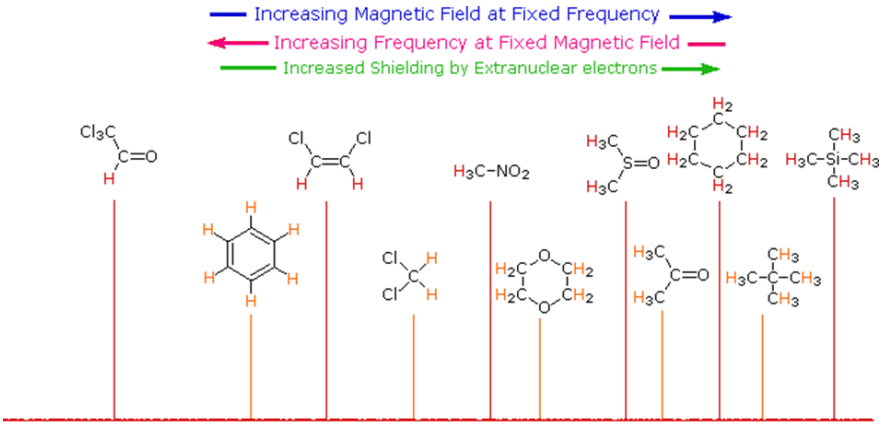

^{1}H NMR Resonance Signals for some Different Compounds

The chemical shift in absolute terms is defined by the frequency of the resonance expressed with reference to a standard compound which is defined to be at 0 ppm. The standard reference that was chosen is tetramethylsilane (TMS). This compound has four -CH_3 methyl groups single bonded to a silicon atom. All of the protons on the methyl groups are in the same electronic environment. Therefore only one NMR signal will be generated. The scale is made more manageable by expressing it in parts per million (ppm) and is **independent** of the spectrometer frequency. The chemical shifts of other resonances are expressed as the difference in electron shielding to the reference nucleus:

$$\delta = \frac{\text{difference between a resonance frequency and that of a reference substance}}{\text{frequency of the spectroscopy}}$$

Thus, an NMR signal at 300 Hz from TMS at an applied frequency of 300 MHz has a chemical shift of:

$$\frac{300\ \text{Hz}}{300 \times 10^6\ \text{Hz}} = 1 \times 10^{-6} = 1\text{ppm}$$

Although the frequency depends on the applied field the chemical shift is independent of it. On the other hand the resolution of NMR will increase with applied magnetic field resulting in ever increasing chemical shift changes.

The general distribution of proton chemical shifts associated with different functional groups is summarized in the following chart. Bear in mind that these ranges are approximate, and may not encompass all compounds of a given class. Note also that the ranges specified for OH and NH protons (colored orange) are wider than those for most CH protons. This is due to hydrogen bonding variations at different sample concentrations.

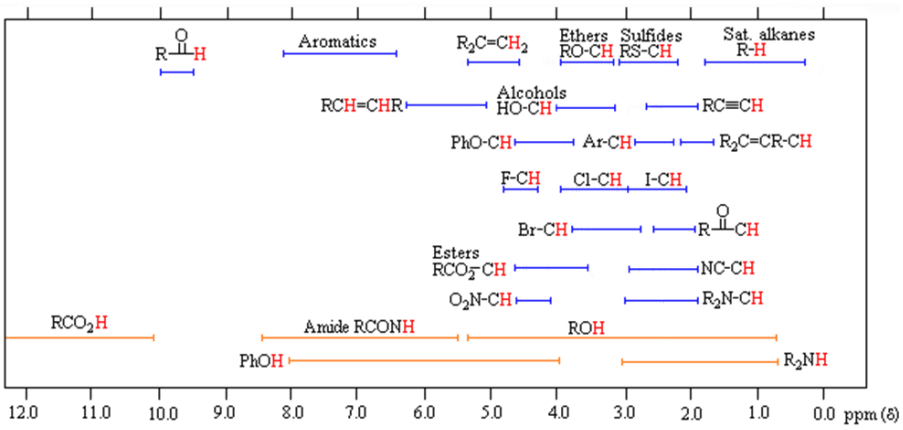

* For samples in $CDCl_3$ solution. The δ scale is relative to TMS at δ = 0.

Chemical Shifts of other Nuclei

Fluorine-19 Chemical Shifts Carbon-13 Chemical Shifts

Carbon-13* Environment	Chemical Shift Range (ppm)	Fluorine-19 Environment	Chemical Shift Range (ppm)
$(CH_3)_2C^*O$	-12	**UF_6**	-540
CS_2	0	**FNO**	-269
CH_3C^*OOH	16	**F_2**	-210
C_6H_6	65	**bare nucleus**	0
CHCl CHCl (cis)	71	**$C(CF_3)_4$**	284
CH_3C^*N	73	**$CF_3(COOH)$**	297
CCl_4	97	**fluorobenzene**	333
dioxane	126	**F-**	338
C^*H_3CN	196	**BF_3**	345
CHI_3	332	**HF**	415

Nitrogen-14* Environment	Chemical Shift Range (ppm)
NO_2Na	-355
NO_3- (aqueous)	-115
N_2 (liquid)	-101
pyridine	-93

Nitrogen-14* Environment	Chemical Shift Range (ppm)
bare nucleus	0
CH_3CN	25
CH_3CONH_2 (aqueous)	152
NH_4+ (aqueous)	245
NH_3 (liquid)	266

Phosphorous-31 Environment	Chemical Shift Range (ppm)
PBr_3	-228
$(C_2H_5O)_3$ P	-137
PF_3	-97
85% phosphoric acid	0
PCl_5	80
PH_3	238
P_4	450

These shifts are all relative to the bare nucleus.

The strong magnets required for NMR/MRI can be dangerous in the wrong hands. This happened several years ago in Denmark.

Now, back to the basics....

5.5: Boltzmann Statistics

Energy Level Spin Distribution

In the absence of a magnetic field the magnetic dipoles are oriented randomly and there is no net magnetization (vector sum of μ is zero). Application of an external magnetic field, as was shown above, creates distinct energy levels based on the spin angular momentum of the nucleus. Each energy level is populated by the spins which have the same angular momentum. To illustrate this, consider a I=1/2 system. There are two energy levels, +1/2 and -1/2, which are populated by spins that have aligned against or with the external magnetic field, respectively.

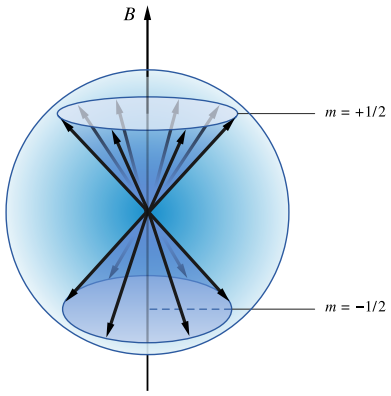

Figure 5.5.1: Spins configurations according to applied magnetic field

The energy separation between these states is relatively small and the energy from thermal collisions is sufficient to place many nuclei into higher energy spin states. The number of nuclei in each spin state can be described by the Boltzmann distribution. The Boltzmann equation expresses the relationship between temperature and the related energy as shown below.

$$\frac{N_{upper}}{N_{lower}} = e^{\frac{-\Delta E}{kT}} = e^{\frac{-h\nu}{kT}}$$

Where N_{upper} and N_{lower} represent the population of nuclei in upper and lower energy states, E is the energy difference between the spin states, k is the Boltzmann constant (1.3805x10-23 J/Kelvin) and T is the temperature in K. At room temperature, the number of spins in the lower energy level, N_{lower}, slightly outnumbers the number in the upper level, N_{upper}.

As the temperature **decreases**, so **does** the ratio N^-/N^+. As the temperature **increases**, the ratio approaches **one**.

The signal in NMR spectroscopy results from the difference between the energy absorbed by the spins which make a transition from the lower energy state to the higher energy state, and the energy emitted by the spins which simultaneously make a transition from the higher energy state to the lower energy state. The signal is thus **proportional** to the population difference between the states. NMR is a rather sensitive spectroscopy since it is capable of detecting these very small population differences. It is the resonance, or exchange of energy at a specific frequency between the spins and the spectrometer, which gives NMR its sensitivity.

5.6: Larmour Frequency

When placed in a magnetic field, charged particles will precess about the magnetic field. In NMR, the charged nucleus, will then exhibit precessional motion at a characteristic frequency known as the **Larmor Frequency**. The Larmor frequency is specific to each nucleus and is measured during the NMR experiment, as it is dependent on the magnetic field that the nucleus experiences.

Precessing Tops

Apply an external magnetic field, $\vec{H}_o$ that defines a direction in space (e.g., z). Assume that $\vec{H}_o$ makes an angle, θ, with $\vec{\mu}$, so that we have:

$$\mu = |\mu| \cos\theta$$
$$\mu_\perp = |\mu| \sin\theta$$

The applied magnetic field exerts a torque, $\vec{\tau}$ on the nucleus that is given by the cross product:

$$\begin{aligned}\vec{\tau} &= \vec{\mu} \times \vec{H}_\circ \\ &= |\mu||H| \sin\theta \\ &= H\mu_\perp\end{aligned}$$

The direction of $\vec{\tau}$ is perpendicular to the plane formed by $\vec{\mu}$ and $\vec{H}_o$. Thus, as shown in Figure 5.6.1, this torque cause to process about the direction of $\vec{H}_o$. The tip sweeps out a cone and $\vec{\tau}$ is an angular force on the spinning nucleus causing it to wobble, just like a gyroscope wobbles in a gravitational field aka a spinning top.

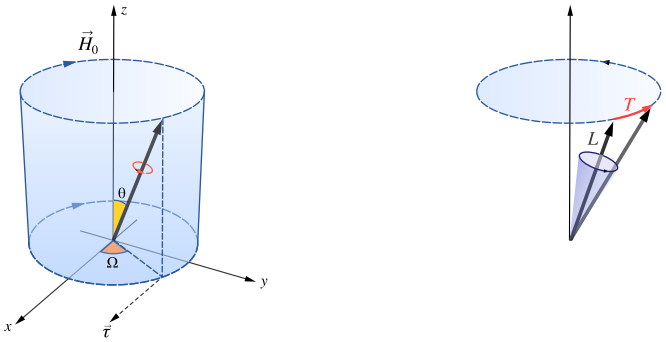

Figure 5.6.1: The wobbling of a spinning nucleus.

The torque is the time derivative of the angular momentum. This is the angular analog of the linear relationships you know in basic physics classes, where the force is the derivative of the linear momentum:

$$\frac{d}{dt}\vec{p} = \frac{d}{dt}m\vec{v} = m\frac{d}{dt}\vec{v} = m\vec{a} = \vec{F}$$

For angular systems

$$\frac{d}{dt}\vec{J} = \hbar\frac{d}{dt}\vec{I} = \vec{\tau} = \vec{\mu} \times \vec{H}_\circ$$

Multiplying by γ gives

$$\frac{d}{dt}\gamma\vec{J} = \frac{d}{dt}\vec{\mu} = \gamma\left(\vec{\mu} \times \vec{H}_\circ\right)$$

Set of three linear differential equations relating the components of $\overrightarrow{mu}$. This can be rewritten

$$\dot{\vec{\mu}} = -\gamma\left(H_\circ \times \vec{\mu}\right)$$

(sign change due to flipping the cross product)

$$\begin{pmatrix} \dot{\vec{\mu}}_x \\ \dot{\vec{\mu}}_y \\ \dot{\vec{\mu}}_z \end{pmatrix} = -\gamma \begin{pmatrix} \vec{i} & \vec{j} & \vec{k} \\ 0 & 0 & H_\circ \\ \mu_x & \mu_y & \mu_z \end{pmatrix}$$

This results from the determent form of the cross product

$$\dot{\vec{\mu}} = -\gamma \left(-\vec{i}\,(H_\circ \mu_y) - \vec{j}\,(H_\circ \mu_x) + \vec{k}(0) \right)$$

Note that $\vec{\mu}_z = 0$. This means that θ is constant defining μ and $\mu_\perp$ from the initial conditions. A solution to this set of equations:

$$\frac{d\mu_x}{dt} = \gamma H_\circ \mu_y$$
$$\frac{d\mu_y}{dt} = -\gamma H_\circ \mu_x$$
$$\frac{d\mu_z}{dt} = 0$$

where μ is the magnitude of $\vec{\mu}$. The equations above represent a rotation of $\mu_\perp$ in the xy-plane with angular frequency ω_0. Same as the precession of $\vec{\mu}$ about $\vec{k}$ at $\omega_\circ$. Substitution gives an expression for this **procession frequency**

$$\frac{d\mu_x}{dt} = \frac{d}{dt}\mu_\perp \cos\omega_0 t = -\mu_\perp \omega_0 \sin\omega_0 t$$
$$= \gamma H_0 \mu_y = -\gamma H_0 \sin\omega_0 t$$

The effect is illustrated below:

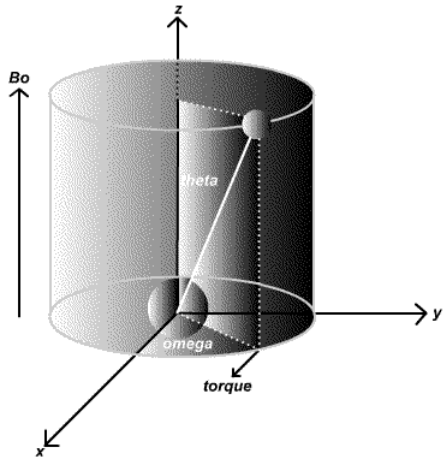

So $\omega_\circ = \gamma H_\circ$ and this is the **Larmour frequency,** which is the procession of the nuclei due to the applied magnetic field which torques via magnetic moment due to the non-zero angular momentum (constantly spinning) of the nuclei.

So $\omega_\circ \propto \gamma$ and $\omega_\circ \propto H_\circ$.

Lamour frequency

- The larger the gyroscopic ratio for a nuclei, the greater the Lamour frequency
- The greater the applied magnetic field, the greater the Lamour Frequency.

Units

In NMR, is usually expressed in units of the **nuclear magneton,** β_N:

$$\vec{\mu}_N = g_N \beta_N$$

Where g_N is the **nuclear g-value** (unique to each nucleus). β_N is defined as

$$\beta_N \equiv \frac{e\hbar}{2m_p c} = 5.05 \times 10^{-27} \mathrm{JT}^{-1}$$

Where c= charge of proton and is the mass of the proton. We have expressed the Larmour frequency in terms of γ, the magnetogyric ratio. Recall:

$$\gamma = \frac{\vec{\mu}_N}{\vec{J}_N} = \frac{g_N \beta_N}{\hbar I} = \frac{2\pi g_N \beta_N}{hI}$$

Since $\omega_0 = \gamma H_0$ or $2\pi v_0 = \gamma H_0$

$$2\pi v_0 = \left(\frac{2\pi g_N \beta_N}{hI} \right) H_0$$

with

$$v_0 = \frac{g_N \beta_N H_0}{hI}$$

Example 5.6.1

For H, with I=1/2, and g_N = 2.793. Calculate the Larmour frequency (in Hertz) for a field of 7.0463 Telsa (=70,463 Gauss).

Solution

$$\begin{aligned} v_\circ &= \frac{g_N \beta_N H_\circ}{hI} \\ &= \frac{(2)(2.793)\left(5.05 \times 10^{-27}\right)(7.0463)}{6.626 \times 10^{-34}} Hz \\ &= 3 \times 10^8 \text{ Hz} \end{aligned}$$

Thus, NMR is commonly carried out at 300 MHz, which requires a 7 T magnetic field. The latter is produced in a superconducting solenoid (see Augustine or Britt labs for these).

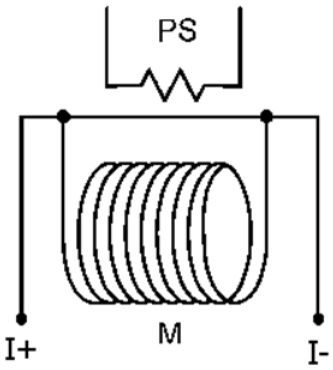

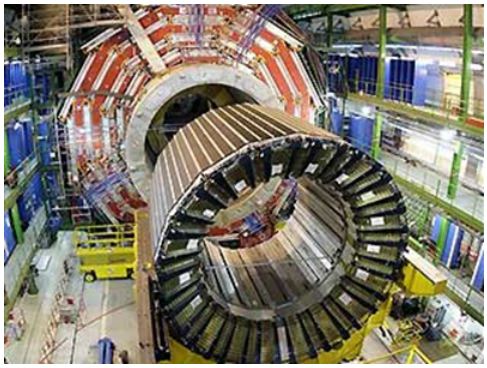

Right: Magnet core of the largest superconducting solenoid magnet at European Organization for Nuclear Research's Large Hadron Collider.

References

1. Duer, M.J., *Solid State NMR Spectroscopy: Principles and Applications*. Blackwell Science Ltd. USA. 2002
2. Fukushima, E., Roeder, S.B.W., *Experimental Pulse NMR A Nuts and Bolts Approach*. Perseus Books Publishing, USA. 1981

5.7: Ensemble Effects

The net magnetization for a sample is the sum of the individual magnetic moments in the sample

$$M = \sum_i \mu_i$$

we have already defined the magnetic moment for a nucleus with spin I. The magnetization can then be written as

$$M = \gamma J$$

where J is the net spin angular momentum.

The torque, T, of the sample will then be

$$T = \frac{dJ}{dt}$$

Substituting M for J we obtain

$$T = M \times B$$

and finally

$$\frac{dM}{dt} = \gamma M \times B$$

then

$$\frac{dM}{dt} = \gamma M B \sin\theta$$

since $\vec{M}$ and $\vec{B}$ are parallel the sin term drops out.

We want to know the rate at which the magnetization is changing with respect to time so we take the second derivative and the result is the **Larmor frequency**

$$\omega_0 = \gamma B$$

since $\vec{M}$ and $\vec{B}$ are both vector quantities, the cross product with $\vec{B}$ in only the Z direction i.e. ($B = (0, 0, B_0)$) then we obtain the Larmor frequency

$$\omega_0 = \gamma B_0$$

Rotating Axis

It is convenient to define a rotating frame of reference which rotates about the Z axis at the Larmor frequency. We distinguish this rotating coordinate system from the laboratory system by primes on the X and Y axes, X'Y'. The motion of $\vec{\mu}$ in a rotating frame with the xy-axis rotate about the z-axis in the **same phase** as the ω_0 procession of sometimes called the **rotating axis** u and v:

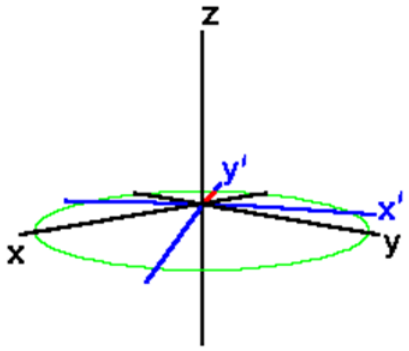

A magnetization vector *rotating at the Larmor frequency* in the laboratory frame appears stationary in a frame of reference rotating about the Z axis. In the rotating frame, relaxation of M_Z magnetization to its equilibrium value looks the same as it did in the laboratory frame.

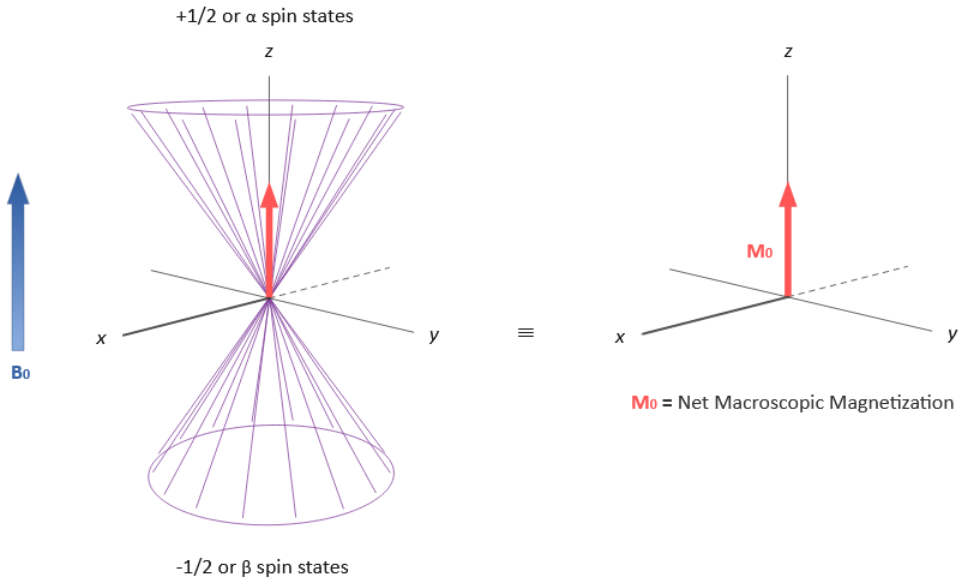

A **transverse magnetization vector** rotating about the Z axis at the same velocity as the rotating frame will appear stationary in the rotating frame.

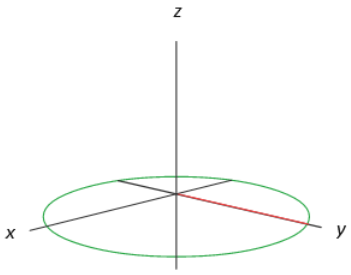

A magnetization vector traveling **faster** than the rotating frame rotates clockwise about the Z axis. A magnetization vector traveling **slower** than the rotating frame rotates counter-clockwise about the Z axis.

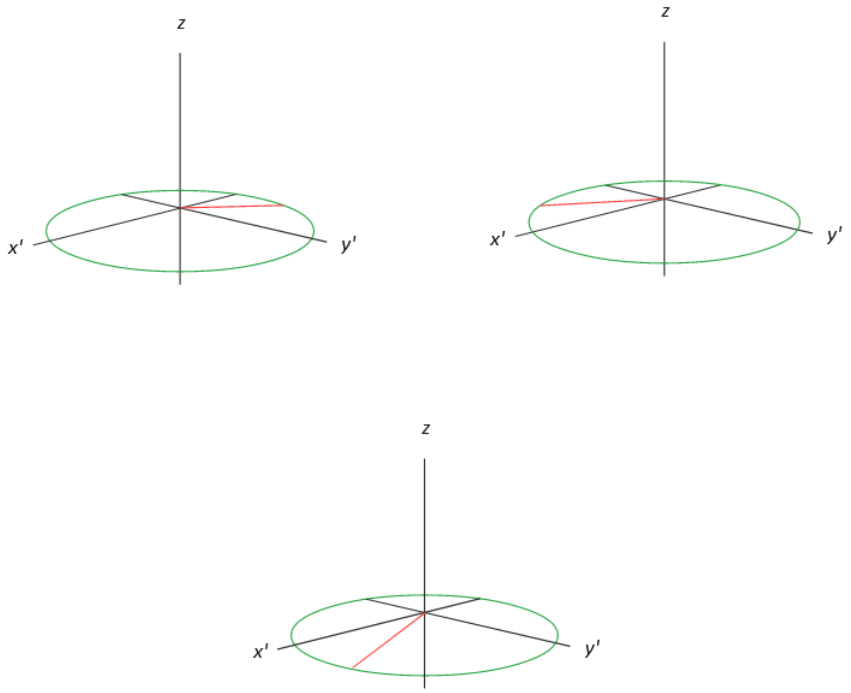

Figure 5.7.1: Paste Caption Here

The two magnetizations can be summarized:

- $\mu_{\perp}$ rotates with ω_0 frequency **counter clockwise**, while u, v rotate with counter **clockwise**.
- $\mu_{||}$ rotates with $\omega = \omega_0 - \omega$ to an observer in the rotating coordinate system that rotates at the frequency ω.

Now

$$\omega_0 = \gamma H_\circ - \omega_1 = \gamma \left(H_\circ - \omega_1 / \gamma \right)$$

where the quantity in the parenthesis has the units of magnetic field. When view in the rotating coordinate system, the procession frequency is , which is what would be produce by an effective field

$$H_{eff} = \left(H_0 - \omega_1 / \gamma \right)$$

The quantity ω_1 / γ behaves like a fictitious field that is directed in the **opposite direction** of H_o. In vectoral units

$$\vec{H}_{eff} = \left(H_0 - \omega_1 / \gamma \right) \vec{k}$$

The equations of motion in the rotating frame are now

$$\begin{aligned} \dot{\vec{\mu}} &= -\gamma \left[\vec{H}_{eff} \times \vec{\mu} \right] = \\ &= -\gamma \left[\vec{H}_\circ - \omega_1 / \gamma \right] \vec{k} \times \vec{\mu} \end{aligned}$$

As $\omega_1 / \gamma \to H_0$ or as $\omega_1 \to \gamma H_0$, the quantity in the brackets goes to zero and $\dot{\vec{\mu}} \to 0$. Thus is stationary in a coordinate system that rotates as the Larmour frequency $\omega_1 = \omega_0$ and $H_{eff} = 0$.

Macroscopic Statistics (magnetization)

In contrast to single molecule optical spectroscopy, the signal strength of NMR is too weak to do with a single molecule, and we need to address an ensemble of nuclei. It is cumbersome to describe NMR on a microscopic scale. A macroscopic picture is more

convenient. The first step in developing the macroscopic picture is to define the spin packet. A spin packet is a group of spins experiencing the same magnetic field strength. In this example, the spins within each grid section represent a spin packet.

At any instant in time, the magnetic field due to the spins in each spin packet can be represented by a magnetization vector.

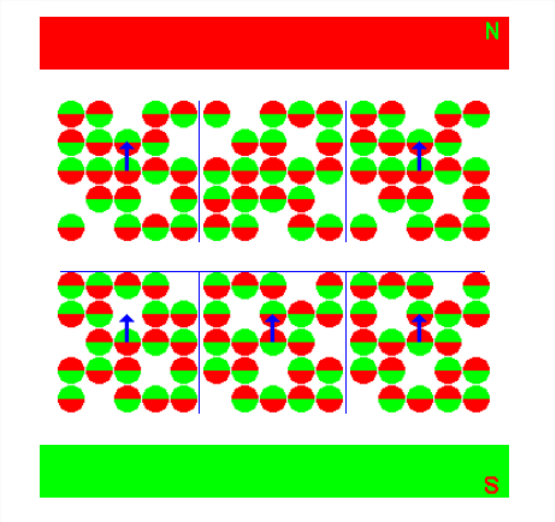

The individual for each member of the ensemble add vectorally to give a resulting **bulk magnetization**

$$\vec{M} = \sum_i \vec{\mu}_i$$

The size of each vector is proportional to (N_+ - N_-) calculated from the Boltzman equation. The vector sum of the magnetization vectors from all of the spin packets is the net magnetization. To describe pulsed NMR, it is necessary from here on to talk in terms of the bulk or net magnetization, $\vec{M}$.

Adapting the conventional NMR coordinate system, the external magnetic field and the net magnetization vector at equilibrium are both along the Z axis. The equation of motions for procession of $\vec{M}$ is the same as for $\vec{M}$.

$$\dot{\vec{M}} = -\gamma \left(H_{eff} \times \vec{M} \right)$$

$\vec{M}$ *at equilibrium* will have no x- or y- components because these average to 0 ($\vec{\mu}_x$ and $\vec{\mu}_y$ are random). However, an equilibrium component in the z-direction will exist, since slightly more spins will line up with $\vec{\mu}_z$ (more parallel than anti parallel).

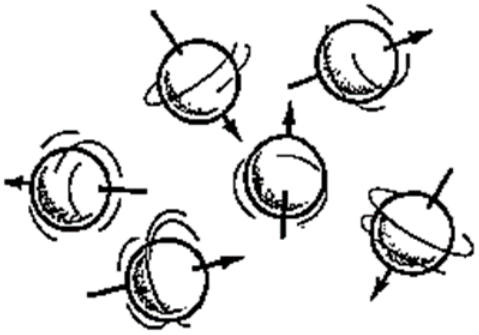

The rotation of the charged protons makes them magnetic. In the absence of field, the directions of the magnetic dipoles are random,

The **equilibrium** magnetization is directed along the applied magnetic field,

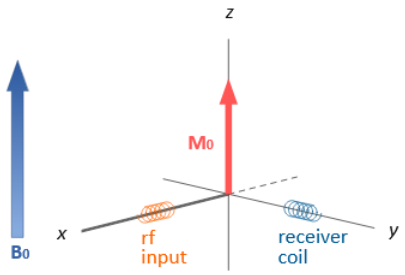

or as a function of all the "individual spins" looks like this:

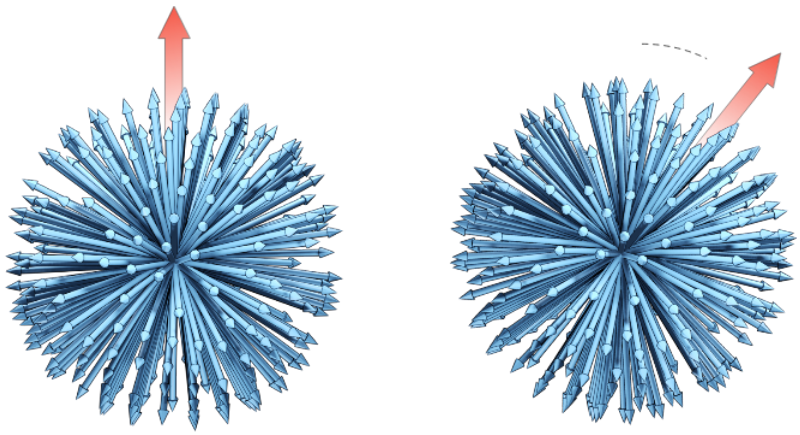

Figure 5.7.1: Equilibrium magnetization before and after application of a strong magnetic field that also makes the spin distribution rotate around the direction of the field (here vertical). (CC BY 4.0; Ümit Kaya via LibreTexts)

The (thermal) bulk magnetization magnitude is given by the **Curie law**:

$$|M_0| = \frac{N_0 \mu^2}{3kT} I(I+1) H_0$$

At very low temperatures, only the lowest energy level is populated the magnetization given is the equilibrium magnetization inherent to a system, when placed in a magnetic H_o. It is often designated as M_o (and will be henceforth). That is, the magnetization is inversely proportional to temperature. This makes sense since the thermal motions are random and act to reduce the net magnetization of the material.

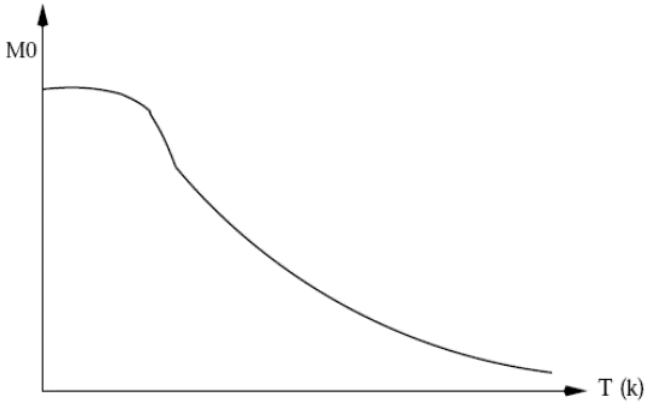

Reference

https://mriquestions.com/rotating-frame.html

5.8: Precession and Relaxation

What happens when you apply a transverse RF field to the sample with a net magnetization

1. First, the net magnetization shifts away from the z-axis and toward the y-axis. This occurs because some of the +1/2 nuclei are excited to the −1/2 state, and the precession about the z-axis becomes coherent (non-random), generating a significant y component to the net magnetization ($|M|$).
2. After irradiation the nuclear spins return to equilibrium in a process called **relaxation**. As the xy coherence disappears and the population of the +1/2 state increases, energy is released and detected by the receiver. The net magnetization spirals back, and eventually the equilibrium state is reestablished.

Step 1: Creating a Magnetization with a Magnetic Field

A difference way of looking at the next magnetization:

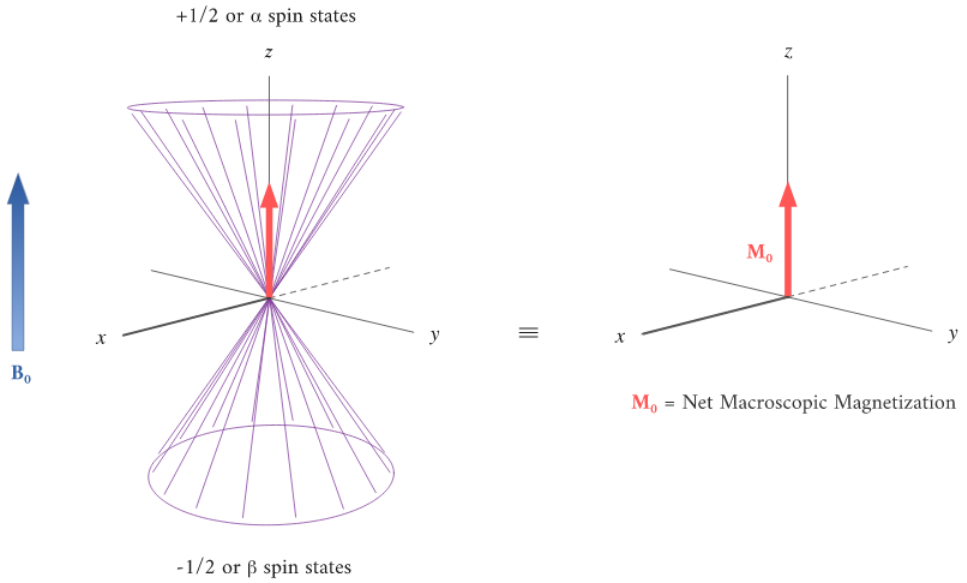

Step 2: Shifting the Magnetization with a Radiofrequency Field

If the net magnetization is placed in the XY plane due to r**esonant radio waves that rotate the equilibrium magnetization in the rotating frame of resonance**, $\vec{M}$ will rotate about the Z axis at a frequency equal to the frequency of the photon which would cause a transition between the two energy levels of the spin at the Larmor frequency.

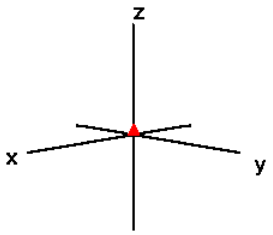

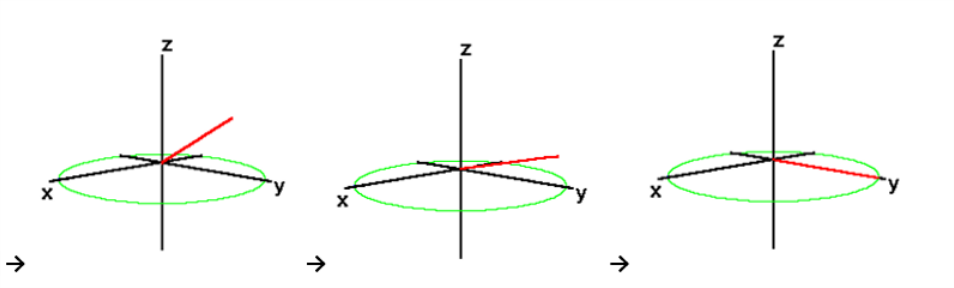

The effect of resonant radio waves is also illustrated in the figure below that shows the rotation of the magnetization distribution resulting from application of a resonant radio frequency pulse

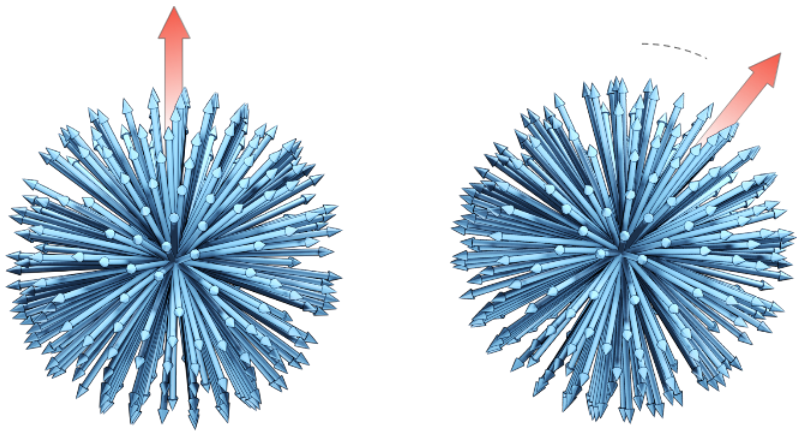

The main magnetic field makes the ensemble of nuclei precess and skews the spin distribution toward the direction of the field as indicated by the higher density of spins along this direction (vertical in the figure). When a resonant radio frequency field is applied, the entire magnetization distribution is rotated around an axis that is rotating perpendicularly to the magnetic field.

Once the magnetication is shifted, it will now rotate (or process)

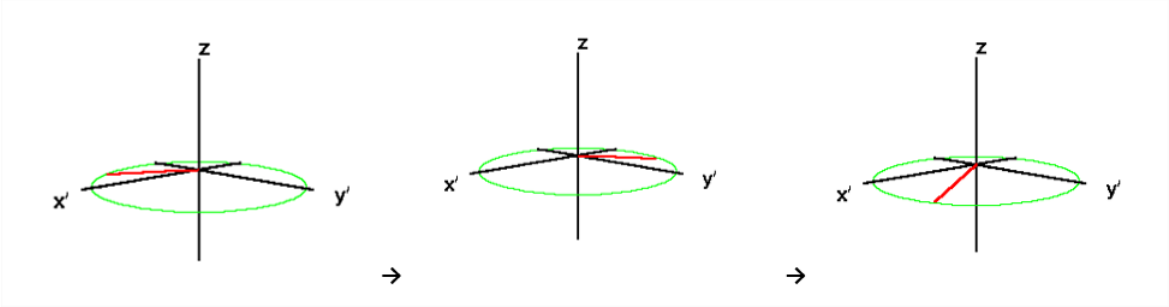

Lab frame evolution (i.e., not rotating frame)

and so forever (that a magnetic field is applied).

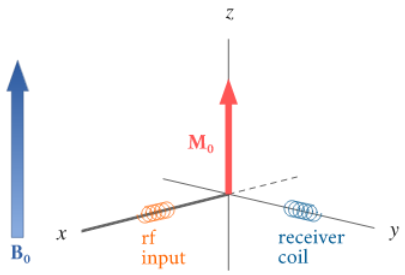

An inherent problem of the NMR experiment must be pointed out here. We have noted that the population difference between the spin states is proportionally very small. A fundamental requirement for absorption spectroscopy is a population imbalance between a lower energy ground state and a higher energy excited state. This can be expressed by the following equation, where A is a proportionality constant. If the mole fractions of the spin states are equal ($\eta_+ = \eta_-$) then the population difference is zero and no absorption will occur. If the rf energy used in an NMR experiment is too high this **saturation** of the higher spin state will result and useful signals will disappear.

$$\text{Probability of Absorption} = A \times \underbrace{\rho(v_0)}_{\substack{\text{radiation} \\ \text{flux}}} \times \underbrace{(\eta_+ - \eta_-)}_{\substack{\text{population} \\ \text{imbalance}}}$$

References

- https://www.drcmr.dk/mr

5.9: Chemical Shifts

The chemical shift feature of NMR makes it a powerful analytical tool. Identical nuclei (e.g. protons) undergo procession at somewhat difference frequencies if they are in a **different electronic environment**. Electron currents in the electronic charge distribution give rise to an induced magnetic field that had a magnitude, $-\delta H_{\circ}$, where δ is a shielding constant. The magnetic field active in on the i^{th} nucleus is then

$$H_i = (1-\delta)H_{\circ}$$

Only if the nuclei are in chemical indistinguishable positions (i.e. related by symmetry operations), will their δ's be the same. The δ's are dimensionless and for proton on at most an order of magnitude of 10^{-7} MHz. Thus the Larmour frequencies of protons only differ by ~10 ppm. For 300 MHz NMR, this is 3000 MHz, but since the linewidths < 1 Hz are common, very small chemical shits differences can be resolved in a 300 MHz instrument.

The Fourier Transform of a sample containing two differently shielded nuclei, σ_1 and σ_2 will contain two Lorentzians separated by $H_0\,(\sigma_1-\sigma_2)\,\gamma/2\pi$ Hz etc.

Δf increases with linearly with H_o, which is characteristic of chemically shifted nuclei. There are charts that correlates the range of various types of protons commonly found in organic molecules. There are given as function of a standard, TMS: $(CH_3)_4Si$. δ is defined as the shift, Δ, in Hz relative to TMS taken at 0 (arbitrary standard). Since Δ is proportional to H_o, this is compensated by dividing by the fixed frequency of the probe, f_o.

The origin of the chemical shift for a nucleus is very complicated. We can derive it initially into local and remote effects. Local effects are from electron on the atoms; remote effects from electrons on neighboring atoms.

Local Shift: Two types of contributions are found: **diamagnetic** and **paramagnetic**.

- Diamagnetic is an induced circulation of charge in the ground state wavefunction that **opposes** the field.
- Paramagnetic is field-induced mixing of the excited state wavefunction that leads to a contribution of opposite sign that **reinforces** the applied field.

Remote Shifts:

- The shielding at an atom like H that has little electron density can be influenced by field induced moment on electron rich neighboring atom. Take H-X, for example: the induced moment on X is the opposite to the field (only considering the diamagnetic part of the local effect). The induced (shielding) field of H depends on the orientation of H_0 relative to the HX axis.

Ring Currents in conjugated systems

The pi electrons in aromatic ring systems contribute to large currents in the present of an external magnetic field. These current induce fields at the positions of the protons that deshielded. The current are produce when the H_0 is perpendicular to the aromatic plane.

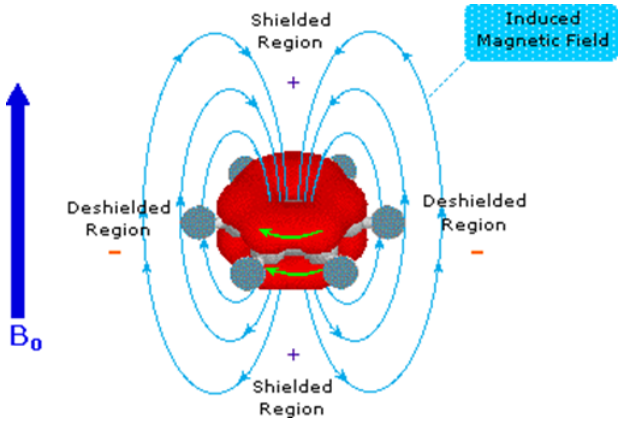

At the position of the H atoms, the direction of the induced fields along Ho reinforce the applied field. This is massive deshielding (downfield shift of resonance)

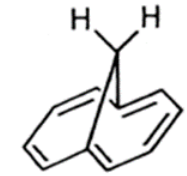

δ (Ring) 7.27; 6.95
δ (CH_2) -0.51

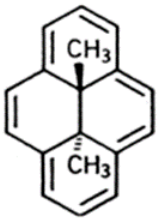

δ (Ring) 8.14 - 8.64
δ (CH_3) - 4.25

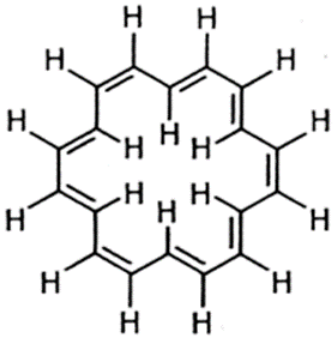

δ (H outer) 9.28
δ (H inner) - 2.99

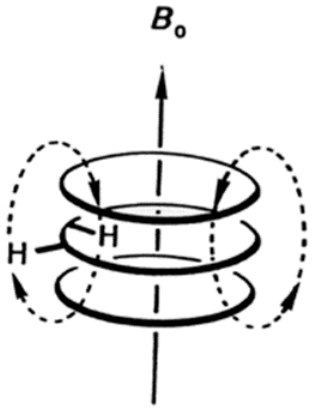

Aromatic compounds show a characteristic deshielding of ring protons (d 6 - 9 ppm vs. d 3 - 4 ppm for alkenes)

Upshot: The interpretation of chemical shift is very complicated; NMR can be used empirically for structural analysis with great success, without having to fully interpret the origin of the chemical shifts. A characteristic useful feature of NMR is the spin-spin splitting that is very useful in structural analysis.

5.10: Fourier Transform (pulsed) NMR - The way things are really done these days

Most applications of NMR involve full NMR spectra, that is, the intensity of the NMR signal as a function of frequency. Early attempts to acquire the NMR spectrum more efficiently than simple CW methods involved irradiating simultaneously with more than one frequency. A revolution in NMR occurred when short pulses of radio-frequency were used (centered at the middle of the NMR spectrum). In simple terms, a short square pulse of a given "carrier" frequency "contains" a range of frequencies centered about the carrier frequency, with the range of excitation (bandwidth) being inversely proportional to the pulse duration (the Fourier transform (FT) of an approximate square wave contains contributions from all the frequencies in the neighborhood of the principal frequency). The restricted range of the NMR frequencies made it relatively easy to use short (millisecond to microsecond) RF pulses to excite the entire NMR spectrum.

Applying such a pulse to a set of nuclear spins simultaneously excites all the single-quantum NMR transitions. In terms of the net magnetization vector, this corresponds to tilting the magnetization vector away from its equilibrium position (aligned along the external magnetic field). The out-of-equilibrium magnetization vector precesses about the external magnetic field vector at the NMR frequency of the spins. This oscillating magnetization vector induces a current in a nearby pickup coil, creating an electrical signal oscillating at the NMR frequency. This signal is known as the free induction decay (FID) and contains the vector-sum of the NMR responses from all the excited spins. In order to obtain the frequency-domain NMR spectrum (**NMR absorption intensity vs. NMR frequency**) this time-domain signal (intensity vs. time) must be FTed. Fortunately the development of FT NMR coincided with the development of digital computers and Fast Fourier Transform algorithms.

An NMR sample may contain many different magnetization components, each with its own Larmor frequency. These magnetization components are associated with the nuclear spin configurations joined by an allowed transition line in the energy level diagram. Based on the number of allowed absorptions due to chemical shifts and spin-spin couplings of the different nuclei in a molecule, an NMR spectrum may contain many different frequency lines.

In pulsed NMR spectroscopy, signal is detected after these magnetization vectors are rotated into the XY plane. Once a magnetization vector is in the XY plane it rotates about the direction of the Bo field, the +Z axis. As transverse magnetization rotates about the Z axis, it will induce a current in a coil of wire located around the X axis.

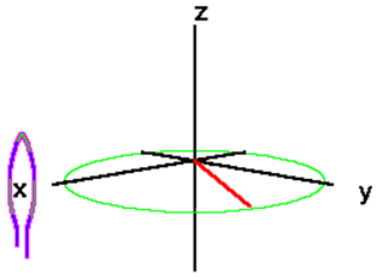

Plotting current as a function of time gives a sine wave.

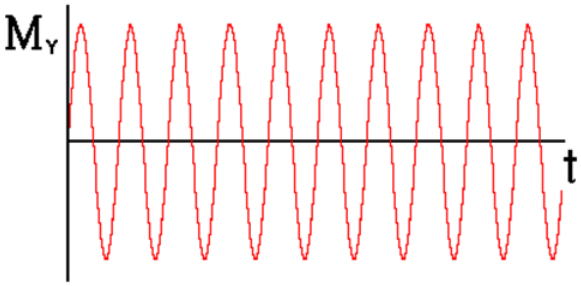

This wave will, of course, decay with time constant T_2^* due to dephasing of the spin packets. This signal is called a **free induction decay** (FID).

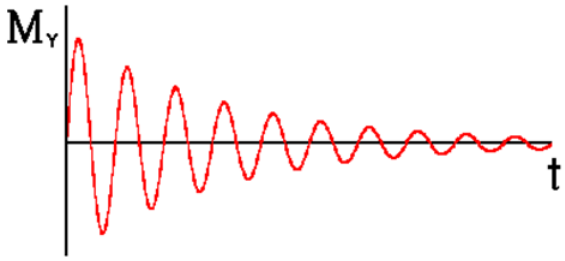

Imagine that $\vec{H}_1$ is turned on @ t=0 exact at a resonance, so that $H_{eff} \sim \vec{H}_1 (\omega_1 = \omega_0)$. $\vec{M}$ will process about $\vec{H}_1$ (along the u-axis) and after a 90-degree procession, it will lie along the v. At this point, $\vec{H}_1$ is turned off and begin with the entire equilibrium magnetization M_o along the v-axis. This called a **90 pulse**, because the $\vec{H}_1$ field is pulsed long enough for M to process 90 degrees about $\vec{H}_1$.

$$\theta = \gamma H_1 t_p$$

where t_p is the time duration of the pulse. If $\vec{H}_1$ is large enough $t_p \ll T_2$ so (transverse) relaxation during the pulse can be ignore.

A $\theta = 90^\circ$ Pulse

$M_v(0) = M_0$, but this will decay with T_2:

$$M_v(t) = M_0 \exp(-t/T_2)$$

in the rotating frame….

A coil setup to pick p the signals will observed a decaying cosine signal

$$M_\perp(t) = M_0 \exp(-t/T_2) \cos(\omega t)$$

with $\omega \approx \omega_\circ$, since not all process at exactly $\omega_\circ$ because of line width or inhomogeneity).

We have a non-periodic $x(t)$ that can be Fourier Transformed. We know that it is a single function of cosine and exponential decay, the Fourier Transform (in frequency space) will be a **convolution** of the Fourier Transforms of $\cos(\omega t)$ and the exponential decay. The factor is analogous to a rectangular window function which produces a $sinc(x)$ function: $\sin(x)/x$ centered at $\pm\omega$. What do we expect for the whole function? A Fourier Transform of $\exp(-t/T_2)$ centered at $\pm\omega$.

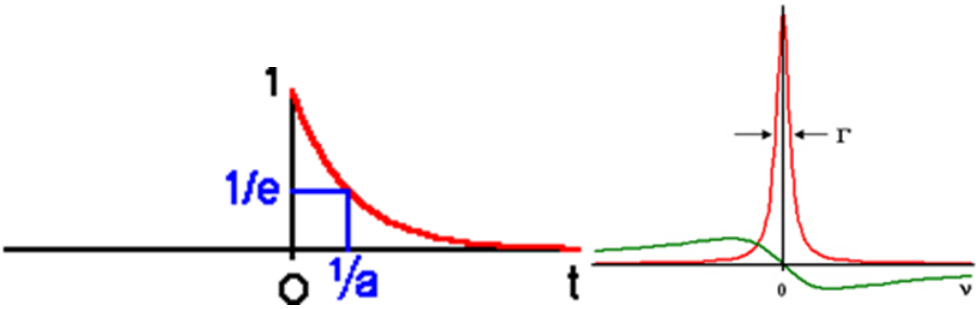

$M_\perp(t)$ is neither symmetric or antisymmetric about $t = 0$, thus we expect non-zero real and imaginary components of $X(\omega)$, the FT of $M_1(t)$.

$$X(\omega) = A(\omega) + iD(\omega)$$

where A and D are the real and imaginary part of the Fourier Transform. Here $A(\omega)$ is the absorption and $D(\omega)$ is the dispersive components to the signal.

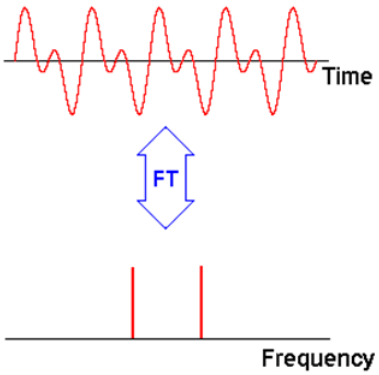

The upshot for FT NMR

Fourier Transform NMR is an example of a set of damped oscillators (nuclei) that have individual resonance frequencies. Each frequency is characterized by its own τ_2; this damping time constant is called T_2. Thus each resonance contributes to the total FT a set of signals analogous to those represented above for a single damped oscillator. All oscillators are excited simultaneously by a broadband radio-frequency pulse. The decaying oscillators are sampled and Fourier Analyzed.

The $\vec{H}_1$ field is applied at f_0 (approximately the Larmour Frequency of **all protons in sample**). The RF is windows through a rectangular window of length t_p.

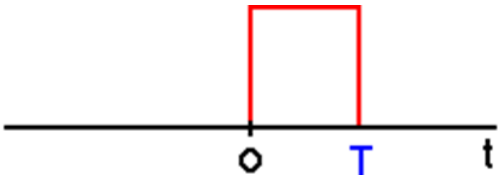

The spectral content is given by the sinc$x$ function center $\pm f_0$: (sin(2 t))/(2 t) with imaginary component: -(sin^2(2 t))/(t)

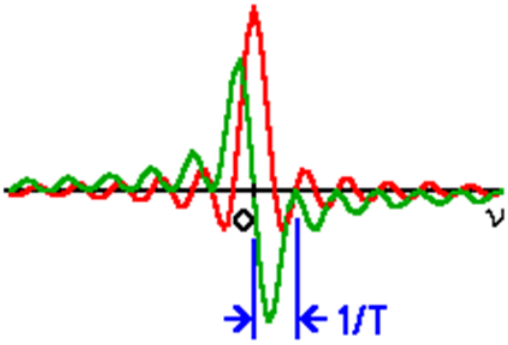

All protons with in a bandwidth of $\sim \Delta f_p = \frac{2}{t_p}$ about f_0 will be tipped away from z toward the v plane and will contribute their own frequencies to the FID. So, if we want Δf_p to be ~2,000 Hz to cover a large range of chemical shifts, we need a t_p of 10^{-3} s.

$$\Delta f_p = \frac{2}{t_p} = 2000 \text{ Hz}$$

so $t_p = 10^{-3} s$.

The convolution theorem says that the FT of a convolution of two functions is proportional to the products of the individual Fourier transforms, and vice versa.

If $f(\omega) = FT(f(t))$ and $g(\omega) = FT(g(t))$ then $f(\omega)g(\omega) = FT(g(t)f(t))$ and $f\omega) \times g(\omega) = FT(g(t)f(t))$.

It will be easier to see this with pictures. In the animation window we are trying to find the FT of a sine wave which is turned on and off. The convolution theorem tells us that this is a sinc function at the frequency of the sine wave.

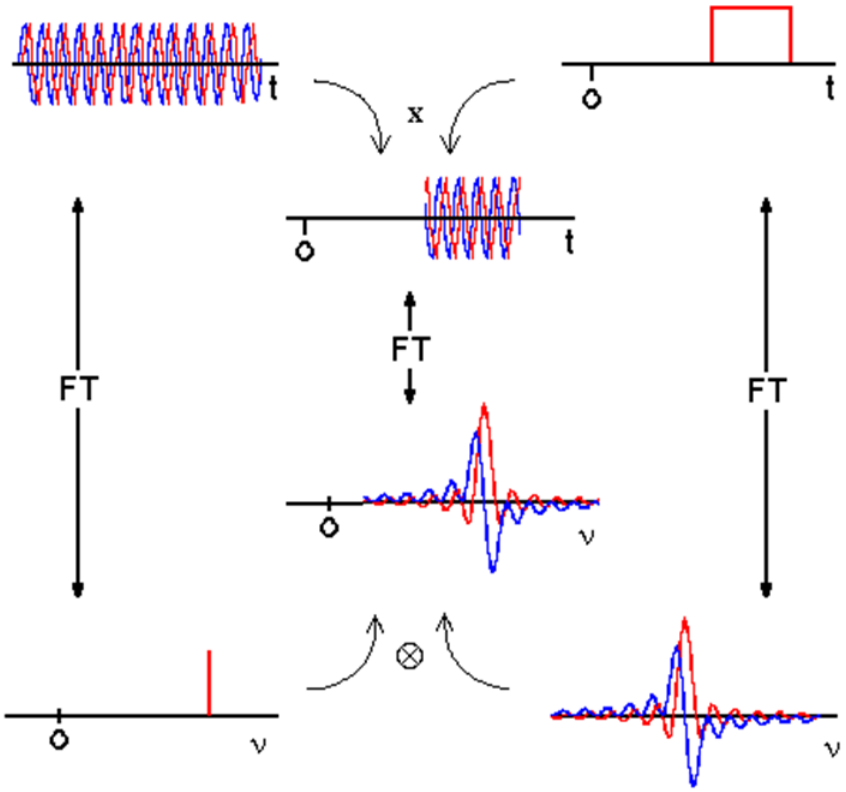

5.11: Spin-Spin, J-Coupling or indirect dipole-dipole coupling (all the same phenomenon)

By a mechanism not discussed here, the magnetic moment induced by nearby nuclear spin can be felt as a contribution to the magnetic field at a nuclear undergoing resonance. Thus if the B spin had two orientations (I=1/2 had only two possible orientations), two possible local fields at A would results and this resonance would be split into two resonances - J.

> *The frequency, J_{AB} is **independent** of H_o (internal forces only), while δ for two different nuclear is **proportional** to H_0. That is how we can tell chemical shifts splitting from spin-spin splitting.*

The resonance frequencies (or field position) of a proton is influenced not only by the shielding parameter, but also by the orientations of other nuclear spins in the molecules with which it is communication (like a correlation length for UV excitations). The interaction between nuclear spins in a molecule is called spin-spin coupling. This leads to structure in the NMR spectra in addition to the intrinsic chemical shift differences discussed above.

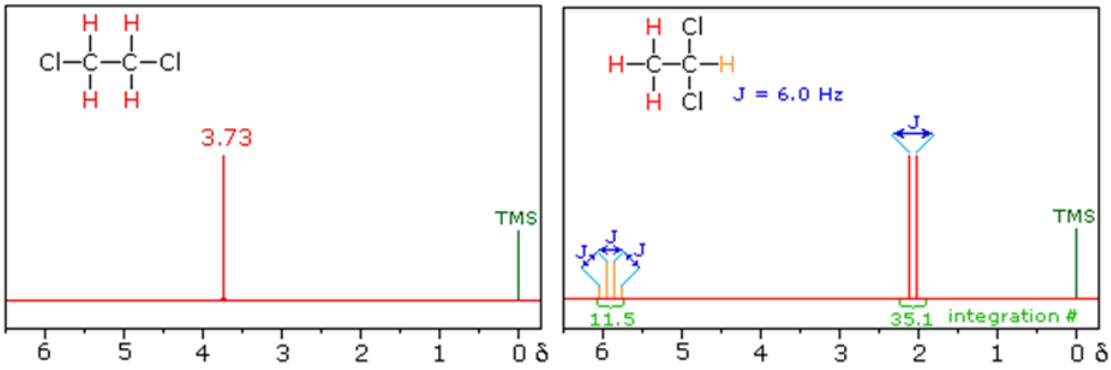

1,2-dichloroethane 1,1-dichloroethane

The splitting patterns found in various spectra are easily recognized, provided the chemical shifts of the different sets of hydrogen that generate the signals differ by two or more ppm. The patterns are symmetrically distributed on both sides of the proton chemical shift, and the central lines are **always stronger** than the outer lines. The most commonly observed patterns have been given descriptive names, such as **doublet** (two equal intensity signals), **triplet** (three signals with an intensity ratio of 1:2:1) and **quartet** (a set of four signals with intensities of 1:3:3:1). Four such patterns are displayed in the following illustration. The line separation is always constant within a given multiplet, and is called the **coupling constant (J)**. The magnitude of J, usually given in units of Hz, is magnetic field independent.

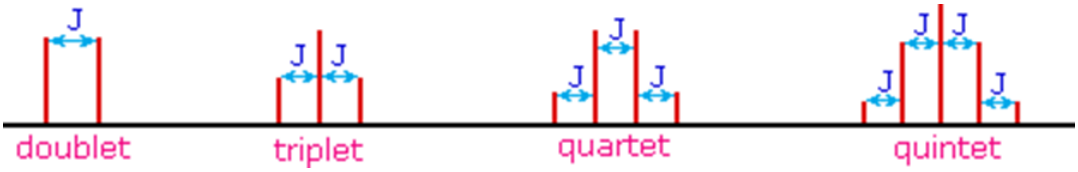

The fine structure pattern of CH_3 protons is due to the fact that the CH_3 protons sense different orientations of the nearby CH_2 protons (**through bond coupling**) in the field.

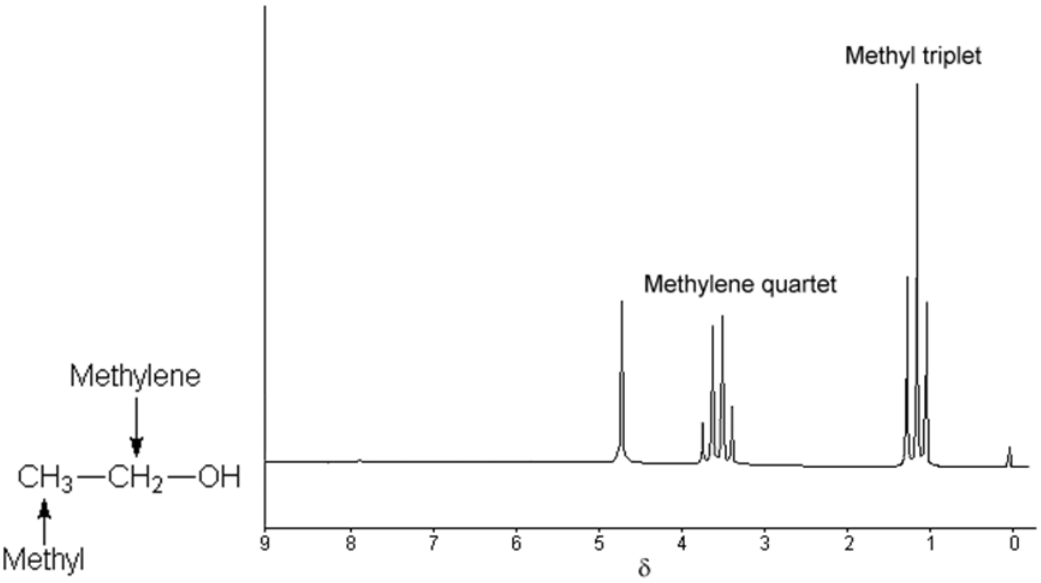

The coupling constant in Hz is $\mathbf{J_{H\text{-}C\text{-}C\text{-}H}}$ **or** $\mathbf{^3J_{H\text{-}H}}$ (superscript indicates that the coupled atoms are 3 bonds apart). The CH_2 protons are split by the same coupling constant $^3J_{H\text{-}H}$ into a quartet with an intensity ratio of 1:3:3:1. There are two **methylene** protons of them, and each can have one of two possible orientations (aligned with or opposed against the applied field). This gives a total of four possible states;

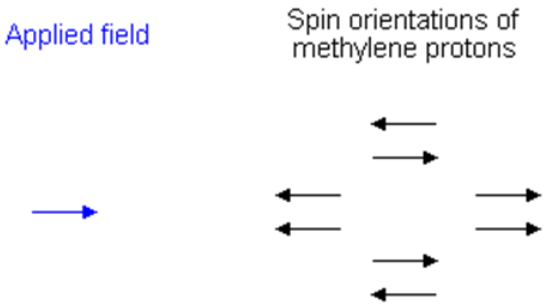

In the first possible combination (left), spins are paired and opposed to the field. This has the effect of reducing the field experienced by the **methyl** protons; therefore a slightly higher field is needed to bring them to resonance, resulting in an upfield shift. Neither combination of spins opposed to each other has an effect on the methyl peak. The spins paired in the direction of the field produce a downfield shift. Hence, the methyl peak is split into three, with the ratio of areas 1:2:1.

Similarly, the effect of the methyl protons on the methylene protons is such that there are **eight** possible spin combinations for the three methyl protons;

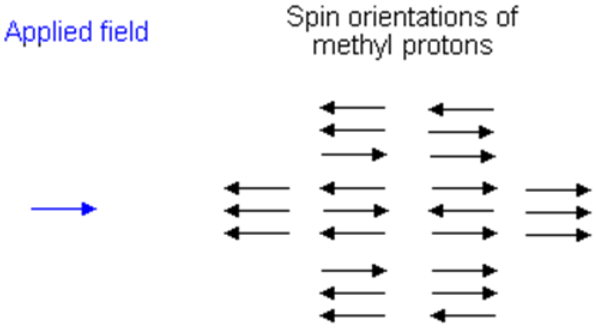

Out of these eight groups, there are two groups of three magnetically equivalent combinations. The methylene peak is split into a quartet. The areas of the peaks in the quartet have the ration 1:3:3:1.

The spin mulitplet pattern of NMR spectra contain much structure info, as witnessed by C_2H_5OH. The intensity patterns of groups of equivalent nuclei of I=1/2 that split a resonance can be obtains by Pascal's triangle (handy way to remember binomial coefficients):

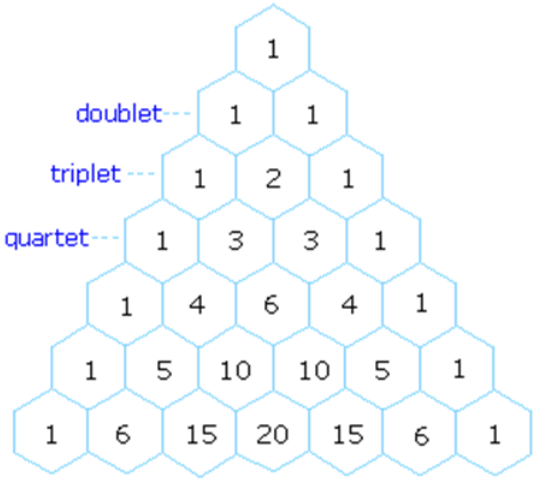

Pascal's Triangle

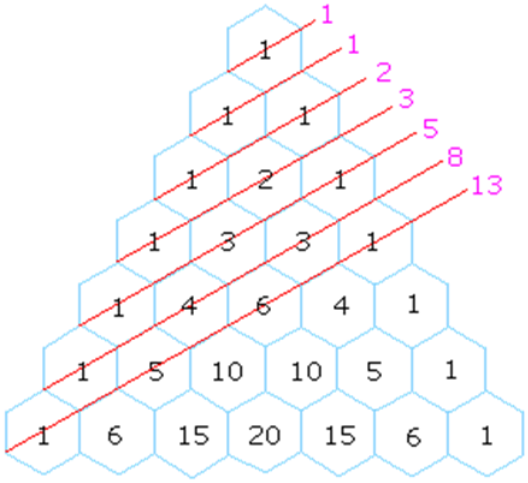

Pascal's Triangle
The Fibonacci Series

Any number is given as the sum of the two adjacent numbers on the preceding row. Each row is the number of nuclei equivalent protons are coupled to starting at 0.

Non I=1/2 splitting

The intensities of the individual lines is given by the spin *I* of the coupling nucleus (not the observed one). The relative intensities of the lines can be derived from Pascal's triangle and similar arrays:

n	*I* = 1/2	*I* = 1	*I* = 3/2
0	1	1	1
1	1 1	1 1 1	1 1 1 1
2	1 2 1	1 2 3 2 1	1 2 3 4 3 2 1
3	1 3 3 1	1 3 6 7 6 3 1	1 3 6 10 12 12 10 6 3 1
4	1 4 6 4 1	1 4 10 16 19 16 10 4 1	1 4 10 20 31 40 44 40 31 20 10 4 1

When done properly, there are 12 distinct main transitions in the CH_2 group and 13 in the CH_3 group of ethanol, but all of them are never resolved. The distance between the different transitions depends on the magnetic field in such a way that at higher fields they are too close to be observed and several transitions often contribute to the same peak.

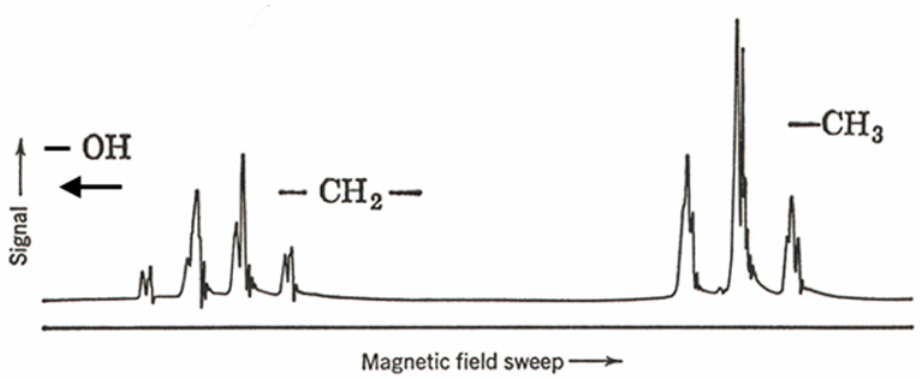

Higher resolution showing greater splitting in the bands in ETOH

Measureable J's are usually observed between protons separated by up to **3-bands**. 4 bands and > coupling are usually not observed. So splitting of CH_3 by OH (four bands) is not seen *(with the exception of aromatic molecules)*.

Coupling Constants (I): $^2J(H,H)$ and $^3J(H,H)$ Coupling Constants of Organic Compounds

The following is a list of H,H coupling constants observed for different structural fragments. Many different fragments give coupling constants in the range of 2-10 Hz so that coupling constants in this range are of limited value as a diagnostic tool for structure elucidation.

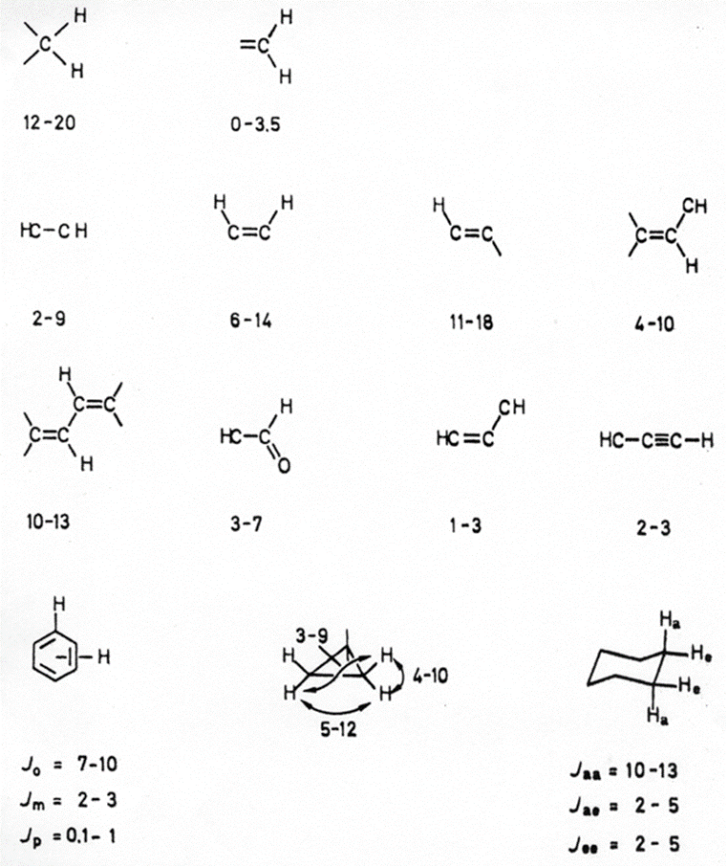

The following general rules summarize important requirements and characteristics for spin 1/2 nuclei

1. Nuclei having the same chemical shift do not exhibit spin-splitting. They may actually be spin-coupled, but the splitting cannot be observed directly.
2. Nuclei separated by **three or fewer** bonds (e.g. vicinal and geminal nuclei) will usually be spin-coupled and will show mutual spin-splitting of the resonance signals (same J's), provided they have different chemical shifts. Longer-range coupling may be observed in molecules having rigid configurations of atoms.
3. The magnitude of the observed spin-splitting depends on many factors and is given by the coupling constant **J** (units of Hz). J is the same for both partners in a spin-splitting interaction and is **independent** of the external magnetic field strength.
4. The splitting pattern of a given nucleus (or set of equivalent nuclei) can be predicted by the **n+1 rule**, where n is the number of neighboring spin-coupled nuclei with the same (or very similar) Js. If there are 2 neighboring, spin-coupled, nuclei the observed signal is a triplet (2+1=3); if there are three spin-coupled neighbors the signal is a quartet (3+1=4). In all cases the central line(s) of the splitting pattern are stronger than those on the periphery. The intensity ratio of these lines is given by the numbers in Pascal's triangle. Thus a doublet has 1:1 or equal intensities, a triplet has an intensity ratio of 1:2:1, a quartet 1:3:3:1 etc.

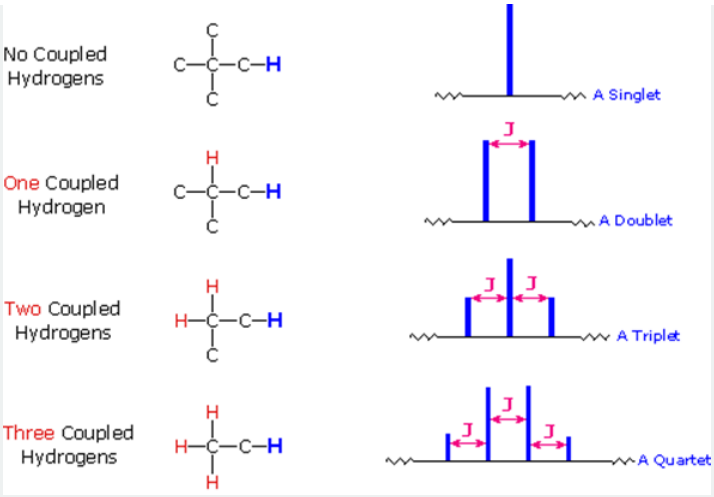

The interpretation of the 1st order spectra is relatively straightforward. Not so for spectra in which the relative chemical shifts are similar to J_{AB}. These give very complex spectra that are hard to interpret. The best solution is to use the strongest applied field as possible to induce the greatest chemical shifts allowing for separation of δ from J **(bigger is better).**

Spin-spin coupling isn't limited to protons with protons, but will all nuclei that have magnetic fields (for example ^{13}C will couple with ^{1}H or ^{13}C with ^{14}N).

Distance Dependence of Coupling Constants

While ^{1}J, ^{2}J or ^{3}J coupling is commonly observed for H,H coupling, coupling constants ^{4}J or higher are usually *too small* to be observed.

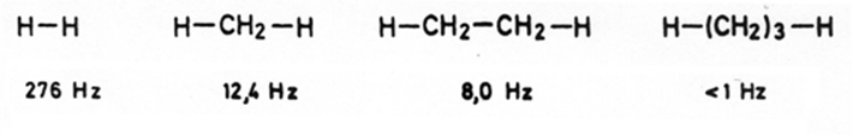

A notable exception are ^{4}J coupling constants in rigid frameworks:

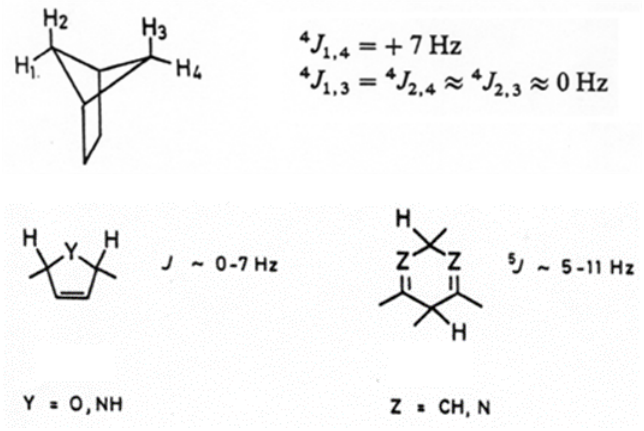

Geometric considerations in J Coupling

The $^{3}J(H,H)$ coupling constants of aliphatic H-C-C-H fragments depend on the dihedral angle. The quantitative relationship is given by the Karplus equation, named after Martin Karplus (Harvard), which describes the correlation between ^{3}J-coupling constants and dihedral torsion angles in nuclear magnetic resonance spectroscopy:

$$J(\phi) = A\cos^2\phi + B\cos\phi + C$$

where J is the ^{3}J coupling constant, φ is the dihedral angle, and A, B, and C are empirically-derived parameters whose values depend on the atoms and substituents involved. The relationship may be expressed in a variety of equivalent ways e.g., involving $\cos^2$ φ rather than cos 2φ —these lead to different numerical values of A, B, and C but do not change the nature of the relationship.

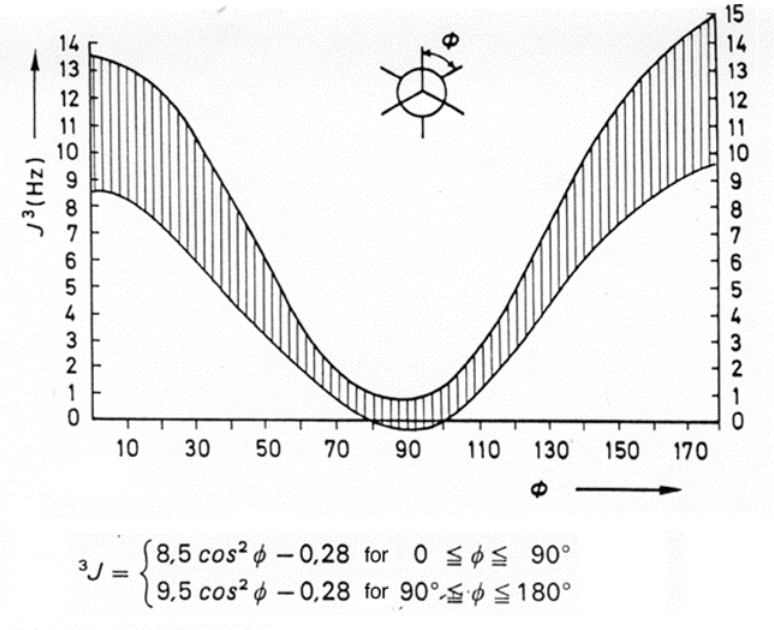

The Karplus equation is extremely important tool for the elucidation of 3D structures via NMR methods.

Example 5.11.1: Sugars

The Karplus equation is a useful tool to distinguish between the equatorial and axial protons present in many natural products. In the following example, the ^{3}J(H,H) coupling constants used to distinguish between a-D-Glucose and b-D-Glucose:

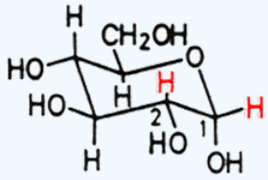

α-D-Glucose

($^3J_{aa}$ = 3,0 Hz)

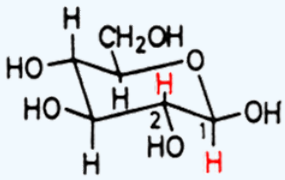

β-D-Glucose

($^3J_{aa}$ = 7,4 Hz)

References

https://chem.libretexts.org/Bookshel...on_NMR_Spectra

5.12: 13-C NMR Spectroscopy

The carbon-12 nucleus does not have a nuclear spin, but the carbon-13 (^{13}C) nucleus does due to the presence of an unpaired neutron. Carbon-13 nuclei make up approximately one percent of the carbon nuclei on earth. Therefore, carbon-13 NMR spectroscopy will be less sensitive (have a poorer SNR) than hydrogen NMR spectroscopy. Therefore, only the few 13C nuclei present resonate in the magnetic field, although this can be overcome by isotopic enrichment of e.g. protein samples. In addition, the gyromagnetic ratio (6.728284 107 rad T^{-1} s^{-1}) is only 1/4 that of ^{1}H, further reducing the sensitivity. The overall signals of ^{13}C is about 4 orders of magnitude lower than ^{1}H.

Chemical Shifts

As with proton NMR, the chemical shift reference standard for ^{13}C is the carbons in tetramethylsilane (TMS), whose chemical shift is set to 0.0 ppm.

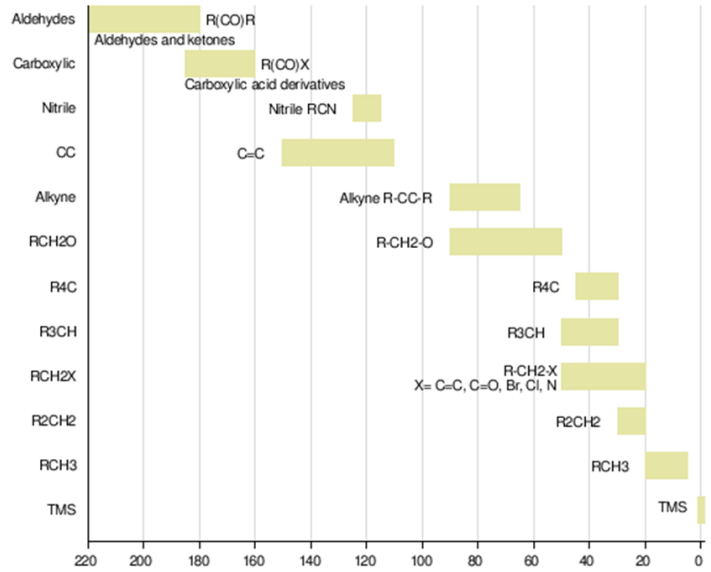

Range of Chemical Shifts

Chemical shift depends on the net magnetic field felt by the nuclei (H,C). The net magnetic field, in turn, depends upon the electron density possessed by the particular atom (Shielding constant). In the case of hydrogen, there is just a single electron and by coordination with others (H-F, CH3-F etc) leads to the slight change in electron density around the hydrogen nuclei, therefore, results in the small range of chemical shift. However, carbon having six electrons, being tetravalent, as well as attached to diverse functionalities leads to the considerable change in electron density around the carbon nuclei thereby, possess broader range of chemical shift values.

This is a simple example of a C-13 NMR spectrum. do not worry about the scale for now - we'll look at that in a minute.

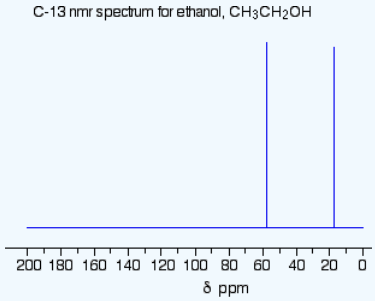

The NMR spectra on this page have been produced from graphs taken from the Spectral Data Base System for Organic Compounds (SDBS) at the National Institute of Materials and Chemical Research in Japan. It is possible that small errors may have been introduced during the process of converting them for use on this site, but these won't affect the argument in any way.

There are two peaks because there are two different environments for the carbons. The carbon in the CH_3 group is attached to 3 hydrogens and a carbon. The carbon in the CH_2 group is attached to 2 hydrogens, a carbon and an oxygen. The two lines are in different places in the NMR spectrum because they need different external magnetic fields to bring them in to resonance at a particular radio frequency.

This is the C-13 NMR spectrum for 1-methylethyl propanoate (also known as isopropyl propanoate or isopropyl propionate).

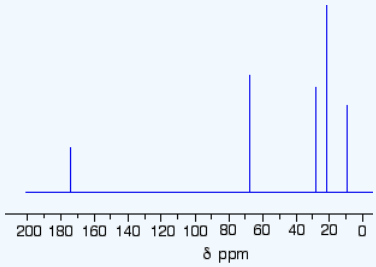

This time there are 5 lines in the spectrum. That means that there must be 5 different environments for the carbon atoms in the compound. Is that reasonable from the structure?

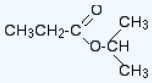

Well - if you count the carbon atoms, there are 6 of them. So why only 5 lines? In this case, two of the carbons are in exactly the same environment. They are attached to exactly the same things. Look at the two CH_3 groups on the right-hand side of the molecule.

You might reasonably ask why the carbon in the CH3 on the left is not also in the same environment. Just like the ones on the right, the carbon is attached to 3 hydrogens and another carbon. But the similarity is not exact - you have to chase the similarity along the rest of the molecule as well to be sure.

The carbon in the left-hand CH_3 group is attached to a carbon atom which in turn is attached to a carbon with two oxygens on it - and so on down the molecule. That's not exactly the same environment as the carbons in the right-hand CH_3 groups. They are attached to a carbon which is attached to a single oxygen - and so on down the molecule.

Heteronuclear Coupling

Many organic molecules contain ^{1}H as only NMR active nucleus and observed couplings are accordingly those between neighboring protons, the situation is more complex if other high abundance I = 1/2 nuclei are present (e.g., ^{13}C, ^{19}F and ^{31}P). The below spectrum is a **^{1}H broadband decoupled ^{13}C spectrum** (shorthand notation: ^{13}C {^{1}H }) of trifluoroacetic acid that shows "hydrogen like " coupling (two quartets).

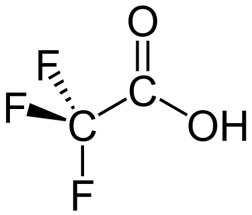

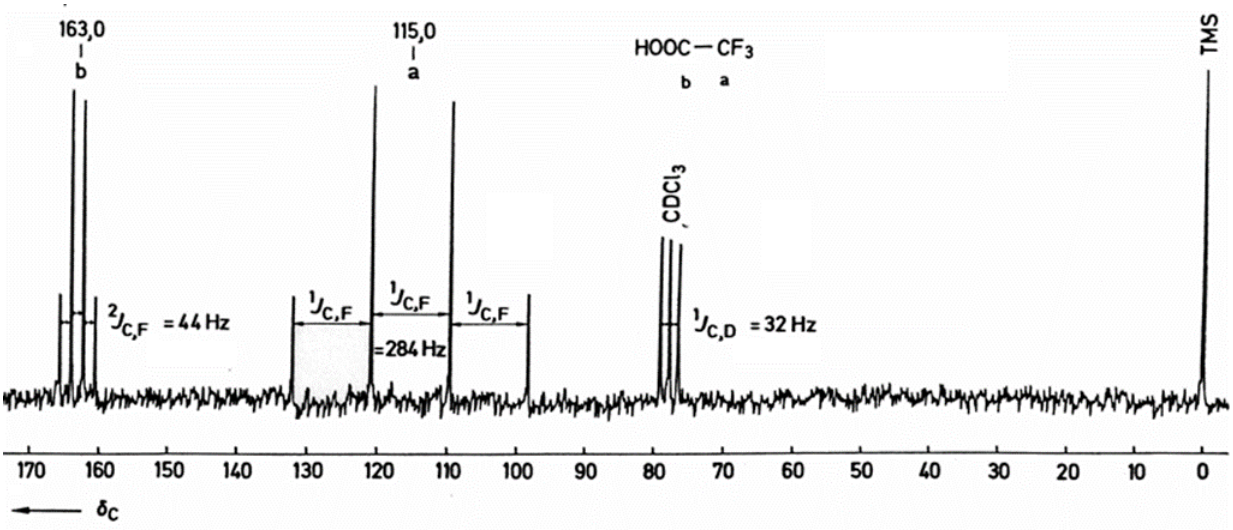

Quadrupolar nuclei (e.g., ^{2}H) can also couple to I=1/2 nuclei, but is usually detected by measuring the quadrupolar nucleus, but rarely by measuring the I=1/2 nucleus (lifetime, T_2, issue). J =1/2 to J =1/2 is generally observed unless **fast exchange** disrupts the bond (loss of through-bond coupling)

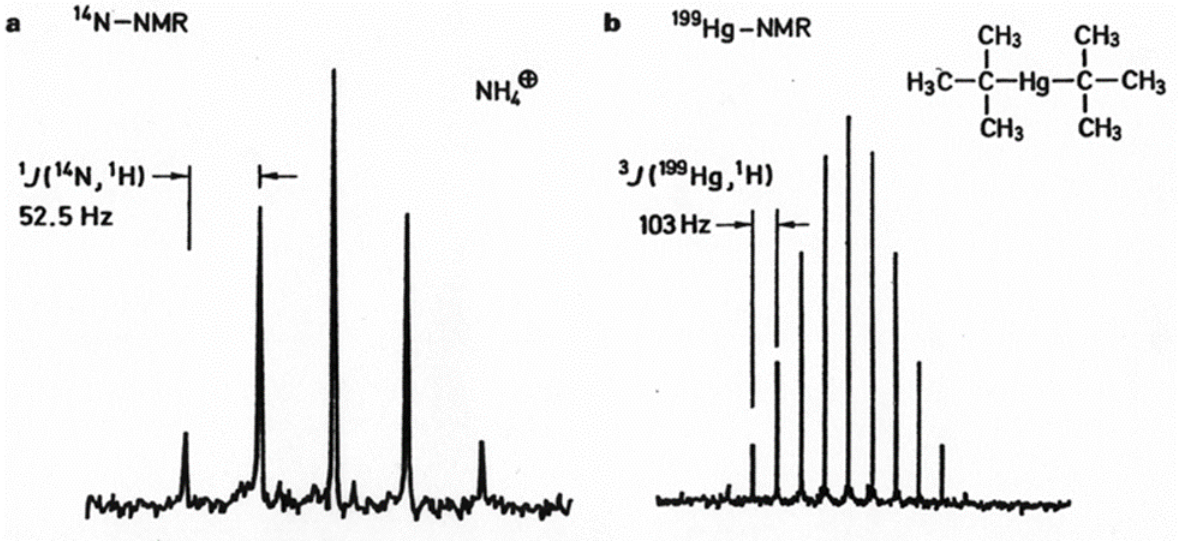

^{14}N NMR Spectrum of ammonium ions (a) and ^{199}Hg NMR spectrum of di-tert-butylmercury (b); Spectrometer frequency 4.33 and 14.3 MHz. b: only 11 of the 19 expected lines are actually observed.

J-coupling constants between carbon and hydrogen are typically from 100 to 250 Hz. To suppress these couplings, which would otherwise complicate the spectra and further reduce sensitivity, carbon-13 NMR spectra are often "proton decoupled" to remove the signal splitting. Typically, ^{13}C-^{13}C couplings can be ignored due to the low natural abundance of ^{13}C (unless specifically synthesized that way in the lab). Hence in contrast to typical proton NMR spectra which show multiplets for each proton position, **carbon NMR spectra typically show a single peak for each chemically non-equivalent carbon atom.**

5.13: Nuclear Overhauser Effect (NOE) and 2-D NMR

The use of pulses of different shapes, frequencies and durations in specifically-designed patterns or pulse sequences allows the spectroscopist to extract many different types of information about the molecule. Multi-dimensional nuclear magnetic resonance spectroscopy is a kind of FT NMR in which there are at least two pulses and, as the experiment is repeated, the pulse sequence is varied. In multidimensional nuclear magnetic resonance there will be a sequence **of pulses** and, at least, one variable time period. In three dimensions, two time sequences will be varied. In four dimensions, three will be varied.

There are many such experiments. In one, these time intervals allow (amongst other things) magnetization transfer between nuclei and, therefore, the detection of the kinds of nuclear-nuclear interactions that allowed for the magnetization transfer. Interactions that can be detected are usually classified into two kinds.

1. There are through-bond interactions and
2. through-space interactions, the latter usually being a consequence of the nuclear Overhauser effect.

Such experiments may be employed to establish distances between atoms, as for example by 2D-FT NMR of molecules in solution. NOE differs from **spin coupling in the respect that NOE is observed through space, not through bonds**. Thus, all atoms that are in close proximity to each other give a NOE, whereas spin coupling is observed only when the atoms are bonded to same or neighboring atoms. Furthermore, the distance can be derived from the observed NOEs, so that the precise, three-dimensional structure of the molecule can be reconstructed.

Other experimental techniques exploiting the NOE include and are not limited to:

- HOESY, Heteronuclear Overhauser Effect Spectroscopy
- ROESY, Rotational Frame Nuclear Overhauser Effect Spectroscopy
- TRNOE, Transferred Nuclear Overhauser Effect
- DPFGSE-NOE, Double Pulsed Field Gradient Spin Echo NOE experiment

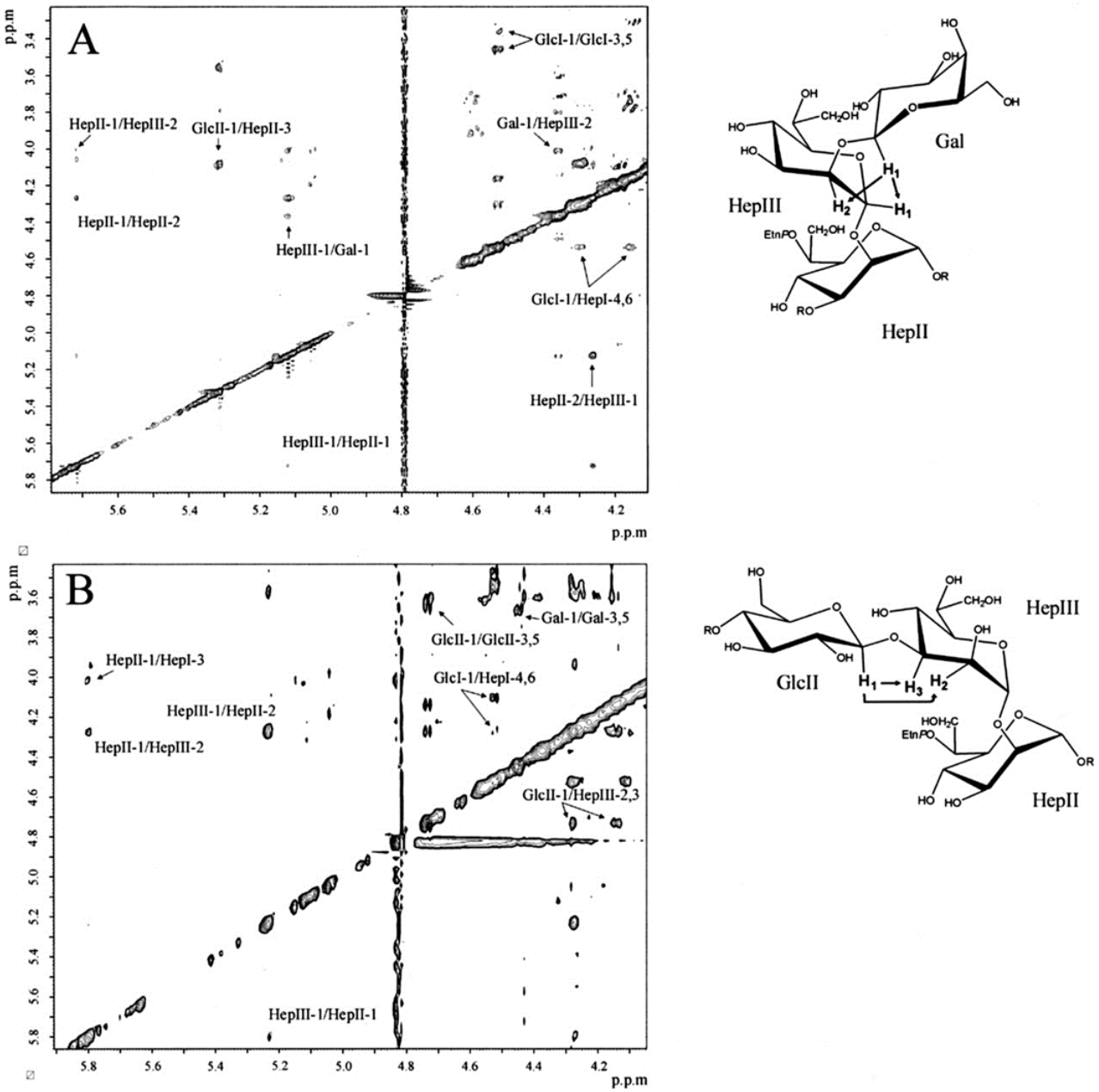

Selected regions from the 500-MHz two-dimensional NOE spectroscopy spectra (mixing time 200 ms) of OS derived from the LPS of 486lpsAEa (*A*) and RdlpsA486 (*B*). Cross-peaks that are characteristic are labeled. The NOE connectivities important for the Hex-HepIII-HepII region are illustrated in the structural elements.

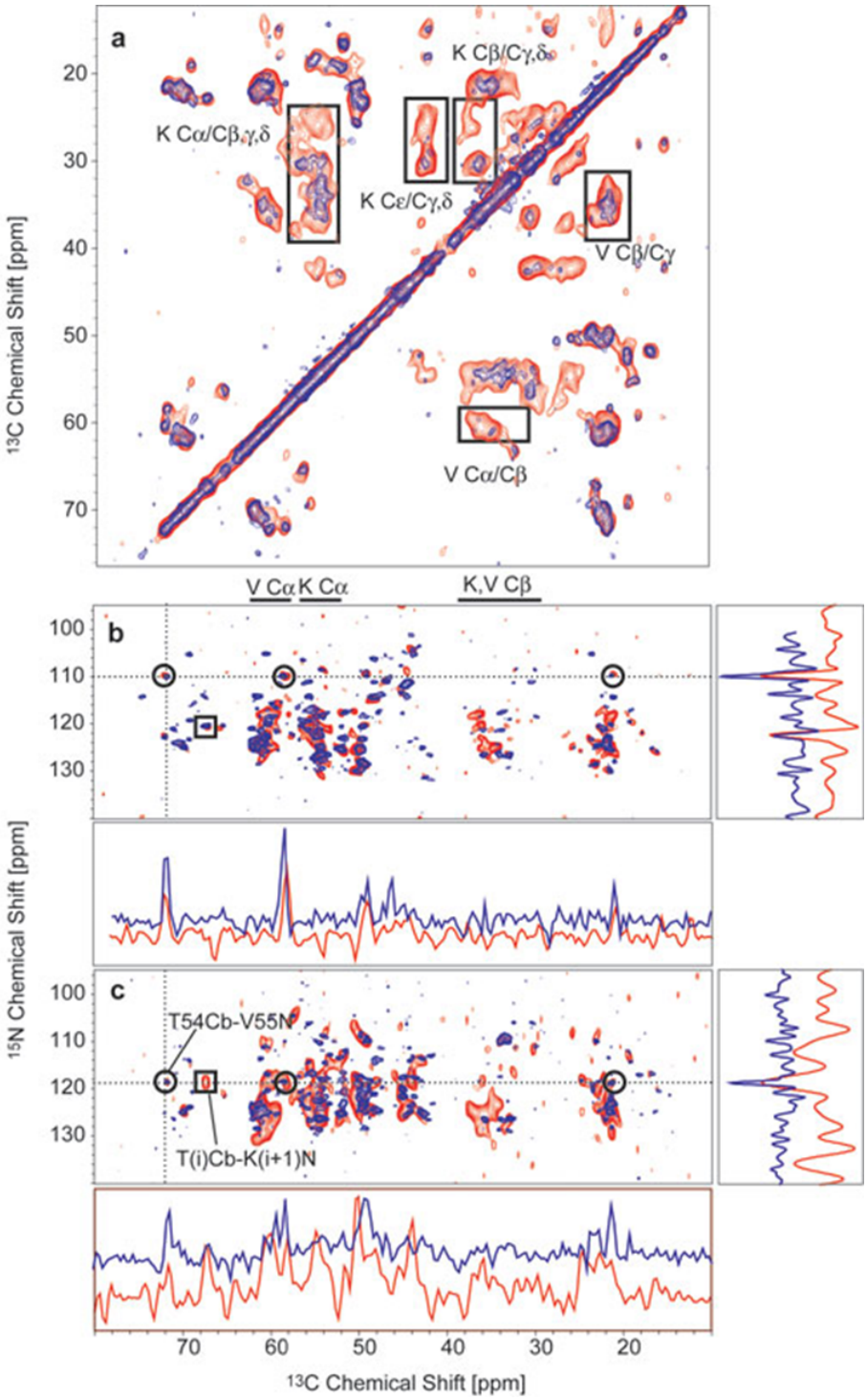

The fastest upshot, is that the **off-diagonal peaks** indicate coupling between the two nuclei (through space of through bond), which gives greater information regarding the structure of a sample (this is the underlying approach to solution-phase NMR structure determination of proteins). See: http://pubs.acs.org/doi/abs/10.1021/ja00353a071

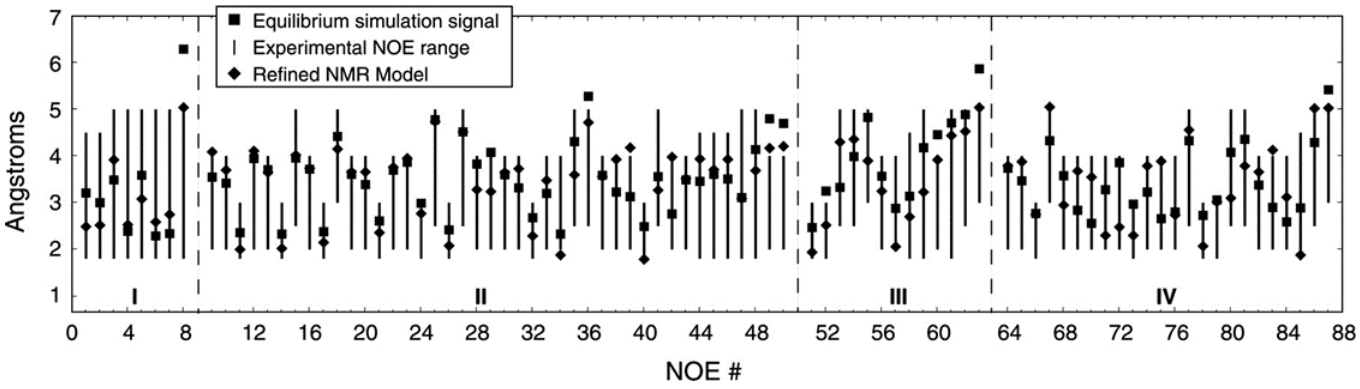

Simulation data are compared to the distance constraints determined from NOE cross peaks

5.14: Electron Paramagnetic Resonance

EPR spectroscopy is possible to come out of any sample that has transiently or statically unpaired electron spins. For instance, radicals and electronic triplet states. Electron paramagnetic resonance spectroscopy (EPR) is a powerful tool for investigating paramagnetic species, including organic radicals, inorganic radicals, and triplet states. The basic principles behind EPR are very similar to the more ubiquitous NMR, except that EPR focuses on the interaction of an external magnetic field with the **unpaired electron(s)** in a molecule, rather than the nuclei of individual atoms. EPR has been used to investigate kinetics, mechanisms, and structures of paramagnetic species and along with general chemistry and physics, has applications in biochemistry, polymer science, and geosciences.

EPR Features

Measured physical quantities

- Energy separation between different electron spin states
- Nuclear hyperfine coupling constants

Information available

- Spin state, S, of paramagnetic center
- Magnitude of hyperfine interactions
- Zero-field splitting of half-integer S > 1/2 states
- Possible identity of paramagnetic center (free radical; metals in metal cluster)
- Possible identity of ligating atoms

Information NOT available, limitations

- No information for diamagnetic sites
- Integer spin states often unobservable

Examples of questions that can be answered

- What are the different paramagnetic centers in the sample?
- How do these centers change with changes in redox potential and pH or during substrate binding or catalysis?

Major advantages

- Volume (300 mL) and concentration (1.0-0.01 mM) often low
- Recording spectrum can be done quickly (usually no more than 15-20 min)
- Spectrum is only of paramagnetic species
- Spectrum is often simple to interpret
- Spectrum often can be recorded *in vivo*

Major disadvantages

- Most paramagnetic metal centers require low (20 K or lower) temperatures for detection

Sample constraints

- Sample volume is ca. 0.3 mL
- Concentration can range from 0.01-1.0 mM
- Sample should be free of any paramagnetic impurities

The degeneracy of the electron spin states is lifted when an unpaired electron is placed in a magnetic field, creating two spin states, $m_s = \pm ½$, where $m_s = - ½$, the lower energy state, is aligned with the magnetic field.

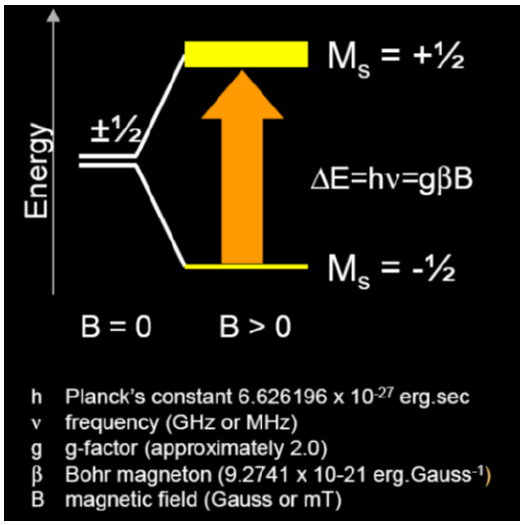

The spin state on the electron can flip when electromagnetic radiation is applied. In the case of electron spin transitions, this corresponds to radiation in the microwave range. The energy difference between the two spin states is given by:

$$\Delta E = E_+ - E_- = h\upsilon = g\beta B \tag{5.14.1}$$

where h is Planck's constant (6.626 x 10^{-34} J s-1), ν is the frequency of radiation, β is the Bohr magneton (9.274 x 10-24 J T^{-1}), B is the strength of the magnetic field in Tesla, and g is known as the **g-factor**.

The g-factor is a unitless measurement of the intrinsic magnetic moment of the electron, and its value for a free electron is 2.0023. The value of g can vary, however, and can be calculated by rearrangement of Equation 5.14.1:

$$g = \frac{h\upsilon}{\beta B}$$

using the magnetic field and the frequency of the spectrometer. Since h, ν, and ß should not change during an experiment, g values decrease as B increases. **The concept of g can be roughly equated to that of chemical shift in NMR**.

Reference

https://egpat.com/test-papers/esr?Page=1

5.15: EPR Instrumentation

EPR spectroscopy can be carried out by either:

- varying the magnetic field and holding the frequency constant or
- varying the frequency and holding the magnetic field constant (as is the case for NMR spectroscopy).

Commercial EPR spectrometers typically vary the magnetic field and holding the frequency constant, opposite of NMR spectrometers. The majority of EPR spectrometers are in the range of 8-10 GHz (**X-band**), though there are spectrometers which work at lower and higher fields: 1-2 GHz (**L-band**) and 2-4 GHz (**S-band**), 35 GHz (**Q-band**) and 95 GHz (**W-band**). These are wavelengths around 1 to 10 centimeters.

EPR experiments often are conducted at X- and, less commonly, Q bands, mainly due to the ready availability of the necessary microwave components (which originally were developed for radar applications). A second reason for widespread X and Q band measurements is that electromagnets can reliably generate fields up to about 1 tesla. High-field-high-frequency EPR measurements are sometimes needed to detect subtle spectroscopic details. However, for many years the use of electromagnets to produce the needed fields above 1.5 T was impossible, due principally to limitations of traditional magnet materials.

The EPR waveband is stipulated by the frequency or wavelength of a spectrometer's microwave source

band	L	S	C	**X**	P	K	**Q**	U	V	E	W	F	D	—	J	—
λ / mm	300	100	75	**30**	20	12.5	**8.5**	6	4.6	4	3.2	2.7	2.1	1.6	1.1	0.83
ν / GHz	1	3	4	**10**	15	24	**35**	50	65	75	95	111	140	190	285	360
B0 / T	0.03	0.11	0.14	**0.33**	0.54	0.86	**1.25**	1.8	2.3	2.7	3.5	3.9	4.9	6.8	10.2	12.8

EPR spectrometers work by generating microwaves from a source (typically a klystron), sending them through an attenuator, and passing them on to the sample, which is located in a microwave cavity (Figure 5.15.1). Microwaves reflected back from the cavity are routed to the detector diode, and the signal comes out as a decrease in current at the detector analogous to absorption of microwaves by the sample.

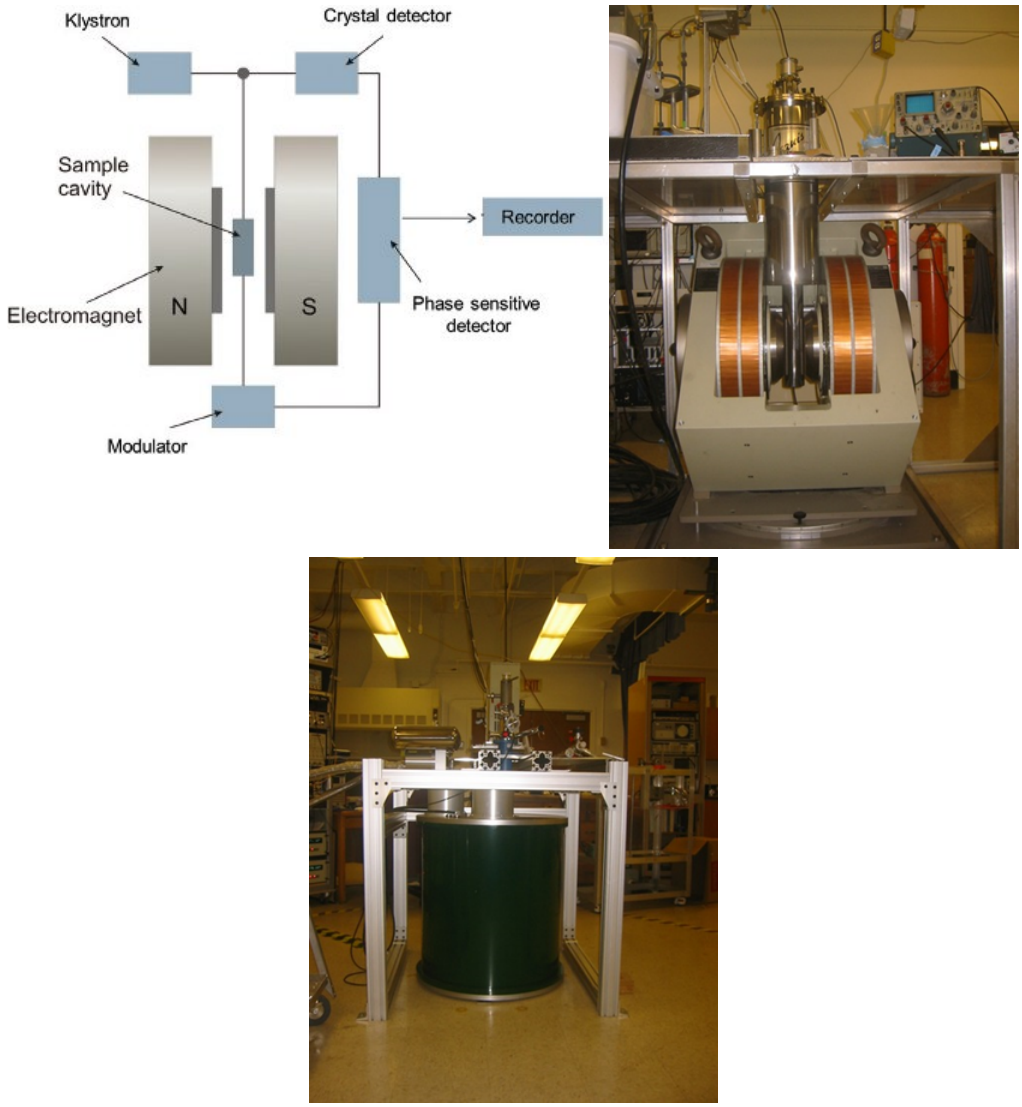

Figure 5.15.1: (left) Basic EPR instrument layout. (B and C) EPR instruments in the Britt Lab at UC Davis.

Microwave Generation

Klystrons are high power microwave vacuum tubes. They are velocity-modulated tubes that are used in radars as amplifiers or oscillators. A klystron uses the kinetic energy of an electron beam for the amplification of a high-frequency signal. Klystrons make use of the transit-time effect by varying the velocity of an electron beam. It is a linear beam device; that is, the electron flow is in a straight line focused by an axial magnetic field. The magnetic field is only used to focalize the electron beam. A klystron has one or more special cavities around the axis of the tube that modulate the electric field. Due to the number of the resonant cavities, klystrons are divided up into two-cavity klystrons, multi-cavity klystrons, and repeller klystrons.

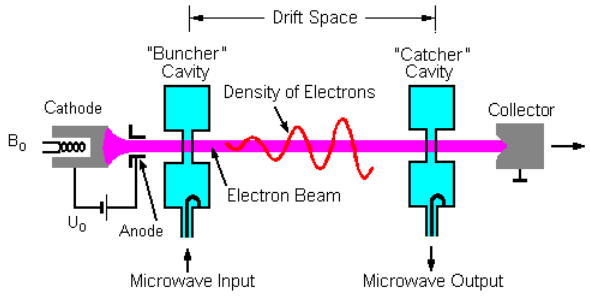

Figure 5.15.1: Two-cavity klystron amplifier. (CC BY-SA 3.0; Charly Whisky via Wikipedia)

In two-cavity klystrons there are two microwave cavity resonators, the "catcher" and the "buncher". When used as an amplifier, the weak microwave signal to be amplified is applied to the buncher cavity through a coaxial cable or waveguide, and the amplified signal is extracted from the catcher cavity.

At one end of the tube is the hot cathode which produces electrons when heated by a filament. The electrons are attracted to and pass through an anode cylinder at a high positive potential; the cathode and anode act as an electron gun to produce a high velocity stream of electrons. An external electromagnet winding creates a longitudinal magnetic field along the beam axis which prevents the beam from spreading.

The beam first passes through the "buncher" cavity resonator, through grids attached to each side. The buncher grids have an oscillating AC potential across them, produced by standing wave oscillations within the cavity, excited by the input signal at the cavity's resonant frequency applied by a coaxial cable or waveguide. The direction of the field between the grids changes twice per cycle of the input signal. Electrons entering when the entrance grid is negative and the exit grid is positive encounter an electric field in the same direction as their motion, and are accelerated by the field. Electrons entering a half-cycle later, when the polarity is opposite, encounter an electric field which opposes their motion, and are decelerated.

Microwave Waveguides

A waveguide is a structure that guides waves, such as electromagnetic waves or sound, with minimal loss of energy by restricting the transmission of energy to one direction. Without the physical constraint of a waveguide, wave intensities decrease according to the inverse square law as they expand into three dimensional space.

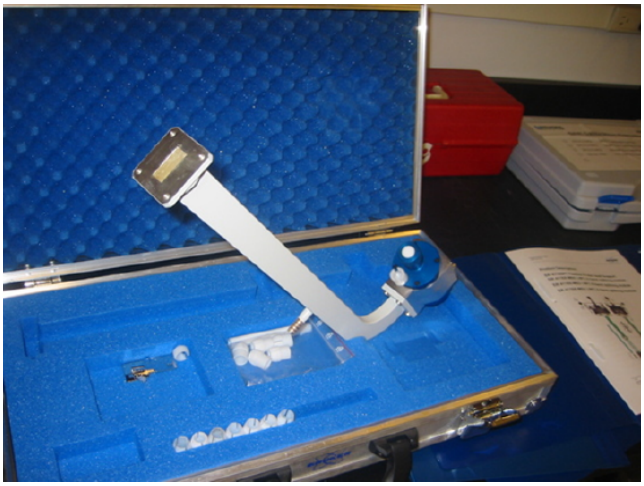

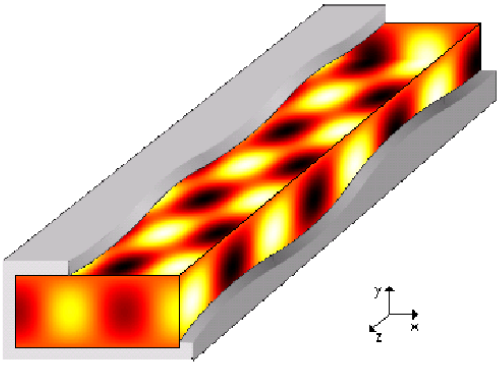

Figure 5.15.2: Microwave waveguides direct microwaves through the EPR instrument. The optical analog would be a fiber optic.

References

- https://sites.cns.utexas.edu/epr_facility/what-epr
- https://www.americanlaboratory.com/9...radiated-Food/

Attributions

- Klystron: https://www.radartutorial.eu/08.tran...ystron.en.html (CC BY-SA 3.0; Christian Wolff)
- Klyston: https://en.Wikipedia.org/wiki/Klystron(CC BY-SA 4.0; Wikipedia)

5.16: EPR Signals

Like most spectroscopic techniques, EPR spectrometers measure the absorption of electromagnetic radiation. A simple absorption spectra will appear similar to the one on the top of Figure 1. However, a phase-sensitive detector is used in EPR spectrometers which converts the normal absorption signal to its first derivative. Then the absorption signal is presented as its first derivative in the spectrum, which is similar to the one on the bottom of Figure 5.16.1. Thus, the magnetic field is on the x-axis of EPR spectrum; dχ″/dB, the derivative of the imaginary part of the molecular magnetic susceptibility with respect to the external static magnetic field in arbitrary units is on the y-axis. In the EPR spectrum, where the spectrum passes through zero corresponds to the absorption peak of absorption spectrum. People can use this to determine the center of the signal. On the x-axis, sometimes people use the unit "gauss" (G), instead of tesla (T). One tesla is equal to 10000 gauss.

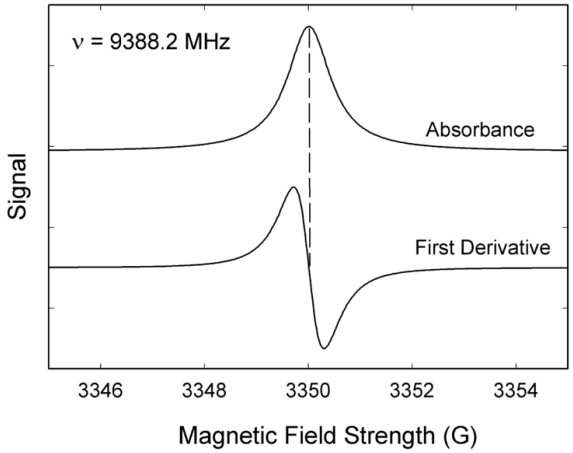

Figure 5.16.1: Comparison of absorption spectrum and EPR spectrum. Image used with permisison (Public Domain).

Proportionality factor (g-factor)

As a result of the Zeeman Effect, the state energy difference of an electron with s=1/2 in magnetic field is

$$\Delta E = g\beta B \tag{5.16.1}$$

where β is the constant, Bohr magneton. Since the energy absorbed by the electron should be exactly the same with the state energy difference ΔE with $\Delta E = h\nu$ (h is Planck's constant), Equation 5.16.1 can be expressed as

$$h\nu = g\beta B \tag{5.16.2}$$

Spectroscopists can control the microwave frequency ν and the magnetic field B. The other factor, g, is a constant of proportionality, whose value is the property of the electron in a certain environment. After plugging in the values of h and β in Equation 5.16.2, g value can be given through Equation 5.16.3:

$$g = 71.4484v(\text{in GHz})/\text{B (in mT)} \tag{5.16.3}$$

A free electron in vacuum has a g value of $g_e = 2.00232$. For instance, at the magnetic field of 331.85 mT, a free electron absorbs the microwave with an X-band frequency of 9.300 GHz. However, when the electron is in a certain environment, for example, a transition metal-ion complex, the second magnetic field produced by the nuclei, ΔB, will also influence the electron. At this kind of circumstance, Equation 5.16.2 becomes

$$h\nu = g\beta(B_e + \Delta B) \tag{5.16.4}$$

since we only know the spectrometer value of B, the Equation 5.16.4 is written as:

$$h\nu = (g_e + \Delta g)\beta B \tag{5.16.5}$$

From the relationship shown above, we know that there are infinite pairs of ν and B that fit this relationship. The magnetic field for resonance is not a unique "fingerprint" for the identification of a compound because spectra can be acquired at different microwave frequencies.

Then what is the fingerprint of a molecule? It is Δg and this contains the chemical information that lies in the interaction between the electron and the electronic structure of the molecule, one can simply take the value of

$$g = g_e + \Delta g$$

as a fingerprint of the molecule.

For organic radicals, the g value is very close to g_e with values ranging from 1.99-2.01. For example, the g value for •CH3 is 2.0026. For transition metal complexes, the g value varies a lot because of the spin-orbit coupling and zero-field splitting. Usually it ranges from 1.4-3.0, depending on the geometry of the complex. For instance, the g value of Cu(acac)2 is 2.13. To determine the g value, we use the center of the signal. By using Equation 5.16.3, we can calculate the g factor of the absorption in the spectrum. The value of g factor is not only related to the electronic environment, but also related to anisotropy. About this part, please refer to EPR:Theory, Parallel Mode EPR: Theory and ENDOR:Theory. An example from UC Davis is shown in Figure 5.16.2(Britt group, Published in J.A.C.S.):

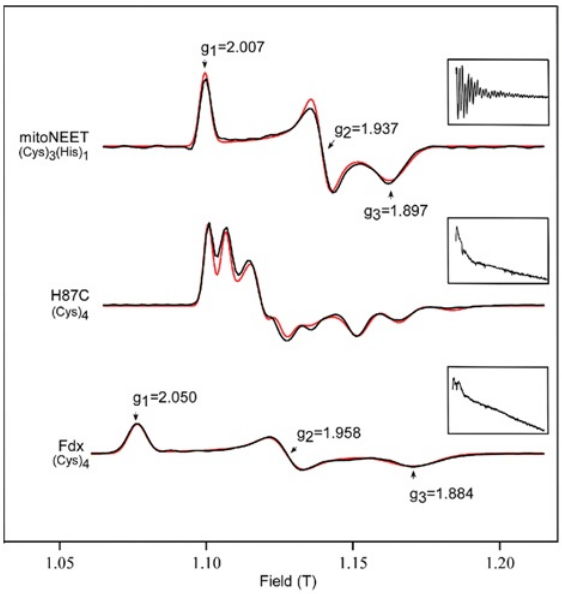

Figure 5.16.2: EPR spectra of some proteins (WT mitoNEET, H87C mitoNEET, and ferredoxin). Frequency is 30.89 GHz.[1]

5.17: EPR - Hyperfine Structure

Besides the applied magnetic field B_0, the compound contains the unpaired electrons are sensitive to their local “micro” environment. These so-called **hyperfine interactions** involves the coupling of the electron spins to the nuclei of the atoms in a molecule or complex that have their own fine magnetic moments. These magnetic moments can produce a local magnetic field intense enough to affect the electron energy.

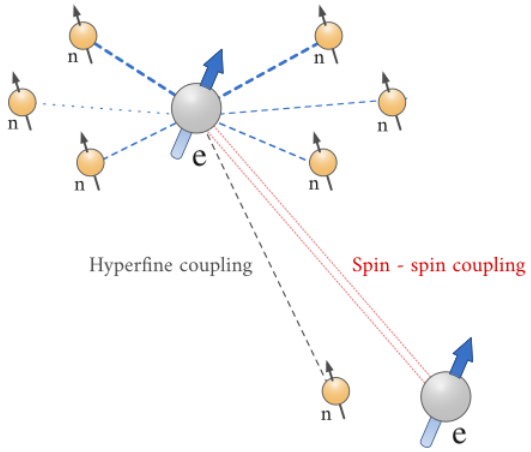

Figure 5.17.1: An unpaired electron can be influenced by surrounding unpaired electron spins (via spin-spin coupling) or via nearby nuclear spins (hyperfine coupling). (CC BY-NC 4.0; Ümit Kaya via LibreTexts)

Hyperfine coupling in EPR is analogous to spin-spin coupling in NMR. There are two kinds of hyperfine coupling:

1. coupling of the electron magnetic moment to the magnetic moment of its own nucleus; and
2. coupling of the electron to a nucleus of a different atom, called **super hyperfine splitting**.

Both types of hyperfine coupling cause a splitting of the spectral lines with intensities following Pascal’s triangle for $I = 1/2$ nuclei, similar to J-coupling in NMR.

Hyperfine interactions can be used to provide a wealth of information about the sample such as the number and identity of atoms in a molecule or compound, as well as their distance from the unpaired electron. Then the energy level of the electron can be expressed as:

$$E = gm_B B_0 M_S + aM_s m_I \tag{5.17.1}$$

with a is the hyperfine coupling constant, m_I is the nuclear spin quantum number.

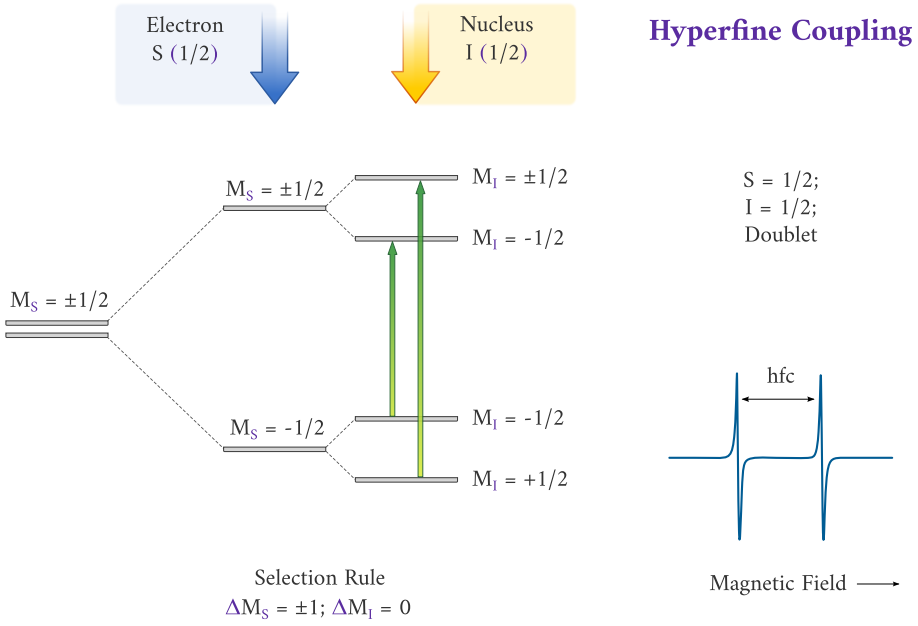

Figure 5.17.1: Hyperfine coupling of an electron with a spin-1/2 nuclus (CC BY-NC 4.0; Ümit Kaya via LibreTexts)

The splitting pattern for a coupling of an electron to a spin-1 nucleus Figure 5.17.3) differs from the coupling to the spin-1/2 nucleus Figure 5.17.2

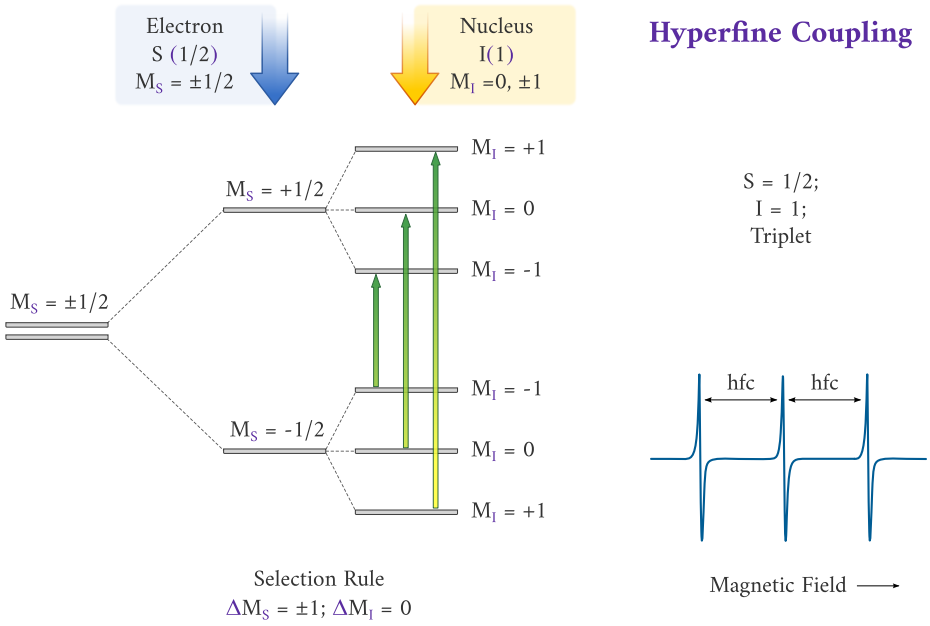

Figure 5.17.3: Hyperfine coupling of an electron with a spin-1 nuclus (CC BY-NC 4.0; Ümit Kaya via LibreTexts)

Splitting Patterns

The rules for determining which nuclei will interact are the same as for NMR. For isotopes which have even atomic and even mass numbers, the ground state nuclear spin quantum number, I, is zero, and these isotopes have no EPR (or NMR) spectra. For isotopes with odd atomic numbers and even mass numbers, the values of I are integers. For example the spin of ^{2}H is 1. For isotopes with odd mass numbers, the values of I are fractions. For example the spin of ^{1}H is 1/2 and the spin of ^{23}Na is 7/2. Here are more examples from biological systems:

The number of lines from the hyperfine interaction can be determined by the formula:

$$2NI+1$$

where N is the number of equivalent nuclei and I is the spin.

For example, an unpaired electron on a V^{4+} experiences *I*=7/2 from the vanadium nucleus. We can see 8 lines from the EPR spectrum. When coupling to a single nucleus, each line has the same intensity. When coupling to more than one nucleus, the relative intensity of each line is determined by the number of interacting nuclei. For the most common $I = 1/2$ nuclei, the intensity of each line follows Pascal's triangle (Figure 5.17.4:

$$\begin{array}{ccccccc} & & & 1 & & & \\ & & 1 & & 1 & & \\ & 1 & & 2 & & 1 & \\ 1 & & 3 & & 3 & & 1 \\ & 1 & & 4 & & 1 & \\ 1 & & 5 & & 10 & & 10 & & 5 & & 1 \end{array}$$

Figure 5.17.4: Pascal's triangle

For example, for •CH_3, the radical's signal is split to 2N*I*+1= 2*3*1/2+1=4 lines, the ratio of each line's intensity is 1:3:3:1. The spectrum looks like this:

A simulated spectrum of the methyl radical is shown in Figure 5.17.3. The line is split equally by the three hydrogens giving rise to four lines of intensity 1:3:3:1 with hyperfine coupling constant a.

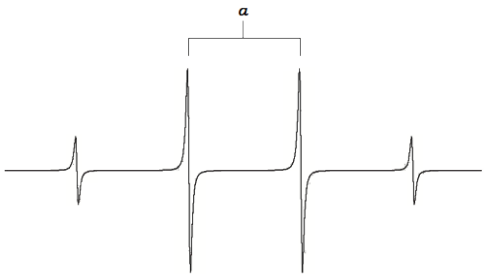

Figure 5.17.3: Simulated spectrum of CH_3 radical with hyperfine coupling constant a.

If an electron couples to several sets of nuclei, first we apply the coupling rule to the nearest nuclei, then we split each of those lines by the coupling them to the next nearest nuclei, and so on. For the methoxymethyl radical, $H_2C(OCH_3)$, there are

$$(2*2*1/2+1)*(2*3*1/2+1) = 12$$

lines in the spectrum, the spectrum looks like this:

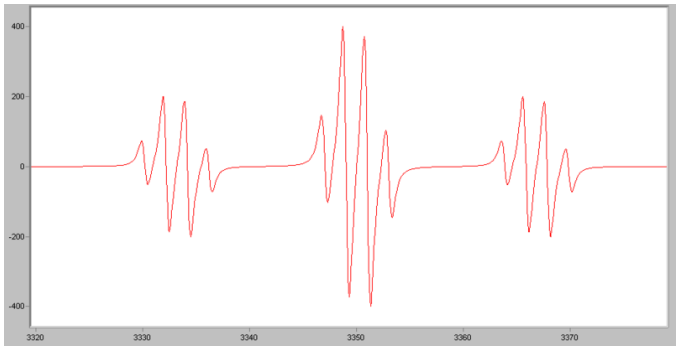

Figure 5.17.4: Simulated EPR spectrum of the $H_2C(OCH_3)$ radical. http://en.Wikipedia.org/wiki/File:EP...hoxymethyl.png

The hyperfine splitting constant (a), can be determined by measuring the distance between each of the hyperfine lines. This value can be converted into Hz using the g value in the equation:

$$hA = g\beta a \tag{5.17.2}$$

EPR experiments often are conducted at X- and, less commonly, Q bands, mainly due to the ready availability of the necessary microwave components (which originally were developed for radar applications). A second reason for widespread X and Q band measurements is that electromagnets can reliably generate fields up to about 1 tesla. EPR spectra of a nitroxide radical as a function of frequency. Note the improvement in resolution from left to right

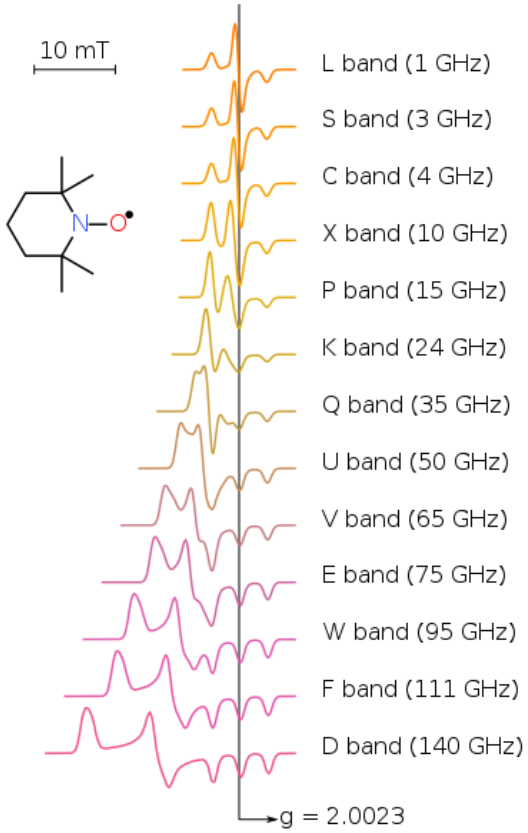

Figure 5.17.4: Variation in the EPR spectrum of the TEMPO nitroxide radical as the microwave band (energy of excitation) changes.[24] Note the improved resolution as frequency rises (neglecting the influence of g strain). (Public Domain; TungstenEinsteinium via Wikipedia)

The EPR spectra have very different line shapes and characteristics depending on many factors, such as the interactions in the spin Hamiltonian, physical phase of samples, dynamic properties of molecules. To gain the information on structure and dynamics from experimental data, spectral simulations are heavily relied. People use simulation to study the dependencies of spectral features on the magnetic parameters, to predict the information we may get from experiments, or to extract accurate parameter from experimental spectra.

References

- https://chem.libretexts.org/Bookshel...R_Spectroscopy
- http://www.sb.fsu.edu/~fajer/Fajerla...cuments/Primer

Index

A

Auger effect
4.6: X-ray Absorption Spectroscopies
Auger electrons
4.6: X-ray Absorption Spectroscopies

B

bathochromic shift
2.13: Assignment of Bands Based on Solvent Effects
binding energy
4.1: Physical Principles
Boltzmann distribution
5.5: Boltzmann Statistics
Bremsstrahlung
4.4: Experimental Details

C

chemical shift
5.4: Chemical Shifts
collisional broadening
2.3: Broadening Mechanisms
configuration interaction
2.9: Configuration Interaction

E

electromagnetic radiation
1.1: Electromagnetic Radiation (Component 1)
extinction coefficient
1.5: Multicomponent Samples

H

heteronuclear coupling
5.12: 13-C NMR Spectroscopy
homogeneous broadening
2.3: Broadening Mechanisms
hyperchromism
2.13: Assignment of Bands Based on Solvent Effects
hyperfine interactions
5.17: EPR - Hyperfine Structure
hyperfine splitting
5.16: EPR Signals
hypochromism
2.13: Assignment of Bands Based on Solvent Effects
hypsochromic shift
2.13: Assignment of Bands Based on Solvent Effects

I

inhomogeneous broadening
2.3: Broadening Mechanisms
isosbestic point
1.5: Multicomponent Samples

K

Koopmans' Theorem
4.2: Photoelectron Spectroscopy - Valence Ionization

L

Larmour frequency
5.6: Larmour Frequency

M

molar absorptivity
1.5: Multicomponent Samples

N

NMR precession
5.8: Precession and Relaxation
NMR relaxation
5.8: Precession and Relaxation
Nyquist theorem
3.8: Fourier Transform IR Spectroscopy
Nyquist wavenumber
3.8: Fourier Transform IR Spectroscopy

O

oscillator strength
2.10: Measures of Transition Amplitudes

P

photoemission
4.4: Experimental Details
Pure dephasing
2.3: Broadening Mechanisms

S

scintillators
4.4: Experimental Details
solvation
2.13: Assignment of Bands Based on Solvent Effects
stationary states
1.2: Matter (Component 2)

T

term symbols
2.11: Term Symbols
transition integrals
2.1: Transition Integrals
transmittance
1.5: Multicomponent Samples

U

Ultraviolet Photoelectron Spectroscopy (UPS)
4.1: Physical Principles

V

vibronic transitions
2.2: Vibronic Transitions

Glossary

Sample Word 1 | Sample Definition 1

Detailed Licensing

Overview

Title: Chem 205: Symmetry, Spectroscopy, and Structure

Webpages: 108

Applicable Restrictions: Noncommercial

All licenses found:

- CC BY-NC-SA 4.0: 97.2% (105 pages)
- Undeclared: 2.8% (3 pages)

By Page

- Chem 205: Symmetry, Spectroscopy, and Structure - *CC BY-NC-SA 4.0*
  - Front Matter - *CC BY-NC-SA 4.0*
    - 0: Agenda - *CC BY-NC-SA 4.0*
    - TitlePage - *CC BY-NC-SA 4.0*
    - InfoPage - *CC BY-NC-SA 4.0*
    - Table of Contents - *Undeclared*
    - Licensing - *CC BY-NC-SA 4.0*
    - 7: Writing Topics - *CC BY-NC-SA 4.0*
      - 7.1: Polarization Sensitive Electronic Spectra (Anisotropy) - *CC BY-NC-SA 4.0*
      - 7.2: Circular Dichroism (Electronic) - *CC BY-NC-SA 4.0*
      - 7.3: Influence of Absorption Spectra based on Molecular Structure - *CC BY-NC-SA 4.0*
      - 7.4: Two-Photon Absorption - *CC BY-NC-SA 4.0*
      - 7.5: Electronic Absorption Selection Rules - *CC BY-NC-SA 4.0*
      - 7.6: Resonant Raman Scattering - *CC BY-NC-SA 4.0*
      - 7.7: Circular Dichroism (Vibrational) - *CC BY-NC-SA 4.0*
      - 7.8: FTIR Operation - *CC BY-NC-SA 4.0*
      - 7.9: Fourier Transform Algorithms in FTIR - *CC BY-NC-SA 4.0*
      - 7.10: Rotational Raman Spectroscopy -Li Wang - *CC BY-NC-SA 4.0*
      - 7.11: Vibrational Absorption Selection Rules - *CC BY-NC-SA 4.0*
      - 7.12: Microwave Rotational Spectroscopy - *CC BY-NC-SA 4.0*
      - 7.13: Two-photon Fluorescence -Rachel Siegel - *CC BY-NC-SA 4.0*
      - 7.14: 2D NMR (General Properties) - *CC BY-NC-SA 4.0*
      - 7.15: Spin Echos - *CC BY-NC-SA 4.0*
      - 7.16: X-ray Photoelectron Spectroscopy (XPS) - Nick Mrachek - *CC BY-NC-SA 4.0*
      - 7.17: Sensitivity of XANES on Oxidation State of Elements - Ivan Opara - *CC BY-NC-SA 4.0*
      - 7.18: Sensitivity of XANES on Chemical Environment (e.g., bonding) - *CC BY-NC-SA 4.0*
      - 7.19: X-Ray Generation and Detection Sources - *CC BY-NC-SA 4.0*
      - 7.20: Analysis of XAFS Spectra -Kingston Robinson - *CC BY-NC-SA 4.0*
      - 7.21: X-Ray Photoelectron Spectroscopy - *CC BY-NC-SA 4.0*
      - 7.22: Magic Angle Spinning Solid-State NMR - Kayla Osumi - *CC BY-NC-SA 4.0*
      - 7.23: Electron-Nuclear Double Resonance (ENDOR) -Liam Twomey - *CC BY-NC-SA 4.0*
      - 7.24: Double Electron-Electron Resonance (DEER) - *CC BY-NC-SA 4.0*
      - 7.25: Nuclear Resonance Vibrational Spectroscopy (NRVS) - *CC BY-NC-SA 4.0*
      - 7.26: Nuclear Overhauser Effect - *CC BY-NC-SA 4.0*
      - 7.27: Total Correlation Spectroscopy (TOCSY) - *CC BY-NC-SA 4.0*
      - 7.28: Nuclear Overhauser Effect Spectroscopy (NOESY) - Joel Shirey - *CC BY-NC-SA 4.0*
      - 7.29: ^{1}H-^{1}H COSY (COrrelated SpectroscopY) - Chris Suarez - *CC BY-NC-SA 4.0*
      - 7.30: Heteronculear Single Quantum Coherence (HSQC) NMR - *CC BY-NC-SA 4.0*
      - 7.31: Rotating frame Overhauser Effect SpectroscopY (^{1}H-^{1}H ROESY) - *CC BY-NC-SA 4.0*
      - 7.32: scanning near-field optical microscopy (SNOM) - Xavier Holmes - *CC BY-NC-SA 4.0*
      - 7.33: Surface-enhanced Raman spectroscopy - Chris Suarez - *CC BY-NC-SA 4.0*
  - 1: Basics of Spectroscopy - *CC BY-NC-SA 4.0*
    - 1.1: Electromagnetic Radiation (Component 1) - *CC BY-NC-SA 4.0*

- 1.2: Matter (Component 2) - *CC BY-NC-SA 4.0*
- 1.3: Different types of Spectroscopy - *Undeclared*
- 1.4: Absorbance and Concentration - *Undeclared*
- 1.5: Multicomponent Samples - *CC BY-NC-SA 4.0*

- 2: Electronic Spectroscopy - *CC BY-NC-SA 4.0*
  - 2.1: Transition Integrals - *CC BY-NC-SA 4.0*
  - 2.2: Vibronic Transitions - *CC BY-NC-SA 4.0*
  - 2.3: Broadening Mechanisms - *CC BY-NC-SA 4.0*
  - 2.4: The Fate of Electronic Transitions - *CC BY-NC-SA 4.0*
  - 2.5: Electronic State and Transitions - *CC BY-NC-SA 4.0*
  - 2.6: Introduction to Symmetry - *CC BY-NC-SA 4.0*
  - 2.7: The Carbonyl Group - *CC BY-NC-SA 4.0*
  - 2.8: Symmetry and Formaldehyde - *CC BY-NC-SA 4.0*
  - 2.9: Configuration Interaction - *CC BY-NC-SA 4.0*
  - 2.10: Measures of Transition Amplitudes - *CC BY-NC-SA 4.0*
  - 2.11: Term Symbols - *CC BY-NC-SA 4.0*
  - 2.12: Absorption Spectrum of Formaldehyde - *CC BY-NC-SA 4.0*
  - 2.13: Assignment of Bands Based on Solvent Effects - *CC BY-NC-SA 4.0*
  - 2.14: Solvent Effect of Fluorescence - *CC BY-NC-SA 4.0*
  - 2.15: Breaking Symmetries - *CC BY-NC-SA 4.0*
  - 2.16: Charge Transfer Bands - *CC BY-NC-SA 4.0*
  - 2.17: Conjugation Length - *CC BY-NC-SA 4.0*
- 3: Vibrational Spectroscopy - *CC BY-NC-SA 4.0*
  - 3.1: Introduction to Vibrations - *CC BY-NC-SA 4.0*
  - 3.2: Polyatomic Molecules - *CC BY-NC-SA 4.0*
  - 3.3: Raman vs. IR Spectroscopies - *CC BY-NC-SA 4.0*
  - 3.4: Resonant Raman Spectroscopy - *CC BY-NC-SA 4.0*
  - 3.5: Classification of Normal Modes - *CC BY-NC-SA 4.0*
  - 3.6: IR and Raman Activity - *CC BY-NC-SA 4.0*
  - 3.7: Non-Fundamental Transations - Hot Bands, Combination Bands, and Fermi Resonances - *CC BY-NC-SA 4.0*
  - 3.8: Fourier Transform IR Spectroscopy - *CC BY-NC-SA 4.0*
  - 3.9: Spectra of Gases - Rovibronic Transitions - *CC BY-NC-SA 4.0*
- 4: X-ray Spectroscopy - *CC BY-NC-SA 4.0*
  - 4.1: Physical Principles - *CC BY-NC-SA 4.0*
  - 4.2: Photoelectron Spectroscopy - Valence Ionization - *CC BY-NC-SA 4.0*
  - 4.3: Back to Basics - *CC BY-NC-SA 4.0*
  - 4.4: Experimental Details - *CC BY-NC-SA 4.0*
  - 4.5: X-ray Photoelectron (XPS) Spectroscopy - *CC BY-NC-SA 4.0*
  - 4.6: X-ray Absorption Spectroscopies - *CC BY-NC-SA 4.0*
  - 4.7: Experimental modes and Data Analysis - *CC BY-NC-SA 4.0*
  - 4.8: Introduction to X-ray Absorption Spectroscopy (XAS) - *CC BY-NC-SA 4.0*
  - 4.9: X-Ray Absorption Near Edge Structure (XANES) - *CC BY-NC-SA 4.0*
  - 4.10: X-ray absorption fine structure (XAFS) - *CC BY-NC-SA 4.0*
- 5: Magnetic Resonance Spectroscopies - *CC BY-NC-SA 4.0*
  - 5.1: Nuclear Magnetic Resonance (NMR) - Intrinsic Spins - *CC BY-NC-SA 4.0*
  - 5.2: Nuclear Magnetic Resonance (NMR) - Turning on the Field - *CC BY-NC-SA 4.0*
  - 5.3: Spin 1/2 Spectra - *CC BY-NC-SA 4.0*
  - 5.4: Chemical Shifts - *CC BY-NC-SA 4.0*
  - 5.5: Boltzmann Statistics - *CC BY-NC-SA 4.0*
  - 5.6: Larmour Frequency - *CC BY-NC-SA 4.0*
  - 5.7: Ensemble Effects - *CC BY-NC-SA 4.0*
  - 5.8: Precession and Relaxation - *CC BY-NC-SA 4.0*
  - 5.9: Chemical Shifts - *CC BY-NC-SA 4.0*
  - 5.10: Fourier Transform (pulsed) NMR - The way things are really done these days - *CC BY-NC-SA 4.0*
  - 5.11: Spin-Spin, J-Coupling or indirect dipole-dipole coupling (all the same phenomenon) - *CC BY-NC-SA 4.0*
  - 5.12: 13-C NMR Spectroscopy - *CC BY-NC-SA 4.0*
  - 5.13: Nuclear Overhauser Effect (NOE) and 2-D NMR - *CC BY-NC-SA 4.0*
  - 5.14: Electron Paramagnetic Resonance - *CC BY-NC-SA 4.0*
  - 5.15: EPR Instrumentation - *CC BY-NC-SA 4.0*
  - 5.16: EPR Signals - *CC BY-NC-SA 4.0*
  - 5.17: EPR - Hyperfine Structure - *CC BY-NC-SA 4.0*
- Back Matter - *CC BY-NC-SA 4.0*
  - Index - *CC BY-NC-SA 4.0*
  - Glossary - *CC BY-NC-SA 4.0*
  - Detailed Licensing - *CC BY-NC-SA 4.0*